INVESTIGATING THE NEURAL CONTROL OF MUSCLE TORQUE USING HIGH-DENSITY SURFACE ELECTROMYOGRAPHY

Robert Hunter

A thesis submitted in partial fulfilment of the requirements of the University of Kent for the degree of Doctor of Philosophy

PhD

School of Sport and Exercise Sciences

University of Kent

September 2022

No part of this thesis has been submitted in support of an application for any degree or other qualification of the University of Kent, or any other University or Institution of learning.

Robert Hunter

ABSTRACT

The use of high-density surface electromyography (HDsEMG) decomposition presents an opportunity to study the behaviour of individual motor units, the smallest functional components of the neuromuscular system involved in movement. The present thesis aimed to investigate the neural control of muscle torque during isometric exercise of the ankle dorsiflexors in healthy adults using decomposition of the tibialis anterior HDsEMG signal. The first experimental study (Chapter 4) investigated the methodological aspects of HDsEMG signal acquisition including the skin-electrode interface, ground electrode configuration, and decomposition processing criteria. No differences in motor unit yield were observed between skin treatments, and at least four ground electrodes resulted in significant reductions in baseline signal noise. The use of adjusted acceptance criteria during the decomposition process resulted in a greater motor unit yield when compared to the original conditions. Furthermore, the low motor unit yields observed with increasing contraction intensities meant that contractions in subsequent studies were performed below 50% maximal voluntary contraction (MVC). Study 2 (Chapter 5) then investigated the effects of fatiguing intermittent exercise performed with arterial occlusion at 30% MVC on the complexity of muscle torque output and the motor unit cumulative spike train. Reductions in the complexity of the tibialis anterior motor unit cumulative spike train were concomitant with a loss of dorsiflexor muscle torque complexity, indicating an increase in the transmission of common synaptic input relative to independent synaptic input to the muscle as task failure approaches. In Study 3 (Chapter 6), the critical torque concept was extended to the ankle dorsiflexors, and the end-test torque from the 5 min all-out test was compared to the critical torque estimated from the conventional method involving multiple submaximal exercise bouts performed until task failure. The 5 min all-out test overestimated the critical torque compared to the conventional method, and the critical torque of the dorsiflexors was shown to be higher than previously reported for the knee extensors. In the final study (Chapter 7), the performance of 6 min prior heavy-intensity exercise had no discernible effects on tibialis anterior motor unit behaviour, suggesting the ‘priming’ effects previously observed for the knee extensors are absent in the dorsiflexor muscles. Collectively, the findings of this

thesis confirm the dorsiflexors as a highly fatigue-resistant muscle group, and suggest that the findings from HDsEMG studies involving the tibialis anterior are not necessarily generalisable to other muscles (such as the knee extensors).

TABLE OF CONTENTS

Page

ABSTRACT iii
LIST OF TABLES vii
LIST OF FIGURES viii
SYMBOLS, ABBREVIATIONS, AND DEFINITIONS xii
PUBLICATIONS AND COMMUNICATIONS xiv
ACKNOWLEDGEMENTS xv
CHAPTER 1 – INTRODUCTION 1
Introduction 2
CHAPTER 2 – REVIEW OF LITERATURE 6
Decomposition of high-density surface electromyography 7
Complexity 13
Critical Power 31
Priming exercise 48
Aims and hypotheses 56
CHAPTER 3 - GENERAL METHODS 58
Introduction 59
Pre-test Procedures 59
Ethics 59
Participant Recruitment and Informed Consent 59
Familiarisation 59
Experimental Controls 60
Procedures 60
Anthropometry 60
Isometric Torque Measurement/Dynamometry 60
High-Density Surface Electromyography 62
Motor Unit Decomposition 64
Statistical Analyses 65
CHAPTER 4 – METHODOLOGICAL ASPECTS OF HIGH-DENSITY SURFACE ELECTROMYOGRAPHY SIGNAL ACQUISITION IN THE TIBIALIS ANTERIOR MUSCLE DURING ISOMETRIC CONTRACTIONS OF VARYING INTENSITY 67
Introduction 68
Methods 71
Results 77
Discussion 83
CHAPTER 5 – LOSS OF MOTOR UNIT CUMULATIVE SPIKE TRAIN COMPLEXITY AND ANKLE TORQUE COMPLEXITY DURING FATIGUING DORSIFLEXOR CONTRACTIONS IN HUMANS 90

Introduction 91
Methods 94
Results 100
Discussion 108
CHAPTER 6 – CRITICAL TORQUE IN THE DORSIFLEXORS – A COMPARISON BETWEEN THE 5 MINUTE ALL-OUT TEST AND THE CONVENTIONAL ESTIMATION OF CRITICAL TORQUE FROM SUBMAXIMAL TESTS PERFORMED TO TASK FAILURE 115
Introduction 116
Methods 118
Results 123
Discussion 130
CHAPTER 7 – THE EFFECTS OF PRIMING EXERCISE ON MOTOR UNIT BEHAVIOUR IN THE TIBIALIS ANTERIOR 137
Introduction 138
Methods 141
Results 145
Discussion 152
CHAPTER 8 – GENERAL DISCUSSION 160
Recapitulation of experimental studies and summary of main findings 161
Fatigue-induced losses of motor unit cumulative spike train complexity in the tibialis anterior 164
Fatigue-resistant properties of the dorsiflexor muscles 166
High-density surface electromyography – a powerful, yet limited technique 169
Conclusions 175
REFERENCES 176
APPENDIX 213

LIST OF TABLES

Chapter 5

Table 5.1. Voluntary torque responses during contractions at 30% MVC with (OCC) and without (OPEN) arterial occlusion. 101

Table 5.2. Torque variability, complexity, and fractal scaling responses during contractions at 30% MVC with (OCC) and without (OPEN) arterial occlusion. ... 102

Table 5.3. Cumulative spike train complexity and fractal scaling responses during contractions at 30% MVC with (OCC) and without (OPEN) arterial occlusion. ... 107

Chapter 6

Table 6.1. Parameters of the 5 min all-out test and the critical torque determined from the conventional method using four or five submaximal tests performed to task failure 127

Chapter 7

Table 7.1. Target torque values for the 6 min heavy exercise bouts. 146

LIST OF FIGURES

Chapter 1

Figure 1.1. The action potentials, or “action currents”, recorded with the concentric needle electrode in the human triceps muscle. A) Beginning of a contraction; B) Follows on from A; C) A “powerful” contraction. From Adrian and Bronk (1929)..... 4

Chapter 2

Figure 2.1. Multichannel HDsEMG decomposition. 9

Figure 2.2. The effective neural drive to the muscle and force from experimental data. From Farina and Negro (2015). 11

Figure 2.3. Examples of mathematical fractals. From Eke et al. (2002). 14

Figure 2.4. Examples of self-similar structures and self-similar fluctuations. From Goldberger (2006)..... 17

Figure 2.5. Stepwise overview of Detrended Fluctuation Analysis. From Hardstone et al. (2012)..... 22

Figure 2.6. The effect of neuromuscular fatigue on knee extensor muscle torque complexity. From Pethick et al. (2021). 26

Figure 2.7. (**A**) Average speed in yards per second plotted against time in seconds for world record running and swimming events up to 1925. The scale for swimming is five times greater than that for running. From Hill, (1925). (**B**) The hyperbolic running speed-time relationship plotted for world record performances. From Jones et al. (2019)..... 32

Figure 2.8. (A) Hyperbolic model of CP. (B) Linear work-time model of CP. (C) The alternative approach to extracting CP and W’ proposed by Whipp et al. (1982). From Craig et al. (2019). 35

Figure 2.9. Exercise intensity domains. From Burnley and Jones (2016)..... 37

Figure 2.10. Individual responses for PCr (A) and pH (B) during submaximal intermittent isometric knee extension contractions performed at 40% MVC in a magnetic resonance spectrometer. From Saugen et al. (1997). 41

Figure 2.11. Peripheral fatigue response to exercise performed above and below the critical torque (CT) from the data of Burnley et al. (2012). From Craig et al. (2019) 43

Figure 2.12. A) Group mean power output during the 3-min all-out test. From Vanhatalo et al. (2007), **(B)** The torque profile during the 5-min all-out test for an individual participant. From Burnley (2009). 46
Figure 2.13. Pulmonary $\dot{V}O_2$ responses to heavy exercise bouts separated by 12 min from Burnley, Doust, Ball, et al. (2002). From Poole and Jones (2012). 50
Figure 2.14. Hypothetical simulation of motor unit recruitment thresholds (A and B) and muscle $\dot{V}O_2$ (C and D) during two bouts of heavy-intensity exercise separated by 12 min recovery. From Burnley et al. (2005). 55

Chapter 3

Figure 3.1. Participant setup. 62
Figure 3.2. A) Linear non-adhesive 16-bar electrode. B) 64-electrode HDsEMG grid. 63
Figure 3.3. Brief overview of the HDsEMG signal decomposition process..... 66

Chapter 4

Figure 4.1. Experimental setup.. 73
Figure 4.2. Contractions performed at 30% MVC for a representative participant. 76
Figure 4.3. Individual values for decomposed motor unit numbers in the tibialis anterior..... 78
Figure 4.4. Individual values for global motor unit discharge rate identified in the tibialis anterior..... 79
Figure 4.5. HDsEMG 64-channel average (A) and middle-channel (B) EMG_{RMS} (µV) values recorded at rest using iterative ground electrode configurations: 80
Figure 4.6. Group mean and individual values for the number of decomposed motor units in the tibialis anterior from the ABR visit using the original acceptance criteria (SIL = 90) and the adjusted acceptance criteria (SIL = 85).. 82

Chapter 5

Figure 5.1. Torque output from submaximal contractions performed at 30% maximal voluntary contraction (MVC) with arterial occlusion. 96

Figure 5.2. Responses of dorsiflexor torque and tibialis anterior motor unit cumulative spike train (CST) during contractions performed at 30% maximal voluntary contraction with arterial occlusion. 99
Figure 5.3. Complexity metrics during each condition. 106
Figure 5.4. Global motor unit discharge rate during contractions performed at 30% MVC. 108

Chapter 6

Figure 6.1. Raw torque output from submaximal contractions performed to task failure (**A**) and the 5 min all-out test from a representative participant (**B**). 121
Figure 6.2. A) Group peak and mean torque for all participants during the 5 min all-out test. **B**) Group peak and mean torque for the knee extensor 5 min-all out test from Burnley (2009). 125
Figure 6.3. Dorsiflexion torque (**A-C**) and tibialis anterior EMG_{RMS} (**D-F**) responses during the 5 min all-out test. 126
Figure 6.4. Critical torque determined using the conventional method and end-test torque from the 5 min all-out test for a representative participant. 128
Figure 6.5. A) The relationship between the critical torque estimated using the conventional method and the end-test torque from the 5 min all-out test for all participants. **B**) The bias and limits of agreement between the critical torque and the end-test torque. 129
Figure 6.6. Group torque responses during the submaximal exercise tests used in the conventional estimation of the critical torque. 130

Chapter 7

Figure 7.1. A: Contraction protocol for the 6 min priming and subsequent exercise bouts. B: Schematic of the experimental trial procedures. C: Each repeat of the ramp-and-hold contractions consisted of a 5 s incline, a 10 s hold phase, and a 5 s decline. D: Torque output for a representative participant from the ramp-and-hold contractions performed immediately after the 6 min priming bout at 10% and 40% MVC. 144
Figure 7.2. Mean discharge rates during ramp-and-hold contractions performed at 10% MVC and 40% MVC before and immediately after 6 min of priming exercise.. 149

Figure 7.3. Mean recruitment (A and B) and de-recruitment (C and D) thresholds during ramp-and-hold contractions performed at 10% MVC and 40% MVC before and immediately after 6 min of priming exercise. 150
Figure 7.4. Tibialis anterior global HDsEMG root mean square (EMG_{RMS}) responses during 6 min of 'heavy' priming exercise (open symbols) and a subsequent bout of 6 min 'heavy' exercise (filled symbols).. 151

Chapter 8

Figure 8.1. The decomposition review window presented after HDsEMG signal decomposition in A) OTBioLab and B) OTBioLab+.. 174

SYMBOLS, ABBREVIATIONS, AND DEFINITIONS

ADP	**Adenosine diphosphate**
ATP	**Adenosine triphosphate**
ANOVA	**Analysis of variance**
ApEn	**Approximate entropy**
CP	**Critical power** (W)
CST	**Motor unit cumulative spike train**
CT	**Critical torque** (N·m)
CV	**Coefficient of variation**
DFA	**Detrended fluctuation analysis**
DFA α	**Detrended fluctuation analysis alpha exponent**
EMG	**Electromyography**
EMG_{RMS}	**Electromyogram root mean square**
HDsEMG	**High-density surface electromyography**
H^+	**Hydrogen ion**
Hz	**Hertz**
iEMG	**Integrated electromyogram**
K^+	**Potassium**
kg	**Kilograms**
m	**Metres**
mmHg	**Millimetre of mercury**
MUAP	**Motor unit action potential**
MVC	**Maximal voluntary contraction**
N·m	**Newton-metre**
O_2	**Oxygen**
PCr	**Phosphocreatine**
pH	**Logarithmic scale used to express acidity and alkalinity of solutions**
P_i	**Inorganic phosphate**
PNR	**Pulse-to-noise ratio**

pps	**Pulses per second**
SampEn	**Sample entropy**
SD	**Standard deviation**
SIL	**Silhouette measure**
µV	**Microvolt**
$\dot{V}O_2$	**Oxygen uptake ($L \cdot min^{-1}$; $mL \cdot min^{-1}$; $mL.kg^{-1}.min^{-1}$)**
W	**Watts**
W'	**Curvature constant of the power-time relationship**

PUBLICATIONS AND COMMUNICATIONS

Communications

Hunter, R., Pethick, J., Winter, S. L., & Burnley, M. (2020). Changes in motor unit behaviour after fatiguing isometric exercise in the tibialis anterior muscle. (Abstract).

European College of Sport Science Congress 2020, online.

ACKNOWLEDGEMENTS

Firstly, I would like to acknowledge my supervisors, Dr Mark Burnley and Dr Samantha Winter. Thank you for the opportunity and for your continued support over the years, especially during the months and weeks leading up to submission. Mark, your words of advice have been invaluable and you have allayed many a fear, probably without even realising it.

I would also like to thank Dr Jamie Pethick, for the long hours of piloting at Medway Park and particularly for your efforts on the second study of this thesis. To Dr Lex Mauger, thank you for stepping in and keeping things ticking over this past year and a half at Kent.

To all those I had the pleasure of sharing the PhD office with over the years, thank you. Friday drinks in the Deep End and evening runs on the St Mary's Island loop kept me sane at times. Thank you to Paul, Sam, Ian, Chris, and Borja for welcoming me with open arms (sort of) when I arrived from the North East, and to everyone else who kept me going – Anna, Arthur, Callum, Carol, Megan, Ryan, and Will. You all made it a home from home.

To the Hunters: thank you for supporting me throughout and for putting up with me during the first of the lockdowns, I know it wasn't easy for you!

Finally, to Mel: thank you for being with me every step of the way throughout my journey to Kent (and back again). You are forever there when I need you most.

CHAPTER 1 – INTRODUCTION

Introduction

Prior to any explicit definitions of the motor unit in the literature, the work of Lucas (1905; 1909) revealed step-like increases in the contraction of muscle in the pithed frog after stimulations of increasing intensity. Similarly, Mines (1913) observed the phenomenon of recruitment thresholds, noting that “each step is the result of the excitation of a fresh nerve fibre or nerve fibres, this bringing a new group of fibres into play”. Sir Charles Sherrington also provided a precursor to his later definition of the motor unit when noting that “… by its branching the motor neurone obtains hold of many muscle-fibres” (Sherrington, 1906). However, the motor unit was first defined by Liddell and Sherrington in 1925 as “the motorneurone-axon and its adjunct muscle fibres” when studying the mechanisms of reflex inhibition in the decerebrate cat (Liddell & Sherrington, 1925). After identifying the generation of action potentials in the axon hillock of the motor neuron, Sherrington (1925) expanded this definition to include “the whole axon of the motorneurone from its hillock in the perikaryon down to its terminals in the muscle”. More recently, the motor unit was simply defined as the motor neuron and the muscle fibres its axon innervates (Heckman & Enoka, 2012). The motor unit is the smallest functional unit of the neuromuscular system that can be voluntarily activated and acts as a biological amplifier of neural activity (Farina & Holobar, 2016). Therefore, the study of motor unit behaviour provides an opportunity to study Sherrington’s “final common path” (Burke, 2007) and the neural control of motor output.

For a given muscle, estimates of the number of motor units which innervate that muscle can range from tens to hundreds (Heckman & Enoka, 2012). For example, the tibialis anterior muscle comprises between 330 (van Cutsem et al., 1997) and 445 (Feinstein et al., 1955) motor units. The muscle fibres innervated by the same motor neuron, and therefore belonging to the same motor unit, are collectively termed a muscle unit (Heckman & Enoka, 2012). The number of fibres in a muscle unit can range from fewer than 10 to almost 2000, but on average, around 300 fibres are innervated by each motor neuron (Enoka & Fuglevand, 2001) and each muscle unit typically occupies around 10% of the length of the muscle (Vieira et al., 2011).

Neural signals, in the form of action potentials, from the axon of the motor neuron are propagated to the neuromuscular junctions of all the muscle fibres in a motor unit and converted into contractile force in the form of cross-bridge interaction (Heckman & Enoka, 2012). Due to the high reliability for synaptic transmission at the neuromuscular junction, there is a one-to-one correspondence between the action potential conducted by the motor neuron and the action potential generated at each innervated muscle fibre (Farina & Holobar, 2016). It is these compound motor unit action potentials that can be recorded as electrical activity with electrodes placed over the surface of the skin (Farina et al, 2010). The sum of the action potentials generated by the active motor units is filtered by the so-called “volume conductor” between the muscle and electrodes and detected at the skin as the surface electromyogram (EMG; Farina et al., 2010). However, due to various factors, such as “amplitude cancellation” in which the sum of the surface action potentials is smaller than the amplitudes of the individual potentials, the amplitude of the surface EMG only provides a crude estimate of neural drive (Enoka & Duchateau, 2015; Farina et al., 2010).

Because motor units transduce action potentials from the motor neuron into muscle forces or torques, motor unit discharge characteristics contain information pertaining to the neural control signal (Farina et al., 2016). Since the pioneering work of Adrian and Bronk (1929; Figure 1.1) and their use of the concentric needle electrode, it has been possible to identify the shape and discharge rate of individual motor unit action potentials. Over the past half a century, as advances in intramuscular EMG sampling techniques have progressed, several successful attempts have been made to decompose the intramuscular EMG signal into its constituent motor unit action potentials using needle electrodes, fine wire electrodes, and multi-channel wire electrodes (De Luca & Adam, 1999; Erim & Lin, 2008; Muceli et al., 2015). Despite this, intramuscular sampling methods have obvious limitations due to their inherent selectivity and invasive nature, meaning relatively few motor units can be sampled simultaneously, often during low-intensity isometric contractions (Farina & Negro, 2012).

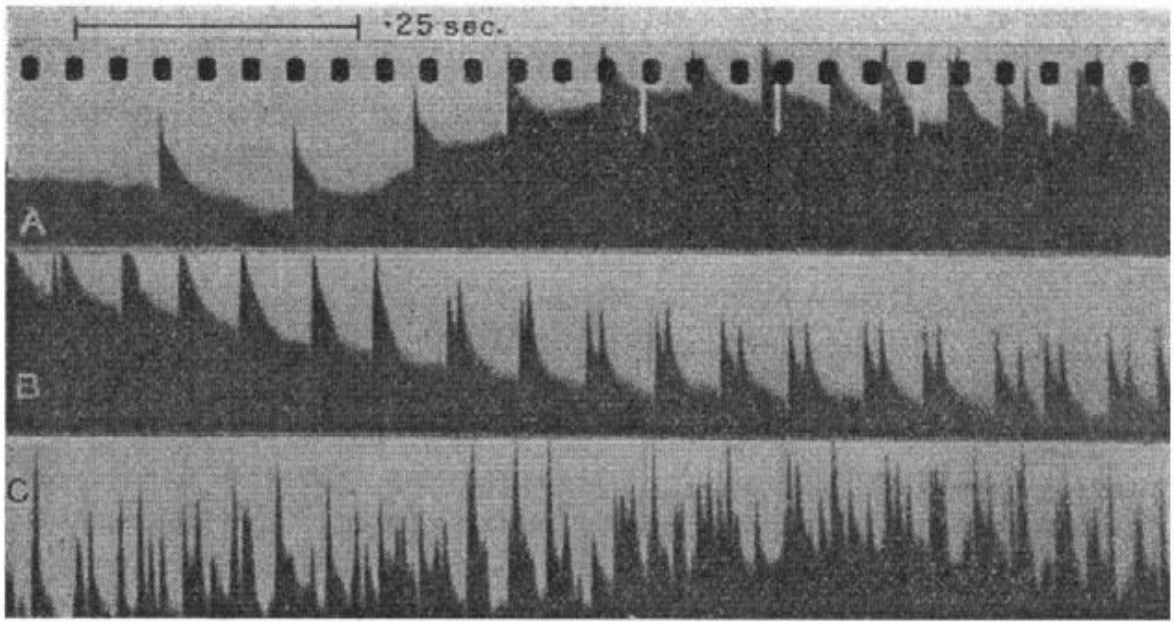

Figure 1.1. *The action potentials, or "action currents", recorded with the concentric needle electrode in the human triceps muscle. A) Beginning of a contraction; B) Follows on from A; C) A "powerful" contraction. From Adrian and Bronk (1929).*

The use of multichannel or high-density surface electromyography (HDsEMG) provides a non-invasive alternative to intramuscular EMG, and recent developments in decomposition techniques present the opportunity to study the behaviour of individual motor units across a range of muscles and contraction intensities (Holobar et al., 2009; Holobar & Zazula, 2007; Negro et al., 2016). Using such techniques, it is possible to identify the discharge timings of tens of concurrently active motor units, from which the neural drive to the muscle can be estimated (Farina & Negro, 2015).

The overall aim of this thesis was to investigate the neural control of muscle torque in the tibialis anterior using decomposition of the high-density surface electromyogram (HDsEMG). Chapter 2 reviews the literature relating to HDsEMG decomposition techniques, as well as the three central themes of this thesis: physiological complexity, the critical power or torque concept, and the use of prior heavy exercise or 'priming'. The general methods are detailed in Chapter 3, before the first experimental chapter (Chapter 4) explores the methodological aspects of

HDsEMG signal decomposition including the skin-electrode interface, the reduction of baseline signal noise, and signal processing. Complexity statistics are applied to both ankle dorsiflexion torque output and the motor unit cumulative spike train during fatiguing intermittent isometric contractions in Chapter 5. Chapter 6 compares the end-test torque estimated from a 5 min all-out test to the critical torque determined from the conventional method of multiple submaximal exercise bouts performed to task failure. The final experimental chapter (Chapter 7) investigates the effects of priming exercise on motor unit behaviour of the tibialis anterior. The collective findings of the thesis are discussed in Chapter 9, including suggestions for future research and concluding remarks.

CHAPTER 2 – REVIEW OF LITERATURE

Decomposition of high-density surface electromyography

HDsEMG decomposition techniques

The Introduction (Chapter 1) highlighted some of the limitations associated with inferring motor unit behaviours from the surface EMG, as well as the inherent issues with the use of intramuscular electrodes. Partly as a consequence of these issues, the past 30 years have seen the proposal of a number of different surface EMG decomposition methods, ranging from blind source separation algorithms (e.g., (Holobar et al., 2014; Holobar & Zazula, 2007; Negro et al., 2016) to algorithms based on motor unit template matching (e.g., De Luca et al., 2006; Nawab et al., 2010). Though the validity of decomposition techniques based on motor unit template matching algorithms has been extensively debated previously (De Luca et al., 2015; De Luca & Nawab, 2011; Farina et al., 2015), this is outside the scope of this thesis. The motor unit decomposition method used in this thesis is based on the convolutive blind source separation technique developed by Negro et al. (2016). Therefore, the following subsections will focus solely on blind source separation methods applied to the HDsEMG signal.

HDsEMG signal acquisition

Reductions in the baseline noise of the HDsEMG signal are paramount for successful and reliable decomposition. Del Vecchio, Holobar et al. (2020) recommend noise levels should be in the order of 10-40 μV RMS to ensure successful decomposition, but this can vary with contraction intensity; at low HDsEMG amplitudes signal noise should be no greater than half of the power of the signal (Del Vecchio, Holobar et al., 2020). A common source of HDsEMG signal noise is the electrode-skin interface, which depends on a number of factors, including the electrode metal and size, but also the condition of the skin (Merletti & Farina, 2016).

Although a number of studies have attempted to investigate the effects of commonly used skin treatments on impedance and noise at the electrode-skin interface, such work has predominantly been carried out on electrocardiography (ECG) electrodes (e.g., Degen & Loeliger, 2007; Grimnes, 1983; Spinelli et al., 2006) and has limited application to HDsEMG recordings. Only one study has looked into effects of skin treatments on the noise and impedance at the electrode-skin interface of surface EMG arrays (Piervirgili et al., 2014). Piervirgili et al. (2014) measured noise and impedance levels at the biceps brachii using a 4 × 1 surface EMG array after the application of three commonly used skin treatments (rubbing with alcohol, rubbing with abrasive paste, and stripping with adhesive tape) with respect to no treatment. The authors concluded that rubbing with abrasive conductive paste was more effective in reducing both impedance and noise compared to no treatment. However, all measurements were performed simultaneously on four portions of the biceps brachii to reduce experimental time and the electrode site was not shaved before treatment, limiting the applicability of the findings to muscles where shaving is often necessary, such as the tibialis anterior (Piervirgili et al., 2014). In addition, the material effect of skin treatment on HDsEMG decomposition outcomes remains to be tested experimentally.

Electronic-amplification noise from equipment can also contaminate the HDsEMG signal (Del Vecchio, Negro et al., 2020), and although a potential solution is to apply ground references directly to equipment, this is rarely reported (e.g., Martinez-Valdes, Guzman-Venegas et al., 2016). Thus, the effect of ground reference configurations on reductions in the HDsEMG signal noise are unclear.

HDsEMG signal processing

Once the HDsEMG signal has been recorded, it is subjected to the decomposition algorithm, which typically estimates one motor unit spike train at a time by iterative optimisation of the motor unit separation filter (Del Vecchio, Holobar et al., 2020). This requires HDsEMG signals of relatively long length, lasting at least 10 s (Negro et al., 2016). The initial decomposition result is then typically assessed against a

normalised reliability index, such as the Silhouette measure (SIL; Negro et al., 2016), or the pulse-to-noise ratio (PNR; Holobar et al., 2014). Once the automatic decomposition is complete the motor unit spike trains are then visually inspected, usually from a raster plot of the discharges (Figure 2.1D).

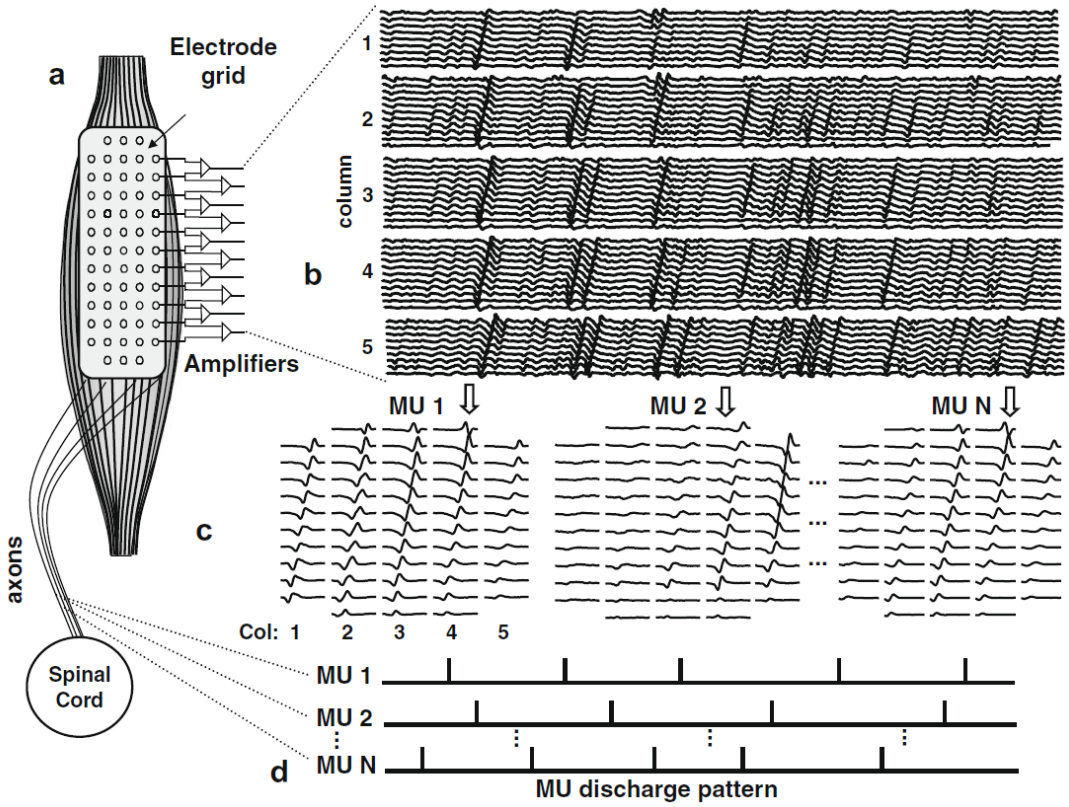

Figure 2.1. *Multichannel HDsEMG decomposition. A) HDsEMG signals are recorded from the muscle using a 13 x 5 electrode grid; B) the HDsEMG signal (500 ms); C) the multichannel action potential profiles for three decomposed motor units; D) the estimated discharge pattern for the three motor units. From Merletti et al. (2008).*

During the visual inspection of motor unit discharge timings, motor units exhibiting interspike intervals (i.e., the duration between consecutive discharge times) outside of a predetermined range can be discarded before further analysis. The coefficient of variation for interspike interval (CoV_{isi}) can also be used as an index of reliability, with only motor unit spike trains displaying CoV_{isi} values below a set threshold accepted for analysis. Reported values for SIL typically range from 0.85 (Afsharipour et al., 2020; Murphy et al., 2019) to 0.90 (Martinez-Valdes, Negro et al., 2020), whereas the PNR is typically set to > 30 dB (e.g., Del Vecchio & Farina, 2019). Likewise, the range in accepted interspike intervals varies considerably between

studies, with excluded durations ranging from discharges separated by < 10 ms (Castronovo et al., 2018) and > 2 s (Del Vecchio, Úbeda, et al., 2018). Similarly, accepted CoV_{isi} values between ≤ 30% (Holobar et al., 2014) and 55% (Almuklass et al., 2018) have been reported. However, despite attempts to provide recommendations on the use of HDsEMG in experimental studies (Del Vecchio, Holobar et al., 2020; Gallina et al., 2022), there are currently no formally agreed standards for decomposition acceptance criteria.

The study of motor unit behaviour using HDsEMG decomposition techniques

During voluntary contractions, the force (or torque) a muscle is able to exert is dependent on the number of activated motor units (recruitment) and the rates at which these motor units discharge (rate coding or modulation; Enoka & Duchateau, 2017). Using HDsEMG decomposition techniques, the spike trains of individual motor units can be identified from the interference signal (Figure 2.1). From these spike trains, the behaviour of individual motor units can be analysed, such as discharge rates, recruitment and de-recruitment thresholds (i.e., the muscle torque at which a motor unit first discharges or last discharges, respectively; Del Vecchio, Holobar et al. 2020).

Common input and torque control

As well as the behaviour of individual motor units, HDsEMG provides an opportunity to study relatively large populations of the motor unit pool, which can provide insights into how the nervous system controls muscle torque (Farina et al., 2016). Broadly, the motor neuron pool receives independent synaptic input (received by individual motor neurons) and common synaptic input (received by all motor neurons) to generate the neural drive to the muscle; motor unit firing behaviour is attributable to the net synaptic input received by the motor neurons (Farina & Negro, 2015). The common input comprises a “control input” necessary for torque control, and a “common noise”, responsible for the oscillations in torque around a target level (Farina & Negro, 2015).

Despite the input-output properties of individual motor units being nonlinear (due to the independent inputs received by each motor neuron), the activation of a large number of motor units partly linearises this transformation and reduces the impact of independent synaptic noise (Farina et al., 2016). The motor neuron pool therefore acts as a filter tuned on common input (Farina & Negro, 2015); the low-pass filtering property of muscle means it is the low-frequency components of the common synaptic input that are responsible for the neural drive to the muscle (Farina et al., 2016; Negro et al., 2009; Figure 2.2). In other words, to effectively regulate torque, the control signal *must* be common to the motor neuron pool (Farina & Negro, 2015).

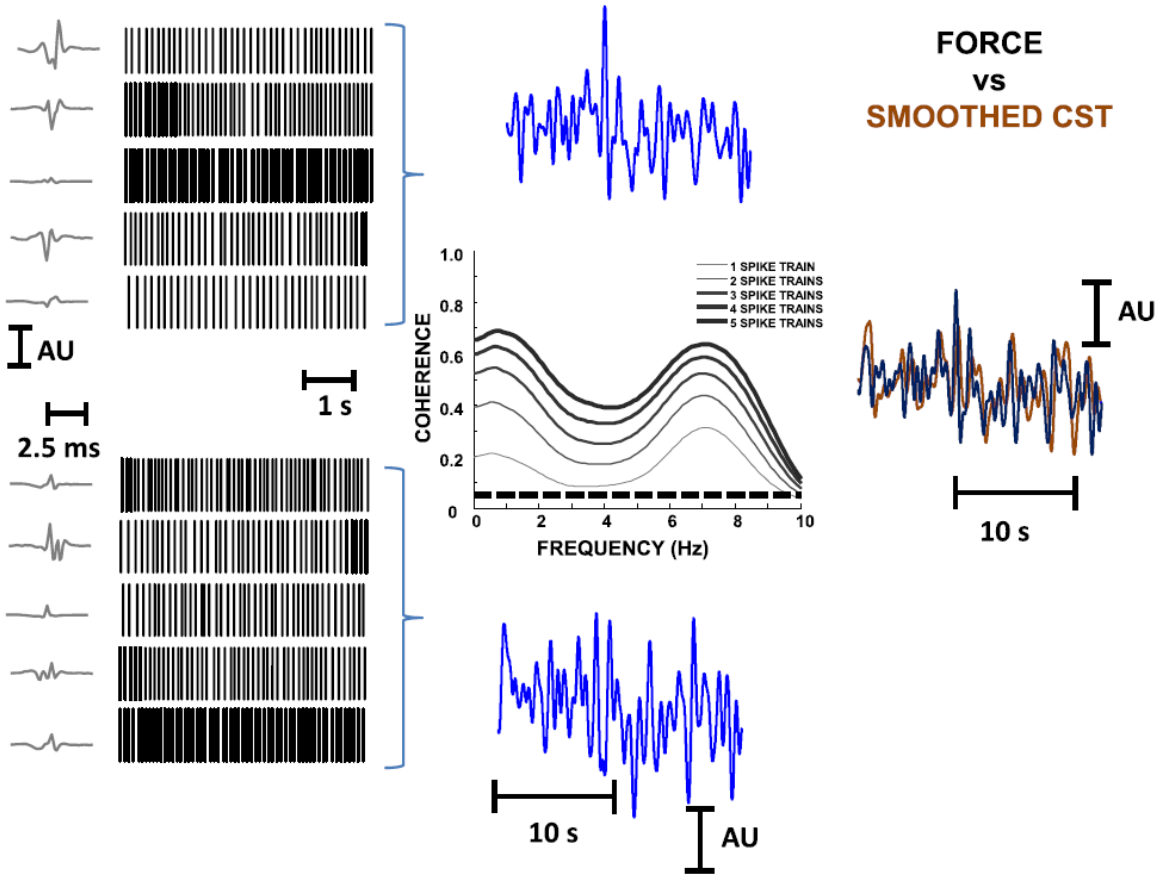

Figure 2.2. *The effective neural drive to the muscle and force from experimental data. Left: raster plots indicating discharge timings for 10 motor units from a 5% maximal voluntary contraction of the abductor digiti minimi muscle. Middle: the spike trains from two sets of five motor units are summed to form cumulative spike trains (CST) and then low-pass filtered in the effective bandwidth for neural drive (< 10 Hz). Right: the low-pass filtered cumulative spike train for all 10 motor units (blue trace) and recorded muscle force (red trace). Note the similarity between the two signals. AU, arbitrary units. From Farina and Negro (2015).*

Because the coherence between common input and the low-frequency (0-10 Hz) content of the cumulative spike train approaches unity when approximately 10 motor units are decomposed, the effective neural drive (control signal) to the muscle can be estimated from the cumulative spike train of decomposed motor units (Farina & Negro, 2015; Farina, Negro et al., 2014; Figure 2.2). It was recently demonstrated by Castronovo et al. (2015) that in response to fatigue, increases in the net excitatory input to the motor neurons results in relative increases in the proportion of common synaptic input compared to the independent synaptic input. At task failure after sustained contractions performed at 20% MVC, there was an increase in coherence values between motor unit spike trains in the low-frequency bands (1-10 Hz; Castronovo et al., 2015). The authors also reported a positive correlation between coherence in the low-frequency bands and force variability, supporting the notion that the force produced by the muscle approximates the low-pass filtered neural drive to the muscle (Figure 2.2). Therefore, the fluctuations in force or torque during isometric contractions are likely explained by the effective neural drive to muscle, which can be investigated by low-pass filtering the cumulative spike train, provided ~10 motor units have been decomposed (Castronovo et al., 2015; Farina & Negro, 2015).

Complexity

The physiological systems of healthy adults involve the interaction of a number of structural components and feedback loops which operate over a large range of temporal and spatial scales (Goldberger, Peng et al., 2002). Consequently, the outputs of healthy physiological systems (e.g., heart rate; Lipsitz & Goldberger, 1992) are characterised by inherently complex fluctuations, even under resting conditions (Goldberger, Amaral et al., 2002). There are a number of related concepts borne from slightly different mathematical approaches that are drawn upon when attempting to quantify the ‘complexity’ of the outputs of physiological systems, and these concepts are outlined below.

Nonlinear dynamics

Linear systems demonstrate proportionality, in the sense that output is proportional to the input, and superposition, in that the individual input-output relationships of the multiple components of a linear system can predict that system’s output (Goldberger, 2006). Overall, the individual components of a linear system are summed to form its behaviour; it is predictable and as expected (Goldberger, 1996; Goldberger, 2006). In contrast, nonlinear systems lack proportionality, and cannot be fully understood by simply “adding up” their individual components (Goldberger, 1996; Peng et al., 2009). In simple terms, "the whole is different to the sum of the parts", an effect described by the term "emergent properties" (Peng et al., 2009). Small changes in nonlinear systems can lead to dramatic, unpredictable results, hindering the ability to predict the long-term behaviour using traditional, linear models (Goldberger, 1996). In the last few decades, the interest in nonlinear systems has been extended to study the extraordinary complexity of physiological systems and, more specifically, the human body.

Fractals

In attempts to quantify and understand the complexity of physiological functions, researchers have also utilised analysis methods based on the concept of fractals (Eke et al., 2002; Lipsitz, 2002). The origins of fractal concepts can be traced back to mathematicians in the late 19th and early 20th century, who generated complex geometrical structures by taking simple objects such as a line, a square, or a cube (termed the initiator), and applying a simple rule of transformation (termed the generator) in an infinite number of iterative steps (Eke et al., 2002). Examples include the von-Koch curve, the Sierpinski gasket, and the Menger sponge, all of which are equally rich in detail at each and every scale of observation, and all of which exhibit self-similarity when smaller pieces of the structure are compared to the whole (Figure 2.3; Eke et al., 2002).

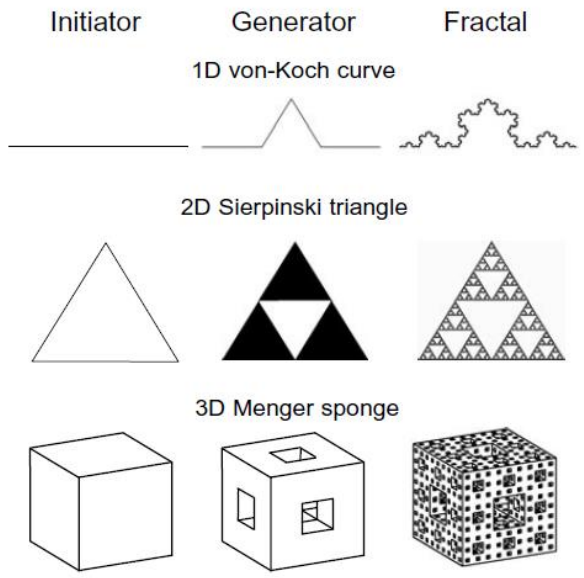

Figure 2.3. *Examples of mathematical fractals: the von-Koch curve, Sierpinski triangle, and Menger sponge. Such structures can be generated by taking a simple object on the largest scale (the initiator) and repetitively applying a single rule of generation (the generator). Only three generations are shown, but complex, self-similar structures are displayed in each case. From Eke et al. (2002).*

Almost 60 years later, Benoit Mandelbrot demonstrated that these geometrical structures actually had many features in common with the complex shapes found in nature (Mandelbrot, 1982; Eke et al., 2002; Peitgen et al., 2004). In doing so,

Mandelbrot (1977) coined the term “fractal” from the Latin verb *frangere*, meaning “to break” into irregular pieces. Fractals were more recently defined as objects composed of subunits and sub-subunits that resemble their larger-scale structures (Goldberger, 1996; Figure 2.4).

The complexity of nature and physiology

Mandelbrot (1967) identified the occurrence of fractals in nature in an attempt to describe the appearance of ever-finer irregular fragments that appear as natural objects and processes are ever-increasingly magnified (Bassingthwaite et al., 1994). In particular, Mandelbrot (1967) highlighted the “statistical self-similarity” of the British coastline (though self-affinity would perhaps be more accurate here, given that the details of the coastline revealed at each scale are not exact copies of one another; Pethick et al., 2021). Using this example, the length of a coastline can be measured using a low-resolution photograph. However, if a bay or peninsula identified on a map is magnified and re-examined, sub-bays and sub-peninsulas become apparent. If this process is repeated, then sub-sub-bays and sub-sub-peninsulas become visible, and so on (Mandelbrot, 1982). Each change in scale adds seemingly infinite new detail, and the measured length of the coastline tends to increase without limit (Mandelbrot, 1967). Many more examples of fractal forms have been observed in nature, including the rough surfaces of mountains, billowing clouds, coral reefs, branching trees, and the Romanesco broccoli (Bradbury & Reichelt, 1982; Glenny et al., 1991; Goldberger, Amaral et al., 2002; Hardstone et al., 2012).

Several complex physiological structures of the human body exhibit fractal-like anatomies (Goldberger, 1996). An object or structure is fractal if the smaller pieces of the object resemble the larger pieces or the object as a whole (Eke et al., 2002). Mathematical fractals such as the von Koch curve are exact fractals, as their smaller pieces are exact rescaled replicas of the whole. In contrast, most natural fractal objects are statistical fractals and as such, their exact self-similar elements cannot be recognised. Their self-similarity is revealed in the power law scaling of the

parameters that characterise their structures at different scales of observation (Eke et al., 2002); such structures can be described as “scale free” (Hardstone et al., 2012). Examples of fractal-like structures in the human body include the bronchial, arterial and venous trees of the lung (Glenny, 2011), the His-Purkinje conduction system (Goldberger et al., 1985), the neurons of the retina (Caserta et al., 1990; Caserta et al., 1995), and other neurons of the central nervous system (Smith et al., 1989). These fractal-like structures all appear to share at least one critical physiological function: instantaneous, efficient transport across complex, spatially distributed networks (Goldberger, Amaral et al., 2002).

As well as scale-free physiological structures, the fractal concept can also be applied to complex physiological processes lacking a single scale of time (Goldberger, Amaral et al., 2002). One such example of a complex physiological process is that of heart rate variability, for which a qualitative understanding of its self-similar nature can be achieved by viewing the original data at different temporal resolutions (Goldberger, 2006). By visually inspecting a healthy individual’s heart rate on the three different timescales outlined in Figure 2.4, the observed irregularity is not distinguishable, but the fluctuations are statistically self-similar (Goldberger, 2006). In addition to heart rate, other physiological processes that display complex fluctuations similar to fractals include ion channel kinetics (Liebovitch et al., 1987), blood pressure (Marsh et al., 1990), gait (Hausdorff et al.,1995), renal blood flow (Wagner & Persson, 1995), respiration (Bruce, 1996), and muscle force/torque output (Slifkin & Newell, 1999).

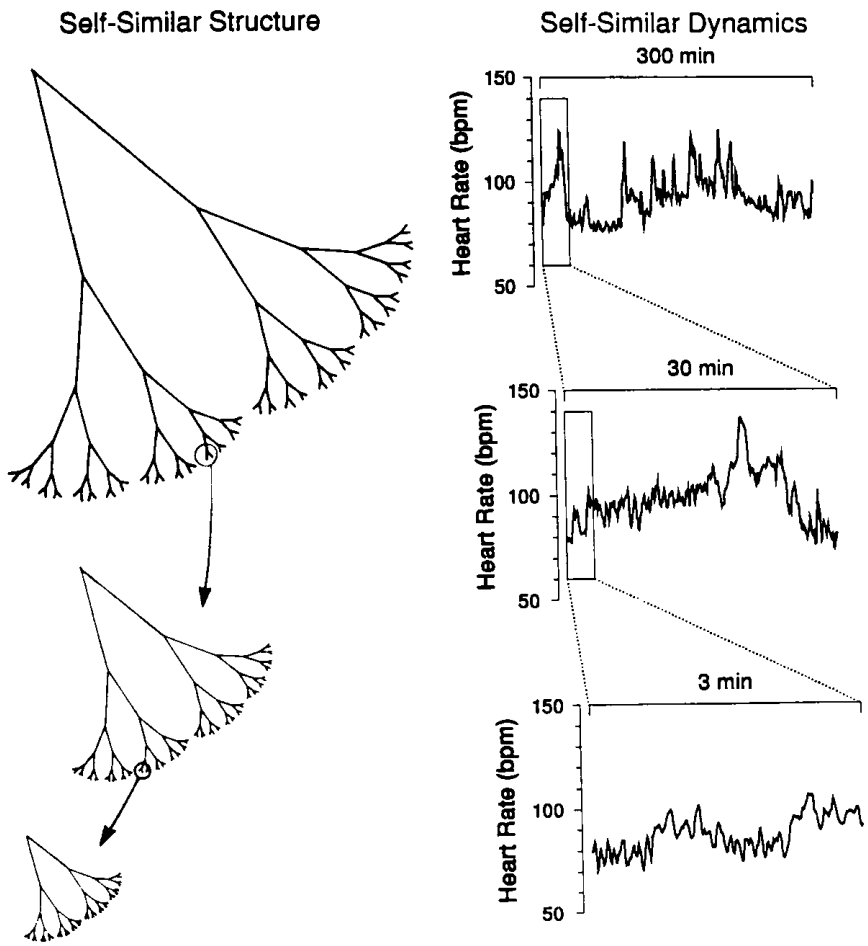

Figure 2.4. *Examples of self-similar structures and self-similar fluctuations. The small-scale structure of the treelike fractal (left) resembles its large-scale form. The fluctuations of a fractal-like process, such as the heart rate of a healthy individual shown on the right, are statistically self-similar on different timescales. From Goldberger (2006).*

Measures of complexity

Even under resting conditions, the outputs of normal physiological systems are inherently complex in nature. Using the example of heart rate, rather than adhering to a regular sinus rhythm, actual measurements reveal fluctuations indicative of fractal scaling (Goldberger, 1992). Fluctuations in the outputs of human physiological systems have traditionally been investigated using measures of magnitude, such as the standard deviation (SD) or coefficient of variation (CV; Rose et al., 2009), and were considered to be uncorrelated random errors or physiological noise (Arsac & Deschodt-Arsac, 2018). However, over the past three decades, the "hidden information" contained within the temporal structure, or complexity, of these

physiological systems has developed into an area of scientific interest (Goldberger, Amaral et al., 2002).

The structure or organisation of the variations in physiological time series can be quantified using measures such as approximate entropy (ApEn; Pincus, 1991), sample entropy (SampEn; Richman & Moorman, 2000), and detrended fluctuation analysis (DFA; Stergiou & Decker, 2011). The regularity of muscle torque output can be determined using ApEn and/or SampEn, and DFA α scaling exponent can provide an estimate of temporal fractal scaling (Peng et al., 1994).

Approximate Entropy

As laid out in the Second Law of Thermodynamics, entropy represents the extent to which nature becomes more disordered or random (Schneider & Kay, 1994), and the entropy of a system tends toward a maximum (Seely & Macklem, 2004). An example of this is given by Seely and Macklem (2004), who describe a smoke ring diffusing into the air as an ordered configuration moving towards a random configuration; the likelihood of this process being spontaneously reversed is so statistically improbable it is all but impossible. Entropy therefore can be seen as a measure of disorder or randomness (Seely & Macklem, 2004).

ApEn can be used in time series analysis to quantify the irregularity or randomness within a system and was introduced by Pincus (1991). Closely related to Kolmogorov-Sinai entropy, which is used as a means of quantifying the rate of new information, ApEn is used to measure the complexity of a physiological signal (Seely & Macklem, 2004; Pincus, 1991). When interpreting ApEn values, smaller values (approaching 0) represent a high degree of regularity, and larger values (approaching 2) represent greater disorder, randomness, or complexity (Seely & Macklem, 2004).

The application of ApEn statistics to the aforementioned physiological time-series data is supported by inherent properties of the method. Pincus (2006) highlighted six such properties: (1) ApEn is nearly always unaffected by noise of a magnitude below a *de facto* specified filter level; (2) ApEn is insensitive to outliers; (3) ApEn has good reproducibility for relatively short time-series (as few as 50 data points, but usually 60 or more; Pincus, 2001); (4) ApEn is finite for stochastic, noisy deterministic and mixed processes (such as biological datasets); (5) an increase in ApEn relates to an increase in the process complexity in the settings of the processes of property 4; and (6) changes in ApEn have been demonstrated to correspond to mechanistic inferences regarding subsystem autonomy, feedback, and coupling in a range of mathematical models (Pincus, 2006).

Sample Entropy

Despite the wide-scale application of ApEn to physiological time-series to estimate system complexity, the approach has been criticised. It was claimed that ApEn statistics can lead to inconsistent results, owing to the bias caused by the ApEn algorithm counting each sequence as matching itself (Richman & Moorman, 2000). This bias was also said to cause a heavy dependence on the record length, leading to uniformly lower than expected values for shorter records (Richman & Moorman, 2000).

To counter the bias of ApEn, Richman and Moorman (2000) developed a new complexity measure, sample entropy (SampEn), that avoids counting self-matches. The authors defined SampEn as being precisely the negative logarithm of the conditional probability that two sequences similar for *m* points remain similar at the next point, while omitting self-matches when calculating the probability (Richman & Moorman, 2000). Other purported benefits of SampEn are the simpler nature of algorithm, resulting in a reduction in calculation time and an improvement in relative consistency compared to ApEn (Richman & Moorman, 2000; Yentes et al., 2013). However, despite SampEn being more consistent for shorter data lengths (particularly ≤200 data points; Yentes et al., 2013), its use for longer data lengths (>

1000 data points) provides no meaningful difference when compared to ApEn. Indeed, Pethick et al. (2015) demonstrated that when more than 5000 data points are used, measures of ApEn and SampEn lead to the same conclusion, and therefore the same interpretation is reached regardless of approach.

Detrended Fluctuation Analysis

Detrended fluctuation analysis (DFA) was initially developed by Peng et al. (1994) to detect long-range correlations in DNA nucleotide sequences but has since been applied to a number of other biological time series data, such as in the evaluation of cardiovascular and respiratory variability (Peng et al., 1995; Seely & Macklem, 2004). In contrast to ApEn and SampEn statistics, which quantify the changing complexity of a signal (Pincus, 1991; Richman & Moorman, 2000), DFA estimates the noise colour and long-range fractal scaling of a signal (Seely & Macklem, 2004).

There are several steps involved in the calculation of DFA, as summarised by Peng et al. (2000): First, the original time series is integrated (Figure 2.5B), before being divided into boxes of equal length, n, to measure the vertical characteristic scale of the integrated time series (Peng et al., 2000). Next, a least squares line (which represents the trend in that box) is fitted to the data for each box of length n (Peng et al., 2000). The integrated time series is then detrended by subtracting the local trend in each box (Figure 2.5C; Peng et al., 2000). For each box of length n, the root mean squared deviation between $y(k)$ and its trend in each box is calculated to give the characteristic size of the fluctuations for this integrated and detrended time series (Goldberger, Amaral et al., 2002; Peng et al., 2000). This process is repeated over all time scales (box sizes) to provide a relationship between $F(n)$ and box size n, with $F(n)$ expected to increase with box size n (Peng et al., 2000). The scaling exponent (self-similarity parameter), α, is determined by the slope of the line relating log $F(n)$ to log n (Goldberger, Amaral et al., 2002; Peng et al., 2000). Figure 2.5 provides a stepwise overview of the calculation of DFA (Hardstone et al., 2012).

The DFA α exponent can be thought of as an indicator of “roughness” of the original time series: larger values represent smoother time series (Peng et al., 2000). Simply put, if $\alpha < 0.5$, the signal is anticorrelated, if $\alpha = 0.5$, there is no correlation, and if $\alpha > 0.5$, there are positive correlations in the signal (Hu et al., 2001). Values observed for physiological signals theoretically range from 0.5 to 1.5 (Seely & Macklem, 2004). Pink (1/*f*-like) noise ($\alpha = 1$) is said to represent healthy function and fractal scaling, or, in other words, a “compromise” between the total unpredictability and very rough “landscape” of white noise ($\alpha = 0.5$), and the far smoother landscape of Brownian noise ($\alpha = 1.5$; Peng et al., 2000).

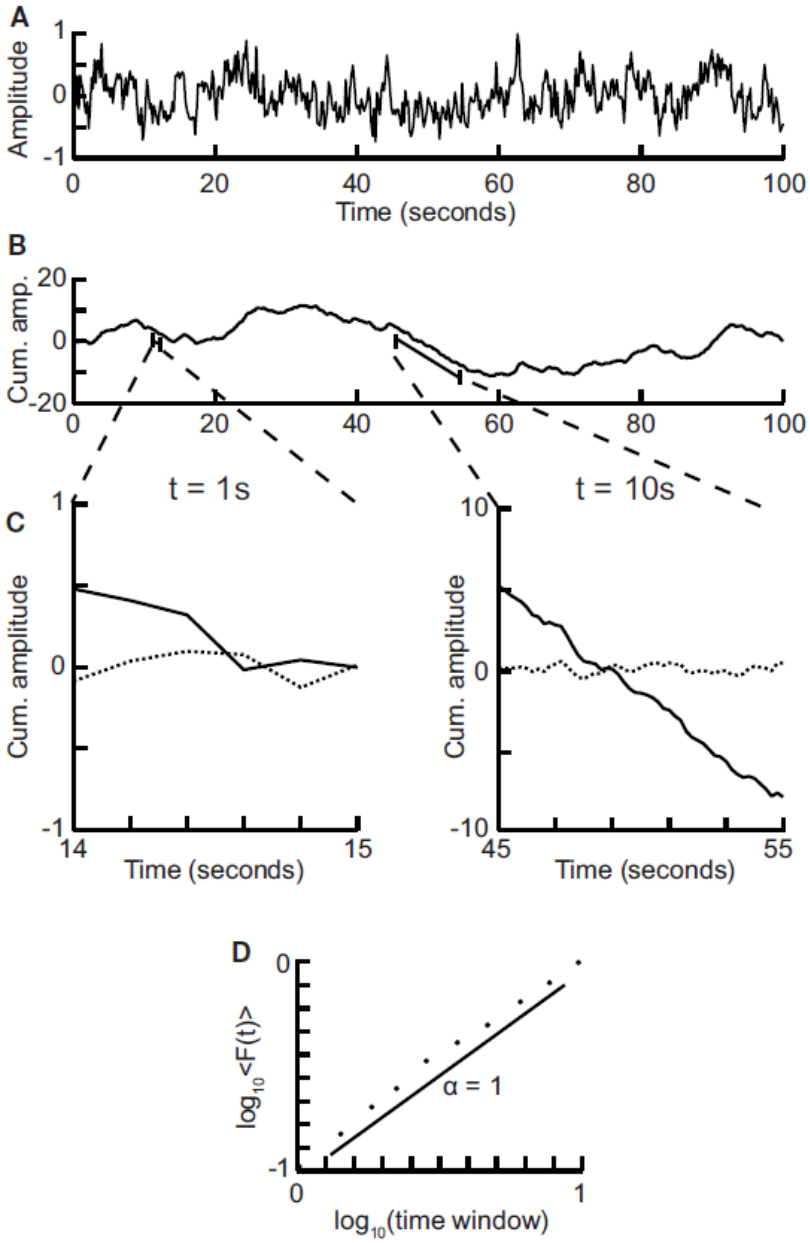

Figure 2.5. *Stepwise overview of Detrended Fluctuation Analysis. (**A**) The original time series, in this case a 1/f signal sampled at 5 Hz lasting 100 s. (**B**) The time series is integrated. (**C**) The linear trend is removed for each box size and the characteristic size of the fluctuations is calculated. The signal is shown as the solid line and the detrended signal is shown as the dotted line. (**D**) The mean fluctuation per box size is plotted against box size on logarithmic axes. The DFA α exponent is determined from the slope of the line (α = 1). From Hardstone et al. (2012).*

Loss of complexity with ageing and disease

First coined by W B Cannon in 1929 (Cannon, 1929), the principle of homeostasis has been one of the overriding theories in the field of physiology ever since (Goldberger, 1991). The concept of homeostasis was originally conceived to describe the automatic adjustments within physiological systems that occur in

response to internal disturbances to prevent wide oscillations and hold internal conditions fairly constant (Cannon, 1929). The conventional view was that homeostasis developed as an evolutionary strategy to ensure that all cellular environments are kept within narrowly defined limits so that cells are able to function without change, therefore allowing the human body to maintain an internal balance (West, 2010). Thus, convention would dictate that for a given physiological measure (e.g. heart rate) a constant, normal value is maintained unless disrupted, before being corrected and returned to its normal steady state value (Goldberger, 1991). However, the recent observation of the fractal dynamics present in the fluctuations of physiological time series has challenged the long-held principles of homeostasis, and new hypotheses have emerged to explain the behaviour of these physiological control systems (West, 2010).

One of the hallmarks of healthy physiological system outputs (such as heart rate, respiration, and muscle torque) is their inherent complexity (Goldberger, Amaral et al., 2002). It has been postulated that the complexity of such outputs reflects the capacity of the system to adapt and function in response to the demands of an ever-changing environment, and that these highly complex systems are the products of a very long evolutionary process (Peng et al., 2009). However, the complexity of these physiological systems appears to degrade in the presence of ageing and disease (Goldberger, Amaral et al., 2002).

A loss of complexity with ageing was first reported by Kaplan et al. (1991), who compared the cardiovascular dynamics of old healthy adults (aged 62-90 years) to those of young healthy adults (aged 21-35 years); a reduction in the complexity (measured using ApEn) of both heart rate and blood pressure variability with ageing was evident. Following the observations of Kaplan et al. (1991) among others, the ‘loss of complexity’ hypothesis was introduced by Lipsitz and Goldberger (1992). The loss of complexity hypothesis describes the observation that ageing is accompanied by a progressive loss of complexity in the dynamics of several physiological outputs including heart rate (Iyengar et al., 1996; Kaplan et al., 1991),

respiratory frequency (Peng et al., 2002), and muscle force/torque (Vaillancourt & Newell, 2003). In short, a loss of complexity is assumed to reflect a loss of system adaptability (Peng et al., 2009), and the loss of complexity hypothesis has since been extended to diseased states (Goldberger, Amaral et al., 2002).

Losses of muscle torque complexity with neuromuscular fatigue

The loss of complexity hypothesis has recently been further extended to the investigation of acute neuromuscular fatigue in healthy adults during isometric contractions (Pethick et al., 2015; Figure 2.6). There is a decrease in the complexity of isometric muscle torque associated with neuromuscular fatigue during intermittent and sustained isometric contractions of both maximal and submaximal intensity (Pethick et al., 2015; Pethick et al., 2019a). In the first of a series of studies, Pethick et al. (2015) investigated the effects of neuromuscular fatigue on knee extensor torque complexity using intermittent maximal and submaximal (40% MVC) contractions. Reductions in the complexity of motor output (quantified using ApEn and SampEn) and increases in the DFA α scaling exponent during both conditions demonstrated that, in addition to the deleterious effects on torque-generating capacity, neuromuscular fatigue also affects the ability of the neuromuscular system to adapt to external perturbations (Pethick et al., 2015).

Given that the submaximal contractions (40% MVC) used by Pethick et al. (2015) were likely performed above the critical torque (~25-35% MVC in the knee extensors; Burnley, 2009), Pethick et al. (2016) then investigated the complexity response to intermittent exercise performed above and below the critical torque. As discussed later in this chapter, the critical torque represents a neuromuscular fatigue threshold, and both neuromuscular and peripheral fatigue develop considerably faster during exercise performed above the critical torque than during exercise below the critical torque (Burnley et al., 2012). Reductions in muscle torque complexity were evident only during contractions performed above the critical torque, suggesting a progressive loss of neuromuscular system adaptability when exercise is performed in the severe domain (Pethick et al., 2016).

A link between the metabolic rate of a system and its output complexity had previously been hypothesised by Seely and Macklem (2012), and muscle metabolic rate (mVO_2) is known to rise inexorably only at intensities above the critical torque or power (Poole et al., 2016). The similarity of the muscle torque complexity response to the mVO_2 response (and other metrics, such as neuromuscular and respiratory perturbations) occurring above the critical torque indicated a possible causal relationship between peripheral fatigue and motor control (Pethick et al., 2016). Indeed, Pethick et al. (2018b) subsequently demonstrated that circulatory occlusion in combination with pre-existing fatigue prevents the recovery of muscle torque complexity. The detrimental impact of circulatory occlusion on recovery gives further credence to the idea that peripheral fatigue is a major factor in the loss of torque complexity during exercise performed above the critical torque. However, the suggestion that this neuromuscular fatigue-induced reduction in muscle torque complexity was mediated solely by peripheral factors was challenged by the observation that knee extensor voluntary activation and the average rectified EMG of the vastus lateralis both failed to recover after circulatory occlusion (Pethick et al., 2018b). Therefore, it is reasonable to conclude that the neuromuscular fatigue-induced reduction in muscle torque complexity is a response to a combination of central and peripheral processes (Pethick et al., 2021).

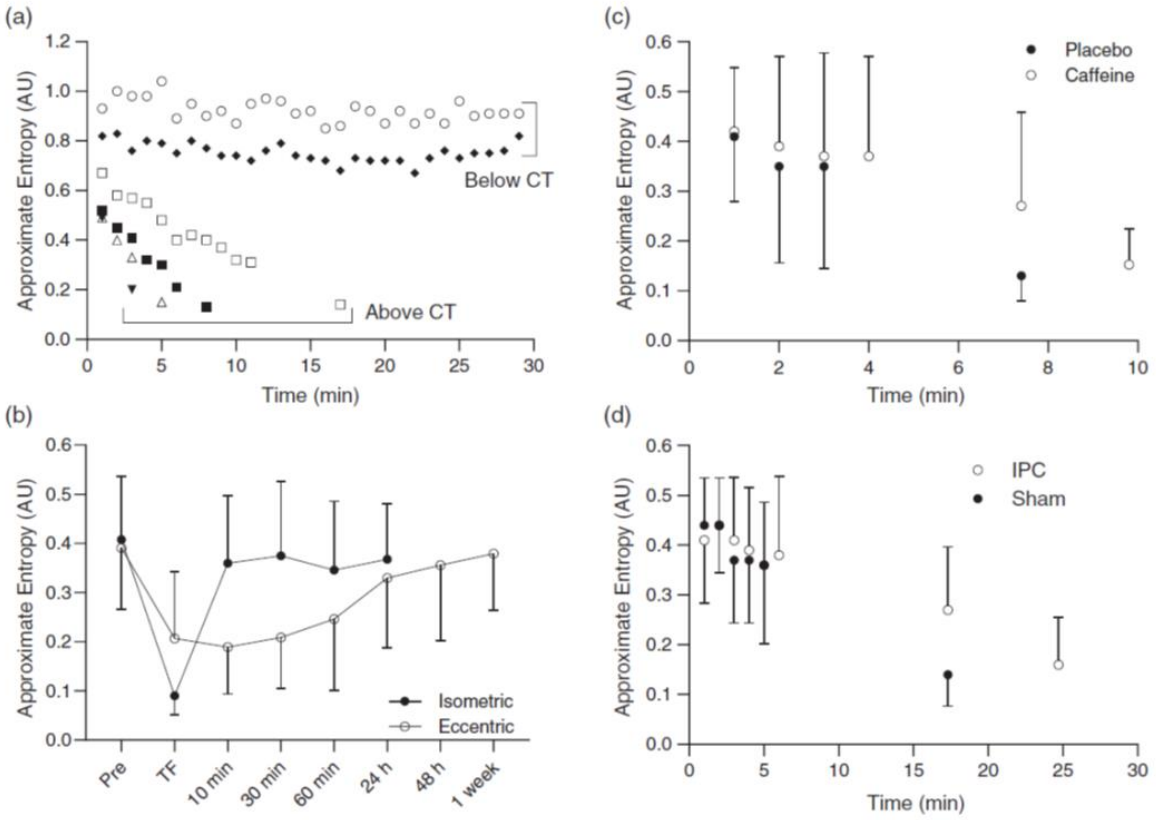

Figure 2.6. *The effect of neuromuscular fatigue on knee extensor muscle torque complexity. (a) Fatigue-induced losses in torque complexity are only evident at contraction intensities above the critical torque (Pethick et al., 2016). (b) Torque complexity was depressed for more than 60 min following eccentric contractions, whereas torque complexity recovered within 10 min following isometric contractions (Pethick, Whiteaway et al., 2019). (c) Caffeine ingestion resulted in elevated torque complexity at task failure when compared to placebo (Pethick et al., 2018b). (d) Losses in torque complexity with fatigue were blunted using ischaemic preconditioning (Pethick, Casselton et al., 2021). From Pethick et al. (2021).*

The neuromuscular fatigue-induced loss of muscle torque complexity can be manipulated using certain interventions and the administration of ergogenic aids. The administration of caffeine (6 mg·kg^{-1} body mass) before fatiguing knee extensor contractions resulted in a slowing of the loss of torque complexity, as well an increase in the time to task failure (Pethick et al., 2018a), when compared to ingestion of a placebo (all-purpose flour). In addition, caffeine ingestion also slowed the rate of decrease in MVC torque and voluntary activation, suggesting that participants maintained a reserve of maximal torque generating capacity at isotime. Interestingly, no differences were observed in the decrease in potentiated doublet torque (a measure of peripheral fatigue) at isotime between conditions, indicating that the caffeine mediated effects on torque complexity were primarily associated

with central mechanisms (Pethick et al., 2018a). At physiological doses, caffeine predominantly acts as a non-competitive adenosine receptor antagonist and exerts several effects on central nervous system function. One such effect is increased α-motor neuron excitability (Walton et al., 2003), which may be explained by increased facilitation of plateau potentials (facilitated by serotonin and noradrenaline) after caffeine ingestion, known to increase the excitability of the membrane (Walton et al., 2002).

Similar findings were reported after the use of repeated cycles of brief ischemia followed by reperfusion (an intervention otherwise known as ischemic pre-conditioning; Pethick, Casselton et al., 2021). As well as a slowing in the loss of muscle torque complexity, ischemic pre-conditioning also attenuated the rates of increase in EMG amplitude and muscle oxygen consumption, indicative of a slowing of the fatigue-induced increase in common synaptic input. The mechanisms that contribute to the ergogenic effects of ischemic pre-conditioning on torque complexity were therefore suggested to be of neural, rather than peripheral, origin.

The addition of a cognitive load (a self-regulated mathematical task) has also been shown to lead to reductions in muscle force complexity during the beginning and middle of a submaximal isometric contraction in the elbow flexors (50% MVC) performed until task failure (Cruz-Montecinos et al., 2018). Interestingly, the time to task failure was greater when exercise was performed with the additional cognitive load, implying that maintaining higher force complexity incurs a significant cost for the neuromuscular system. However, the findings of Cruz-Montecinos et al. (2018) were in sedentary males, and it remains to be seen whether similar findings are replicated in active, healthy participants.

Complexity of the electromyogram

The first application of complexity statistics to the surface EMG demonstrated that the fractal dimension of the interference pattern increased in line with contraction

intensity, indicative of greater complexity at higher force levels (Gitter & Czerniecki, 1995). As previously highlighted, a plausible explanation for the more recently described losses in muscle torque complexity is a fatigue-induced reduction in the ability of the output to the motor unit pool to adapt in response to external perturbations (Pethick et al., 2015). However, attempts to investigate whether such changes occur using bipolar surface EMG during fatiguing maximal or submaximal isometric contractions performed until task failure have thus far yielded equivocal results.

Cashaback et al. (2013) observed a loss in the complexity (quantified using multiscale entropy) of the biceps brachii surface EMG signal during the final third of a sustained isometric elbow flexion trial. It was concluded that neuromuscular fatigue compromised the fast-acting regulatory mechanisms of muscular force control, resulting in a reduction in complexity. The authors suggested that the observed reduction in complexity may have been caused by impaired peripheral factors (including decreases in both motor unit action potential velocity and amplitude), as well as reductions in motor unit discharge rates and altered recruitment strategies (Cashaback et al., 2013). Similar findings were reported by Hernandez and Camic (2019), who demonstrated fatigue-induced losses of vastus lateralis surface EMG complexity (measured using SampEn and DFA α) after the performance of 30 MVCs interspersed with 3 s rest. The magnitude of this fatigue-induced loss of complexity was also dependent on the contraction type used; greater losses were evident after both concentric and isometric compared to eccentric contractions, further supporting the notion that the mechanisms responsible for losses in surface EMG complexity are, at least in part, of peripheral origin (Hernandez & Camic, 2019).

Changes in surface EMG complexity have also been reported during dynamic exercise, namely cycling. Enders et al. (2015) demonstrated changes in the regularity of short-term fluctuations of the surface EMG using entropic half-life (a complexity metric derived from SampEn). Higher entropic half-life, and therefore a

more regular signal, was observed with increased power output demands during cycling, which led the authors to conclude that a more constrained “solution space” allows for less randomness in the execution of a movement task. In other words, a reduced solution space translates to a reduction in available “solutions” for the neuromuscular system to complete the task successfully (similar to the previously discussed loss of system adaptability; Pethick et al., 2015). The observation that complexity reduces with increased power output demands aligns with the decreases in torque complexity observed in the presence of neuromuscular fatigue, where the relative task demands are higher when compared to exercise without (or in the ‘fresh’ muscle; Pethick et al., 2015).

At odds with the studies discussed above, Pethick et al. (2019a) failed to observe a decrease in the complexity or fractal scaling of the vastus lateralis surface EMG signal during either maximal or submaximal knee extensor contractions. Though this contrast in findings could be attributed to methodological differences, it is more likely a reflection of the limited sensitivity of bipolar surface EMG to detect subtle changes in motor unit behaviour. The bipolar surface EMG provides only a crude estimate of the neural drive to the active muscle (Farina, Merletti et al., 2014), therefore its use cannot *confirm* any potential link between muscle torque complexity and motor unit behaviour. In contrast, the use of multiple electrodes in one- (linear) or two-dimensional (high-density surface EMG; HDsEMG) arrays allows for the identification of the conduction velocity and/or discharge timings of individual motor units. Several studies have attributed fatigue-induced reductions in the complexity of global HDsEMG measures (assessed using fractal dimension) to increases in motor unit synchronisation (Mesin et al., 2016; Beretta-Piccoli et al., 2015; Boccia et al., 2016), but the complexity of individual motor unit behaviour has received less attention.

Using fine-wire electrode recordings of the first dorsal interosseus muscle, Jordan et al. (2013) investigated the complexity of single motor unit discharge timings during a force-matching task with varying levels of visual feedback gain. They

observed more random discharge times for both old and young adults when provided with large amounts of visual feedback (high gain), mainly driven by a decrease in discharge regularity at the highest gains in the old adults. Further analysis demonstrated that the main effect of gain on discharge regularity was driven by a difference between the no-vision condition and the two highest gain trials, and led the authors to conclude that both age and visual feedback effect the regularity of motor unit discharge timings. At odds with the findings of Jordan et al. (2013), Chen et al. (2017) observed lower short-time multi-scale entropy values in older adults when exposed to high-frequency error amplification during a low-intensity (20% MVC) force-matching task, a finding not apparent in young adults, and in line with the loss of complexity with ageing hypothesis (Lipsitz & Goldberger, 1992).

In a computer simulation study, Dideriksen et al. (2022) investigated the correlation between ApEn of the synaptic input to the motor neuron pool, the neural drive to muscle (the cumulative spike train), and the force output. Their conclusions were threefold. First, the degree to which the ApEn of muscle force reflects the motor ApEn of the control signal is lower in the presence of high levels of synaptic noise or low magnitudes of the variability in the descending command signal. Second, the greater the number of motor units recruited during a contraction, the smaller the influence of synaptic (or independent) noise and the lower the ApEn of the resultant muscle force. Third, the contractile properties of the motor units decrease the signal bandwidth, an important determinant of the muscle force ApEn. The authors recommended that to reliably estimate the complexity of the control signal to muscles, the analysis should be applied to the cumulative spike train rather than to the force signal Dideriksen et al. (2022). However, the complexity response of the motor unit cumulative spike train during fatiguing exercise is yet to be investigated experimentally. The use of HDsEMG is required to establish whether the previously suggested changes in motor unit behaviour occur concomitantly with changes in muscle torque complexity, and this will be investigated in Chapter 5.

Critical Power

Historical foundations of the critical power model

Human history has been shaped by the constraints of the power-duration (or speed-duration) relationship outlined in Figure 2.7. Over thousands of years, the critical power and *W'* parameters have bound the performances of soldiers, craftsmen, and athletes moving across land, through water, and, more recently, even in human-powered flight (Jones et al., 2010). Moreover, the centuries-long dominance of the Roman military across Europe and further afield was likely due, at least in part, to the marching guidelines for Legionaries, fascinatingly preserved in the writings of Vegetius:

"For nothing should be maintained more on the march or in battle, than that all soldiers should keep ranks as they move." (Milner, 1996).

Whipp et al. (1996; 1998) calculated that to march for several hours at the "military step" (2.85 mph, 4.6 $km \cdot h^{-1}$) whilst carrying armour, weapons, and rations equivalent to 43.25 lb (19.6 kg), a sustained metabolic demand of between 1.4 and 1.7 L of $O_2 \cdot min^{-1}$ would be required. Since failure to maintain the required marching pace was punishable by death, it can be assumed that the laden "military step" was set below the critical speed/velocity for even the most poorly accomplished Legionaries (Whipp et al., 1996; Whipp et al., 1998).

In more recent times, the hyperbolic relationship between power output and the time to task failure was first identified by the British physiologist A. V. Hill in the 1920s. Hill and Lupton (1923) observed a strong relationship between the "maximum duration of an effort" and the intensity of that effort. Hill subsequently plotted the average speed against time for world record performances of that era in both men's and women's running and swimming events (as well as men's cycling and rowing) over various distances and observed a hyperbolic relationship in each case (Hill, 1925; Figure 2.7A). It is interesting to note that this relationship remains true when current-day world records of running events lasting between ~2 min and 15-20 min are used (Jones et al., 2019; Figure 2.7B).

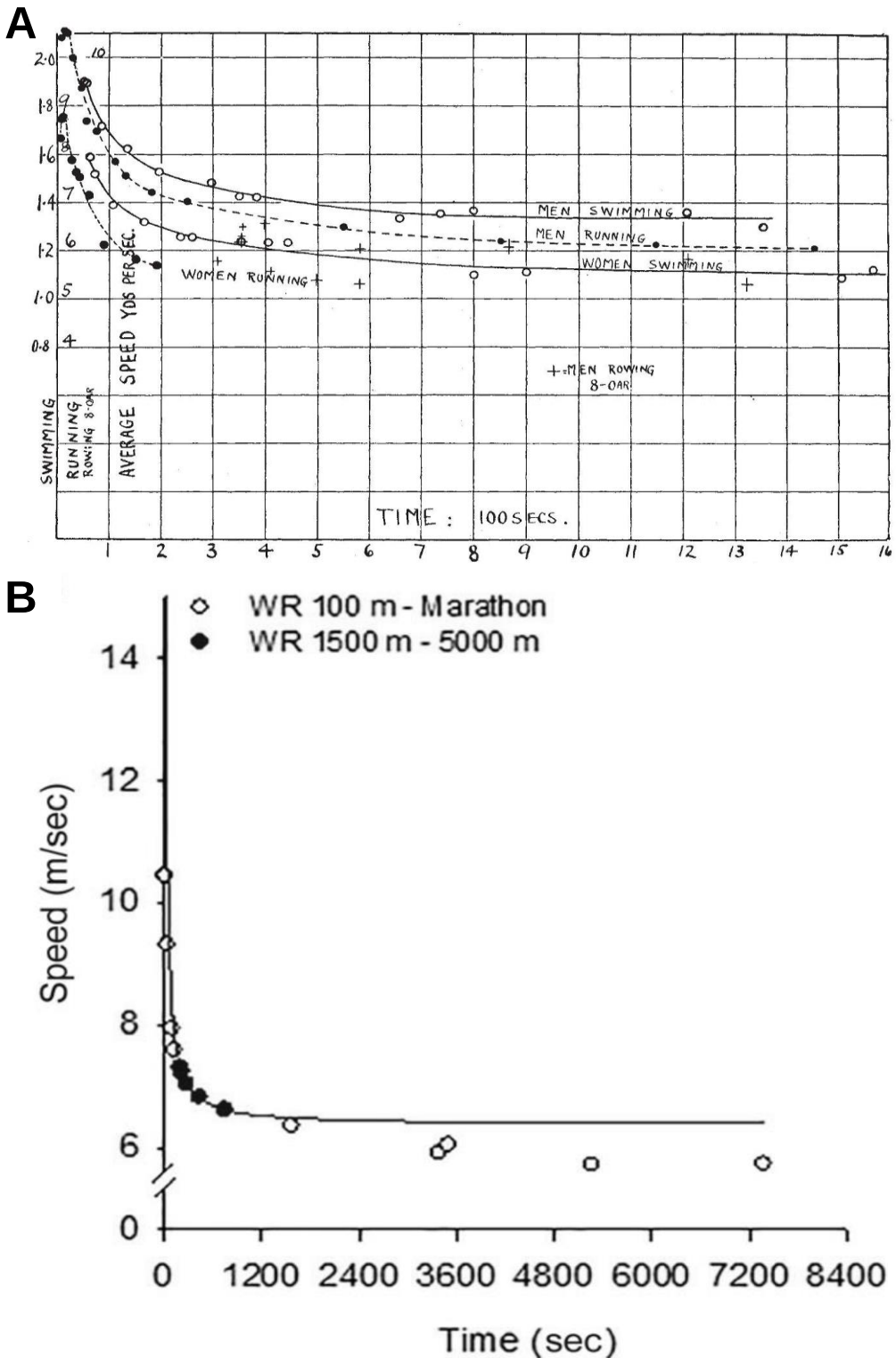

Figure 2.7. *(**A**) Average speed in yards per second plotted against time in seconds for world record running and swimming events up to 1925. The scale for swimming is five times greater than that for running. From Hill, (1925). (**B**) The hyperbolic running speed-time relationship plotted for world record performances from 1500 m to 5000 m as of March 2019. Note the lack of good fit for events over shorter or longer distances. From Jones et al. (2019).*

Rohmert (1960) was the first to identify the hyperbolic force-duration relationship in his investigation into “static work” in the industrial workplace when plotting the maximum hold time against the percentage of maximum force of a muscle group. Hold time was demonstrated to be “theoretically infinite” at or below ~15% MVC in muscle groups of the arm, trunk, and leg (Rohmert, 1960). Rohmert’s findings seemingly provided inspiration for the work of Monod and Scherrer (1965), who originally defined the critical power of a muscle or a muscular group as “the maximum rate it can keep up for a very long time without fatigue”. In doing so, Monod and Scherrer (1965) provided the basis for the current understanding of the critical power concept.

Current definition of the critical power model

Monod and Scherrer plotted “limit work” (or total work done; W) against “limit time” (time-to-task-failure; $Tlim$) for three or four independent dynamic and isometric exercise bouts at different force values. In doing so, they were able to outline two parameters, the critical power (*CP*) and a limited “energy reserve” of work performable above the critical power (now known as *W’*; W prime). An intercept corresponding to *W’* was returned using linear regression, and the slope of the parallel line displaced downward to project from the origin gave the *CP* (Jones et al., 2010; Figure 2.8B). This hyperbolic relationship was expressed as follows:

$Tlim = W' / (P - CP)$ *Equation 1*

which can be expressed in its mathematically equivalent linear form:

$W = W' + CP \times Tlim$ *Equation 2*

Alternatively, power can be plotted against the inverse of time (1/time) to extract the critical power and *W’* parameters (Whipp et al., 1982; Figure 2.8C):

$P = \frac{W'}{t} + CP$ *Equation 3*

Mathematically, the critical power is simply defined as the asymptote of the power-duration relationship (Figure 2.8A; Jones et al., 2010). However, the mathematical modelling of the critical power or torque presents some inherent issues. As with most measures of performance, the critical power and time to task failure are naturally associated with some margin of error (quantifiable using 95% confidence intervals [CIs]; Jones et al., 2019), in addition to the influence of day-to-day biological variability (Jones et al., 2019; Poole et al., 1988). The confidence limits associated with the point estimate of the critical power or torque have been reported to be at least 5-10% of the respective critical power or torque value at best (Smith & Hill, 1993; Burnley et al., 2012; Black et al., 2017; Mitchell et al., 2018).

Studies performed at the critical power have resulted in reports of both steady state (Poole et al., 1988) and non-steady state (Jenkins & Quigley, 1990; Brickley et al., 2002; Pringle & Jones, 2002) responses, indicative of exercise performed in the heavy-intensity and severe-intensity domains, respectively. To avoid such equivocal responses, researchers using the critical power or torque parameters typically set the exercise intensity above or below the aforementioned confidence intervals (Pethick et al., 2020). Recently, Pethick et al. (2020) investigated this 'grey area' during intermittent isometric knee extensor exercise. They reported that exercise performed above the critical torque, but within the confidence limits of the critical torque parameter estimate (+2 CIs = ~107% CT) resulted in heavy-domain responses (including muscle $\dot{V}O_2$, surface EMG amplitude, and torque complexity). Therefore, rather than a sudden threshold, the critical torque represents a continuous phase transition between the heavy and severe-intensity exercise domains (Pethick et al., 2020).

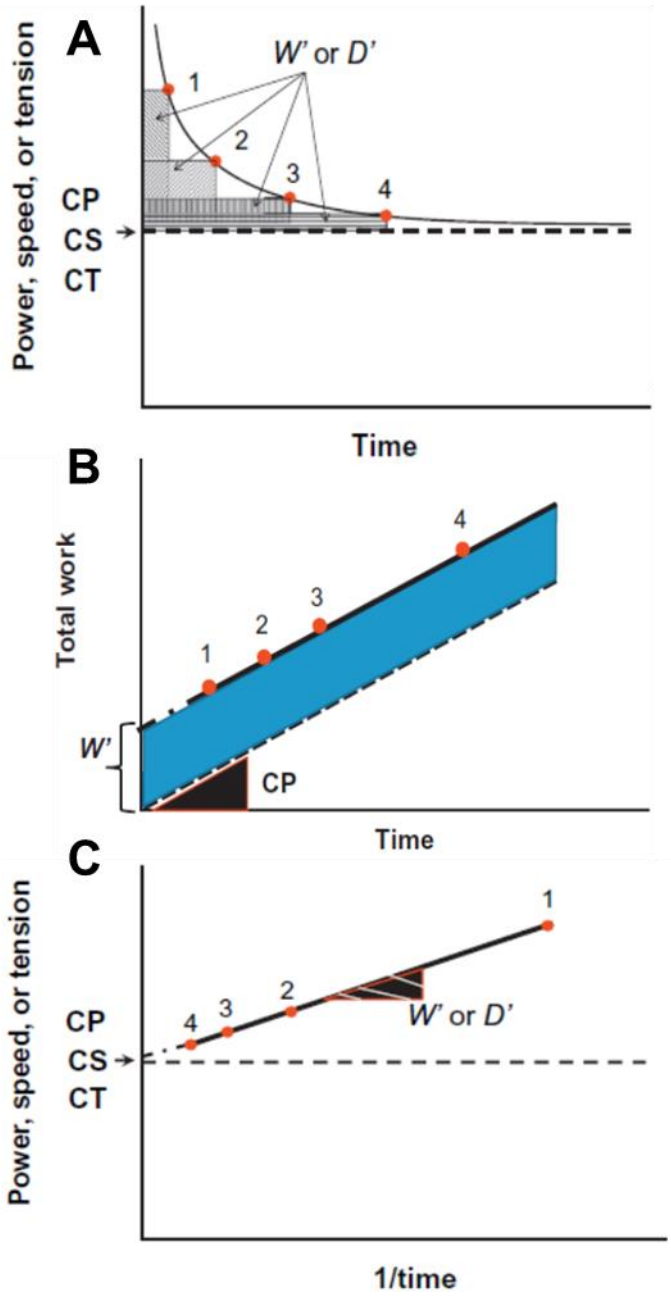

Figure 2.8. *(A) Hyperbolic model of CP. (B) Linear work-time model of CP. (C) The alternative approach to extracting CP and W' proposed by Whipp et al. (1982). The hyperbolic relationship shown above can be linearized by plotting power against 1/time. The parameters CP and W' are given by the Y-intercept and the slope of the line, respectively. From Craig et al. (2019).*

Physiological determinants of the critical power

The observation that intermittent contractions resulted in a greater time to task failure when compared to continuous isometric contractions led Monod and Scherrer (1965) to postulate that the critical power, but not *W'*, was strongly dependent on

blood flow, and thus oxygen delivery, to the working muscle(s). Subsequent research has confirmed this assumption, and it is now accepted that the critical power is determined by oxidative function (Jones et al., 2010). In their attempts to outline the relationship between the critical power and other markers of aerobic function, different research groups incorrectly estimated the critical power to be equal to $\dot{V}O_{2max}$ (Wilkie, 1980) or the previously termed anaerobic threshold, now known as the lactate threshold (LT) or gas exchange threshold (Moritani et al., 1981).

The critical power has since been described as representing the highest sustainable rate of oxidative metabolism, occurring at a similar power output to that of the maximal lactate steady state (MLSS), with the two indices commonly thought to be synonymous (Jones et al., 2019; Poole et al., 1988). However, the MLSS does not correspond to a complete physiological steady state (Baron et al., 2003), and it was later reported that the critical power consistently occurred at a higher power output than that of the MLSS (~7% on average; Dekerle et al., 2003; Dekerle et al., 2005; Jones et al., 2019; Pringle & Jones, 2002). Subsequent studies would go on to define the critical power as a distinct parameter between the gas exchange threshold and $\dot{V}O_{2max}$, and it is now thought to delimit the boundary between the heavy and severe-intensity exercise domains, therefore representing the genuine demarcator of the maximal *metabolic* steady state (Craig et al., 2019; Jones et al., 2019; Figure 2.9). The exact position of the critical power in relation to LT and $\dot{V}O_{2max}$ depends on the training and health status of the individual, but the critical power *always* occurs at a higher $\dot{V}O_2$ than LT (Craig et al., 2019; Figure 2.9A). In extremely well-trained individuals, an upward compression in the LT-$\dot{V}O_{2max}$ range is typically observed; LT and the critical power lie in closer proximity when compared to non-trained individuals (Jones & Poole, 2009; Poole et al., 1990). In contrast, a downward compression in this range (likely caused by a reduction in $\dot{V}O_{2max}$) is reported in those with chronic disease, such as chronic obstructive pulmonary disease (Neder et al., 2000).

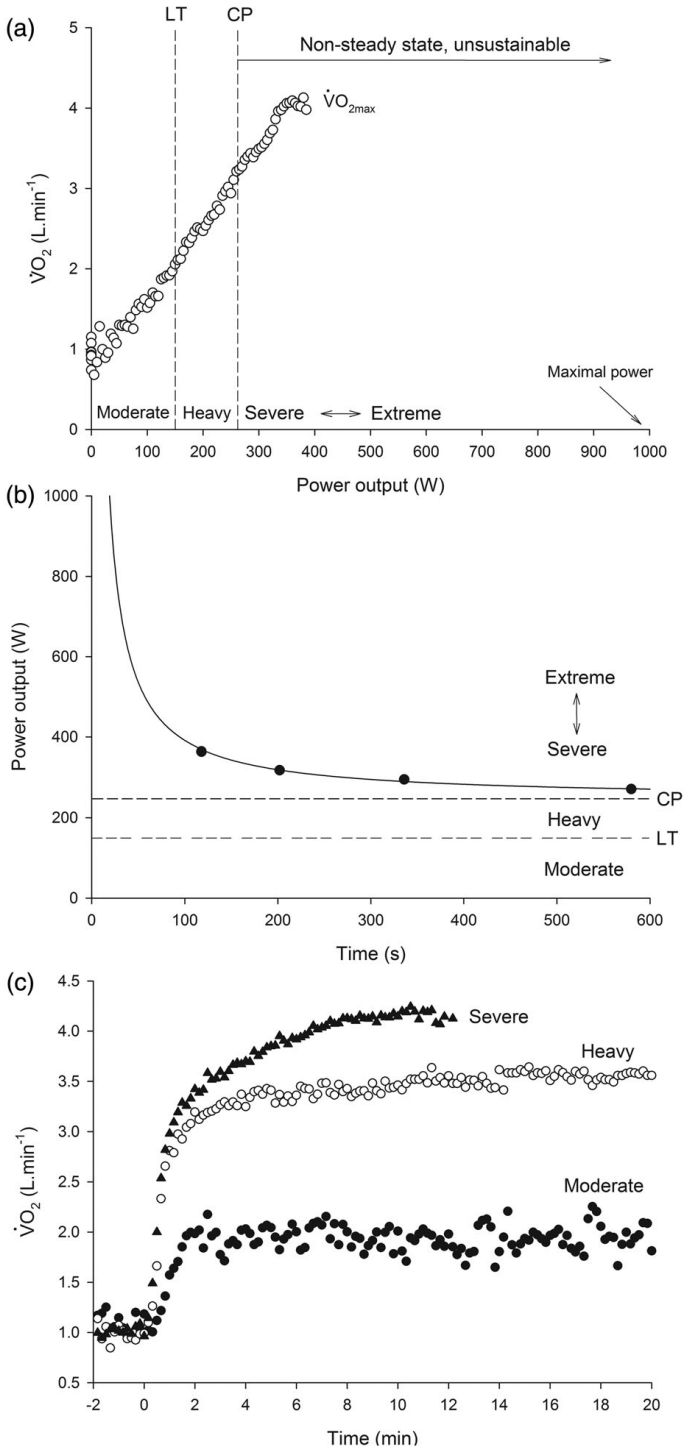

Figure 2.9. *Exercise intensity domains. a) The $\dot{V}O_2$ response to incremental exercise; b) Schematic representation of the power-duration relationship with reference to the moderate, heavy, severe, and extreme-intensity exercise domains; c) The $\dot{V}O_2$ response to constant-load cycling exercise performed in the moderate, heavy, and severe-intensity exercise domains. From Burnley and Jones (2016).*

In their original outlining of the critical power concept, Monod and Scherrer (1965) erroneously stated that “when the imposed power is inferior or equal to the critical

power, it is evident… that exhaustion cannot occur." Whilst the view that exercise performed at the critical power should be limitless is mathematically justifiable, in practice, exercise at this intensity is unlikely to be sustained beyond ~30 min (Brickley et al., 2002). Hence, the critical power represents the lower limit of the applicable range of the critical power concept and accordingly, the concept is not able to predict the tolerable limit of exercise below this work intensity (Jones et al., 2019; Vanhatalo, Jones et al., 2011).

Physiological determinants of W'

The curvature constant parameter, *W'*, represents a maximum amount of work that can be performed to task failure above the critical power (in the severe intensity domain), irrespective of the selected work rate above the critical power (Figure 2.8A; Jones et al., 2010). In comparison to the critical power, the physiological determinants of *W'* are less clear. Historically, *W'* was defined as a fixed anaerobic energy reserve (Monod & Scherrer, 1965), which is in line with the positive correlation between muscle cross-sectional area of the thigh and *W'* reported for cycling ergometer exercise (Miura et al., 2002). *W'* is now thought to be related to the accumulation of metabolites associated with the fatigue process (including H^+ and P_i) and a decrease in intracellular pH (Fitts, 1994; Jones et al., 2008), as well as reductions in intramuscular PCr and glycogen (Miura et al., 1999; Miura et al., 2000).

More recently, *W'* has been shown to be tightly coupled with the development of the $\dot{V}O_2$ slow component during severe-intensity cycle ergometer exercise, in which the increase in $\dot{V}O_2$ is curtailed at the $\dot{V}O_{2max}$ (Murgatroyd et al., 2011; Vanhatalo, Poole et al., 2011). This tight coupling of *W'* with the $\dot{V}O_2$ slow component, in concert with the sensitivity of *W'* to manipulation of O_2 delivery (Vanhatalo et al., 2010), highlights the argument that viewing the critical power and *W'* as aerobic and anaerobic parameters, respectively, is too simplistic; both exist as entities in an "integrated bioenergetic system" (Jones et al., 2010; Poole et al., 2016).

Application of the critical power model to different exercise modalities and species

First reported by Monod and Scherrer (1965) in a single exercising muscle group and later extended to cycling by Moritani et al (1981), the robustness of the critical power concept has been demonstrated by its applicability in describing exercise tolerance across a wide array of exercise modalities. This includes both isotonic (Jones et al., 2008) and isometric (Burnley et al., 2012) muscle contraction protocols, running (Hughson et al., 1984), swimming (Wakayoshi et al., 1992), kayaking (Clingeleffer et al., 1994), wheelchair propulsion (Arabi et al., 1999), rowing (Hill et al., 2003), and weightlifting (Morton et al., 2014). The broad applicability of the power-duration relationship has also been demonstrated in different participant populations (from those with chronic cardiorespiratory disease through to highly-trained endurance athletes, and from young through to elderly individuals; e.g., Jenkins & Quigley, 1990; Neder et al., 2000). In addition to human studies, the power-duration relationship has also been shown to characterise locomotory exercise tolerance across a range of different species including ghost crabs (Full & Herreid, 1983), lungless salamanders (Full, 1986), horses (Lauderdale & Hinchcliff, 1999), mice (Billat et al., 2005), and rats (Copp et al., 2010).

Critical torque during investigations of single muscles/muscle groups

As previously discussed, the power-duration relationship is universally applicable to muscular exercise in humans, and isometric contractions present a powerful means of studying the mechanisms of neuromuscular fatigue, particularly in isolated muscle groups (Craig et al., 2019). The characteristic hyperbolic force/torque-duration relationship, first identified in the arm, leg, and trunk muscles by Rohmert (1965) and then by Monod & Scherrer (1965) was also observed during sustained isometric contractions of the elbow flexors (Hagberg, 1981), and subsequently during intermittent diaphragmatic contractions (Bellemare & Grassino, 1982). The above findings supported the theory that the mechanisms of fatigue are likely consistent during “high-intensity” contractions (i.e., above critical power) and consequently, time to task failure is highly predictable at such intensities (Craig et al., 2019).

The manipulation of pedal frequency in cycling studies can affect estimations of critical power, with lower values reported for faster pedalling frequencies compared to slower pedalling frequencies (Barker et al., 2006). Likewise, manipulation of the analogue to pedalling frequency during studies of isometric contractions, the contraction duty factor, affects the resulting critical torque. For example, during sustained isometric contractions, equivalent to a duty factor of 1, critical torque values of ~15% are typically reported (Rohmert, 1960; Monod & Scherrer, 1965). By comparison, reducing the duty factor to 0.6, the critical torque increases to ~30% MVC (Burnley, 2009; Burnley et al., 2012), and a duty factor of 0.5 results in a critical torque of 40% MVC (Monod & Scherrer, 1965). It is important to note that factors such as muscle architecture will likely affect the absolute critical torque values for different muscle groups (Craig et al., 2019).

Despite the hyperbolic relationship between torque (or force) and time to task failure, the critical torque is rarely used to set exercise intensity during studies of muscle fatigue (Burnley, 2009). This is perhaps due to the considerable time burden for investigators and participants alike during the repeated exhaustive exercise trials that are needed if using the conventional method to establish critical torque (discussed below). In experimental designs investigating the fatigue response to exercise in single muscle groups, the intensity of exercise is commonly prescribed using submaximal isometric contractions performed to task-failure at a % of an individual's MVC. However, this runs the risk of some participants exercising below their respective critical torque. For example, Saugen et al. (1997) examined the muscle metabolic responses to intermittent knee extensor isometric exercise performed in a magnetic resonance spectrometer at 40% MVC using a duty factor of 0.6. Despite most participants exhibiting the expected limited time to task failure and non-steady state muscle metabolic profiles for exercise performed above the critical torque (Jones et al., 2008), at least two participants displayed markedly smaller reductions in muscle pH and PCr in addition to extended times to task failure (Saugen et al., 1997; Figure 2.10). Such responses indicate that for those participants the exercise intensity (even at 40% MVC) did not exceed their critical torque, thereby highlighting the potential worth of including estimations of, and

thereby prescribing torque demands relative to, the critical torque in study designs investigating fatigue mechanisms (Poole et al., 2016).

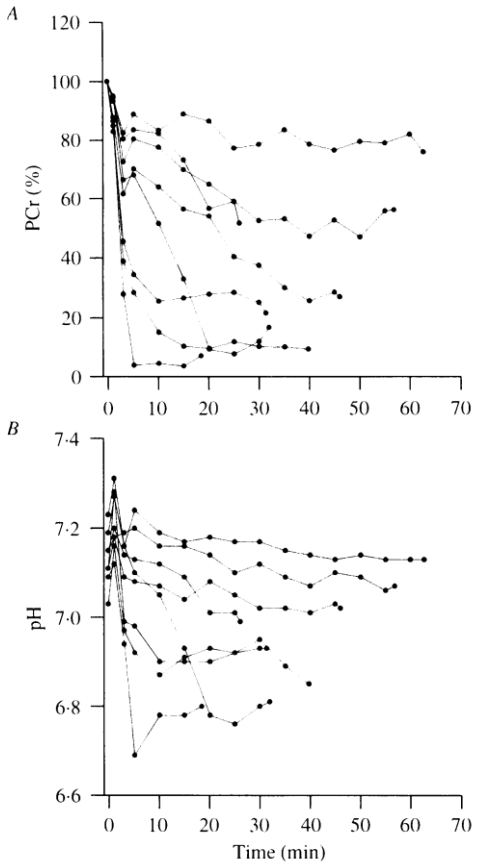

Figure 2.10. *Individual responses for PCr (A) and pH (B) during submaximal intermittent isometric knee extension contractions performed at 40% MVC in a magnetic resonance spectrometer. Note the markedly different responses for the two participants whose time to task failure was > 50 min. From Saugen et al. (1997).*

Broadly speaking, fatigue mechanisms can be categorised into three types: *peripheral fatigue*, *central fatigue*, and "*global fatigue*" (or *neuromuscular fatigue* per se; Poole et al., 2016). In the context of torque demands, torque losses attributable to mechanisms distal to the neuromuscular junction (within the muscle fibres) describe peripheral fatigue, torque losses attributable to mechanisms proximal to the neuromuscular junction (within the central nervous system) describe central fatigue, and the combined effects of peripheral *and* central fatigue resulting in a loss of MVC torque describes neuromuscular fatigue (Burnley et al., 2012; Place et al., 2009; Poole et al., 2016). It is generally accepted that during submaximal exercise tasks, "low-intensity" contractions (typically sustained contractions performed at ≤

15% MVC or intermittent contractions performed below 30% MVC) result in substantial levels of central fatigue (Smith et al., 2007; Søgaard et al., 2006; Yoon et al., 2007). In contrast, during “high-intensity” contractions (typically sustained contractions performed above 20% MVC or intermittent contractions performed above 30%) peripheral fatigue mechanisms dominate, with only small contributions from central fatigue mechanisms (Bigland-Ritchie et al., 1986; Saugen et al., 1997; Poole et al., 2016). However, the way in which “low“ and “high“ intensity contractions are defined in neuromuscular fatigue research is often unclear (Poole et al., 2016).

A gradual transition from central to peripheral fatigue mechanisms in proportion with increases in torque demands is one possibility. The other is that there exists an identifiable threshold, above and below which distinct mechanisms of fatigue are evident. Speculating that the critical torque might represent such a fatigue threshold, Burnley et al. (2012) investigated the global, central, and peripheral fatigue responses (using measures of MVC, voluntary activation, and the potentiated doublet, respectively) to exercise performed above and below the critical torque. When exercise was performed below the critical torque (~90% critical torque), both central and peripheral fatigue developed with modest neuromuscular adjustments as exercise continued (inferred from small increases in the average rectified EMG; Burnley et al., 2012). However, when exercise was performed just above the critical torque (~111% critical torque), both peripheral and global neuromuscular fatigue developed four- to fivefold faster (Burnley et al., 2012; Figure 2.11). As previously discussed in this chapter, the critical torque also represents a critical threshold for fatigue-induced losses in knee extensor muscle torque complexity (Pethick et al., 2016; Figure 2.6A).

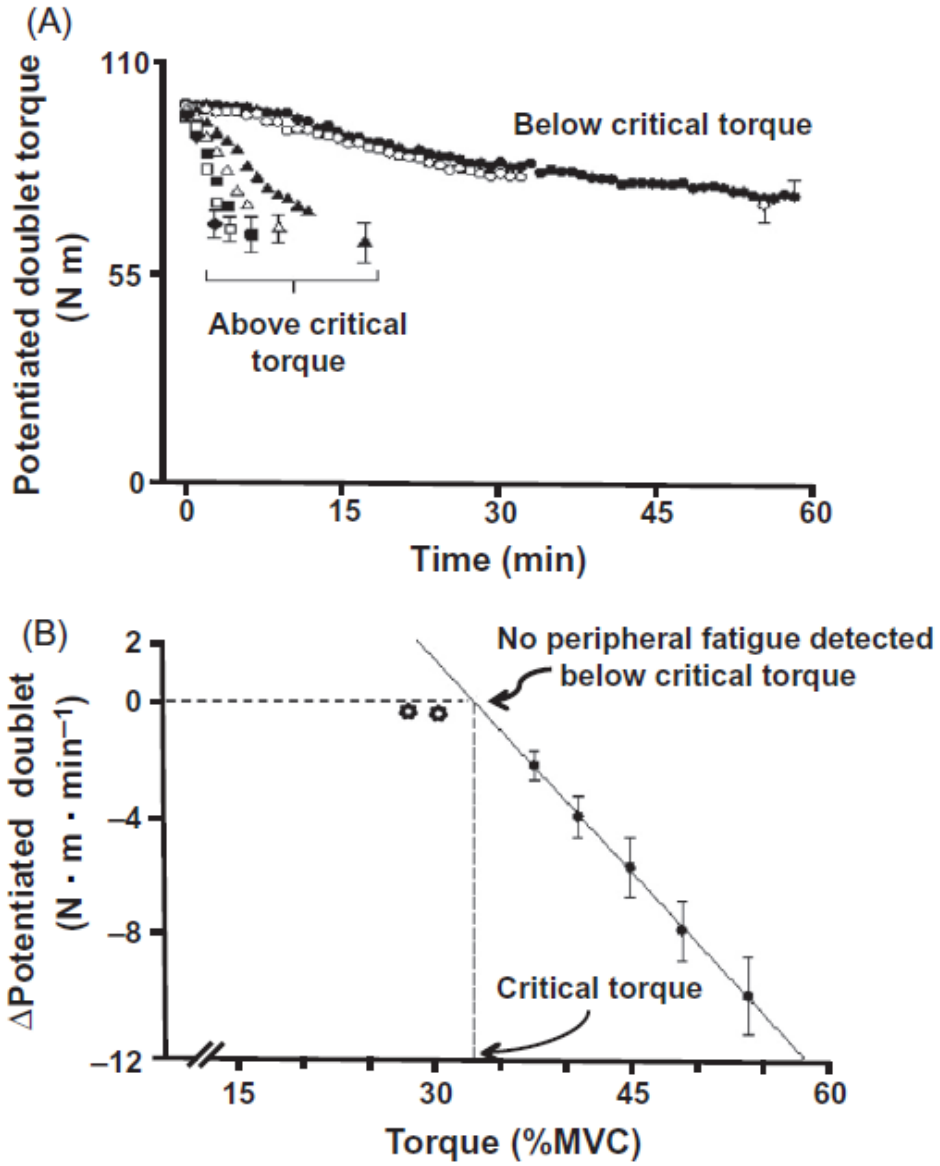

Figure 2.11. *Peripheral fatigue response to exercise performed above and below the critical torque (CT) from the data of Burnley et al. (2012). A) Potentiated doublet response for exercise above (triangles, squares, and diamonds) and below (80%, filled circles; 90%, open circles) the CT. Note the accelerated peripheral fatigue in the tests performed above CT. B) Rate of change for the potentiated doublet response (mean ± standard error) for each test. Filled circles represent tests above CT, open circles represent tests below CT. The solid line denotes the line of best fit for linear regression for data above CT. From Craig et al. (2019)*

Regardless of exercise duration above the critical torque, it appears that the same degree of peripheral fatigue is reached at task failure (Burnley, 2009; Burnley et al., 2012), a finding also apparent in the muscle PCr, P_i, and pH responses at task failure during dynamic contractions performed above the critical power (Vanhatalo et al., 2010). Collectively, these findings suggest there exists a constant amount of

impulse or work the muscle can amass above the critical torque or power (i.e., the *W'*; Craig et al., 2019). Therefore, the critical torque represents a critical neuromuscular fatigue threshold demarcating intensity exercise domains, above and below which distinct fatigue mechanisms are evident (Craig et al., 2019). However, as previously discussed, it is now known that the critical torque is not a sudden threshold, but a continuous phase transition between the heavy and severe intensity exercise domains that exists within the confidence limits of its estimation (Pethick et al., 2020).

Conventional method of critical power determination

Whilst the critical power represents a specific metabolic rate (Barker et al., 2006; Vanhatalo et al., 2016), it differs with regard to other physiological thresholds in that it is determined based on measures of performance, namely mechanical work done and time-to-task-failure (Jones et al., 2010). The conventional method to determine the critical power typically involves three or more independent constant-power exercise trials performed in the severe-intensity domain until task failure (Poole et al., 1988; Vanhatalo et al., 2007). The selected work intensities should ideally cause task failure in 2-15 min and there should be the widest possible range (8-12 min) between the shortest and longest trials (Jones et al., 2019). Higher power outputs leading to task failure in less than 2 min are avoided due to the likely inability of participants to achieve $\dot{V}O_{2max}$ (Hill, et al., 2002). Likewise, lower power outputs resulting in exercise times above 15 min are usually avoided because $\dot{V}O_{2max}$ is seldom reached and to continue to the point of task failure, factors such as motivation become more important (Jones et al., 2010). That said, it has been suggested that increasing the duration of one of the exercise trials to ~20 min may generate the most precise approximation of the critical power and *W'* (Mattioni Maturana et al., 2018).

In keeping with the conventional method to establish critical power, four (Pethick, et al., 2016; 2020) or five (Burnley, 2009; Burnley et al., 2012) intermittent isometric contraction trials performed to task failure at submaximal intensities between 35 and

60% MVC are typically used to establish the critical torque; each independent submaximal trial should elicit task failure in between 2 and 15 min. Indeed, Monod and Scherrer (1965) highlighted that the relationship between W_{lim} (force or torque multiplied by contraction time) and *Tlim* was only linear for tests lasting more than 2 min in the case of intermittent contractions. It is important to note that when using intermittent contraction regimes, the maximum work time must be differentiated from the total duration of the test, since contractions are only performed for a fraction of the test time (Monod & Scherrer, 1965). Despite the effectiveness of the conventional methods to determine the critical power (or torque), it has been argued that the use of repeated exhaustive exercise bouts has likely hindered the wider application of the concept (Vanhatalo et al., 2007). To remedy this, time-efficient, all-out exercise tests to estimate the critical power or torque in a single visit were conceptualised.

All-out tests to estimate the critical power/torque

When investigating peak oxygen uptake and the maximal steady state, Burnley, Doust and Vanhatalo (2007) observed a plateau equating to a ~70% reduction in peak power output during the final 60 s of a 3 min maximal cycling effort. This led to the development of the 3-min all-out test which, as the name suggests, involves 3 min of maximal cycling exercise to provide an estimate of the critical power (Vanhatalo et al., 2007; Figure 2.12A). As well as during cycling exercise (Simpson et al., 2015; Vanhatalo et al., 2007; 2008), the 3-min all-out test has subsequently been shown to be both valid and reliable in its estimation of the critical power (or critical speed) during outdoor track running (Broxterman et al., 2013; Pettitt et al., 2012), rowing (Cheng et al., 2012), and during swimming in highly trained swimmers (Piatrikova et al., 2018).

Consistent with earlier findings of the 3-min all-out test, Burnley (2009) evidenced a plateau in torque during the final 30 s of a 5 min series of intermittent knee extensor MVCs (3 s contraction and 2 s rest). The “end-test torque” was demonstrated to correspond to the critical torque determined using the conventional five-visit

approach, providing an analogue to the aforementioned 3 min all-out test used for cycling (Figure 2.12B). The above findings give credence to the supposition that all-out exercise eventually results in the attainment of critical power (or torque), regardless of the selected exercise modality (Jones et al., 2010).

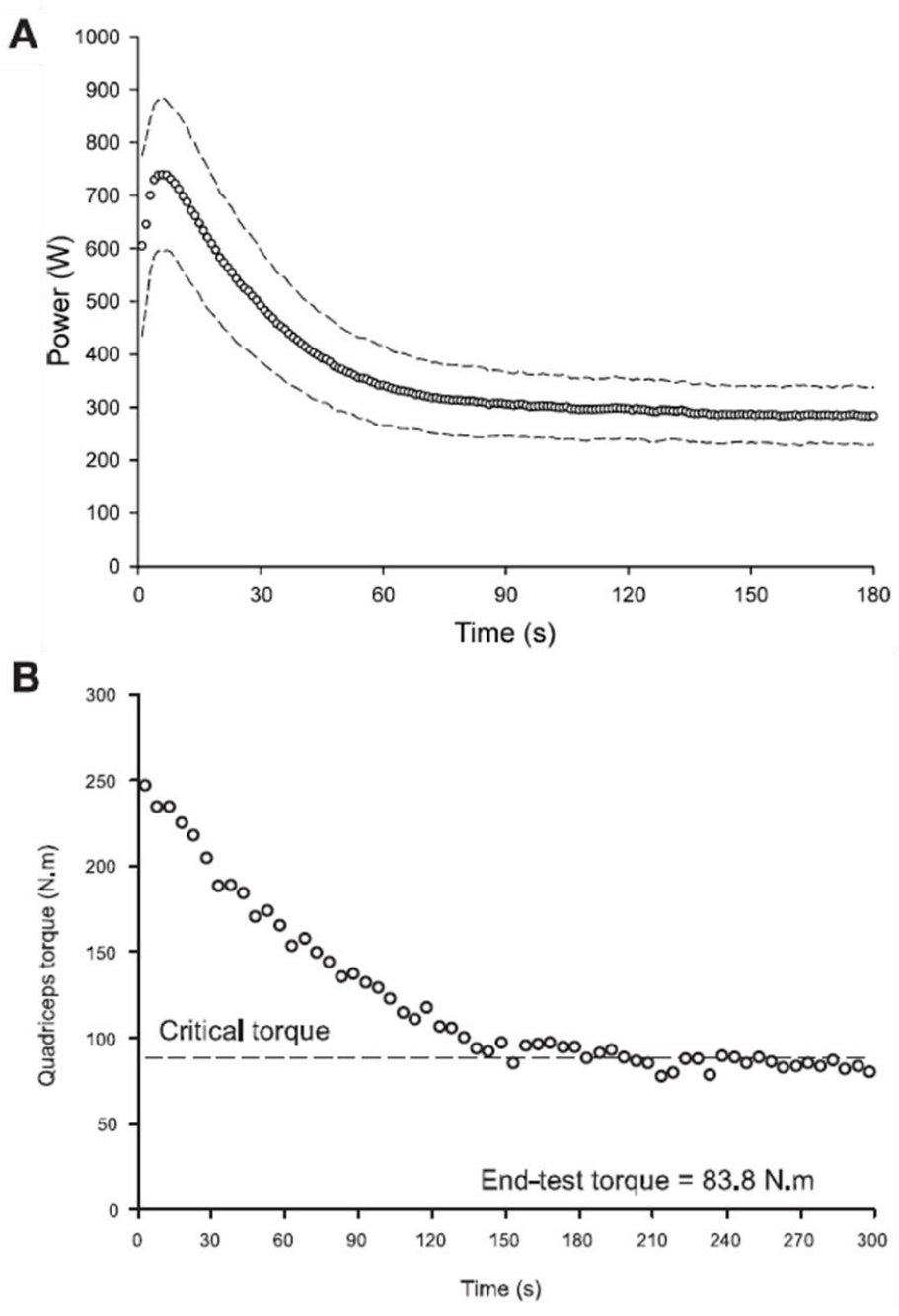

Figure 2.12. A) *Group mean power output during the 3-min all-out test. Dashed lines indicate the standard deviation. Note the plateau in power output during the final 45 seconds of the test (i.e., the "end-test power"). From Vanhatalo et al. (2007),* ***B)*** *The torque profile during the 5-min all-out test for an individual participant. Note the plateau in torque during the final 30 seconds of the test (i.e., the "end-test torque"). From Burnley (2009).*

In addition to the knee extensors, all-out tests have also been used to estimate the critical torque (or force) in the forearm flexors (Kellawan & Tschakovsky, 2014) and the plantarflexors (Abdalla et al., 2018). Interestingly, the critical torque values reported by Abdalla et al. (2018) for the plantarflexors (~40% MVC) were higher than for the knee extensors (~29%). This is in line with an analysis of endurance times reported by Frey-Law and Avin (2010), in which the ankle joint was determined to be more fatigue-resistant than the knee joint during sustained contractions. Furthermore, similar “power fatigue” curves were predicted for both ankle plantarflexion and dorsiflexion contractions (Frey-Law & Avin, 2010), suggesting the critical torque for the dorsiflexors also likely occurs at a higher fraction of MVC relative to the knee extensors.

To date, no study has investigated the critical torque in the dorsiflexor muscle group. The tibialis anterior muscle (primary ankle dorsiflexor) is commonly used in HDsEMG research wherein a uniform % MVC is used to set the contraction intensity (e.g., Castronovo et al., 2015; Del Vecchio, Negro et al., 2019; Martinez-Valdes, Negro et al., 2020). Given the significance of the critical torque as a threshold for accelerated neuromuscular fatigue (Burnley et al., 2012), the development and validation of methods to efficiently determine the critical torque in the dorsiflexors is vital. If the 5-min all-out test (Burnley, 2009) provides an estimate of dorsiflexor critical torque in agreement with the conventional approach, this valuable parameter could be used in addition to, or in place of, % MVC as a way to prescribe the intensity of muscular contractions in HDsEMG studies investigating neuromuscular fatigue; this will be investigated in Chapter 6.

Priming exercise

Warm-up exercise

The use of warm-up exercise is a universally accepted practice performed by athletes before subsequent training or competition, but the optimal intensity and duration of warm-up exercise is relatively unknown (Bishop, 2003; Jones, Koppo et al., 2003). However, one acute "warm-up" intervention that has received considerable attention in the literature is that of priming exercise, specifically the use of prior heavy-intensity exercise and its effects on the time course of the oxygen uptake response (i.e., $\dot{V}O_2$ kinetics) during a subsequent bout of exercise (Jones, Koppo et al., 2003).

$\dot{V}O_2$ kinetics across the exercise intensity domains

The four distinct exercise intensity domains that have thus far been identified were briefly introduced earlier in this chapter (Figure 2.9), but will be reaffirmed in this section as the $\dot{V}O_2$ kinetics differ between each domain. The moderate intensity domain refers to exercise performed at intensities below the lactate threshold. The heavy intensity domain refers to exercise performed at intensities above the lactate threshold but below the critical power. The severe intensity domain denotes exercise intensities above the critical power that can be sustained until attainment of maximal oxygen uptake ($\dot{V}O_{2max}$). The final intensity domain is termed extreme and refers to exercise performed at such an intensity that task failure occurs *before* $\dot{V}O_{2max}$ is reached (Burnley & Jones, 2018).

At moderate-intensity exercise, the transition from rest to constant-load exercise is characterised by the attainment of steady-state pulmonary $\dot{V}O_2$ within 2-3 min (Whipp et al., 1982), wherein the $\dot{V}O_2$ response can be partitioned into three distinct phases (Burnley & Jones, 2007). It is important to note that pulmonary $\dot{V}O_2$ does not immediately reflect muscle $\dot{V}O_2$ due to a 10-20 s delay from oxygen unloading at the muscle and the appearance of the same blood at the pulmonary vasculature (Burnley & Jones, 2007). It is this delay which characterises Phase I of the $\dot{V}O_2$ response to exercise, termed the "cardiodynamic" phase (Burnley & Jones, 2007).

An exponential increase in $\dot{V}O_2$ signals the onset of Phase II or the "primary component", at which point pulmonary $\dot{V}O_2$ *does* reflect muscle $\dot{V}O_2$ (Rossiter et al., 1999). This increase in $\dot{V}O_2$ ultimately leads to the attainment of steady-state (Phase III) after 2-3 min of exercise. However, when exercise is performed in the heavy or severe exercise domains, the emergence of an additional delayed "slow component" of the $\dot{V}O_2$ response is apparent (Jones, Koppo et al., 2003). Quite unlike the response observed during moderate intensity exercise, $\dot{V}O_2$ rises above the predicted steady-state and can result in the attainment of $\dot{V}O_{2max}$ during exercise performed in the severe domain (Gaesser & Poole, 1996). The amplitude of the $\dot{V}O_2$ slow component is thought to signify an increased metabolic inefficiency as exercise continues (Barstow et al., 1990; Jones, Koppo et al., 2003). In addition, the $\dot{V}O_2$ slow component is known to correlate with indices of anaerobic exercise performance (Berger & Jones, 2007). Therefore, interventions designed to attenuate the $\dot{V}O_2$ slow component amplitude (as well as those that speed the overall $\dot{V}O_2$ kinetics) might have the potential to improve exercise tolerance, not only for athletes but also for aged and patient populations (Poole & Jones, 2012).

The effects of prior heavy exercise on $\dot{V}O_2$ kinetics and performance

It has long been known that the performance of prior warm-up exercise can serve to "prime" the physiological response to subsequent exercise, particularly in relation to the $\dot{V}O_2$ response (Gutin et al., 1976; Ingier & Strømme, 1979; Pendergast et al., 1983), but the lack of temporal resolution in these early studies precluded any accurate description of the specific time course of this response (Burnley et al., 2005). However, the work of Gerbino et al. (1996) renewed interest in the area after the use of prior heavy-intensity (but not moderate-intensity) warm-up exercise, or "priming", was demonstrated to "speed" the $\dot{V}O_2$ kinetics during a subsequent bout of heavy exercise performed 6 min after the first. Similar findings were reported by MacDonald et al. (1997), and both groups suggested that the overall speeding of $\dot{V}O_2$ kinetics after heavy exercise was in part due to a speeding of the primary kinetics. Subsequent work determined that priming exercise did not speed the phase II $\dot{V}O_2$ kinetics (Burnley et al., 2000), but instead the overall speeding of $\dot{V}O_2$ kinetics was attributed to an increase in the primary amplitude and a reduction in the $\dot{V}O_2$

slow component amplitude (Burnley et al., 2001; Koppo & Bouckaert, 2001). The characteristic effect of heavy prior exercise on the subsequent heavy exercise $\dot{V}O_2$ response is shown in Figure 2.13.

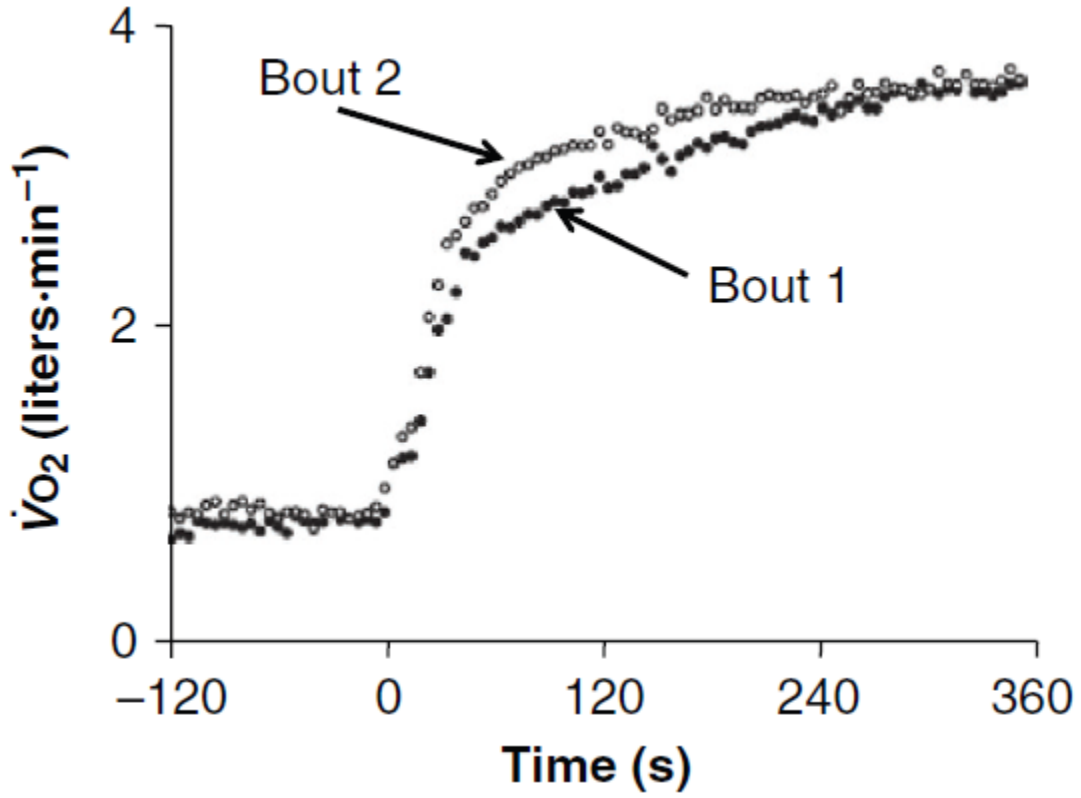

Figure 2.13. *Pulmonary $\dot{V}O_2$ responses to heavy exercise bouts separated by 12 min from Burnley, Doust, Ball, et al. (2002). An increased primary amplitude and a reduced $\dot{V}O_2$ slow component are evident in bout 2. From Poole and Jones (2012).*

It has since been demonstrated that the observed effects on the $\dot{V}O_2$ response are preserved for at least 30-45 min following prior heavy exercise (Burnley et al., 2006). Provided the recovery time between bouts is sufficient (>9-10 min), priming exercise performed in the heavy or severe intensity domain has also been shown to lead to increases in time to exhaustion of between 10-60% in a subsequent bout of exercise (Bailey et al., 2009; Burnley et al., 2011; Carter et al., 2005; Jones, Wilkerson, et al., 2003). Despite research outlining the beneficial effects of priming exercise on $\dot{V}O_2$ kinetics and performance during subsequent exercise, the mechanisms responsible for such effects remain unresolved, though several have been proposed.

Mechanisms for changes in $\dot{V}O_2$ kinetics after prior heavy exercise

It is likely that multiple mechanisms contribute to the changes in $\dot{V}O_2$ kinetics observed after prior exercise, but the evidence for those investigated so far is either scant or inconclusive (Poole & Jones, 2012). For example, an increase in leg muscle temperature (~3°C) elicited by wearing hot-water-perfused pants was shown by Koga et al. (1997) to result in a slight, but statistically significant, reduction in the amplitude of the $\dot{V}O_2$ slow component. The authors speculated that a lowered viscous resistance in the muscle led to improved mechanical efficiency, and consequently a reduced $\dot{V}O_2$ slow component. However, when the leg muscles were passively warmed to temperatures equal to, or greater than, those achieved during 6 min of heavy exercise, no reductions in the $\dot{V}O_2$ slow component amplitude were observed (Burnley, Doust & Jones, 2002; Koppo et al., 2002). Therefore, muscle temperature *per se* is not thought to account for the effects of priming exercise on the $\dot{V}O_2$ response.

Another proposed mechanism for the observed changes in $\dot{V}O_2$ kinetics after heavy prior exercise is improved muscle perfusion. It has consistently been shown that, following a bout of prior heavy exercise, O_2 delivery is increased at the onset of a subsequent bout of exercise (e.g., Bangsbo et al., 2001; Burnley, Doust, Ball et al., 2002), which would be expected to reduce the primary time constant value and speed the primary $\dot{V}O_2$ kinetics. On the contrary, most studies have found no effect on the primary $\dot{V}O_2$ time constant (Poole & Jones, 2012; Whipp et al., 2002), indicating that improved blood flow to the working muscle(s) is not essential for a priming effect to occur (Endo et al., 2005, Fukuba et al., 2004). However, it should be noted that for certain exercise modalities (e.g., supine exercise; Koga et al., 1999) and conditions (e.g., hyperoxia; MacDonald et al., 1997), both the primary component and the $\dot{V}O_2$ slow component might be sensitive to O_2 delivery (Burnley et al., 2005).

Increased activation of the pyruvate dehydrogenase complex (PDC) resulting from increased substrate availability has also been proposed as a potential mechanism

for the speeding of $\dot{V}O_2$ kinetics (Campbell-O'Sullivan et al., 2002). However, this is unlikely because administration of dichloroacetate, which increases PDC activation by inhibition of pyruvate dehydrogenase kinase has been shown to actually *reduce* the amplitude of the primary component (Rossiter et al., 2003). Nevertheless, there remains another plausible explanation for the effect of prior heavy exercise on the $\dot{V}O_2$ kinetics response during subsequent exercise, which is discussed below.

Motor unit recruitment patterns

It has long been hypothesised that a change in motor unit recruitment patterns might explain the development of the $\dot{V}O_2$ slow component during heavy exercise (Poole et al., 1991; Whipp, 1994). This was supported experimentally by observations that the integrated electromyogram (iEMG) increases in tandem with $\dot{V}O_2$ slow component development during heavy exercise (Perrey et al., 2001; Saunders et al., 2000; Shinohara & Moritani, 1992). Given this association, it was postulated that alterations in motor unit recruitment patterns might also explain the reduction of the $\dot{V}O_2$ slow component amplitude after prior heavy exercise (Burnley et al., 2001). In addition, it was also speculated that the characteristic increase in primary component amplitude observed in the second of two bouts of heavy-intensity exercise might be a result of increased motor unit recruitment (Burnley et al., 2001). Burnley Doust, Ball et al. (2002) subsequently reported a significant 19% increase in the iEMG of three leg muscles (gluteus maximus, vastus lateralis, and vastus medialis) during the second of two bouts of heavy exercise separated by 12 min recovery, concomitant with an increase in the amplitude of the $\dot{V}O_2$ primary component. Additionally, qualitative support for the notion that continual recruitment of additional motor units during the second bout might explain the reduction in amplitude of the $\dot{V}O_2$ slow component was inferred from the smaller gradient of iEMG increase during the final 3 min of the second exercise bout. However, despite the findings of Burnley, Doust, Ball et al. (2002), results from other studies were more equivocal on the contribution of motor unit recruitment to the development of the $\dot{V}O_2$ slow component (Scheuermann et al., 2001; Tordi et al., 2003).

Both Scheuermann et al. (2001) and Tordi et al. (2003) were unable to detect significant changes in the leg muscle iEMG signal during a subsequent bout of heavy cycling exercise, despite trends towards higher iEMG values in the second exercise bout in both studies. Such divergent findings between the aforementioned studies might result from the limited sensitivity of bipolar surface EMG in detecting subtle changes in motor unit behaviour during cycling exercise (Burnley et al., 2005). Using a two-leg knee-extension exercise test, Layec et al. (2009) investigated the effects of a prior 6 min “heavy-intensity” exercise (performed at 35% MVC) bout on energy production and muscle fibre recruitment during a subsequent 6 min heavy-intensity exercise bout, separated by 6 min of passive recovery. Surface EMG was recorded from the vastus lateralis of the left leg, and the ratio between the iEMG and power output (W) was reported. In line with the findings of Burnley, Doust, Ball et al. (2001), an increase in the iEMG/W ratio was observed during the first 2 min of the subsequent exercise bout, which was interpreted as increased motor unit recruitment at the onset of the second exercise bout (Layec et al., 2009). However, the use of bipolar surface EMG techniques, even in an isolated muscle model, is limited since the amplitude and frequency content of the signal can only provide a crude approximation of motor unit behaviour (Farina, 2008; Holobar, et al., 2016).

In studies of individual motor unit behaviour using intramuscular or subcutaneous EMG techniques, the recruitment (and de-recruitment) thresholds of motor units have been demonstrated to change after fatiguing contractions were performed to task failure (Adam & De Luca, 2003; Carpentier et al., 2001; Enoka et al., 1989). For example, the recruitment threshold was shown to decrease in high threshold and increase in low threshold motor units of the first dorsal interosseus during submaximal fatiguing isometric ramp-and-hold contractions performed at 50% MVC (Carpentier et al., 2001). In contrast, during submaximal isometric knee extension ramp-and-hold contractions performed to task failure at 20% MVC, Adam and De Luca (2003) reported decreases in the recruitment threshold of all observed motor units in the vastus lateralis, a finding that was universal amongst high and low threshold motor units. Furthermore, the time taken for restoration of the original recruitment thresholds in motor units appears to be similar to the time course for the

lasting effects of prior heavy-intensity cycling exercise on the $\dot{V}O_2$ response (between 15-30 min post-exercise; Carpentier et al., 2001).

Based on the findings of Carpentier et al. (2001) and Adam and De Luca (2003), Burnley et al. (2005) presented a hypothetical model of the effect of additional motor unit recruitment on the $\dot{V}O_2$ kinetics response to two heavy exercise bouts separated by 12 min recovery (Figure 2.14). An additional assumption of the model was that motor unit recruitment adheres to the size principle (i.e., the idea that motor units are recruited in an orderly fashion, from smallest to largest [Henneman, 1985]). The model predicts that during a subsequent bout of heavy exercise, the lowered recruitment thresholds induced by the first exercise bout would result in additional motor units being recruited at that power output (Figure 2.14B), resulting in an increased primary $\dot{V}O_2$ amplitude (Burnley et al., 2005). Rates of fatigue, lactate accumulation, and PCr degradation would all be reduced based on the assumption that more motor units would share the power output during the second exercise bout, and this would result in the recruitment of fewer motor units as exercise progressed. This, in turn, would reduce the $\dot{V}O_2$ slow component (Figure 2.14D). However, the behaviour of individual motor units in response to heavy prior exercise is thus far unknown, and the model presented by Burnley et al. (2005) is yet to be tested experimentally. It remains to be seen whether the findings from Carpentier et al. (2001) and De Luca and Adam (2003) are applicable to heavy-intensity exercise.

The results of the studies of individual motor unit behaviour discussed above were obtained using intramuscular electrodes (Adam & De Luca, 2003; Carpentier et al., 2001) or subcutaneous electrodes (Enoka et al., 1989), which as well as being invasive, often result in relatively few motor units being sampled at a time (Farina et al., 2008). In contrast, the recent development of HDsEMG recording techniques and subsequent advances in HDsEMG decomposition algorithms presents the opportunity to non-invasively identify larger pools of motor units than typically achieved using intramuscular techniques (Holobar, et al., 2014; Negro et al., 2016). The behaviour of individual motor units in response to 6 min of prior heavy exercise is yet to be confirmed, and this will be investigated using HDsEMG signal decomposition in Chapter 7.

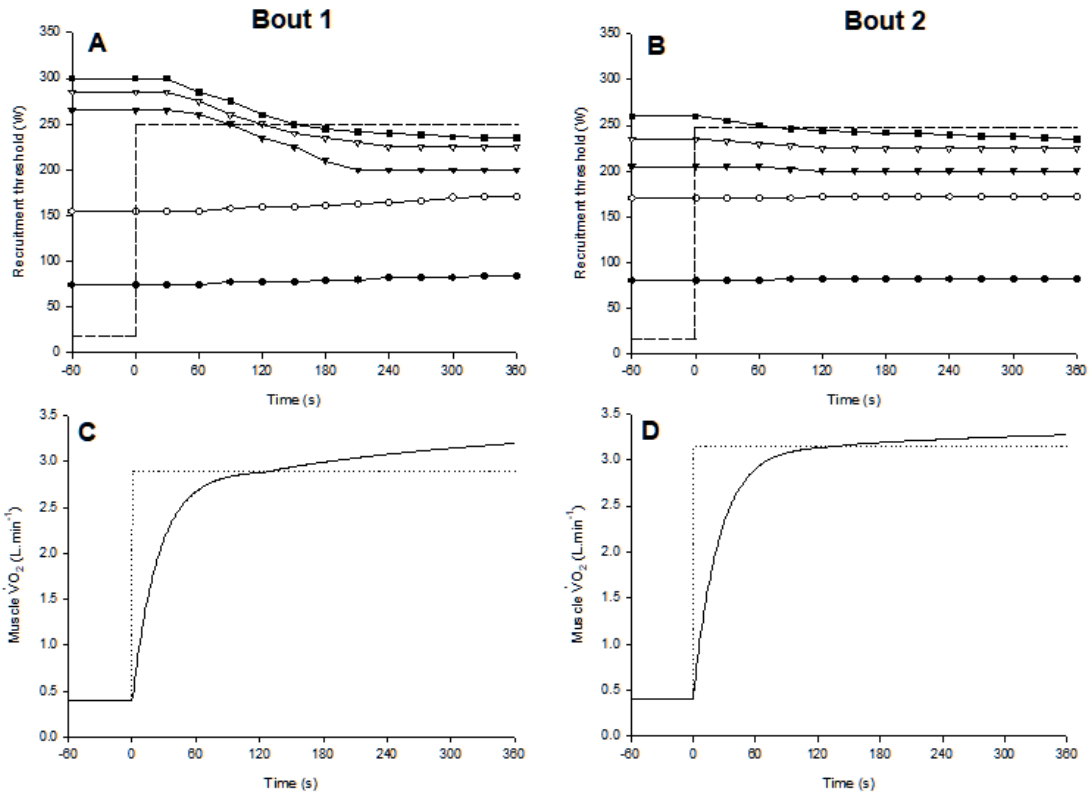

Figure 2.14. *Hypothetical simulation of motor unit recruitment thresholds (A and B) and muscle $\dot{V}O_2$ (C and D) during two bouts of heavy-intensity exercise separated by 12 min recovery. From Burnley et al. (2005).*

Aims and hypotheses

It should be noted here that data collection for Chapters 6 and 7 (Studies 3 and 4) was delayed from Spring of 2020 until Autumn 2020 due to the Coronavirus restrictions in place at the time. Consequently, the participant sample for both studies is one and the same. Other than participant characteristics and anthropometrics, the only other data shared between these studies are the critical torque estimations from Chapter 6 which were used to set the exercise intensity in Chapter 7. Furthermore, due to unavoidable restrictions on participant recruitment when laboratories reopened, participant sample numbers are low (n = 6).

The overall aim of this thesis was to investigate the neural control of muscle torque in the tibialis anterior using HDsEMG decomposition. The specific aims and hypotheses of the four experimental studies are as follows:

Chapter 4 – Study 1

Title: Methodological aspects of high-density surface electromyography signal acquisition in the tibialis anterior muscle during isometric contractions of varying intensity

Aim: To work towards an optimal HDsEMG signal acquisition process in the tibialis anterior to identify individual motor units and their discharge properties during isometric contractions across a range of target torques, including during ramp-and-hold contractions.

Hypothesis: The use of abrasive paste would result in greater numbers of decomposed motor units across all contraction intensities. A greater number of ground electrodes would result in reductions in the noise of the HDsEMG signal. It also was hypothesised that by using less conservative acceptance criteria during the HDsEMG decomposition process, the motor unit yield would increase.

Chapter 5 – Study 2

Title: Loss of motor unit cumulative spike train complexity and ankle torque complexity during fatiguing dorsiflexor contractions in humans

Aim: To determine the complexity of the motor unit cumulative spike train and that of torque output during fatiguing and non-fatiguing contractions of the tibialis anterior muscle.

Hypothesis: Ankle dorsiflexion contractions performed at 30% MVC with arterial occlusion would result in significant neuromuscular fatigue and a reduction in torque complexity which would be accompanied by a fall in motor unit cumulative spike train complexity, whereas contractions performed at 30% MVC without occlusion would result in no changes.

Chapter 6 – Study 3

Title: Critical torque in the dorsiflexors – a comparison between the 5 minute all-out test and the conventional estimation of critical torque from submaximal tests performed to task failure

Aim: To establish if the end-test dorsiflexor torque calculated from a 5 min all-out test is a valid measure of the critical torque estimated using the conventional method.

Hypothesis: The end-test dorsiflexor torque estimated from the 5-minute all-out test would not differ from the critical torque calculated using the conventional method.

Chapter 7 – Study 4

Title: The effects of priming exercise on motor unit behaviour in the tibialis anterior

Aim: To investigate the effects of prior ‘heavy’ exercise on motor unit behaviour of the tibialis anterior muscle.

Hypothesis: Priming exercise would lead to a reduction in motor unit recruitment threshold during subsequent contractions and would also result in an increase in global HDsEMG amplitude during a subsequent bout of ‘heavy’ exercise.

CHAPTER 3 - GENERAL METHODS

Introduction

This chapter outlines the general methods used in the studies contained in this thesis. Details specific to particular studies are included within the relevant experimental chapters. All experiments were conducted in the University of Kent exercise physiology laboratory at Medway Park.

Pre-test Procedures

Ethics

Before commencement of data collection, full ethical approval was granted by the School of Sport and Exercise Sciences Research Ethics Advisory Group (SSES REAG) at the University of Kent (see Appendix). All studies were conducted in adherence with the World Medical Association's *Declaration of Helsinki* (1964).

Participant Recruitment and Informed Consent

Participants were recruited from the student and staff population at the University of Kent. Participants provided written informed consent then completed a health and physical activity questionnaire (see Appendix) to confirm they were suitably healthy to take part in high-intensity exercise, before a written informed consent form (see Appendix) was signed. All participants were assigned an alpha-numerical code (e.g. P01) to ensure confidentiality and to anonymise subsequent data relating to each participant.

Familiarisation

Familiarisation trials were conducted during all studies to ensure participants were introduced to the laboratory surroundings, equipment and protocols to be used in the subsequent visits. With the exception of the first experimental study (Chapter 4), no data from these visits were used in the following analyses.

Experimental Controls

Participants were instructed to attend each session well-rested and well-hydrated, not to consume caffeine or eat in the 2 h prior to exercise, and not to consume alcohol or undergo heavy exercise in the preceding 24 h. Participants were also requested to wear shorts to allow access to the recording site over the tibialis anterior muscle and to wear the same footwear during each visit to ensure the angle of the ankle remained consistent between experimental sessions. Each visit was separated by 48 h and conducted at the same time of day (± 2 h) to minimise the influence of diurnal variation on muscle contractility (Racinais et al., 2005) and maximal voluntary torque production (Tamm et al., 2009).

Procedures

Anthropometry

Before commencement of each study, the date of birth (converted into age; years), stature (measured to the nearest mm using a wall-mounted Harpenden Stadiometer; Holtain Ltd., Crymych, UK), and body mass (measured to the nearest 0.1 kg using calibrated laboratory scales; Seca GmbH & Co., Hamburg, Germany) were recorded. Measurements of stature and body mass were recorded with participants standing upright, unshod, and wearing the clothing in which they were to complete the subsequent experimental procedures.

Isometric Torque Measurement/Dynamometry

All visits of each study involved measuring isometric ankle dorsiflexor torque (N·m) production during voluntary contractions using a Cybex isokinetic dynamometer (HUMAC Norm; CSMi, Massachusetts, USA). The dynamometer was initialised and calibrated according to the manufacturer's instructions. Participants were seated in the chair of the dynamometer with their trunk reclined to 15° (with 0° being seated upright), their right leg fully extended, and ankle at 90° (Figure 3.A). The right limb was used throughout all experimental chapters; Škarabot et al. (2019) reported no

differences in measurements of isometric MVC torque, creatine kinase, motor evoked potentials, H-reflex, or transcranial magnetic stimulation responses when comparing ankle dorsiflexion exercise in the non-dominant limb to the dominant limb. A padded Velcro strap firmly secured the right foot into a foot plate attached to the dynamometer lever arm (Figure 3.1B), which was adjusted such that the lateral malleolus was in line with the axis of rotation of the lever arm. Straps across both shoulders and the waist were used to limit any extraneous movement, and a further strap was secured around the distal portion of the thigh to limit the use of the knee extensors during the isometric contractions. During the first visit of each study, the seating position and dynamometer settings for each participant were recorded and replicated for each visit thereafter.

Torque data were acquired from the dynamometer through a BNC cable via a CED Micro 1401-3 (Cambridge Electronic Design, Cambridge, UK), which was connected to a personal computer. The data were collected using Spike2 (Version 7; Cambridge Electronic Design, Cambridge, UK) and sampled between 1000 and 2048 Hz. Instantaneous torque was displayed on a screen (positioned ~2 m in front of the participant) and a horizontal cursor was superimposed on the display as a target to enable participants to match their instantaneous torque output to the target torque during each contraction.

After a short warm up, three maximal voluntary contractions (MVCs) lasting ~3 s were performed at the beginning of each experimental visit. The determination of the MVC torque allowed for the target torque of the subsequent submaximal contractions to be set. In Chapters 4, 5, and 7, submaximal ramp-and-hold contractions were used to investigate motor unit behaviour. The specific contraction regime(s) used differed between studies and these differences are detailed in the respective chapters.

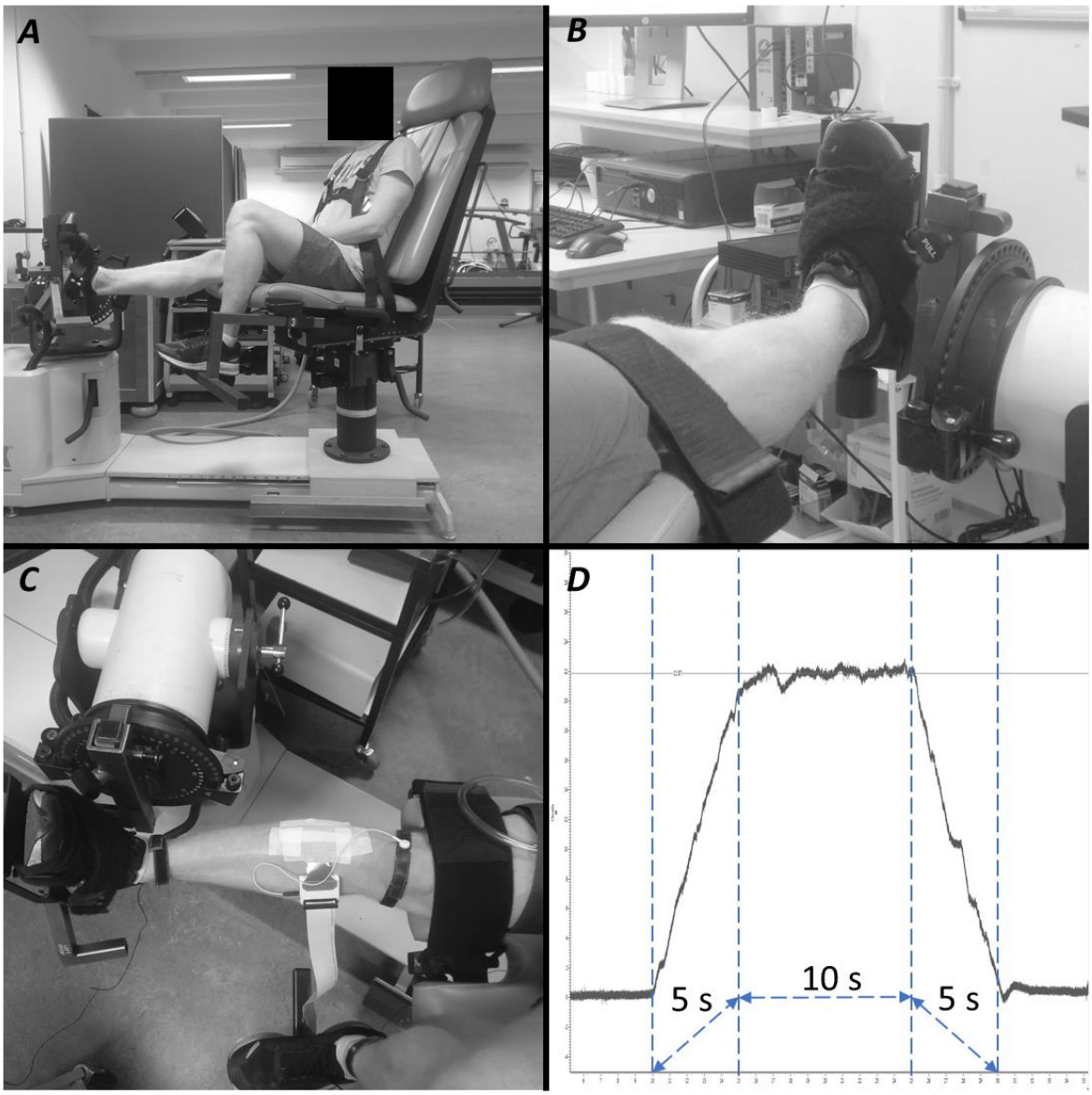

***Figure 3.1**. Participant setup. (A) Seating position; (B) The right foot of the participant secured in the dynamometer foot plate; (C) Electrode grid placement over the right tibialis anterior muscle; (D) Ramp-and-hold contraction profile. Dashed lines are superimposed to highlight the up, plateau, and down phases of the contraction.*

High-Density Surface Electromyography

High-density surface electromyography (HDsEMG) was recorded from the tibialis anterior muscle of the right leg. Prior to placement of the electrode grid, the skin over the tibialis anterior was shaved and rubbed with medical grade abrasive paste (Spes Medica, Battipaglia, Italy). Over a reference line between the tibial tuberosity and the intermalleolar line, drawn using the *Atlas of muscle innervation zones* guidelines (Barbero et al., 2012), a linear non-adhesive electrode (16 bar electrode,

5 mm inter-electrode distance; OT Bioelettronica, Torino, Italy; Figure 3.2A) was used to detect the location of the tibialis anterior innervation zone and tendon during a brief submaximal contraction at ~10% MVC (Masuda et al., 1985). The array was moved over the tibialis anterior to estimate the anatomical direction of muscle fibres that corresponded to the observation of action potentials propagating along the column of electrodes without substantial changes in waveform shape. Once this was established, HDsEMG signals were detected from the proximal region of the tibialis anterior muscle using a grid of 64 electrodes (5 columns and 13 rows, with an electrode missing in the upper right corner of the grid; gold-coated; 4 mm diameter; 8 mm interelectrode distance; ELSCH064NM2, OT Bioelettronica, Torino, Italy; Figure 3.2B). The electrode grid was attached to the skin using disposable bi-adhesive foam pads (Spes Medica, Battipaglia, Italy), and the holes corresponding to each electrode were filled with conductive paste to ensure skin-electrode contact (Spes Medica, Battipaglia, Italy).

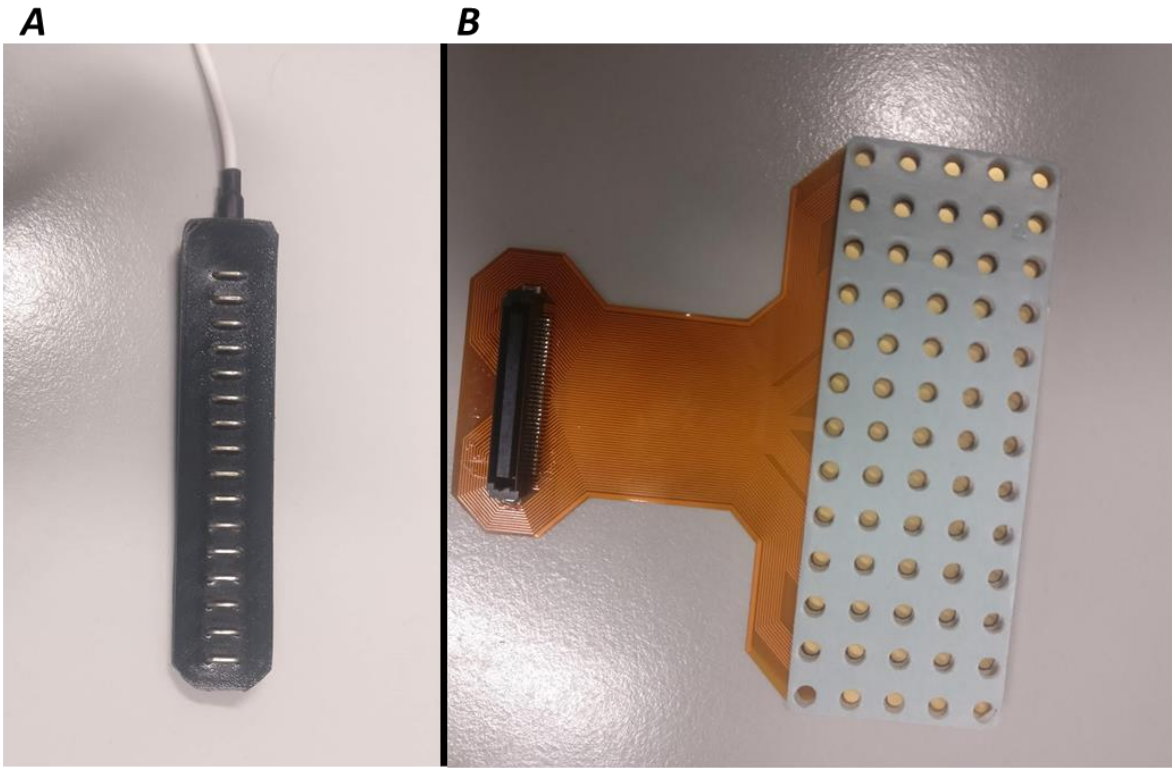

Figure 3.2. *A) Linear non-adhesive 16-bar electrode. B) 64-electrode HDsEMG grid.*

After HDsEMG electrode grid placement, the location was marked on the skin using a surgical pen, and participants were asked to keep the site marked to ensure consistent placement between visits. The electrode grid was further secured over the skin using adhesive dressing tape (Hypafix, BSN medical Ltd, Hull, UK). Strap ground electrodes were dampened with water and placed around the wrists and ankles bilaterally. Two ground electrodes (Nessler Medizintechnik, Innsbruck, Austria) were attached directly to the dynamometer. A further dampened strap electrode was placed around the patella of the right leg, connected to the HDsEMG pre-amplifier, and used as a reference electrode.

HDsEMG signals were acquired in monopolar mode, sampled at 2048 Hz, and converted to digital data by a 12-bit analogue-to-digital converter (EMG-USB2+, 64-channel EMG amplifier; OT Bioelettronica, Torino, Italy; 3 dB, bandwidth 10-500 Hz). EMG signals were amplified using a gain of 500 to 2000. Care was taken to optimise the gain, both on an individual basis and with respect to the contraction level, to maximise the EMG signals without saturating any of the channels, which could affect decomposition results.

Motor Unit Decomposition

The HDsEMG signals obtained for each submaximal contraction were decomposed offline using OT BioLab (v2.0.6775.0, OT Bioelettronica, Torino, Italy; Figure 3.3). The decomposition feature of this software, *Decomponi*, is based on the convolution kernel algorithm which provides semi-automatic decomposition (Holobar & Zazula, 2007; Negro et al., 2016). This algorithm and similar approaches have been validated using simulation models (Holobar et al., 2009) and experimental data across a range of contraction forces in different muscles (Holobar et al., 2014; Marateb et al., 2011). Briefly, the decomposition algorithm differentiates individual motor unit action potentials from the interference signal. The estimated motor unit spike trains were assessed against a silhouette measure (SIL; Negro et al., 2016), which was used as a normalised index of reliability similar to the pulse-to-noise ratio (PNR; Holobar et al., 2014). SIL was initially set at 0.90, and in no case was a SIL

below 0.85 used. Following decomposition, the motor unit spike trains were visually inspected and spike trains exhibiting inter-spike intervals of < 10 ms or > 2 s were discarded before further analysis, along with any duplicated motor units (i.e., after visual inspection, the motor unit displaying the higher coefficient of variation for interspike interval for any units displaying identical action potential waveforms was discarded).

Statistical Analyses

Relevant data were extracted from the original files using MATLAB (The MathWorks, Massachusetts, USA). Statistical analyses for all experimental chapters were carried out using the Statistical Package for Social Sciences (SPSS; v27, SPSS Inc., Chicago, IL, USA). Normality was assessed for all parameters using the Shapiro-Wilk test. Where repeated measures analysis of variance (ANOVA) were used, sphericity was verified with Mauchly's test and the Greenhouse-Geisser correction was applied if this assumption was violated. Effect sizes were calculated as partial eta squared (η_p^2) from the ANOVAs (Cohen, 1973). Specific details relating to data extracted and statistical analyses procedures are outlined in the respective experimental chapters. Statistical significance was set at $P < 0.05$ and all results are presented as mean ± SD, unless otherwise stated.

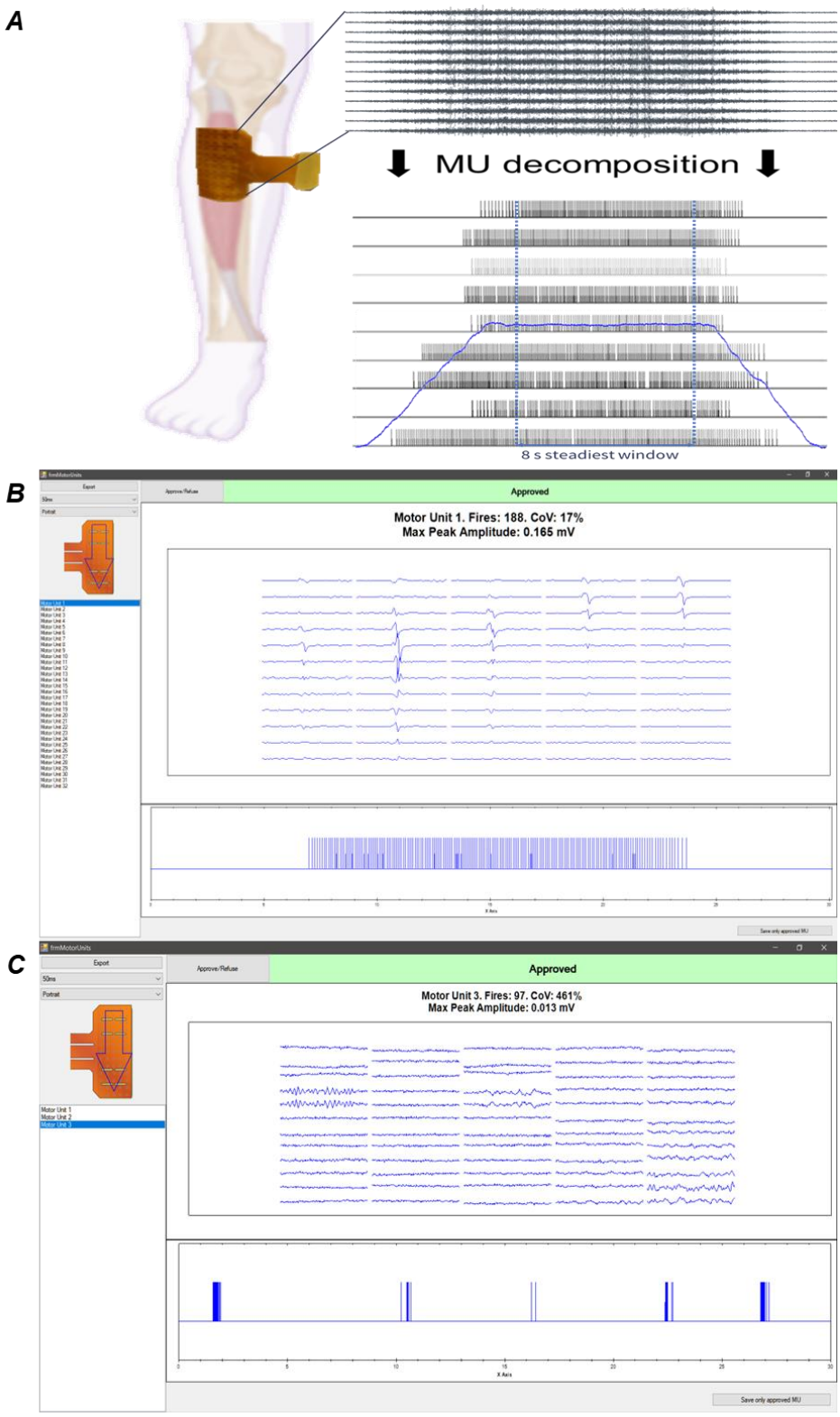

Figure 3.3. *A) Brief overview of the HDsEMG signal decomposition process. In this case, the steadiest 8 s of the contraction was used to analyse motor unit behaviour. Figure created with BioRender.com. The decomposition review window in OT BioLab showing an identified motor unit accepted for further analysis (B) and an identified motor unit discarded before further analysis (C). The SIL was set to 0.90 in both cases. Note the noise apparent in the multichannel surface action potentials of the motor unit identified in C and the sparseness of the motor unit spike train when compared to that of B.*

CHAPTER 4 – METHODOLOGICAL ASPECTS OF HIGH-DENSITY SURFACE ELECTROMYOGRAPHY SIGNAL ACQUISITION IN THE TIBIALIS ANTERIOR MUSCLE DURING ISOMETRIC CONTRACTIONS OF VARYING INTENSITY

Introduction

The use of electromyography (EMG) presents an opportunity to record the action potentials discharged by motor neurons in the form of electrical activity from the muscle fibres (Farina & Negro, 2012). Since the work of Adrian and Bronk (1929), and the use of the concentric needle electrode, it has been possible to identify the shape and firing rate of motor unit action potentials (MUAPs). Over the past four decades, as advances in intramuscular EMG sampling techniques have progressed, several successful attempts have been made to decompose the intramuscular EMG signal using needle electrodes and fine wire electrodes (De Luca & Adam, 1999; Erim & Lin, 2008; Muceli et al., 2015). Despite this, both sampling methods have obvious limitations due to their inherent selectivity and invasive nature, meaning relatively few motor units can be sampled simultaneously, often during low-intensity isometric contractions (Farina & Negro, 2012).

More recently, the development of high-density surface EMG (HDsEMG) decomposition techniques has introduced the possibility of sampling a larger pool of motor unit activity non-invasively (Holobar et al, 2009). However, this larger pool of motor unit activity leads to a more complicated EMG signal than that detected by intramuscular EMG techniques, meaning the classic methods of decomposition have little application and more complex algorithms are needed (Merletti, et al., 2008). One such method that has been developed for HDsEMG decomposition is the convolution kernel compensation (CKC) technique, which uses a blind source separation algorithm (Holobar & Zazula, 2007). The CKC method has subsequently been validated using simulation models (Holobar et al., 2009) and experimental data (Negro et al., 2016) across a range of muscles and contraction forces (between 5% and 70% maximal voluntary contraction; MVC), and also provides reliable estimates of motor unit behaviour both within and between visits (Holobar et al., 2014; Marateb et al., 2011; Martinez-Valdes, Laine et al., 2016).

The sum of the single fibre action potentials within a muscle unit form a compound potential (MUAP), which can be interpreted as biologically amplified neural activity, owing to the one-to-one correspondence between action potentials of the motor neuron and their corresponding MUAPs (Farina & Holobar, 2016). Nevertheless, to detect such action potentials at the surface of the skin using HDsEMG, they must pass through the subcutaneous tissue (termed the volume conductor), which acts as a low-pass filter, deforming the signal and resulting in similar MUAP shapes for different motor units (Farina & Holobar, 2016). Furthermore, when using HDsEMG, the electrode-skin contact itself presents potential problems as the smaller the electrode surface, the greater the impedance and noise (Merletti & Farina, 2016). Therefore, in order to successfully decompose the HDsEMG signal, correct preparation of the electrode-skin interface and the experimental setup is of the utmost importance to ensure the signal-to-noise ratio (SNR) is as high as possible. During pilot work we encountered large amounts of instrument noise attributed to the isokinetic dynamometry setup. Noise levels for reliable HDsEMG decomposition are recommended to be in the order of 10-40 μV RMS, but this can vary with contraction intensity; at low HDsEMG amplitudes signal noise should be no greater than half of the power of the signal (Del Vecchio et al., 2020). One potential solution is to apply one or more ground references directly to equipment, though this is rarely reported (e.g., Martinez-Valdes, Guzman-Venegas et al., 2016).

Whilst previous attempts have been made to investigate the effects of commonly used skin treatments on impedance and noise at the electrode-skin interface, they have been primarily carried out on electrocardiography (ECG) electrodes (Degen & Loeliger, 2007; Grimnes, 1983; Spinelli et al., 2006). To investigate the effects of three commonly used skin treatments on electrode-skin impedance and noise, Piervirgili et al. (2014) used a 4 × 1 surface EMG array. The authors concluded that rubbing with abrasive conductive paste was more effective in reducing both impedance and noise compared to no treatment. However, the measurements were performed on four portions of the same biceps brachii simultaneously to reduce experimental time and shaving was deemed not necessary, potentially limiting the

applicability of the findings to other sites in which the skin is typically covered in hair, such as the tibialis anterior muscle.

The dorsiflexor muscles play an important functional role during human locomotion (Byrne et al., 2007; Hase & Stein, 1998). Though four muscles contribute to ankle dorsiflexion (tibialis anterior, extensor hallucis longus, extensor digitorum longus, and peroneus tertius), the tibialis anterior is typically considered to be the primary dorsiflexor, accounting for almost half (42%) of the generated maximal voluntary torque (Marsh et al., 1981) and is thought to represent 50-66% of the total dorsiflexor cross-sectional area (Fukunaga et al., 1996). Moreover, the superficial morphology and high motor unit yield of the tibialis anterior relative to other leg muscles has resulted in its inclusion in several recent HDsEMG studies (e.g., Castronovo et al., 2015 Del Vecchio, Casolo et al., 2019; Martinez-Valdes, Negro, Farina et al., 2020; Negro et al., 2016).

Once the signal noise is of an acceptable level, the HDsEMG signals recorded during isometric contractions are then subjected to blind source separation decomposition algorithms, for which the reported acceptance criteria can vary. The initial decomposition result is typically assessed against a normalised accuracy index, such as the silhouette measure (SIL; Negro et al. 2016) or the pulse-to-noise ratio (Holobar et al., 2014). After automatic decomposition, the motor unit spike trains are then visually inspected for interspike intervals (the duration between consecutive discharge times) that lie outside a specified duration (e.g., those displaying discharges separated by <10 ms or >250 ms; Castronovo et al., 2018), before being accepted for further analysis. The coefficient of variation for interspike interval (CoV_{isi}) is another index that is commonly used to accept or reject motor unit spike trains, with acceptable CoV_{isi} values of between 30% and 55% reported (Almuklass et al., 2018; Holobar et al., 2014). Though attempts have been made to provide recommendations on the use of HDsEMG in experimental studies (Del Vecchio et al., 2020; Gallina et al., 2022), no definitive consensus exists regarding the standardisation of motor unit decomposition acceptance criteria.

Therefore, the purpose of the current study was to work towards an optimal HDsEMG signal acquisition process in the tibialis anterior to identify individual motor units and their discharge properties during isometric contractions across a range of target torques, including during ramp-and-hold contractions. The study aimed to achieve this by focusing on three fundamental areas: 1) The effects of three different skin treatments on motor unit yield after decomposition. The three skin treatments were: cleaning with water, rubbing using alcohol, and rubbing using an abrasive conductive paste; 2) The effects of different ground electrode configurations on the noise (calculated from the root mean squared value) of the baseline HDsEMG signal; 3) The impact of acceptance criteria on motor unit decomposition yield. It was hypothesised that the use of abrasive paste would result in greater numbers of decomposed motor units across all contraction intensities. Based on prior observations from our own pilot work, we predicted that a greater number of ground electrodes would result in reductions in the noise of the HDsEMG signal. Finally, it also was hypothesised that by using less conservative acceptance criteria during the HDsEMG decomposition process, the motor unit yield would increase.

Methods

Participants

After approval from the SSES REAG at the University of Kent, and in accordance with the *Declaration of Helsinki*, ten healthy, physically active adults (7 male, 3 female; mean ± SD: age 26 ± 3 years; stature 1.76 ± 0.08 m; body mass 67.2 ± 8.5 kg) took part in the study. After being fully advised of the procedures involved in the study, each participant completed a PAR-Q Health Questionnaire and provided written informed consent. Participants were instructed to attend each session well-rested and well-hydrated, not to consume caffeine or eat in the 2 h prior to exercise, and not to consume alcohol or undergo heavy exercise in the preceding 24 h. Participants were also requested to wear shorts to allow access to the tibialis

anterior recording site and to wear the same footwear during each visit to ensure the angle of the ankle remained consistent between experimental sessions.

Experimental Design

Participants were required to visit the laboratory on three occasions, separated by at least 48 hours. Each visit was conducted at the same time of day (± 2 h) to minimise the influence of diurnal variation on muscle contractility (Racinais et al., 2005). The first visit was used to familiarise participants with all equipment, to record the dynamometer settings, and formed the first experimental session. During all visits, participants performed maximal and submaximal (10%, 30%, 50%, and 70% MVC) voluntary contractions to investigate the behaviour of individual motor units during those submaximal contractions following the application of three different skin treatments (a different treatment was applied during each visit, see *Skin Preparation and Treatment*). The order of skin treatments and contraction intensities were randomised.

Experimental Setup

Participants were seated in a Cybex isokinetic dynamometer (HUMAC Norm; CSMi, Stoughton, MA, USA), with the trunk reclined to ~15°, the distal thigh of the right leg strapped to the chair, and the foot firmly strapped into a foot plate for ankle joint torque measurement attached to the dynamometer lever arm. The knee was fully extended and the ankle was fixed in the neutral position (~90°). The dynamometer lever arm, seating position, and foot plate were adjusted to ensure the lateral malleolus was directly in line with the rotational axis of the lever arm (Figure 4.1).

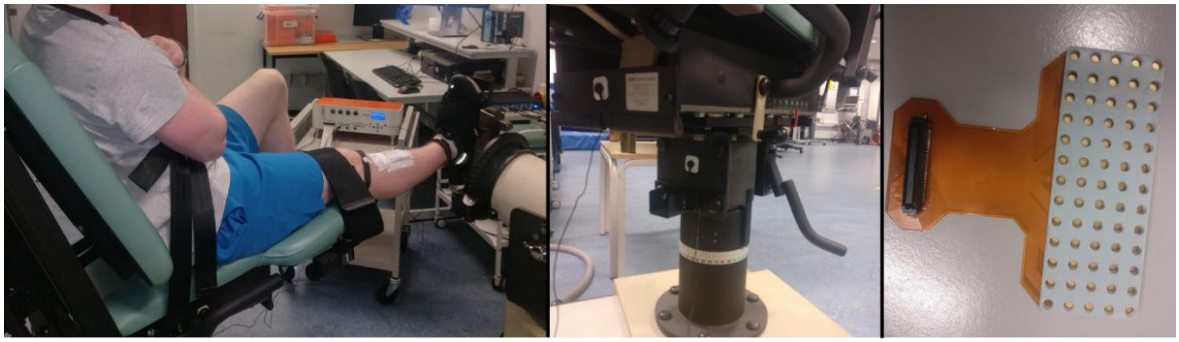

***Figure 4.1**. Experimental setup. Left: Participants were seated in an isokinetic dynamometer with their right foot firmly strapped to a foot plate for ankle joint torque measurement. One high-density grid of electrodes (64 channels) was placed over the tibialis anterior muscle. Middle: The position of the ground electrodes placed on the uppermost and lowermost portions of the underside of the dynamometer chair. Right: The high-density grid of electrodes (64 channels).*

Surface HDsEMG signals were acquired from the tibialis anterior muscle using the methods described in Chapter 3. A strap electrode, dampened with water, was placed over the malleolus of the right leg, and used as the main ground electrode. A second dampened strap electrode was placed around the patella of the right leg, connected to the HDsEMG pre-amplifier, and used as a reference electrode. The outline of the HDsEMG grid was marked on the skin using a surgical pen, and each participant was asked to keep the area marked to allow consistent positioning of the grid across visits.

Skin Preparation and Treatment

Before HDsEMG electrode grid placement, the skin over the tibialis anterior muscle of the right leg was prepared using one of three different treatments, randomised for each visit: (a) the skin was shaved and cleaned with water (WAT); (b) the skin was shaved and rubbed using a 70% alcohol swab (ALC); (c) the skin was shaved, rubbed using medical grade abrasive paste (Spes Medica, Genova, Italy) and a cotton wool pad then cleaned with water (ABR).

Ground Electrode Configuration

A further three dampened electrode straps were placed on the following locations and in the following order: the styloid process of the ulna of the right arm, the styloid process of the ulna on the left arm, and the malleolus of the left leg. Two additional adhesive Ag/AgCl electrodes (32 mm × 32 mm; Swaromed, Nessler Medizintechnick, Innsbruck, Austria) were placed on the uppermost and lowermost portions of the underside of the dynamometer chair (Figure 4.1; middle). During the first visit, baseline HDsEMG was recorded over six 5 s periods of rest to calculate signal noise. This started with only the first ground electrode strap previously mentioned in *Experimental Setup*. Participants completed five more 5 s resting periods with each additional ground electrode iteratively added to the existing configuration.

Experimental Protocol

After the placement of the HDsEMG electrode grids, participants completed a short warm-up before performing three brief (~3 s) ankle dorsiflexion MVCs to measure maximal torque, each separated by 2 min of rest. The highest torque value achieved in each session was used as a reference value for the definition of the subsequent submaximal torque targets. After 5 min of rest, participants completed ramp-and-hold contractions (requiring a 5 s increase in torque, 10 s hold phase, and a 5 s decrease in torque; Figure 4.2A) and ‘rectangular’ 20 s contractions (participants increased torque from rest to the target line and maintained a steady contraction for 20 s; Figure 4.2B) at 10%, 30%, 50%, and 70% MVC, in a randomised order, with rest periods of 2, 3, 4, and 5 min between contractions, respectively. The target torque was projected onto a large screen ~2 m away from the participant.

Data Acquisition

High-density Surface Electromyography: HDsEMG signals were sampled at 2048 Hz and converted to digital data by a 12-bit analogue-to-digital converter (EMG-USB2+, 64-channel EMG amplifier; OT Bioelettronica, Torino, Italy; 3 dB, bandwidth 10-500 Hz). HDsEMG signals were amplified using a gain of 2000, 1000, 500, and 500 for the contractions at 10%, 30%, 50%, and 70% MVC, respectively.

Torque: Torque data was acquired using Spike2 (Version 7; Cambridge Electronic Design, Cambridge, UK) via a CED Micro 1401-3 (Cambridge Electronic Design, Cambridge, UK) with a personal computer and was sampled at 1000 Hz.

Data Processing

Motor Unit Decomposition: The HDsEMG signals acquired during each submaximal isometric contraction were decomposed offline using OT BioLab (OT Bioelettronica, Torino, Italy) as described in the General Methods (Chapter 3). Each motor unit spike train was initially only considered acceptable if the SIL was greater than 0.90. Additionally, only motor unit spike trains with a coefficient of variation of inter-spike interval (CoV_{isi}) ≤ 30% were used for further analysis (Holobar et al., 2014). The acceptance criteria used here will be referred to as SIL = 90 hereafter.

The HDsEMG signals from contractions performed during the ABR visit were reprocessed using less conservative selection criteria (referred to hereafter as SIL = 85). The ABR skin treatment was chosen based on the recommendations of Piervirgili et al. (2014). The SIL was lowered to 0.85 (Afsharipour et al., 2020; Murphy et al., 2019) and the CoV_{isi} raised to ≤ 55% (Almuklass et al., 2018). Any motor unit spike trains with discharges separated by > 2 s (Del Vecchio, Úbeda, et al., 2018) or < 10 ms (Castronovo et al., 2018) were excluded from further analysis, along with any duplicated motor units (i.e., after visual inspection, the motor unit displaying the higher CoV_{isi} for any units displaying identical action potential waveforms was discarded).

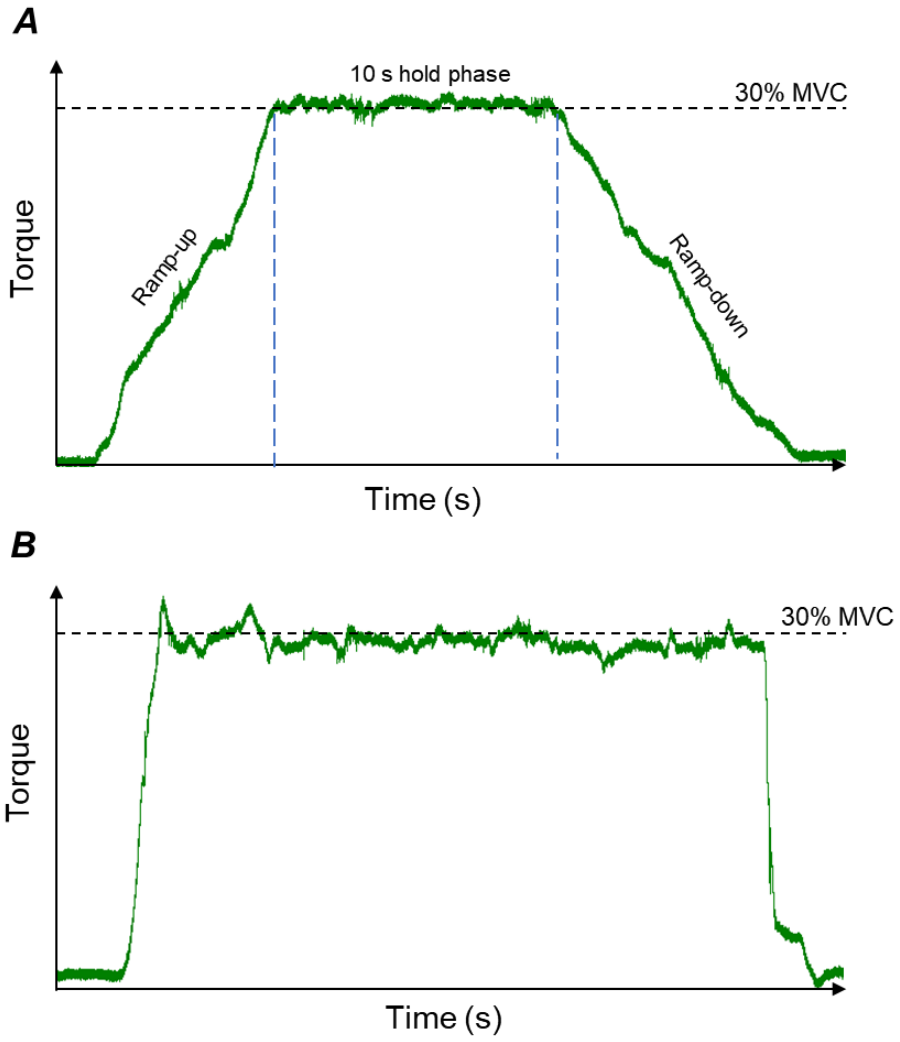

Figure 4.2. *Contractions performed at 30% MVC for a representative participant. A) A ramp-and-hold contraction with a 5 s ramp-up phase, 10 s hold phase, and a 5 s ramp-down phase. B) A 20 s 'rectangular' contraction.*

The number of motor units during each contraction, identified by their discharge times, and the global discharge rate (the mean discharge rate observed between 5 and 15 s during the 20 s contractions and during the hold phase of the ramp-and-hold contractions) were used as the main outcome variables. The root mean square HDsEMG amplitude (EMG_{RMS}) was calculated as a 64-channel average value and from the central channel of the HDsEMG electrode grid using 0.5 s epochs from the 5 s of rest at each ground electrode configuration.

Statistical Analysis

One-way ANOVAs were performed to ascertain whether there were significant differences in motor unit numbers and global discharge rates at each contraction intensity between sessions (and skin treatments). One-way repeated-measures ANOVA was also performed to determine if the EMG_{RMS} differed between ground electrode configurations. The motor unit numbers of the reanalysed ABR contractions were compared using Student's paired-samples *t*-tests. If normality was violated, the Wilcoxon signed-rank test was performed instead.

Results

Motor Unit Numbers and Skin Treatment

The results of the one-way repeated-measures ANOVA showed no effect of skin treatment on the number of decomposed motor units observed between for the ramp-and-hold contractions at 10% ($F_{2, 18} = 0.047$, $P = 0.954$, $\eta_p^2 = 0.005$), 30% ($F_{2, 18} = 1.737$, $P = 0.204$, $\eta_p^2 = 0.162$), or 50% MVC ($F_{2, 18} = 0.679$, $P = 0.52$, $\eta_p^2 = 0.07$; Figure 4.3). Mauchly's test indicated that the assumption of sphericity had been violated for 70% MVC ($\chi^2(2) = 11.61$, $P = 0.003$), therefore, degrees of freedom were corrected using Greenhouse-Geisser estimates of sphericity ($\varepsilon = 0.57$). There was no significant effect of skin treatment on the number of decomposed motor units for the 70% MVC ramp-and-hold contraction ($F_{1.1, 10.1} = 0.84$, $P = 0.394$, $\eta_p^2 = 0.09$; Figure 4.3). Similarly, no significant effect of skin treatment on numbers of decomposed motor units were observed for the 20 s contractions at 10% ($F_{2, 18} = 0.553$, $P = 0.585$, $\eta_p^2 = 0.058$), 30% ($F_{2, 18} = 0.553$, $P = 0.585$, $\eta_p^2 = 0.058$), 50% ($F_{2, 18} = 1.565$, $P = 0.236$, $\eta_p^2 = 0.148$), or 70% MVC ($F_{2, 18} = 0.61$, $P = 0.556$, $\eta_p^2 = 0.06$; Figure 4.3).

Global Motor Unit Discharge Rate

There were no significant effects of skin treatment on global motor unit discharge rate observed for the ramp-and-hold contractions at 10% (n = 7; $F_{2, 12}$ = 2.099, P = 0.165, η_p^2 = 0.259), 30% (n = 6; $F_{2, 10}$ = 1.155, P = 0.354, η_p^2 = 0.188), 50% (n = 4; $F_{2, 6}$ = 0.896, P = 0.456, η_p^2 = 0.23; Figure 4.4, left). For the ramp-and-hold contractions at 70% MVC, motor units were identified for only one participant across the three conditions, meaning the ANOVA could not be conducted. Likewise, there were no significant effects of skin treatment on global motor unit discharge rate observed for the 20 s contractions at 10% (n = 9; $F_{2, 16}$ = 0.807, P = 0.463, η_p^2 = 0.092), 30% (n = 9; $F_{2, 16}$ = 1.209, P = 0.324, η_p^2 = 0.131), 50% (n = 6; $F_{2, 10}$ = 0.514, P = 0.613, η_p^2 = 0.093; Figure 4.4, right). For the 20 s contractions at 70% MVC, motor units were identified for only two participants across all three conditions, meaning the ANOVA was not conducted.

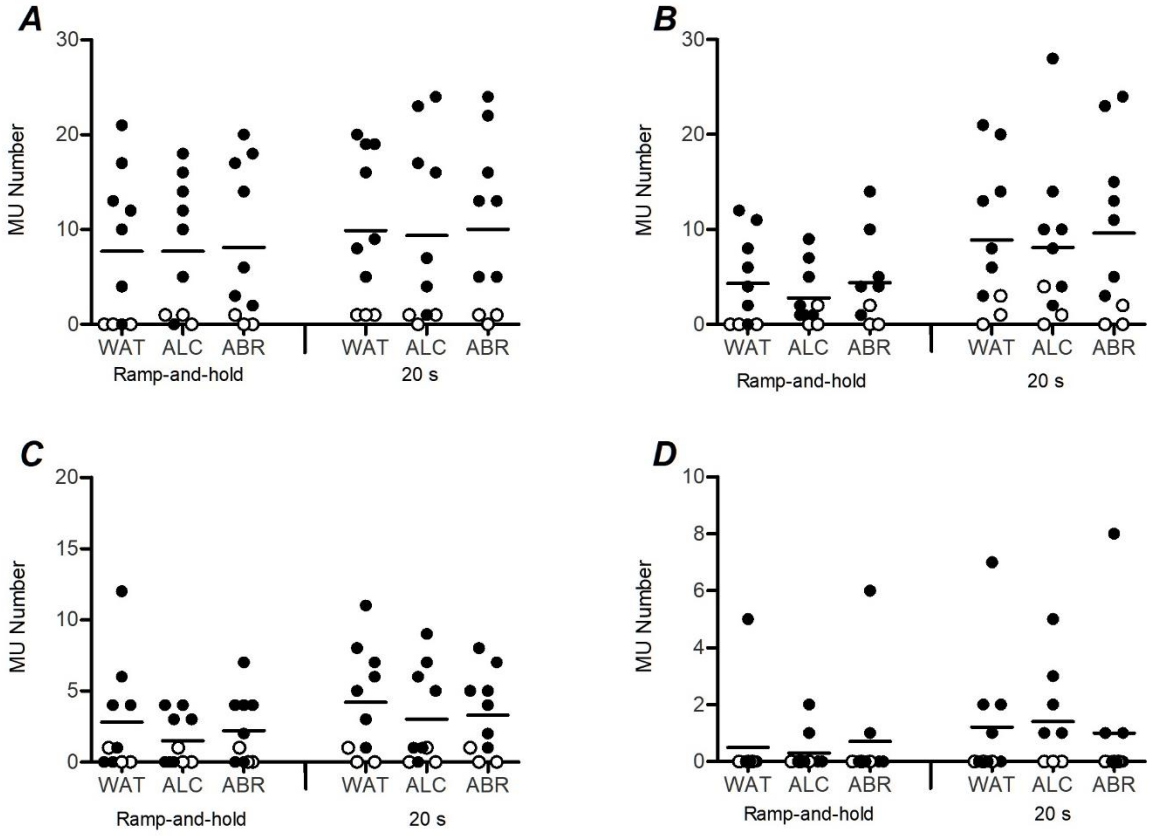

***Figure 4.3**. Individual values for decomposed motor unit numbers in the tibialis anterior. Values are presented for both ramp and hold (5 s up, 10 s hold, 5 down) and 20 s contractions at all torque levels, including A) 10%, B) 30%, C) 50%, and D) 70% of the maximal voluntary contraction across the three skin treatment sessions. Open circles represent female participants; male participants are represented by filled circles. Horizontal lines indicate the mean. Error bars omitted for clarity.*

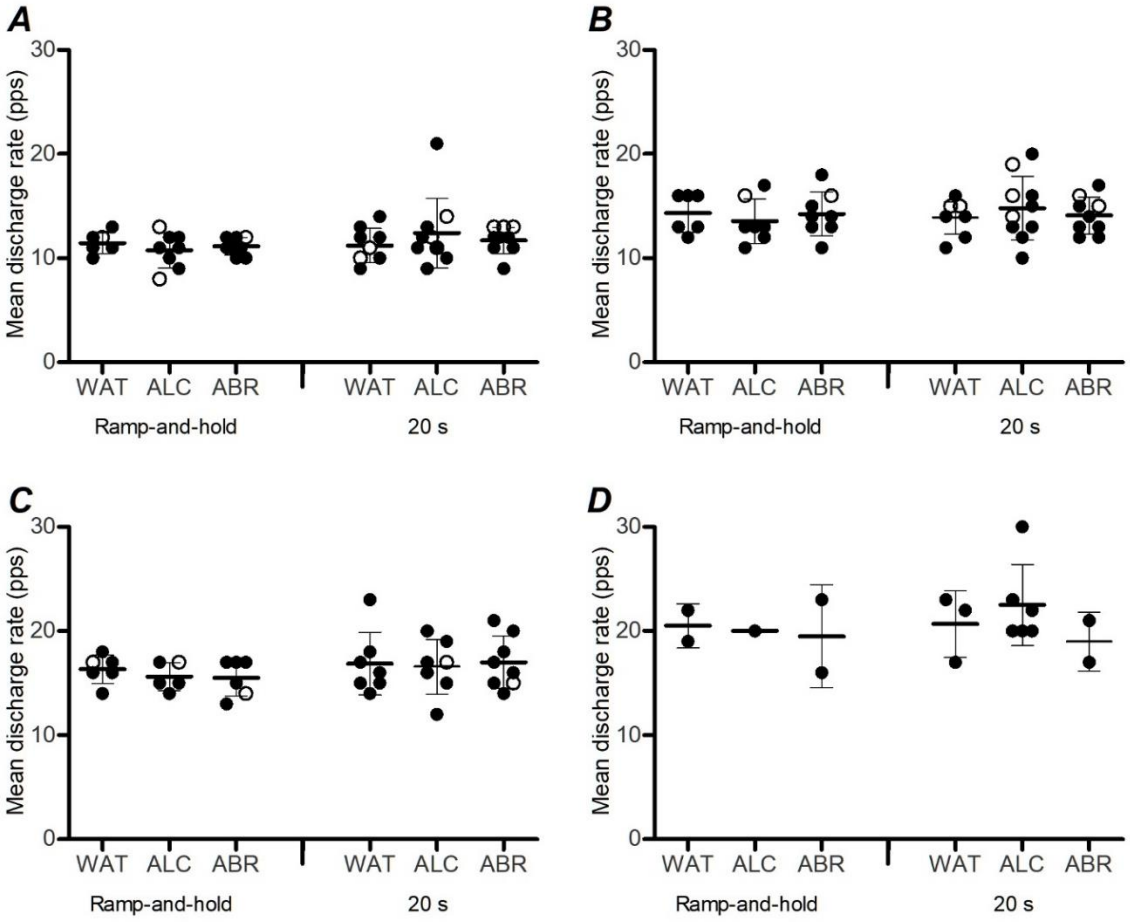

Figure 4.4. *Individual values for global motor unit discharge rate identified in the tibialis anterior. Values are presented for both ramp-and-hold (5 s up, 10 s hold, 5 down; left) and 20 s contractions (right) at all torque levels (10%, 30%, 50%, and 70% of the maximal voluntary contraction) across the three skin treatment sessions. Open circles represent female participants; male participants are represented by filled circles. Horizontal lines represent the mean and error bars represent the SD.*

Ground Reference Configuration and Signal Noise

64-channel average: The assumption of sphericity was violated, as assessed by Mauchly's test of sphericity, $\chi^2(2) = 30.59$, $P = 0.009$. Therefore, a Greenhouse-Geisser correction was applied ($\varepsilon = 0.483$). Results of the one-way repeated-measures ANOVA showed that there was a significant main effect of ground electrode configuration on the 64-channel average EMG_{RMS} ($F_{2.4,\ 21.7} = 42.988$, $P < 0.001$, $\eta_p^2 = 0.827$). Bonferroni post-hoc tests showed that EMG_{RMS} with six ground electrodes (14.5 ± 5.7 µV) was significantly lower than configurations with one (39.0 ± 7.6 µV; $P < 0.001$), two (26.3 ± 8.5 µV; $P = 0.016$), and three (22.6 ± 6.6 µV; $P = 0.017$) ground electrodes. However, no significant differences in EMG_{RMS} were

observed when 6 ground electrodes were compared to configurations consisting of four (18.6 ± 5.0 µV; $P > 0.05$) or five (14.8 ± 4.3 µV; $P > 0.05$) ground electrodes.

Central channel of HDsEMG electrode grid: The assumption of sphericity was violated, as assessed by Mauchly's test of sphericity, $\chi^2(2) = 34.47$, $P = 0.003$. Therefore, a Greenhouse-Geisser correction was applied ($\varepsilon = 0.474$). Results of the one-way repeated-measures ANOVA showed that there was a significant main effect of ground electrode configuration on the 64-channel average EMG_{RMS} ($F_{2.4, 21.3} = 37.49$, $P < 0.001$, $\eta_p^2 = 0.806$). Bonferroni post-hoc tests showed that EMG_{RMS} with six ground electrodes (11.9 ± 5.2 µV) was significantly lower than configurations with one (39.8 ± 10.6 µV; $P < 0.001$), two (25.0 ± 7.8 µV; $P = 0.022$), and three (21.6 ± 6.0 µV; $P = 0.021$) ground electrodes. However, no significant differences in EMG_{RMS} were observed when six ground electrodes were compared to configurations consisting of four (15.8 ± 4.5 µV; $P > 0.05$) or five (11.7 ± 2.7 µV; $P > 0.05$) ground electrodes.

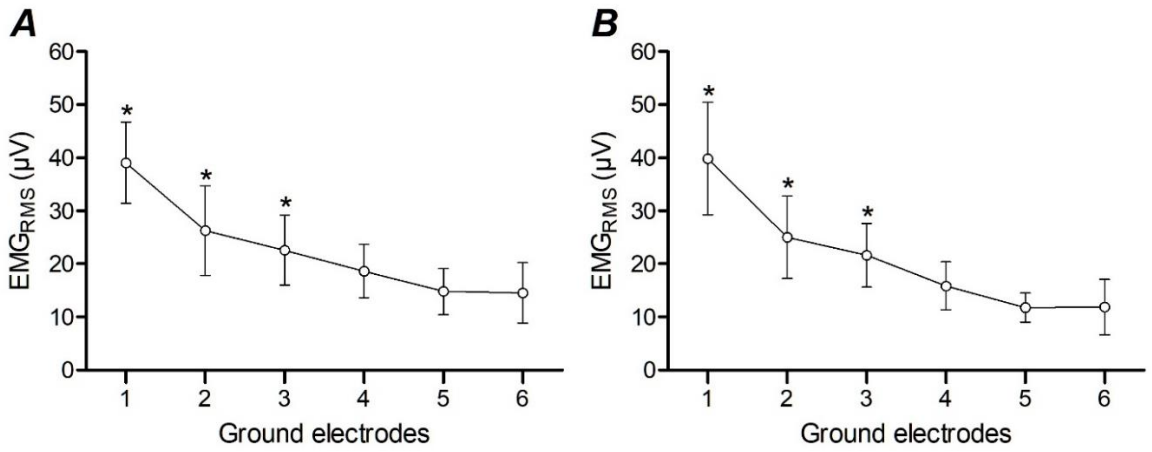

Figure 4.5. *HDsEMG 64-channel average (A) and middle-channel (B) EMG_{RMS} (µV) values recorded at rest using the following iterative ground electrode configurations: 1) Strap electrode placed over the malleolus of the right leg; 2) Strap electrode placed over the styloid process of the ulna of the right arm; 3) Strap electrode placed over the styloid process of the ulna of the left arm; 4) Strap electrode placed over the malleolus of the left leg; 5) Ag/AgCl electrode placed on the uppermost portion of the underside of the dynamometer chair; 6) Ag/AgCl electrode placed on the lowermost portion of the underside of the dynamometer chair. * significantly different from the configuration using 6 ground electrodes.*

HDsEMG Decomposition Acceptance Criteria

Group mean and individual values for the motor units decomposed after the different acceptance criteria were used are shown for each contraction intensity in Figure 4.6. A significantly greater number of motor units were decomposed when the adjusted acceptance criteria was applied (SIL = 85) compared to the original acceptance criteria (SIL = 90) for ramp-and-hold contractions performed at 10% (12 ± 10 vs 8 ± 8; mean difference, 95% CIs: 4; 2, 6; t = 4.06, P = 0.003), 30% (11 ± 8 vs 4 ± 4; mean difference, 95% CIs: 7; 4, 9; t = 5.20, P < 0.001), and 50% MVC (5 ± 4 vs 2 ± 2; mean difference, 95% CIs: 3; 2, 5; t = 4.40, P = 0.002). Normality was violated for the values at 70% MVC, therefore the Wilcoxon signed-rank test was performed. For the ramp-and-hold contractions performed at 70% MVC, there was a significant median increase in the number of motor units after decomposition for SIL = 85 compared to SIL = 90 (median difference: 1; z = 2.80, P = 0.005).

Likewise, significantly more motor units were decomposed when the adjusted acceptance criteria was applied (SIL = 85) compared to the original acceptance criteria (SIL = 90) for 20 s contractions performed at 10% (15 ± 10 vs 10 ± 9; mean difference, 95% CIs: 5; 3, 6; t = 5.24, P < 0.001) and 30% MVC (15 ± 10 vs 10 ± 9; mean difference, 95% CIs: 5; 3, 7; t = 5.02, P < 0.001). Normality was violated for the values at 50% and 70% MVC, therefore the Wilcoxon signed-rank test was performed. There were significantly more motor units decomposed for SIL = 85 compared to SIL = 90 during the 20 s contractions performed at 50% MVC (median difference: 4; z = 2.67, P = 0.009) and 70% MVC (median difference: 3; z = 2.52, P = 0.014).

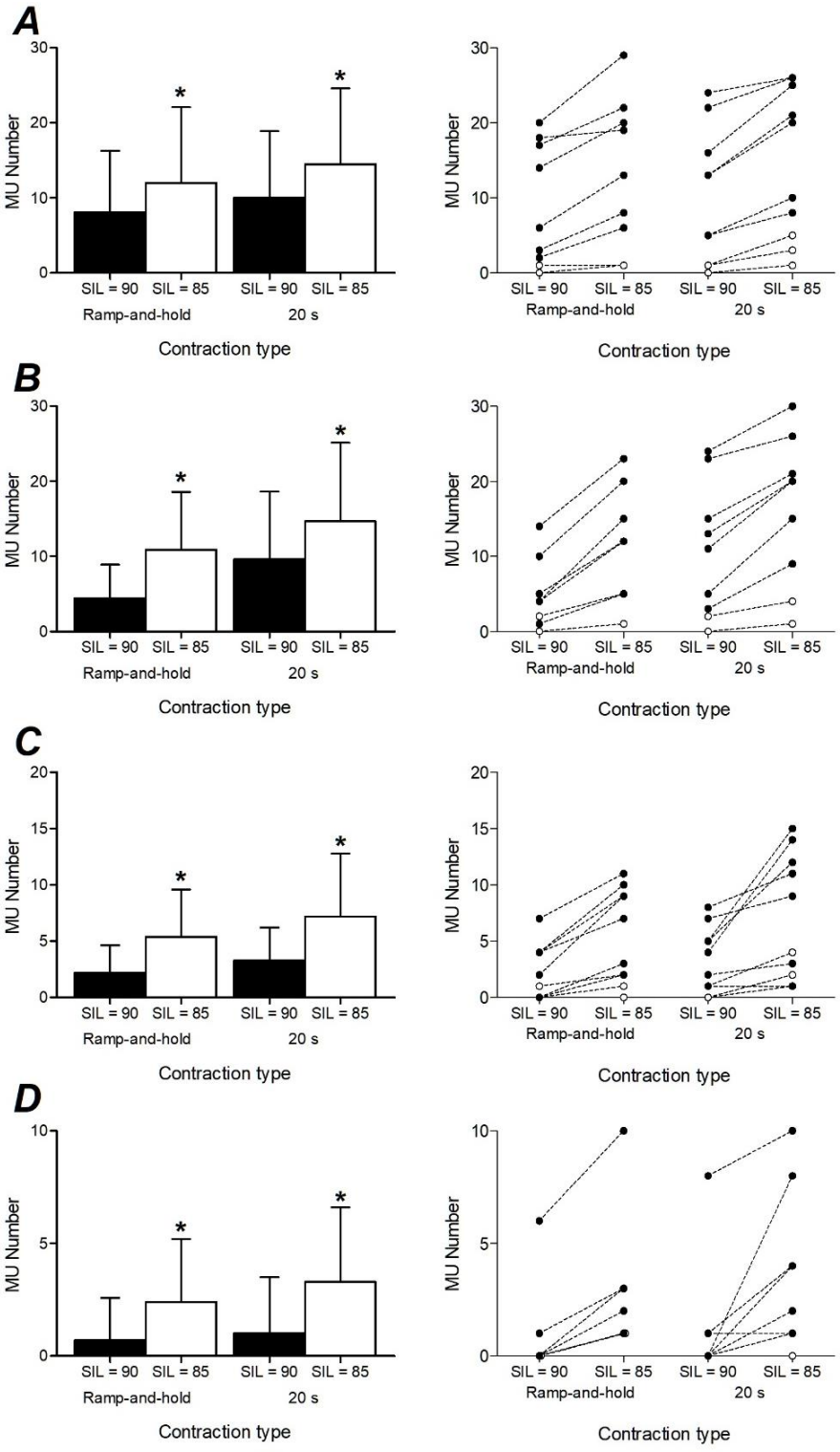

Figure 4.6. *Group mean and individual values for the number of decomposed motor units in the tibialis anterior from the ABR visit using the original acceptance criteria (SIL = 90) and the adjusted acceptance criteria (SIL = 85). Values are presented for both ramp-and-hold and 20 s contractions at all torque levels: A) 10%, B) 30%, C) 50%, and D) 70% maximal voluntary contraction). Values in the panels to the left are mean ± SD. Values in the panels to the right are individual responses. Open circles represent female participants; male participants are represented by filled circles. Note the consistently smaller values for female participants, even after the adjusted acceptance criteria was applied. * significantly different from the value obtained using SIL = 90. MU, motor unit; SIL, silhouette measure.*

Discussion

The present study aimed to investigate the effects of different skin treatments on the number of decomposed motor units of the tibialis anterior during isometric dorsiflexion contractions of varying intensity. No differences were observed between skin treatments for motor unit numbers or global motor unit discharge rates across all isometric contraction types and intensities. These findings suggest that during both ramp-and-hold and 20 s sustained isometric contractions, the effect of the three skin treatments on the material outcomes of motor unit decomposition is negligible. A secondary aim of the study investigated the effects of different ground electrode configurations on the baseline noise of the HDsEMG signal using the current experimental setup. Additionally, at least for the experimental setup employed in the current study, the use of up to four ground electrodes resulted in significant reductions to the baseline noise of the HDsEMG signal, suggesting that the quality of the HDsEMG signal is reduced below this number.

The data of the present study demonstrate that investigators using this technique should consider using at least four ground electrodes in various locations to maximise the signal-to-noise ratio. The current study also aimed to establish if the application of less conservative acceptance criteria (SIL = 85) resulted in a greater motor unit yield after HDsEMG decomposition when compared to the original acceptance criteria (SIL = 90). Motor unit yield was significantly greater across all contraction intensities, suggesting that, provided caution is applied (e.g., visual inspection of each motor unit spike train after automatic decomposition), this approach can improve motor unit yield.

Skin Preparation

Although most previous studies focusing on the effects of commonly used skin treatments on impedance and noise at the electrode-skin interface have been carried out using ECG electrodes (e.g., Spinelli et al., 2006), to the best of our knowledge, just one study has used a surface EMG array (Piervirgili et al., 2014).

Of the skin treatments used by Piervirgili et al. (2014), only the use of abrasive conductive paste resulted in reductions in both noise and impedance when compared to no treatment. However, the results of the present study suggest that regardless of any reductions in noise or impedance (not measured in the current study), there may be no material effect on motor unit decomposition outcomes between the skin treatments used, provided that the skin is carefully shaved and cleaned as part of the preparatory process. Both motor unit numbers and discharge rates were comparable across conditions, suggesting that similar populations of motor units were sampled during each visit, and no shift toward the identification of lower or higher threshold motor units was present.

Signal Acquisition

During pilot work we encountered substantial instrument noise from the Cybex isokinetic dynamometer used in this study. While other research groups have used similar isokinetic dynamometer setups (e.g., Biodex System 3; Castronovo et al. 2015; Martinez-Valdes Negro, Farina et al., 2020), custom-made ankle dynamometers or load cell setups are commonly used instead (e.g., Del Vecchio et al., 2019; Taylor et al., 2022). However, because a custom-built setup was not an option within our laboratory, this necessitated the systematic approach to reduce baseline HDsEMG signal noise employed in the present study. Using a similar approach to Martinez-Valdes, Guzman-Venegas et al. (2016), we applied ground references bilaterally to the wrists and ankles, while also referencing the dynamometer in two locations. This iterative application of ground references to both wrists and ankles in the current study reduced the baseline HDsEMG signal noise toward the lower end of the recommendations (signal noise of between 10-40 µV EMG_{RMS}) of Del Vecchio et al. (2020). While there were no additional significant reductions after the application of further electrodes to the base of the dynamometer, baseline noise was ~15 µV, and all but three participants demonstrated a trend toward lower values when the fifth and sixth ground references were applied. This study is the first to systematically investigate the effect of ground electrode configuration on HDsEMG signal noise, and we recommend that future work using a similar experimental setup to ours (i.e., a Cybex isokinetic

dynamometer) should use at least four ground electrodes to improve the quality of the HDsEMG signal ahead of acquisition.

HDsEMG Decomposition Acceptance Criteria

Due to the consistently low motor unit yields for female participants in the current study (discussed separately below), only data from male participants will be discussed here. During the initial analysis (SIL = 90) for the contractions performed at 10% MVC in the present study, it was possible to identify an average of 11 and 14 motor units during the ramp-and-hold and 20 s contractions, respectively. For the contractions performed at 30% MVC, it was possible to identify an average of 6 and 13 motor units during the ramp-and-hold and 20 s contractions, respectively. However, there was considerable variance in the motor unit yield between male participants in the present study, and for some participants no motor units were identified, even at the lowest torque targets (Figure 4.3).

It is difficult to compare motor unit yields directly with those of other studies due to reporting inconsistencies (e.g., average motor units per participant reported across all tasks rather than at each contraction intensity; Del Vecchio, Ubeda et al., 2018) and methodological differences (e.g., sustained isometric contractions at different intensities; Castronovo et al., 2015). Nevertheless, the mean numbers of identified motor units in the present study are lower than those reported by Castronovo et al. (2015), who reported 21 motor units per participant across all contraction forces (20, 50, and 70% MVC), and Castronovo et al. (2018) who reported 18 motor units per participant during contractions held for 30 s at 20% MVC. Likewise, Del Vecchio and Farina (2019) reported ~21, ~19, and ~14 identified motor units for ramp-and-hold contractions performed at 35, 50, and 70%, respectively. More recently, Martinez-Valdes Negro, Farina et al. (2020) reported 14 motor units per participant were tracked during ramp-and-hold contractions performed at 20% MVC and 11 for contractions at 70% MVC.

When the adjusted decomposition criteria (SIL = 85) was applied, average motor unit yields increased to 17 (ramp-and-hold contraction at 10% MVC) and 19 (20 s contraction at 10% MVC), and 15 (ramp-and-hold contraction at 30% MVC) and 20 (20 s contraction at 30% MVC), which is more in line with those reported in the aforementioned studies. At SIL = 85, considerable variance was still evident, with just 5-6 motor units detected for some participants during the contractions performed at 10% and 30% MVC (Figure 4.6A-B). Though the tibialis anterior muscle is thought to be covered by lower levels of adipose tissue than other lower limb muscles (e.g., the vasti muscles), it is possible that participant-specific differences may have influenced the decomposition algorithm (Holobar et al., 2014). Such a relationship remains to be confirmed for the tibialis anterior muscle.

The coherence between common input and the low-frequency (< 10 Hz) content of the cumulative spike train (the summed discharge trains of concurrently active motor units) approaches unity when ~10 motor units are decomposed, therefore this number is likely sufficient to infer the control signal, or neural drive, to the muscle (Farina & Negro, 2015; Farina, Negro et al., 2014). Using the original decomposition processing criteria, only one participant yielded ≥ 10 motor units across all contractions at 50% (Figure 4.3C), and at 70% MVC no participant reached this value (Figure 4.3D). This finding suggests that using the current experimental setup, contractions should be performed below 50% MVC to obtain motor unit yields high enough to sufficiently infer the neural drive to muscle.

Low Motor Unit Yields in Female Participants

In female participants, the majority of contractions resulted in just one or two motor units being identified, regardless of contraction intensity or treatment. In only one contraction in one participant were more than three motor units decomposed during the initial analysis (four motor units were identified for the ALC 20 s contraction performed at 30% MVC; Figure 4.3B). Even after adjustments were made to the HDsEMG decomposition acceptance criteria, female participants yielded fewer than half the amount of motor units when compared to males, with only one participant

yielding five motor units (Figure 4.6A-B). Low motor unit yields in female participants have recently been reported elsewhere (Afsharipour et al., 2020; Del Vecchio et al., 2020; Hug et al., 2021; Taylor et al., 2022), suggesting that, when compared to those of male participants, the motor unit populations of females are more difficult for HDsEMG decomposition algorithms to identify.

One potential explanation for such findings might be sex differences in human adipose tissue, as females are generally thought to have higher levels of adipose tissue than males (Karastergiou et al., 2012). Previous simulation studies have suggested that a greater subcutaneous fat layer introduces unwanted low-pass filtering effects on the surface EMG signal (Farina et al., 2002; Farina & Holobar, 2016; Kuiken et al., 2003). However, Taylor et al. (2022) observed no sex differences between body mass index (BMI), and reported that females with the lowest motor unit yield also had the lowest body mass index. That said, BMI does not the reflect subcutaneous fat under the electrode, and further work is warranted to understand the poor motor unit yield in female participants.

Ultrasound measurements can provide an accurate estimate of the thickness of the subcutaneous layer (Holobar et al., 2010; de Oliveira et al., 2022; Trevino et al., 2019), but were not used in the current study. The use of ultrasound and magnetic resonance imaging has recently been used to demonstrate that subcutaneous tissue in the biceps brachii muscle is negatively correlated with motor unit yield, particularly at low forces (de Oliveira et al., 2022). It is unclear whether this supposition holds for the subcutaneous tissue over the tibialis anterior muscle in female participants, but Trevino et al. (2019) reported no significant differences in vastus lateralis subcutaneous fat levels between males and females. Therefore, the reason for the sex difference in motor unit yields reported here and elsewhere remains unclear, and future work should urgently investigate this.

Limitations

While the current study investigated the effects of different skin treatments on the functional outcome measure of the number of decomposed motor units, the impedance of the electrode-gel-skin contact was not measured. Piervirgili et al. (2014) used a custom-built impedance meter and a low noise amplifier in order to measure impedance and noise of the electrode-gel-skin contact after the application of different skin treatments. Such a setup was not available in the current study and as such we opted to focus on direct motor unit decomposition outcomes instead (i.e., the number of motor units decomposed and their discharge rates). Additionally, the lack of a dedicated familiarisation visit may have impacted upon participants' ability to accurately match the torque targets, particularly during the contractions at the highest (70% MVC) torque target values. Nevertheless, participants were given time at the beginning of the first visit to become accustomed to the contraction protocols and progression to experimental recordings was only made once task proficiency was demonstrated (i.e., participants were able to smoothly track the ramp-and-hold contractions).

The HDsEMG and torque signals were not synchronised in the present study due to difficulties delivering a trigger signal from the torque acquisition system to the HDsEMG amplifier. This meant that outcome measures such as recruitment threshold (the torque value at which a motor unit first discharges) and de-recruitment threshold could not be calculated. Furthermore, synchronisation of the HDsEMG and torque signals is necessary for investigations into the neural control of muscle torque, such as the concurrent analysis of the low-pass filtered cumulative spike train of discharge times from identified motor units and the muscle torque signal (Farina & Negro, 2015).

Conclusions

The current study demonstrated that motor unit yield or global discharge rates of the tibialis anterior did not differ between different skin treatments during dorsiflexion contractions of varying intensity. Additionally, incremental reductions in the

HDsEMG signal noise were observed with increasing numbers of ground electrodes, suggesting investigators using a similar experimental setup to that employed in the present study should use at least four ground references for each participant. Finally, motor unit yield was increased across all participants when the HDsEMG decomposition acceptance criteria was widened, though low yields were still obtained for female participants relative to males. Together, these data will help to inform similar experimental setups used in future work, including the subsequent experimental chapters of the present thesis.

CHAPTER 5 – LOSS OF MOTOR UNIT CUMULATIVE SPIKE TRAIN COMPLEXITY AND ANKLE TORQUE COMPLEXITY DURING FATIGUING DORSIFLEXOR CONTRACTIONS IN HUMANS

Introduction

Neuromuscular fatigue, defined as a loss of maximal voluntary contraction (MVC) force or torque that is reversible by rest (Allen et al., 2008; Enoka & Ducheteau, 2008; Gandevia, 2001; also termed “performance fatigability” Enoka & Ducheteau [2016]), has profound effects on the neuromuscular system. Fatigue is usually a combination of functional decline of central (events proximal to the neuromuscular junction, including spinal and supraspinal processes; Gandevia, 2001) and peripheral origin (events distal to the neuromuscular junction, including declines in excitation–contraction coupling and cross–bridge turnover; Allen et al., 2008). The rate at which performance fatigability develops is strongly influenced by exercise intensity. Specifically, during intermittent contractions performed to task failure above the so–called “critical torque” (CT; Burnley, 2009), an intensity known as the severe domain, peripheral fatigue develops 4-5 times faster than during contractions just below CT (i.e., the heavy domain; Burnley et al., 2012). It is therefore important to ensure that contractions are performed definitively below or above the CT.

The development of performance fatigability involves a number of feedback loops within and between the muscle and central nervous system (CNS), and results in a loss of motor control, originally identified as a decline in force or torque steadiness (Furness et al. 1977; Galganski et al. 1993), quantified by an increase in the standard deviation (SD) and coefficient of variation (CV) of force around a target value (Galganski et al. 1993; Hunter & Enoka, 2003; Contessa et al. 2009). Recently, we have demonstrated that the temporal pattern of knee extensor torque fluctuations (the “complexity” of torque output) changes in a characteristic fashion when relatively high–intensity contractions are performed (Pethick et al., 2015). The complexity of torque output decreases (measured using approximate entropy, ApEn, [Pincus, 1991] and detrended fluctuation analysis, DFA [Peng et al., 1994]. These statistics characterise the regularity and noise colour of a time series, respectively). Simply put, the torque fluctuations become more regular and tend towards Brownian noise as fatigue progresses (Pethick et al., 2015; Pethick et al., 2016).

The functional significance of the fatigue-induced loss of torque complexity is that the ability of the neuromuscular system to respond to external perturbations (such as changing torque demands during typical motor activity) is reduced. In other words, the neuromuscular system becomes less adaptable (Peng et al., 2009). Fatigue has been shown to result in reduced force steadiness (Contessa et al., 2009) and increased error during tracking tasks (Huysmans et al., 2008). Furthermore, task failure during fatiguing intermittent contractions is associated with low torque output complexity (Pethick et al., 2015). For example, during intermittent contractions performed above the critical torque, the complexity of torque output declines to similarly low levels at task failure irrespective of the absolute torque demands of the task (Pethick et al., 2016; Pethick, Winter et al., 2020). The mechanism which underpins the fatigue-induced loss of complexity is presently unclear, but the fact that these effects are only evident during relatively high-intensity contractions suggests that peripheral fatigue mechanisms are a significant contributor (Pethick et al., 2016). Nevertheless, we have also demonstrated that caffeine ingestion can blunt the fall in knee extensor complexity without altering the rate of peripheral fatigue development (Pethick et al., 2018a), suggesting that central mechanisms can also contribute to the loss of torque complexity. The fatigue-induced loss of torque complexity therefore appears to be an integrated response to the global development of neuromuscular fatigue.

The fluctuations present in a torque time series have been attributed to the ensemble behaviour of the motor unit pool (Farina & Negro, 2015). Mathematical modelling (Farina & Negro, 2015) as well as intramuscular and high-density surface EMG decomposition (HDsEMG; Negro et al., 2009; Farina et al., 2014) have demonstrated a close association between fluctuations in the cumulative motor unit spike train (CST; that is, a representation of the ensemble firing of active motor units) during isometric contractions and the fluctuations in torque or force output. The fluctuations in the CST, in turn, are thought to reflect the common synaptic input to the motor unit pool, with high-frequency independent input (“synaptic noise”) being filtered out by virtue of the common input being amplified and transmitted

(Farina & Negro, 2015), with further low-pass filtering occurring due to muscle contractile properties represented by individual twitch forces (Dideriksen et al., 2012). Force output is thus thought to be a low-pass filtered version of the CST, which itself represents the common synaptic input to the motor neuron pool (Farina et al., 2014). Importantly, the relationships between common synaptic input, the CST, and force are preserved during fatiguing contractions (Castronovo et al., 2015). Thus, given that force fluctuations reflect the low-pass filtered CST, a loss of force or torque complexity should be associated with a loss of CST complexity. Alternatively, peripheral fatigue may distort the twitch forces to such an extent that the loss of torque complexity is not reflected in a loss of CST complexity. However, to date, CST complexity has not yet been quantified in the presence of fatigue, and thus whether it is sensitive to the fatigue process is unknown. The primary aim of the present study was to use HDsEMG and motor unit decomposition to determine the change in CST complexity and torque output complexity simultaneously during fatiguing contractions.

Extraction of cumulative motor unit behaviours using HDsEMG is a powerful technique, but it is not without some practical limitations in the context of neuromuscular fatigue development. First, given its architecture and proximity to the skin surface, the lower limb muscle with arguably the best motor unit yield using the HDsEMG technique is the tibialis anterior (TA). However, given its role in locomotion and postural control this muscle is fatigue resistant (Fourchet et al., 2012), and the high force contractions necessary to cause fatigue yield fewer motor units during decomposition due to the increased difficulty in extracting unique motor unit waveforms as the number of active motor units increases (Holobar et al., 2009; Del Vecchio et al., 2020; Hug, Avrillon et al., 2021). Since the effects of interest in the present study occur above the critical torque (usually ~25–35% MVC in the knee extensor group [Burnley et al., 2012], but likely higher in the dorsiflexors), we had to take steps to reduce the critical torque experimentally. To achieve this, in one condition we performed dorsiflexion contractions at 30% MVC with blood flow occluded (OCC), whilst in the other we left the circulation open (OPEN). The OCC condition effectively reduced critical torque to zero (Broxterman et al., 2015),

allowing us to study the fatigue process and decompose a sufficient number of motor units to produce a representative motor unit CST even when severely fatigued, and compare it to a condition in which little or no fatigue occurred (OPEN).

The aim of the present investigation was to determine the complexity of the motor unit CST and that of torque output during fatiguing and non-fatiguing contractions of the tibialis anterior muscle. It was hypothesised that performing dorsiflexor contractions at 30% MVC with occluded arterial inflow (OCC) would result in significant neuromuscular fatigue and a reduction in torque complexity which would be accompanied by a fall in motor unit CST complexity, whereas contractions at 30% MVC with an open circulation (OPEN) would result in no change in the complexity of torque or motor unit CST.

Methods

Participants

After approval by the SSES REAG at the University of Kent and in adherence to the Declaration of Helsinki, eleven healthy, physically active male adults (mean ± SD): age 26 ± 6 years; stature 1.78 ± 0.05 m; body mass 71 ± 10 kg) participated in the study. Each participant was fully advised of the procedures involved in the study before completing a PAR-Q Health Questionnaire and providing written informed consent. Participants were asked to attend each visit well rested and well hydrated, to abstain from caffeine or food consumption in the 2 h prior to exercise, and to avoid heavy exercise or alcohol consumption in the preceding 24 h. Each visit to the laboratory was conducted at the same time of day (± 2 h) to limit the influence of diurnal variation on muscle contractility (Racinais et al., 2005).

Experimental Design

Participants were required to visit the laboratory on three separate occasions, with a minimum of 48 hours between each visit. During the first visit, participants were familiarised with all testing equipment and experimental procedures, the dynamometer settings were recorded, and the location of the HDsEMG electrode grid was established. The remaining two visits were used to investigate the effects of fatiguing intermittent isometric submaximal contractions (and arterial occlusion) on muscle torque complexity and motor unit discharge properties of the tibialis anterior. The order of experimental visits was randomised.

Dynamometry

On arrival at the laboratory, participants were seated in the chair of a Cybex isokinetic dynamometer (HUMAC Norm; CSMi, Massachusetts, USA), with their trunk reclined to 15° (with 0° being seated upright), their right leg fully extended and ankle at 90°. A padded Velcro strap firmly secured the right foot into a foot plate attached to the dynamometer lever arm, with this adjusted such that the lateral malleolus was in line with the axis of rotation of the lever arm. Straps across both shoulders and the waist were used to limit any extraneous movement, and a further strap was secured around the distal portion of the thigh to prevent the use of the knee extensors during the isometric contractions. The instantaneous torque was projected onto a large screen placed ~2 m in front of the participant. A horizontal cursor was superimposed on the display to act as a target to enable participants to match their instantaneous torque output to the target torque during each contraction. The dynamometer chair settings were recorded during the first visit and reproduced during each visit thereafter.

Experimental Procedures

Participants performed a series of three isometric MVCs, each lasting ~3 s and separated by a minimum of 60 s rest. The highest MVC value was used to set the target torques for the subsequent submaximal contractions. After the establishment of maximal torque, participants rested for 5 min before performing the main experimental test. Participants performed intermittent submaximal isometric

dorsiflexion contractions at 30% MVC, with either open (OPEN) or closed (OCC) circulation; with arterial occlusion in the latter being accomplished by rapidly inflating a blood pressure cuff around the right quadriceps to a pressure of 300 mmHg using a sphygmomanometer (AG101, D.E.Hokanson Inc., Washington, USA).

In both conditions, the contraction regime consisted of a 2 s rise, 10 s hold, and 2 s fall, followed by 6 s rest, meaning participants performed three such contractions each minute. This ramp-and-hold contraction regime was chosen to assess the ongoing effects of fatigue on motor unit behaviour and muscle torque complexity. The 10 s hold phase allowed for an 8 s 'steady window' to be determined offline, which was then subjected to complexity analysis (see *Data Analysis*). OPEN contractions continued until task failure or for 30 min, whichever occurred sooner, and OCC contractions were performed until task failure. Task failure was defined as the inability to achieve the target torque during the 10 s hold phase of the repeated contractions. Immediately after task failure, participants performed an MVC (Figure 5.1).

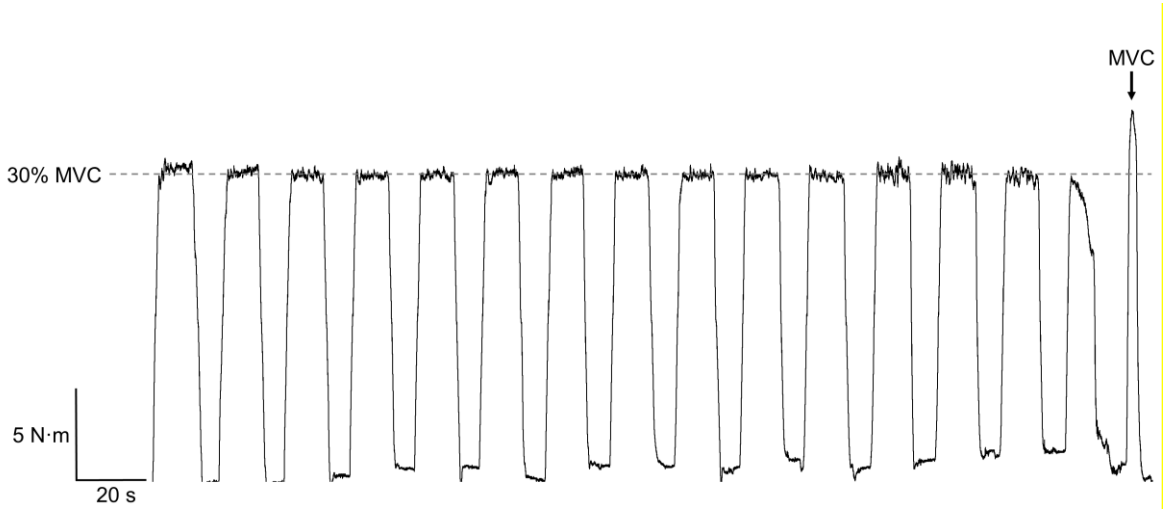

Figure 5.1. *Torque output from submaximal contractions performed at 30% maximal voluntary contraction (MVC) with arterial occlusion. Note the inability to reach the target torque at the end of the trial. The performance of a 3 s MVC immediately after task failure only resulted in the attainment of 35% of the pre-exercise MVC value.*

High-Density Surface Electromyography

The skin over the tibialis anterior was shaved and rubbed with medical grade abrasive paste (Spes Medica, Battipaglia, Italy). The methods used for the placement of the HDsEMG electrode grid are described in the General Methods (Chapter 3).

Data Acquisition

HDsEMG signals were acquired in monopolar mode, sampled at 2048 Hz, and converted to digital data by a 12-bit analogue-to-digital converter (EMG-USB2+, 64-channel EMG amplifier; OT Bioelettronica, Torino, Italy; 3 dB, bandwidth 10-500 Hz). HDsEMG signals were amplified using a gain of 500 to 1000. Care was taken to optimise this on an individual basis to maximise the HDsEMG signals without saturating any of the channels, which could affect decomposition results.

Torque data was sampled at 2048 Hz and acquired in Spike2 (Version 7; Cambridge Electronic Design, Cambridge, UK) via a CED Micro 1401-3 (Cambridge Electronic Design) interfaced with a personal computer. HDsEMG and torque signals were synchronised offline using a trigger signal delivered by the Micro 1401-3 to the EMG-USB2+ amplifier.

Motor Unit Decomposition

The HDsEMG signals obtained for each submaximal contraction were decomposed offline using OT BioLab (OT Bioelettronica, Torino, Italy) as described in the General Methods (Chapter 3). SIL was initially set at 0.90, but lowered to 0.85 in the event of the detection of fewer than 5 motor units for each contraction, and in no case was a SIL below 0.85 used. Following decomposition, the motor unit spike trains were visually inspected and spike trains exhibiting inter-spike intervals of < 10 ms or > 2 s were discarded before further analysis. The spike trains of each motor unit were summed to produce the cumulative spike train (CST) to estimate the neural drive to the muscle (Del Vecchio, Ubeda et al., 2018). The CST was then low-pass filtered

(2nd order Butterworth) at 10 Hz to extract the low-frequency components of the neural drive responsible for force production (Farina & Negro, 2015), before being subjected to complexity analysis using ApEn, sample entropy (SampEn), and DFA α exponent calculations (detailed below).

Data Analysis

Data were extracted from raw files using custom-written code in MATLAB R2020a (The MathWorks, Massachusetts, USA). Torque data were low-pass filtered (2nd order Butterworth) at 40 Hz prior to analysis. Mean and peak torque were calculated for each contraction in both trials. MATLAB code identified the 8 s 'steady window' of each contraction with the lowest SD, before calculating the mean and peak torque values. This was chosen to extract only torque values of the hold phase of each contraction and to exclude the rise and fall portions of each ramped contraction. The same 8 s was extracted from the synchronised CST.

The SD and coefficient of variation (CV) were used to quantify the amount of variability in the torque output of each contraction. The SD provides a measure of the absolute amount of variability in a time series, and the CV provides a measure of relative variability in a time series normalised to the mean of that time series.

The temporal structure, or complexity, of torque output and the motor unit CST was investigated using multiple time domain analyses (Goldberger, Peng et al., 2002). The regularity of each time series was determined using ApEn (Pincus, 1991) and SampEn (Richman & Moorman 2000). Both ApEn and SampEn quantify a continuum from 0 to 2; high values (approaching 2; e.g. white noise) represent less regular signals and greater complexity, whereas low values (close to 0; e.g. for a sinusoid time series) represent regular signals and lower complexity. However, high ApEn and/or SampEn values do not necessarily represent a physiologically complex signal (e.g. in the case of a random signal such as white noise), so DFA analysis was used to distinguish complexity from randomness. The DFA α scaling exponent

(Peng et al., 1994) was used to provide an estimate of the temporal fractal scaling of each time series; a DFA α value of 0.5 represents uncorrelated white noise, a DFA α value of 1 represents pink noise, and a DFA α value of 1.5 represents Brownian noise (“red noise”). Therefore, an increase in the DFA α exponent from 1 to 1.5 represents a move toward a less complex signal.

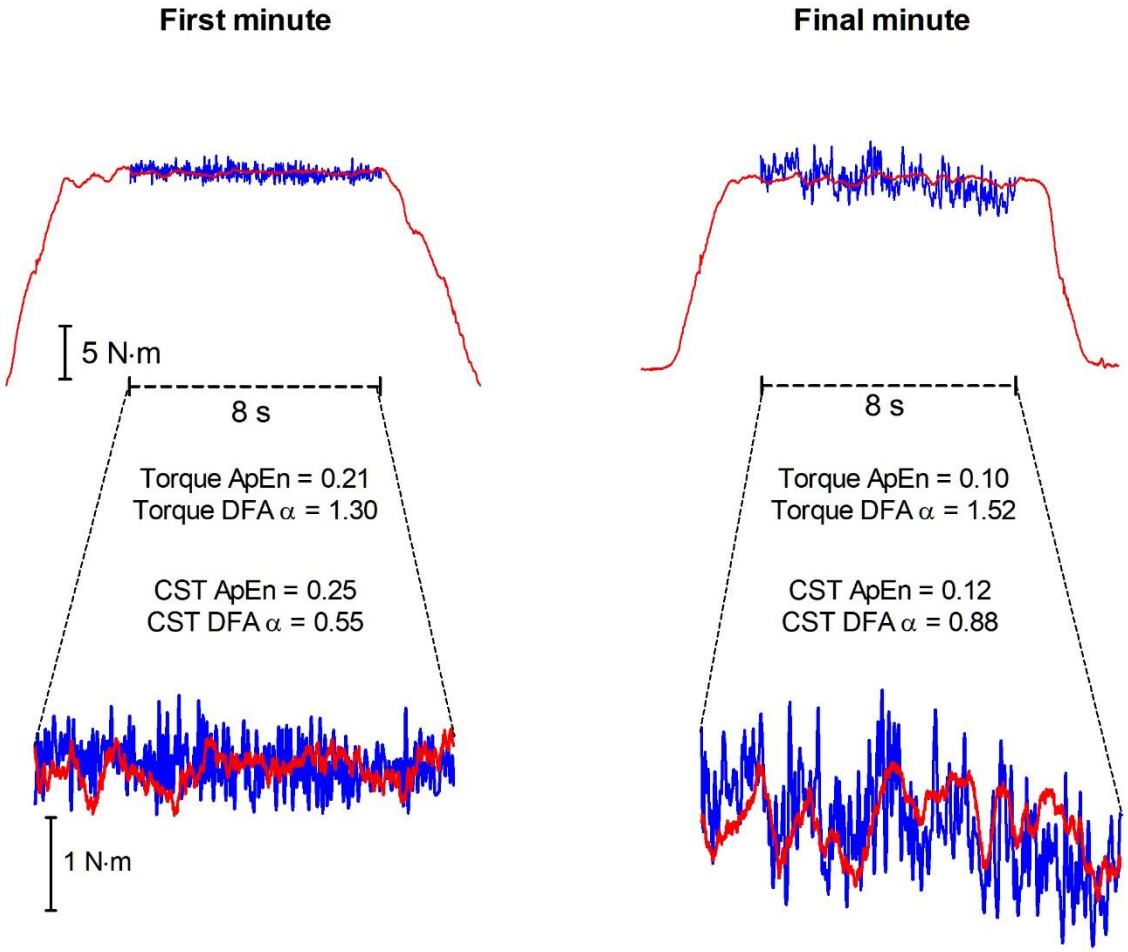

Figure 5.2. *Responses of dorsiflexor torque and tibialis anterior motor unit cumulative spike train (CST) during contractions performed at 30% maximal voluntary contraction with arterial occlusion. Data show the responses in one representative participant: one in the first minute, one in the final minute before task failure. Task failure occurred after 5 min of exercise. A reduction in complexity (lower ApEn values) and an increase in fractal scaling (greater DFA α values) was observed for both torque and the CST during the final minute of contractions before task failure.*

ApEn, SampEn, and DFA α scaling exponent analyses were used in a similar fashion to Pethick et al. (2015). Briefly, both ApEn and SampEn were calculated with the template length, *m*, set at 2 and the tolerance, *r*, set at ~10% of the SD of

torque output, and DFA was calculated across timescales (76 boxes ranging from 2000 to 4 data points). If a degree of crossover was identified in the log-log plot of fluctuation size versus box size (demonstrated by an $r < 0.95$), an iterative piecewise least squares linear regression was used to fit two lines to each respective plot, and two α exponents were calculated (Hu et al., 2001). The second of these (α_2) represents longer, physiological timescales and was used in the DFA α exponent analysis (Pethick et al., 2019b).

Statistical Analysis

Two-way repeated-measures ANOVA (condition × time) was used to investigate differences between conditions and time points for torque variability and complexity, CST complexity, and for pre-exercise and task failure MVC torque. *Post-hoc* Bonferroni-adjusted pairwise comparisons were performed to identify specific differences when significant main or interaction effects were observed. Student's paired-samples *t*-tests and 95% confidence intervals were used to investigate differences in rates of change for all parameters between OCC and OPEN conditions. All measures were analysed using mean values for the first minute and final minute before task failure/end.

Results

Time to task failure and MVC torque

Time to task failure at 30% MVC during OCC was 5.7 ± 1.5 min, whereas all participants were able to reach 30 min without task failure at 30% MVC during OPEN. Torque output for contractions from a representative participant during OCC are shown in Figure 5.1. There was a significant interaction effect (condition × time) for peak MVC torque ($F_{1, 10} = 17.03$, $P = 0.002$, $\eta_p^2 = 0.63$). Peak MVC torque was significantly lower at task failure when compared to the pre–exercise value during both OCC (first minute vs final minute: 43.0 ± 13.1 vs 20.1 ± 8.1 N·m; mean

difference; 95% CIs: –22.9; –29.0, -16.8 N·m, $F_{1, 10}$ = 70.46, P < 0.001), and OPEN (first minute vs final minute: 43.8 ± 14.5 vs 35.0 ± 12.5 N·m; mean difference; 95% CIs: –8.8; –13.0, –4.5 N·m, $F_{1, 10}$ = 21.16, P < 0.001). However, peak MVC torque was significantly lower at task failure during OCC compared with OPEN (mean difference; 95% CIs: -14.90; -22.5, -7.4, N·m, $F_{1, 10}$ = 19.56, P = 0.001) and the rate of decrease in peak MVC torque was significantly greater during OCC than OPEN (mean difference; 95% CIs: –3.8; –5.6, –2.7 N·m·min^{-1}; t = -6.34, P < 0.001). Voluntary torque response data are presented in Table 5.1.

Table 5.1. *Voluntary torque responses during contractions at 30% MVC with (OCC) and without (OPEN) arterial occlusion.*

Parameter	OPEN	OCC
Target torque, N·m	12.8 ± 3.9	12.8 ± 3.9
Time to task end/failure, min	30.0 ± 0.0	5.7 ± 1.5
Neuromuscular fatigue		
Pre-exercise peak MVC, N·m	43.8 ± 14.2	43.0 ± 12.4
Peak MVC at task end/failure, N·m	35.4 ± 12.5*	20.6 ± 8.1*†
Δ peak MVC/Δt, N·m·min^{-1}	-0.3 ± 0.2	-4.4 ± 2.2†

*N = 11; values are mean ± SD. MVC, maximal voluntary contraction; Δ, change; t, time. Symbols indicate a statistically significant difference compared to the following: * pre-exercise value, † OPEN.*

Torque variability and complexity

Torque variability and complexity data are presented in Table 5.2. There was no significant interaction effect (condition × time: $F_{1, 10}$ = 0.05, P = 0.821, η_p^2 = 0.01) or main effect for time ($F_{1, 10}$ = 2.50, P = 0.146, η_p^2 = 0.20) for SD. There were no significant differences in the SD of torque fluctuations in the final minute when compared to the first minute of exercise during both OCC (mean difference; 95% CIs: 0.06 N·m; –0.04, 0.15 N·m; $F_{1, 10}$ = 1.77, P = 0.213) and OPEN (mean difference; 95% CIs: 0.05 N·m; –0.02, 0.12 N·m; $F_{1, 10}$ = 2.53, P = 0.143). However, there were main effects of condition for the SD of torque fluctuations ($F_{1, 10}$ = 5.66, P = 0.039, η_p^2 = 0.36). There were significantly higher values in the final minute of OCC when compared to OPEN for the SD (OCC vs. OPEN: 0.34 ± 0.20 vs. 0.23 ± 0.12; mean difference; 95% CIs: 0.11; 0.02, 0.20 ; $F_{1, 10}$ = 7.33, P = 0.022).

There was no significant interaction effect (condition × time: $F_{1, 10} = 0.35$, $P = 0.570$, $\eta_p^2 = 0.03$) or main effect for time ($F_{1, 10} = 3.81$, $P = 0.080$, $\eta_p^2 = 0.28$) for the CV of torque fluctuations. There were no significant differences in the CV in the final minute when compared to the first minute of exercise during both OCC (mean difference; 95% CIs: 0.48%; –0.10, 1.06%; $F_{1, 10} = 3.45$, $P = 0.093$) and OPEN (mean difference; 95% CIs: 0.33%; –0.18, 0.84%; $F_{1, 10} = 2.09$, $P = 0.179$). However, there was a main effect of condition for the CV of torque fluctuations ($F_{1, 10} = 5.77$, $P = 0.037$, $\eta_p^2 = 0.37$), with significantly higher values in the final minute of OCC when compared to OPEN (OCC vs. OPEN: 2.47% ± 1.02% vs. 1.70% ± 0.64%; mean difference; 95% CIs: 0.76%; 0.11, 1.41%; $F_{1, 10} = 6.83$, $P = 0.026$).

Table 5.2. *Torque variability, complexity, and fractal scaling responses during contractions at 30% MVC with (OCC) and without (OPEN) arterial occlusion.*

Parameter		OPEN	OCC
SD			
	SD at task beginning, N·m	0.18 ± 0.08	0.28 ± 0.25
	SD at task end/failure, N·m	0.23 ± 0.12	0.34 ± 0.20†
	ΔSD/Δt, $N \cdot m \cdot min^{-1}$	0.002 ± 0.003	0.009 ± 0.023
CV			
	CV at task beginning, %	1.38 ± 0.44	1.99 ± 1.28
	CV at task end/failure, %	1.70 ± 0.64	2.47 ± 1.02†
	ΔCV/Δt, %/min	0.01 ± 0.03	0.08 ± 0.14
ApEn			
	ApEn at task beginning	0.38 ± 0.13	0.27 ± 0.14
	ApEn at task end/failure	0.33 ± 0.16	0.21 ± 0.15*†
	ΔApEn/Δt	-0.002 ± 0.004	-0.010 ± 0.013
SampEn			
	SampEn at task beginning	0.37± 0.13	0.26 ± 0.14
	SampEn at task end/failure	0.32 ± 0.16	0.21 ± 0.14*†
	ΔSampEn/Δt	-0.002 ± 0.004	-0.009 ± 0.012
DFA α			
	DFA α at task beginning	1.23 ± 0.14	1.32 ± 0.18
	DFA α at task end/failure	1.21 ± 0.15	1.38 ± 0.19†
	ΔDFA α/Δt	-0.001 ± 0.005	0.010 ± 0.032

*N = 11; values are mean ± SD. SD, standard deviation; CV, coefficient of variation; ApEn, approximate entropy; SampEn, sample entropy; DFA α, detrended fluctuation analysis; Δ, change; t, time. Symbols indicate a statistically significant difference compared to the following: * value at task beginning, † OPEN.*

There were no significant differences in the rates of change between conditions for both SD (mean difference; 95% CIs: 0.01 N·m.min^{-1}; –0.01, 0.02 N·m.min^{-1}; t = 1.14, P = 0.282) and CV (mean difference; 95% CIs: 0.07%.min^{-1}; –0.02, 0.15%.min^{-1}; t = 1.70, P = 0.121).

There was no significant interaction effect for ApEn (condition × time: $F_{1, 10}$ = 0.05, P = 0.821, η_p^2 = 0.01), but there was a main effect of time ($F_{1, 10}$ = 8.86, P = 0.014, η_p^2 = 0.47) and condition ($F_{1, 10}$ = 13.15, P = 0.005, η_p^2 = 0.57). ApEn was significantly lower in the final minute than in the first minute of exercise during OCC (mean difference; 95% CIs: –0.06; –0.11, –0.01; $F_{1, 10}$ = 6.88, P = 0.025; Figure 5.3). There was no difference between ApEn in the final minute when compared to the first minute of exercise during OPEN (mean difference; 95% CIs: –0.05; –0.12, 0.03; $F_{1, 10}$ = 2.10, P = 0.178; Figure 5.3). ApEn was significantly lower (OCC vs. OPEN: 0.21 ± 0.15 vs. 0.33 ± 0.16; mean difference; 95% CIs: -0.12; -0.21, -0.02; $F_{1, 10}$ = 6.87, P = 0.026) during the final minute of OCC when compared to OPEN.

There was no significant interaction effect for SampEn (condition × time: $F_{1, 10}$ = 0.02, P = 0.883, η_p^2 = < 0.01), but there was a main effect of time ($F_{1, 10}$ = 9.07, P = 0.013, η_p^2 = 0.48) and condition ($F_{1, 10}$ = 14.79, P = 0.003, η_p^2 = 0.60). SampEn was significantly lower in the final minute than in the first minute of exercise during OCC (mean difference; 95% CIs: –0.05; –0.10, –0.01; $F_{1, 10}$ = 7.23, P = 0.023). There was no difference between SampEn in the final minute when compared to the first minute of exercise during OPEN (mean difference; 95% CIs: –0.05; –0.12, 0.02; $F_{1, 10}$ = 2.18, P = 0.171). SampEn was significantly lower (OCC vs. OPEN: 0.21 ± 0.14 vs. 0.32 ± 0.16; mean difference; 95% CIs: -0.12; -0.21, -0.02; $F_{1, 10}$ = 7.51, P = 0.021) during the final minute of OCC when compared to OPEN.

There was no significant interaction effect for DFA α (condition × time: $F_{1, 10}$ = 2.68, P = 0.133, η_p^2 = 0.21) and no main effect of time ($F_{1, 10}$ = 0.52, P = 0.487, η_p^2 = 0.05), but there was a main effect of condition ($F_{1, 10}$ = 12.56, P = 0.005, η_p^2 = 0.56). The DFA α scaling exponent was not significantly different in the final minute compared

to the first minute of exercise during both OCC (mean difference; 95% CIs: 0.07; –0.02, 0.16; $F_{1, 10}$ = 2.99, P = 0.115) and OPEN (mean difference; 95% CIs: –0.02; –0.12, 0.08; $F_{1, 10}$ = 0.17, P = 0.691). However, the DFA α scaling exponent was significantly greater (OCC vs. OPEN: 1.38 ± 0.19 vs. 1.21 ± 0.15; mean difference; 95% CIs: 0.17; 0.042, 0.30; $F_{1, 10}$ = 8.82, P = 0.014), during the final minute of OCC when compared to OPEN.

There were no significant differences in the rates of change between conditions for ApEn (mean difference; 95% CIs: –0.01; –0.018, 0.002; t = –1.82, P = 0.099), SampEn (mean difference; 95% CIs: –0.01; –0.017, 0.002; t = –1.80, P = 0.102), or the DFA α scaling exponent (mean difference; 95% CIs: 0.01; –0.01, 0.03; t = 1.12, P = 0.289).

Cumulative spike train complexity

A representative participant's torque output and CST time series is shown in Figure 5.2. We identified 251 motor units for data processing from the OCC condition, including 130 (mean per participant: 12 ± 4) from the first minute and 121 (9 ± 5) from the final minute. 264 motor units were accepted from the OPEN condition, including 124 (11 ± 4) from the first minute, and 140 (13 ± 5) from the final minute. CST complexity and fractal scaling data are presented in Table 5.3.

There was a significant interaction effect (condition × time) for motor unit CST ApEn ($F_{1, 10}$ = 13.73, P = 0.004, η_p^2 = 0.58). Motor unit CST ApEn was significantly lower in the final minute than in the first minute of exercise during OCC (mean difference; 95% CIs: –0.06; –0.09, –0.03; $F_{1, 10}$ = 23.00, P < 0.001; Figure 5.3). There was no difference between ApEn in the final minute when compared to the first minute of exercise during OPEN (mean difference; 95% CIs: –0.01; –0.02, 0.01; $F_{1, 10}$ = 0.63, P = 0.445; Figure 5.3).

There was a significant interaction effect (condition × time) for motor unit CST SampEn ($F_{1, 10}$ = 13.57, P = 0.004, η_p^2 = 0.58). Motor unit CST SampEn was significantly lower in the final minute than in the first minute of exercise during OCC (mean difference; 95% CIs: –0.06; –0.09, –0.03; $F_{1, 10}$ = 22.18, P < 0.001). There was no difference between SampEn in the final minute when compared to the first minute of exercise during OPEN (mean difference; 95% CIs: –0.004; –0.02, 0.01; $F_{1, 10}$ = 0.25, P = 0.629).

There was a significant interaction effect (condition × time) for motor unit CST DFA α: ($F_{1, 10}$ = 13.18, P = 0.005, η_p^2 = 0.57). The DFA α scaling exponent was significantly greater in the final minute compared to the first minute of exercise during OCC (mean difference; 95% CIs: 0.18; 0.06, 0.29; $F_{1, 10}$ = 11.92, P = 0.006), but not during OPEN (mean difference; 95% CIs: –0.05; –0.12, 0.02; $F_{1, 10}$ = 2.46, P = 0.148).

In the final minute of contractions, there was significantly lower complexity in the motor unit CST during OCC compared to OPEN, as evidenced by lower ApEn (OCC vs. OPEN: 0.14 ± 0.03 vs. 0.21 ± 0.15; mean difference; 95% CIs: -0.07; -0.09, -0.04; $F_{1, 10}$ = 36.03, P < 0.001) and SampEn (OCC vs. OPEN: 0.13 ± 0.03 vs. 0.20 ± 0.02; mean difference; 95% CIs: -0.06; -0.09, 0.04; $F_{1, 10}$ = 38.03, P < 0.001), and a significantly higher DFA α scaling exponent (OCC vs. OPEN: 0.78 ± 0.17 vs. 0.57 ± 0.09; mean difference; 95% CIs: 0.21; 0.09, 0.33; $F_{1, 10}$ = 15.97, P = 0.003).

The rate of decrease in both ApEn (mean difference; 95% CIs: –0.011; –0.016, –0.006; t = –4.70, P < 0.001) and SampEn (mean difference; 95% CIs: –.010; –0.015, –0.005; t = –4.58, P = 0.001) was significantly greater during OCC than during OPEN, and the rate of increase in DFA α scaling exponent was significantly greater during OCC than OPEN (mean difference; 95% CIs: 0.03; 0.01, 0.06; t = 3.37, P = 0.007).

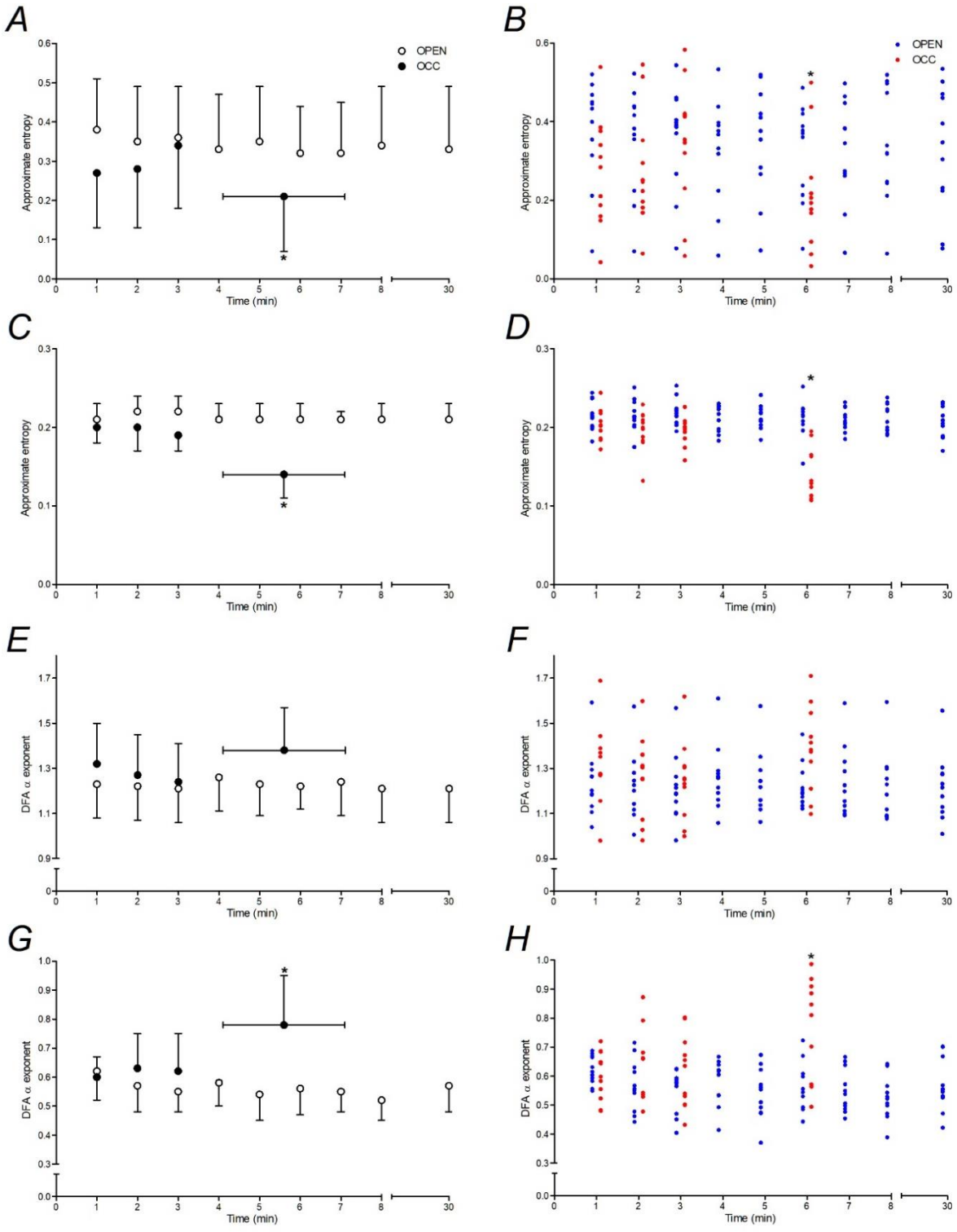

Figure 5.3. *Complexity metrics during each condition. Panels show ApEn for torque output (A and B), Cumulative spike train (C and D), and DFA α exponent for torque (E and F) and Cumulative spike train (G and H). Panels on the left show group mean (SD) responses, and panels on the right show individual responses. Open circles represent OPEN values and closed circles represent OCC values. In the individual panels, blue symbols represent the OPEN condition, and red the OCC condition. Values are averaged over 1 min (3 contractions per min). For the OCC trial, the final datapoint represents task failure, with the preceding value (at 3 min) being the final common timepoint. *indicates a statistically significant difference compared to the first minute of exercise. N = 11.*

Table 5.3. *Cumulative spike train complexity and fractal scaling responses during contractions at 30% MVC with (OCC) and without (OPEN) arterial occlusion.*

Parameter	OPEN	OCC
ApEn		
ApEn at task beginning	0.21 ± 0.02	0.20 ± 0.02
ApEn at task end/failure	0.21 ± 0.02	0.14 ± 0.03*†
ΔApEn/Δt	-0.0003 ± 0.0037	-0.0114 ± 0.0078†
SampEn		
SampEn at task beginning	0.20 ± 0.02	0.19 ± 0.02
SampEn at task end/failure	0.20 ± 0.02	0.13 ± 0.03*†
ΔSampEn/Δt	-0.0001 ± 0.0009	-0.0105 ± 0.0075†
DFA α		
DFA α at task beginning	0.62 ± 0.05	0.60 ± 0.08
DFA α at task end/failure	0.57 ± 0.09	0.78 ± 0.17*†
ΔDFA α/Δt	-0.002 ± 0.004	0.031 ± 0.032†

*N = 11; values are mean ± SD). ApEn, approximate entropy; SampEn, sample entropy; DFA α, detrended fluctuation analysis; Δ, change; t, time. Symbols indicate a statistically significant difference compared to the following: * value at task beginning, † OPEN.*

Motor unit behaviour

There was a significant interaction effect (condition × time) for global motor unit discharge rate ($F_{1, 10}$ = 12.41, P = 0.006, η_p^2 = 0.55). Global motor unit discharge rate was significantly higher in the final minute (15.1 ± 3.5 pulses per second [pps]) than in the first minute (12.7 ± 1.9 pps) of exercise during OCC, an increase of 2.5 pps (95% CIs: 0.83, 4.1 pps; $F_{1, 10}$ = 11.15, P = 0.008; Figure 5.4). There was no difference between global motor unit discharge rate in the final minute (14.0 ± 2.1 pps) when compared to the first minute (14.5 ± 2.0 pps) of exercise during OPEN (mean difference; 95% CIs: –0.5 pps; –1.7, 0.6 pps; $F_{1, 10}$ = 1.08, P = 0.323). There was no significant difference between final minute global motor unit discharge rate during OCC and OPEN (mean difference; 95% CIs: -1.17 pps; -3.01, 0.67 pps; $F_{1, 10}$ = 2.00, P = 0.188). The rate of increase in global motor unit discharge rate was significantly greater during OCC (0.5 ± 0.4 pps.min^{-1}) than during OPEN (–0.02 ± 0.06 pps.min^{-1}), (mean difference; 95% CIs: 0.5; 0.2, 0.8), t = 3.89, P = 0.003.

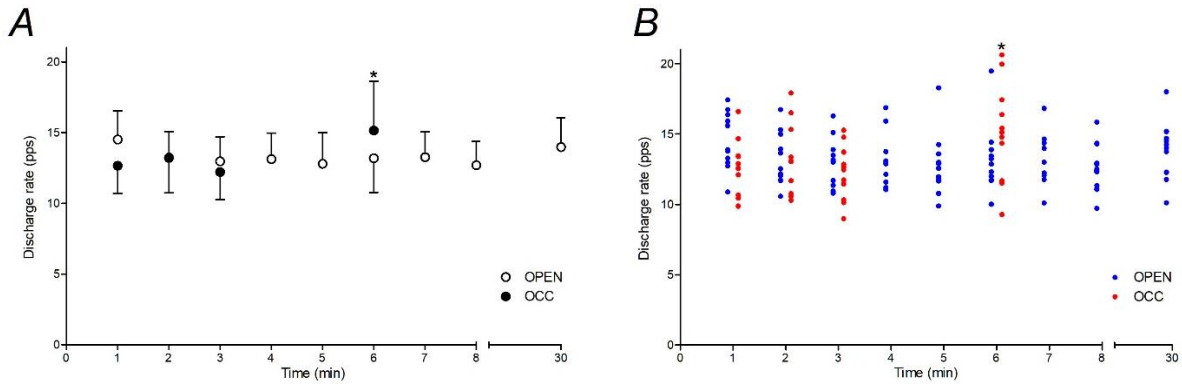

Figure 5.4. *Global motor unit discharge rate during contractions performed at 30% MVC. Open circles represent OPEN values and filled circles represent OCC values. Panel A represent group mean (SD), panels on the right represent individual data. In the individual panels, blue symbols represent the OPEN condition, and red the OCC condition. Values are averaged over 1 min (3 contractions per min). For the OCC trial, the final datapoint represents task failure, with the preceding value (at 3 min) being the final common timepoint. pps, pulses per second. * indicates a statistically significant difference compared to the first minute of exercise. N = 11.*

Discussion

The present study demonstrated that contractions of the tibialis anterior muscle at 30% MVC with occluded blood flow (OCC) resulted in a loss of torque complexity which was accompanied by a loss of complexity in the motor unit CST. In contrast, contractions of the same muscle at the same torque requirement with open circulation (OPEN) resulted in no change in the complexity of torque output or the motor unit CST. Thus, the present study is the first to show that a fatigue-induced loss of torque complexity occurs in tandem with a loss of complexity in the firing patterns of the motor units responsible for torque production. Although the motor unit yield from surface EMG decomposition techniques provides an incomplete picture of the behaviour of the motor unit pool (Enoka & Farina, 2021), the fact that motor units share a common drive suggests that a change in the transduction of common drive to the motor unit pool is primarily responsible for the fatigue-induced loss of torque complexity observed in the present study.

Limitations

The interpretation of this study is subject to several limitations which need to be appreciated before the results are interpreted physiologically. Despite being a valid and reliable means of detecting and classifying motor unit behaviour, with the potential to detect significantly more motor units than intramuscular methods, the motor unit yield from surface HDsEMG decomposition is a small proportion of the TA motor unit pool (<30 per participant vs. 300 in the TA; Van Cutsem et al., 1997). Thus, HDsEMG decomposition techniques can detect ~10-20% of the active motor units in a muscle, and these will be drawn from those with fibres closest to the surface. Nevertheless, this number is likely to be sufficient to infer the control signal due to the amplification of the common synaptic input alluded to above, and since the coherence between common input and the CST approaches unity when ~10 motor units are decomposed (Farina et al., 2014). Furthermore, the approach taken in the present study (quantifying complexity using the ensemble behaviour of a sample of the motor unit pool) was also recommended by a recent simulation study (Dideriksen et al., 2022).

The focus on the fatigue-resistant TA is another potential limitation due to our previous work on torque complexity being conducted using knee extension exercise. We addressed this limitation through experimental design, using arterial occlusion in our fatigue condition. This resulted in a time to task failure for the OCC condition similar to that in experiments in which we have performed intermittent contractions of the vastus lateralis at 50% MVC (Pethick et al., 2016). Ideally, these experiments would also have been conducted sampling the vastus lateralis, but in pilot work the motor unit yield from the vastus lateralis was low in comparison to the TA. For similar reasons, we did not recruit female participants; only 1-2 motor units could be detected in females performing pilot work even with the TA as the target muscle group. The anatomical or physiological basis of such low motor unit yields in female participants is not known (Del Vecchio et al., 2020; Hug, Avrillon et al., 2021; Taylor et al., 2022), but needs to be addressed urgently given the differences in performance fatiguability between the sexes (see Hunter [2016] for review).

Neuromuscular fatigue in each condition and effects on torque output complexity

The development of fatigue in each condition demonstrated that the OPEN condition was performed below the critical torque and the OCC condition was performed above it: the MVC declined an order of magnitude faster in the OCC condition (Table 5.1), and task failure occurred in ~6 min. In contrast, all participants completed 30 min of contractions in the OPEN condition, with a smaller, but significant, decline in the MVC torque at the end of the task. The OCC condition, therefore, resulted in a greater degree of fatigue development which progressed at a substantially faster rate than in the OPEN condition. This is indicative of each condition being positioned either side of the critical torque boundary (Burnley et al., 2012; Poole et al., 2016). As a result, the OCC condition should have resulted in the same changes in complexity as we previously observed in knee extensor torque complexity (Pethick et al., 2015), whereas a fatigue-induced loss of complexity should have been absent in the OPEN condition.

The results of the present experiments demonstrated that the torque complexity of the tibialis anterior muscle was significantly reduced in the OCC condition but not during contractions in the OPEN condition (Table 5.2, Figure 5.3). Due to substantial high-frequency system noise, we filtered the torque signal with a 40 Hz low-pass filter. The majority of the power in the force or torque frequency spectrum occurs below 20 Hz, and so removal of dynamometer system noise (which was present above 100 Hz) was justified in this case. This may, however, explain why the ApEn values were lower than previously reported for the knee extensor group (e.g., Pethick et al., 2015), in which filtering of this kind was not required. Nevertheless, a fatigue-induced loss of complexity (measured by a decrease in ApEn and SampEn, indicating increased signal regularity) has been consistently observed in the knee extensors (Pethick et al., 2015; Pethick et al., 2016), and the present work extends this to the TA. However, despite an increase in the DFA α exponent value, this was not statistically significant. Therefore, the change in complexity observed in this study represented an increase in the regularity of TA torque without a change in its

noise colour, which was in the same range as previously observed (i.e., pink to red noise, 1.0-1.5; Figure 5.3). These observations are in contrast to measures of variability (SD and CV), which showed no change in response to fatiguing contractions in the OCC condition. Thus, complexity measures detected changes that measures of variability could not.

Fatigue-induced loss of motor unit cumulative spike train (CST) complexity

The second major finding of the present study was that a reduction in torque complexity in the OCC condition was accompanied by a reduction in the complexity of the CST in the detected TA motor units (Figure 5.3). In the OPEN condition, the modest development of fatigue and unchanged complexity was mirrored by no changes in the complexity of the CST, with neither ApEn, SampEn, nor the DFA α exponent changing. In the OCC condition, ApEn, SampEn and the DFA α exponent significantly changed as the contractions progressed. The ApEn values were significantly reduced during fatiguing contractions, whilst the DFA α exponent increased. Qualitatively, these results are consistent with those of our previous studies (e.g., Pethick et al., 2015), and strongly suggest that the decrease in TA torque complexity is a consequence, in large part, of a decrease in CST complexity. The change in CST complexity was accompanied by an increase in the motor unit pool mean firing rate (Table 5.2, Figure 5.4). This response is similar to that recently reported by Martinez-Valdes et al. (2020) in sustained contractions of the knee extensors, in which firing frequency increased as task failure approached. In short, increased regularity in the CST and increased motor unit firing frequency were the only identifiable changes in motor unit function in the present experiments.

The loss of CST complexity during the OCC condition, but not during the OPEN condition, suggests that the loss of torque complexity is not simply a direct effect of peripheral fatigue, but rather was attributable to a direct effect on motor unit firing behaviour. That behaviour is, itself, attributable to the net synaptic input the motoneurons receive (Farina & Negro, 2015). This input can be broadly separated into two sources: independent inputs received by individual motoneurons, and

common synaptic input received by all motoneurons. The latter input is thought to carry the dominant signal for force control and, consequently, is thought to represent the effective neural drive to the muscle (Farina et al., 2014). It also accounts for the fluctuations in force during steady contraction tasks (Castronovo et al., 2015; Enoka & Farina, 2021). This is because the motoneurons act as a linear low-pass filter of synaptic input, ensuring that the common input is ultimately translated into muscle force output via the CST of the motor unit pool, explaining both its amplitude (as a percentage of MVC) as well as the size and complexity of its fluctuations. Although independent input can influence the firing probability of a motor unit, and thus add to the fluctuations in force, its influence is thought to be greatest at low levels of excitation, and thus force output (Castronovo et al., 2015).

Whilst the above neurophysiological model can explain the presence of complex output in the CST, it does not explain why fatigue caused that complexity to be lost as the contractions progressed in the OCC condition. The effects of neuromuscular fatigue are wide-ranging, but in the present experiments the use of occlusion meant that the effect of peripheral fatigue was accentuated. Metabolite accumulation (P_i, ADP, H^+, and/or K^+) and depletion (e.g., phosphocreatine, ATP) in various parts of the muscle cell can directly or indirectly result in a reduction in muscle force for a given level of muscle stimulation (Allen et al., 2008), requiring an increase in net excitation (Carpentier et al., 2001; Adam & De Luca, 2004; Dideriksen et al., 2011). This increase in excitatory drive has been shown to improve the coherence between CST and force during increments in muscle force output and neuromuscular fatigue, most likely reflecting an increase in the strength of the common synaptic input relative to the independent input (Castronovo et al., 2015). Finally, reduced motoneuron gain requires greater than normal excitation to exceed the motor unit recruitment threshold (McNeil et al., 2011), which will also tend to amplify the common component of synaptic input. These processes could result in the effective neural drive to the muscle being transmitted with progressively less noise as the muscle fatigues. In turn, this would be observed as a reduction in CST complexity and, therefore, torque output complexity.

Functional significance of reduced CST complexity

Although we cannot rule out a reduction in the complexity of effective neural drive to the muscle in producing a loss of CST complexity, there is currently no evidence to suggest that the fluctuations in common synaptic input change in this way in response to fatigue. More importantly, the above explanation provides a potentially important conceptual advance in the meaning of “complexity” in neuromuscular function. Since the formulation of the “loss of complexity hypothesis” (Lipsitz & Goldberger, 1992), a loss of complexity has been assumed to reflect a loss of system adaptability (that is, system components become more isolated and less able to respond to inputs from other systems; Peng et al., 2009). The present results provide the first evidence that a loss of complexity may represent the emergence and amplification of the dominant control signal as the capacity of the system itself is systematically declining. This is because the loss of torque and CST complexity observed here most likely reflects the amplification of the required signal for force control (i.e., the common synaptic input; Farina & Negro, 2015). In the context of neuromuscular fatigue, the loss of adaptability is primarily caused by a loss of peripheral force-generating capacity. The loss of CST complexity, and thus torque complexity is a necessary consequence of compensatory adjustments to continue the required task, and thus an attempt to *maintain* adaptability.

The suggestion that a fatigue-induced loss of torque and CST complexity represents an outcome of the typical neurophysiological adjustments to neuromuscular fatigue is consistent with previous observations that a loss of torque complexity has so far only been observed during contractions above the critical torque (Pethick et al., 2016; Pethick et al., 2020), wherein fatigue progresses much more rapidly than lower contractile intensities (Burnley et al., 2012), as well as those in which the recovery from peripheral fatigue was prevented by arterial occlusion (Pethick et al., 2018b). The latter would necessitate the maintenance of high levels of central motor drive to achieve the target torque in the face of significant inhibitory metaboreceptor input, which would maximise the transmission of effective motor drive as expressed in the CST. Additionally, the loss of peripheral function (muscle fibre twitch force and/or area), would further smooth the torque output resulting in the very low levels

of complexity observed under these conditions (Pethick et al., 2018b). Further work is necessary to establish whether the CST complexity does indeed reflect these effects.

Conclusions

In conclusion, a fatigue-induced reduction in dorsiflexor torque complexity during contractions at 30% MVC under arterial occlusion was accompanied by a reduction in TA motor unit CST complexity. When the same contractile intensity was performed with open circulation, neither torque nor CST complexity changed. The loss of torque and CST complexity when occluded contractions were performed was accompanied by an increase in TA motor unit discharge rate. These results indicate that the loss of torque complexity previously reported is a consequence of changes in motor unit firing behaviour, likely reflecting the increased transmission of the effective drive to the muscle as the contractions progressed, as well as a likely attenuation of the transmission of independent synaptic input.

CHAPTER 6 – CRITICAL TORQUE IN THE DORSIFLEXORS – A COMPARISON BETWEEN THE 5 MINUTE ALL-OUT TEST AND THE CONVENTIONAL ESTIMATION OF CRITICAL TORQUE FROM SUBMAXIMAL TESTS PERFORMED TO TASK FAILURE

Introduction

The Review of Literature (Chapter 2) discussed the concept of the critical power, which is thought to delimit the boundary between the heavy and severe-intensity exercise domains during whole body exercise (Craig et al., 2019; Jones et al., 2019; Poole et al., 1988). The critical power therefore represents the maximum power output at which a metabolic steady state can be attained (Craig et al., 2019; Jones et al., 2019). Analogous to the critical power, the so-called critical torque (or force) has been explored in studies involving isometric contractions of single agonist muscle groups (most commonly the knee extensors; Ansdell et al., 2019a; Broxterman et al., 2017; Burnley et al., 2012; Pethick et al., 2016). In addition to the muscle metabolic steady state, the critical torque demarcates a threshold for accelerated peripheral fatigue development, with rates four to five-fold greater observed during exercise performed above the critical torque (Burnley et al., 2012). Furthermore, losses of muscle torque complexity are only evident above the critical torque, indicating that attempts to elucidate both the central and peripheral mechanisms of such losses should focus on exercise intensities above this threshold (Pethick et al., 2016). Thus, the use of the critical torque parameter is of the utmost importance when investigating the mechanisms of neuromuscular fatigue, and particularly the effects of training and rehabilitation interventions on such mechanisms (Burnley, 2009; Burnley et al., 2012; De Ruiter et al., 2014).

In experimental designs investigating the fatigue response to submaximal isometric muscle contractions, a predetermined percentage of MVC (typically ranging from 20% to 75% MVC; Rossato et al., 2022; Castronovo et al., 2015; Murphy et al., 2019) is commonly used to prescribe exercise intensity across all participants. However, this can lead to markedly different physiological responses, with some participants exercising above, and some below, their unique critical torque. This was particularly evident from the work of Saugen et al. (1997), in which intermittent contractions performed at 40% MVC until task failure resulted in at least two participants exercising below the critical torque, thereby exhibiting less metabolic stress (inferred from smaller reductions in muscle PCr and pH) and exercising for

much longer than the rest of the group. Indeed, to avoid such disparate responses across participants in Chapter 5 it was necessary to ‘simulate’ exercise above the critical torque in the dorsiflexor muscles using arterial occlusion, effectively reducing the critical torque to 0 N·m (Broxterman et al., 2015).

Conventionally, the critical torque (or power) is estimated across three or more visits, usually on separate days, during which submaximal exercise tests are performed until task failure (Broxterman et al., 2015; Burnley et al., 2012; Pethick et al., 2020). However, this presents a considerable time burden for both participant and experimenter, and all-out tests have been proposed to overcome such practical shortcomings (Burnley 2009; Vanhatalo et al., 2007). All-out tests developed so far include those for the knee extensors, plantarflexors, and forearm flexors (Abdalla et al. 2018; Burnley, 2009; Kellawan & Tschakovsky 2014). To date, no study has investigated the critical torque in the dorsiflexor muscles. The dorsiflexors, namely the tibialis anterior muscle, are frequently investigated in studies utilising HDsEMG techniques (Castronovo et al., 2015; Cogliati et al., 2020; Martinez-Valdes et al., 2020). Given the aforementioned importance of the critical torque as a threshold for accelerated neuromuscular fatigue, the development of methods to accurately and efficiently estimate the critical torque in the dorsiflexor muscle group is essential. If the 5 min all-out test provides an estimate of dorsiflexor critical torque in agreement with the conventional approach, this valuable parameter could be used in addition to, or in place of, % MVC to prescribe the intensity of isometric contractions in experimental designs using HDsEMG.

The aim of the current study was therefore to ascertain if the end-test dorsiflexor torque calculated from a 5 min all-out test is a valid measure of the critical torque estimated using the conventional method (i.e., a series of submaximal, constant-intensity exercise tests performed to task failure). It was hypothesised that the end-test dorsiflexor torque estimated from the 5-minute all-out test would not differ from the critical torque calculated using the conventional method.

Methods

Participants

Following approval from the SSES REAG at the University of Kent, and in accordance with the Declaration of Helsinki, six physically active male adults (mean ± SD: age 29 ± 7 years; stature 181 ± 5 cm; body mass 74 ± 11 kg) volunteered to participate in the study and provided written informed consent. Participants were instructed to attend each session well rested and hydrated, to not consume caffeine or eat in the 2 h prior to exercise, and to not consume alcohol or undergo heavy exercise in the preceding 24 h.

Experimental Design

Participants were required to visit the laboratory on six separate occasions, with at least 48 h between visits. Sessions were conducted at the same time of day (± 2 h) to minimise the influence of diurnal variation on muscle contractility (Racinais et al., 2005). The first visit was used to familiarise participants with all equipment and procedures, and record individual chair settings. During *visits 2-5*, the critical torque was calculated using a series of intermittent isometric contractions to task failure. During the sixth visit, critical torque was approximated using the “5 min all-out test” (Burnley, 2009).

Experimental Setup

Torque: The methods used for the setup of the dynamometer are described in the General Methods (Chapter 3). The seating position was recorded during the first visit and replicated thereafter.

Bipolar surface EMG measurements: Before electrode placement, the skin was shaved, rubbed using abrasive paste, and cleaned with water. Adhesive bipolar EMG electrodes (AgCl; 24mm diameter; 1.6 cm interelectrode distance; OT Bioelettronica, Torino, Italy) were placed over the proximal portion of the tibialis anterior during the 5 min all-out test. The electrode pair were secured over the skin

to prevent movement artifacts using adhesive dressing tape (Hypafix, BSN medical Ltd, Hull, UK). A strap ground electrode was dampened with water and placed around the right ankle of the participant.

Experimental Protocol

Visit 1 – Familiarisation: Participants completed a series of three isometric MVCs, each lasting 3 s and separated by at least 1 min of recovery. After 5 min rest, participants then performed the "5 min all-out test" (Burnley, 2009). Briefly, participants performed 60 intermittent MVCs using a contraction regime of 3 s contraction and 2 s rest, which is designed to result in a plateau in torque during the final 60 s of the test (Figure 6.1). Participants were encouraged to equal or exceed their previous MVC values during the first 2-3 contractions. Participants were also told to expect their torque to decrease by over 50% during the test, but to still produce maximal effort during each contraction. During the test, participants were strongly encouraged to maximise their torque, but were not informed of the number of completed contractions, nor the elapsed time. An audio signal was used to prompt participants to contract and stop. After completion of the 60th contraction, the test ended. The end-test torque during the 5 min all-out test was defined as the mean of the last six contractions (Burnley, 2009; Vanhatalo, et al., 2007).

Visits 2-5 - Submaximal trials to establish the critical torque: During *visit 2*, participants performed 3 MVCs and the highest instantaneous measure of voluntary torque was recorded as the peak MVC torque. The target torques for the submaximal contractions in *visits 2-5* were calculated from this value. The target for the submaximal contractions in *visit 2* was set at 10% above the end-test torque measured during the 5 min all-out test completed in *Visit 1*. Submaximal contractions were performed until task failure, using a contraction regime of 3 s contraction and 2 s rest (Burnley, 2009). Participants were instructed to match their instantaneous torque to the target displayed on the screen in front of them for as much of the 3 s contraction as possible, and were not informed of the elapsed time but were informed of each "missed" contraction. After 3 missed contractions, participants were asked to immediately perform a 3 s MVC.

Visits 3-5 were performed in an identical manner, with the only difference being the percentage of MVC used. The subsequent tests were conducted in a randomised order and were designed to produce trial durations of between 2 and 15 min, as recommended for the determination of critical torque (Burnley, 2009).

Visit 6 – 5 min all-out test: During *Visit 6*, critical torque was estimated using the 5 min all-out test as outlined in *Visit 1*. The data from this visit were used to calculate the end-test torque and impulse above end-test torque (see *Data Analysis*).

Data Acquisition

Bipolar EMG signals were acquired in OT BioLab software, sampled at 2048 Hz and converted to digital data by a 12-bit analogue-to-digital converter (EMG-USB2+, 64-channel EMG amplifier; OT Bioelettronica, Torino, Italy; 3 dB, bandwidth 10-500 Hz). EMG signals were amplified using a gain of 500-1000 V/V (participant dependant) during the 5 min all-out test to avoid EMG signal saturation, which could affect interpretation of EMG amplitude results. Torque data was sampled at 2048 Hz in Spike2 (Version 7; Cambridge Electronic Design, Cambridge, UK) via a CED Micro 1401-3 (Cambridge Electronic Design, Cambridge, UK) and stored on a computer hard disk before offline analysis. EMG and torque signals were synchronised using a trigger delivered in Spike2.

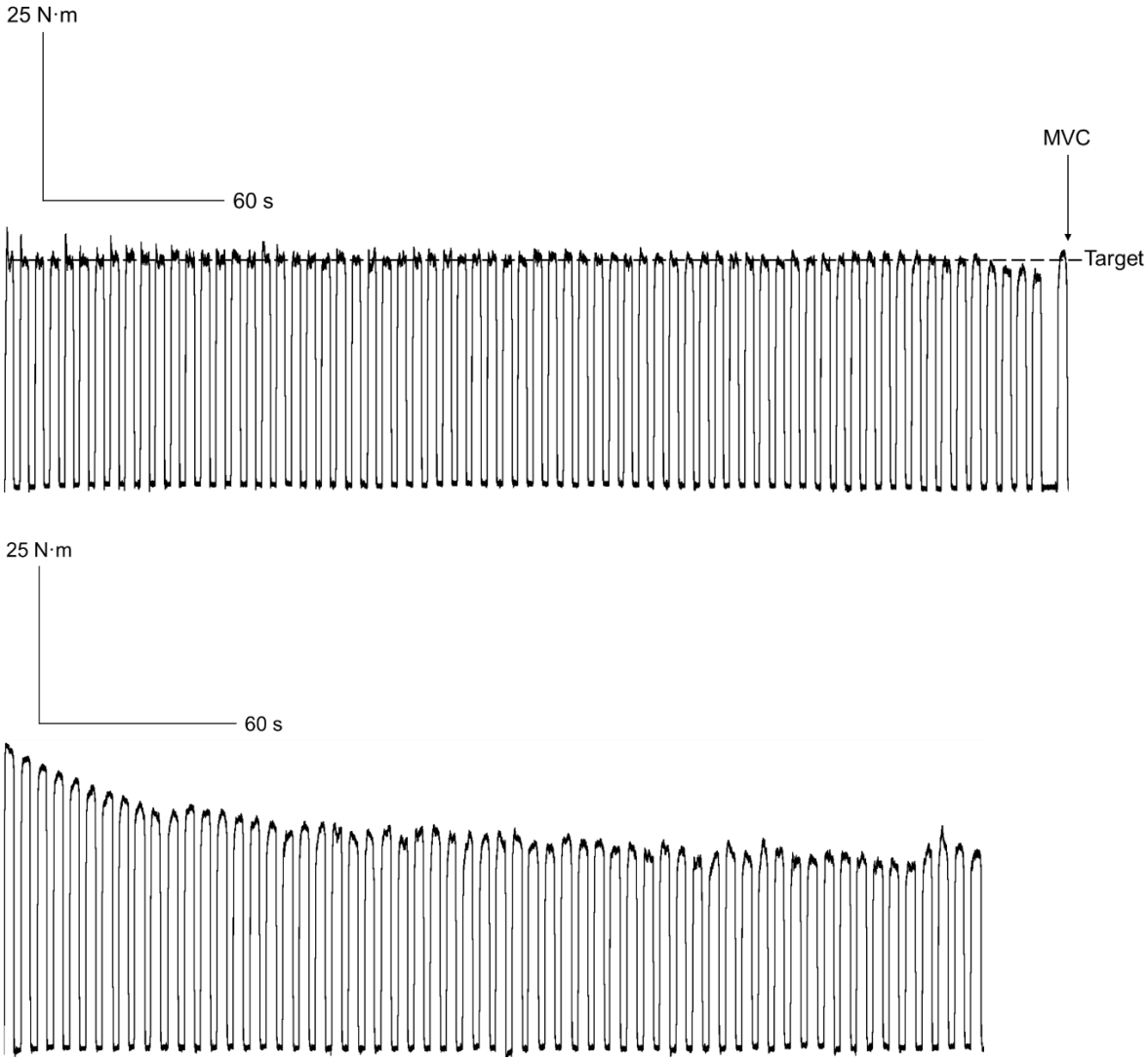

Figure 6.1. *Raw torque output from submaximal contractions performed to task failure (**A**) and the 5 min all-out test from a representative participant (**B**). **A** shows submaximal contractions performed until task failure at a target torque of 32.9 N·m. Note the inability to achieve the target torque during the final contractions of the test. The performance of a MVC at task failure resulted in a peak torque value of 35.2 N·m. **B** shows the torque profile during the 5 min all-out test for the same representative participant.*

Data Analysis

Torque – 5 min all-out test: Code written in MATLAB R2020a (The MathWorks, Massachusetts, USA) was used to analyse all torque data from the 5 min all-out test. In a similar fashion to Burnley (2009), peak torque and mean torque were calculated for each 3 s contraction, and the torque impulse was calculated as the area under the torque-time curve. End-test torque was determined using the mean

torque of the final six contractions in the 5 min all-out test (i.e., the final 30 s; Burnley, 2009; Vanhatalo et al., 2007).

Torque – submaximal tests: In keeping with the analysis of the 5 min all-out test, the mean torque and torque impulse were calculated for each contraction of the submaximal tests, and were used to establish the overall mean torque during each test and the total torque impulse for each test, as well as the time to task failure. However, owing to the inevitable rise and fall in torque when attempting to reach the target value during intermittent contractions, it is necessary to determine the *actual* test torque for each submaximal test to establish an accurate time to task failure. The actual test torque was calculated as the mean torque of the first 12 contractions (or the 1st min of the test; Burnley, 2009). Using the actual test torque rather than the target torque, task failure was then deemed to have occurred when the mean torque recorded during three consecutive contractions was more than 1 N·m below this value. The first of these three 'missed' contractions represented the point and time of task failure. Using all contractions prior to the point of task failure, the overall mean torque was calculated, and the total torque impulse and total contraction time were calculated as the sum of respective values for each individual contraction before this point.

The impulse-time model was used to determine the critical torque from the four (or in the case of two participants, five) submaximal tests performed to task failure. First, for each participant and for each submaximal test, the torque impulse was plotted against the total contraction time (Burnley, 2009). Next, using linear regression, the critical torque and the curvature constant (*W'*) were calculated from the slope of the line and the intercept of the line, respectively (Burnley et al., 2012):

$$\text{Torque impulse} = W' + \text{CT} \times t \qquad [1]$$

where CT represents the critical torque and t is the time to task failure.

Bipolar EMG analysis: Using code written in MATLAB, the EMG signal from the tibialis anterior was full-wave rectified. The root mean square EMG amplitude (EMG_{RMS}) was then calculated for each contraction of the 5 min all-out test and

normalised by expressing the EMG_{RMS} as a percentage of the EMG_{RMS} calculated from the pre-test MVC.

Statistical Analysis

Student's paired-samples *t*-tests were used to compare the critical torque estimated from the submaximal tests with the end-test torque from the 5 min all-out test. The same procedures were also used to compare the *W'* with the impulse measured above the end-test torque. One-way repeated measures ANOVA was used to analyse mean torque and EMG_{RMS} across the 5 min all-out test. Inspection of boxplots identified one outlier in the EMG_{RMS} data from the 120-150 s time bin onwards. In addition, Shapiro-Wilk's test indicated violations of normality for the EMG_{RMS} 180-210 s, 210-240 s, and 240-270 s time bin data (all $P > 0.05$). Consequently, Friedman's nonparametric test was performed for the EMG_{RMS} dataset. When significant changes were found, this was followed by *post-hoc* Bonferroni-adjusted pairwise comparisons to determine if differences were present between the end-test torque time bin (270-300 s) and all other time points. Linear regression and 95% limits of agreement were used to establish the relationship between the end-test torque and the critical torque. Linear regression was also used to establish if mean torque plateaued during the final 30 s of contractions during the 5 min all-out test. The slope of the line was then compared to zero by means of a one-sample *t*-test.

Results

5 min all-out test torque and bipolar EMG profiles

The torque profile for a representative participant during the 5 min all-out test is shown in Figure 6.1B. The group mean data for mean torque and peak torque during the 5 min all-out test are shown in Figure 6.2. Peak torque declined from 98.1 ± 8.8% MVC (first contraction) to 50.1 ± 14.7% MVC (the end-test torque) across the duration of the test. The ANOVA revealed statistically significant decreases in mean torque over time as the 5 min all-out test progressed ($F_{9, 45} = 14.853$, $P < 0.001$, η_p^2

= 0.748; Figure 6.3A). However, Bonferroni-adjusted pairwise comparisons revealed no significant differences between the end-test torque time bin (270 to 300 s) and all other time points (all $P > 0.05$). Linear regression showed the slope of torque during the final 30 s of the 5 min all-out test (the contractions used to establish the end-test torque) was -0.06 N·m/s (Table 6.1), which was not significantly different to zero ($P = 0.634$).

EMG_{RMS} (normalised to a pre-test MVC) declined from 94.7 ± 3.3% during the first 30 s time bin to 70.6 ± 22.4% during the final 30 s time bin, and Friedman's test revealed significant differences across the duration of the test ($\chi^2(9) = 21.782$, $P = 0.010$; Figure 6.3D). However, Bonferroni-adjusted pairwise comparisons revealed no significant differences between the end-test EMG_{RMS} time bin (270 to 300 s) and all other time points (all $P > 0.05$), with the exception of the first time bin (0 to 30 s; $P < 0.001$), indicating that neural drive did not change beyond the first 30 s of the test (Figure 6.3D).

Comparison of end-test torque with critical torque

End-test torque in the 5 min all-out test (22.8 ± 6.4 N·m) was significantly greater than critical torque estimated using the conventional method (16.8 ± 5.8 N·m; mean difference; 95% CIs: 6.0 N·m; 1.4, 10.7 N·m, t (5) = 3.34, $P = 0.020$). Parameters of the 5 min all-out test and the critical torque estimated using the conventional method are presented in Table 6.1 for all participants. The conventional estimation of the critical torque and the mean torque profile during the 5 min all-out test are shown for a representative participant in Figure 6.4A and Figure 6.4B, respectively.

The conventional determination of the critical torque using the impulse-time model provided a good fit across participants (r^2 = 0.893 – 0.999; Figure 6.4). The relationship and bias ± 95% limits of agreement between the end-test torque and the critical torque are shown in Figure 6.5A and Figure 6.5B, respectively. The impulse above end-test torque (983.7 ± 676.7 N·m·s) was not different from the curvature constant (W') estimated from the conventional method (1438.2 ± 590.8

N·m·s; mean difference; 95% CIs: -454.5 N·m·s; -1317.8, 408.7 N·m·s, *t* (5) = -1.35, *P* = 0.234).

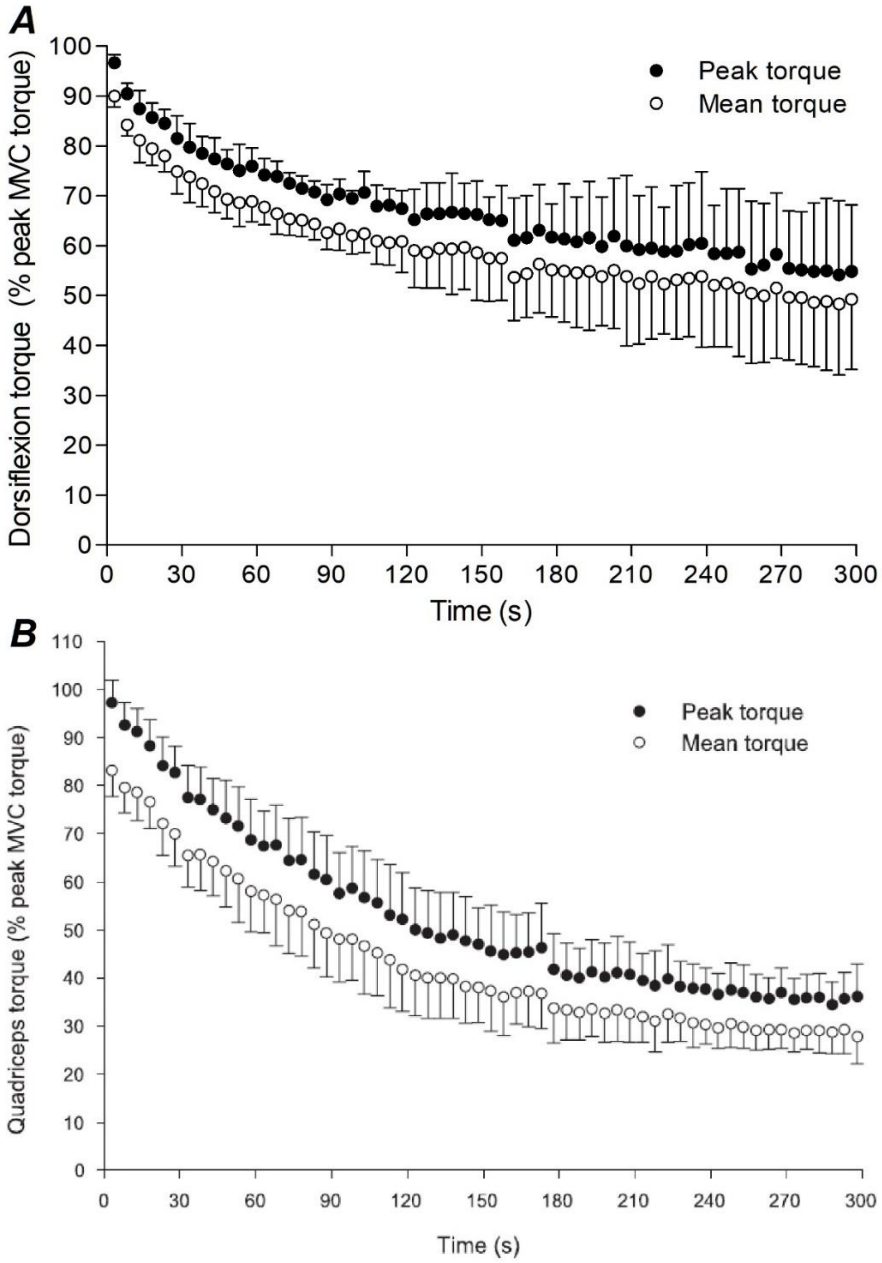

Figure 6.2. A*) Group peak and mean torque for all participants during the 5 min all-out test. Peak torque was calculated as the highest instantaneous torque measured during each 3 s contraction, and mean torque was calculated as the average torque over the duration of each contraction. Contractions were normalised to the instantaneous peak value of a control maximal voluntary contraction performed 10 min before the test began.* ***B****) Group peak and mean torque for the knee extensor 5 min-all out test from Burnley (2009).*

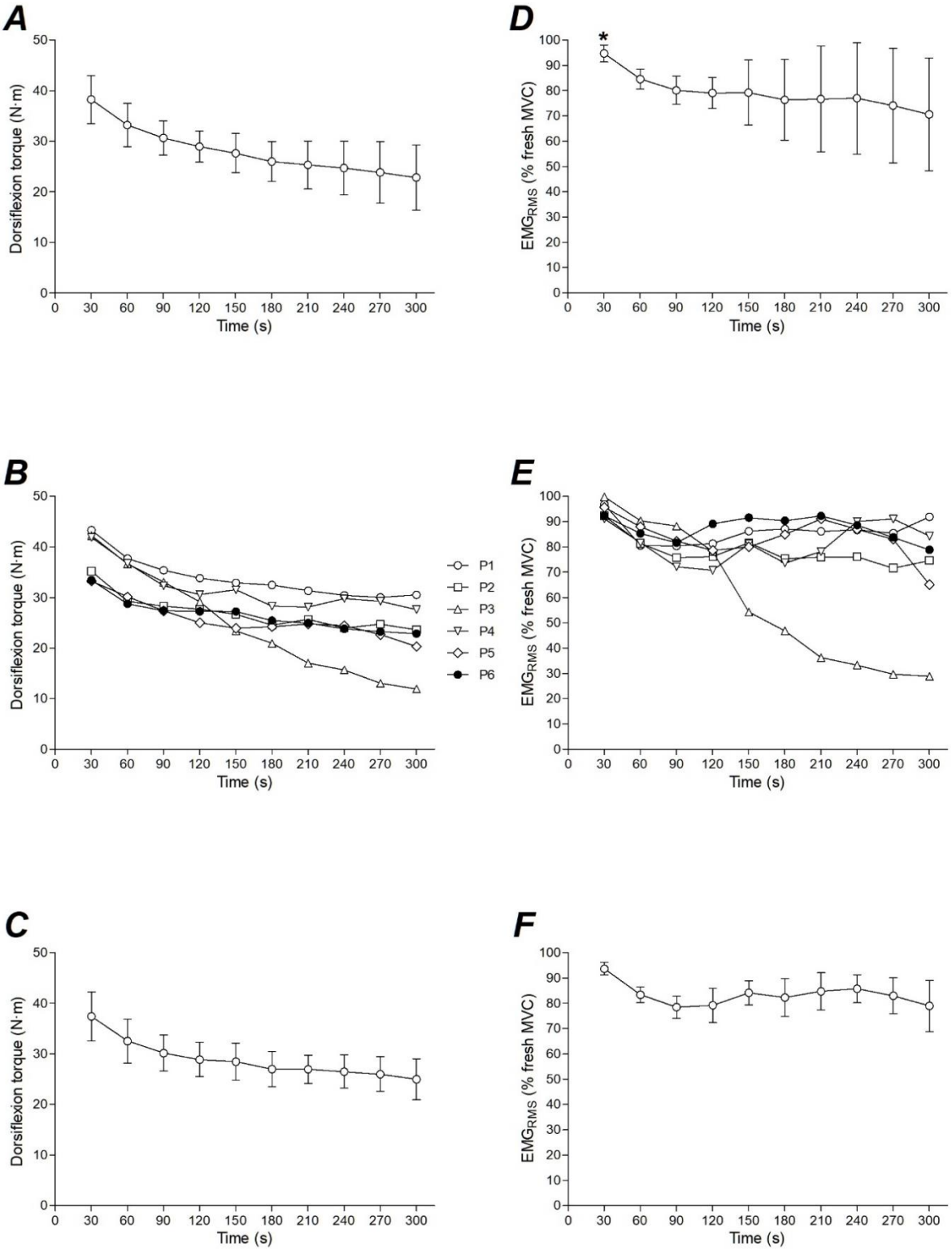

Figure 6.3. *Dorsiflexion torque (**A-C**) and tibialis anterior EMG_{RMS} (**D-F**) responses during the 5 min all-out test. **A** and **D** are mean ± SD responses for all participants (n = 6). Individual responses are displayed in **B** and **E**. Note the divergent responses of participant 3 (P3) from 150 s onwards; both responses further support the close agreement of the end-test torque and critical torque for P3 shown in Table 6.1. **C** and **F** are mean ± SD responses for all participants except P3 (n = 5). Six-contraction (30 s) time bins were used for analysis. *Significantly different from the end-test torque value (270-300 s; P < 0.05).*

Table 6.1. *Parameters of the 5 min all-out test and the critical torque determined from the conventional method using four or five submaximal tests performed to task failure*

	5MAOT						Submaximal Tests		
	Peak Torque		End-test Torque			Impulse Above End-test Torque, N·m·s			
Participant	N·m	% MVC	N·m	% MVC	Slope of Torque (N·m/s)		Critical Torque, N·m	% MVC	Curvature Constant (*W'*), N·m·s
1	49.6	86.5	30.5	53.2	0.45	621.6	28.0	48.8	766.8
2	45.4	109.3	23.6	57.0	-0.35	601.8	12.9	31.2	1878.4
3	51.5	90.3	11.9	20.9	-0.34	2340.6	12.4	21.7	1573.4
4	48.9	104.2	27.6	58.8	0.07	750.3	16.9	36.1	2186.1
5	38.0	95.2	20.3	50.9	-0.14	943.8	14.0	35.1	1506.3
6	39.5	102.9	22.9	59.5	-0.06	644.2	16.4	42.6	718.4
Mean	45.5	98.1	22.8	50.1	-0.06	983.7	16.8*	35.9	1438.2
SD	5.6	8.8	6.4	14.7	0.30	676.7	5.8	9.3	590.8

*MVC, maximal voluntary contraction; peak torque, highest torque measured during the test; end-test torque, mean torque measured in the last six contractions of the 5 min all-out test. *Significantly different from 5 min all-out test (P < 0.05).*

Submaximal tests

The time to task failure during the submaximal tests across all participants ranged from 110.4 ± 38.7 s in the test with the highest target torque (28.0 ± 5.2 N·m; 60.5 ± 9.7 % MVC) to 502.7 ± 81.4 s in the test with the lowest target torque (19.2 ± 5.4 N·m; 41.3 ± 8.8 % MVC). The torque generated during the MVC performed immediately after task failure of each test was not significantly different to the mean torque, with the exception of the test with the lowest target torque (mean difference; 95% CIs: 7.3 N·m·s; 1.2, 13.4 N·m·s, t (5) = 3.09, P = 0.027; Figure 6.6), indicating that to match the required torque at the end of the test, a maximal effort was required.

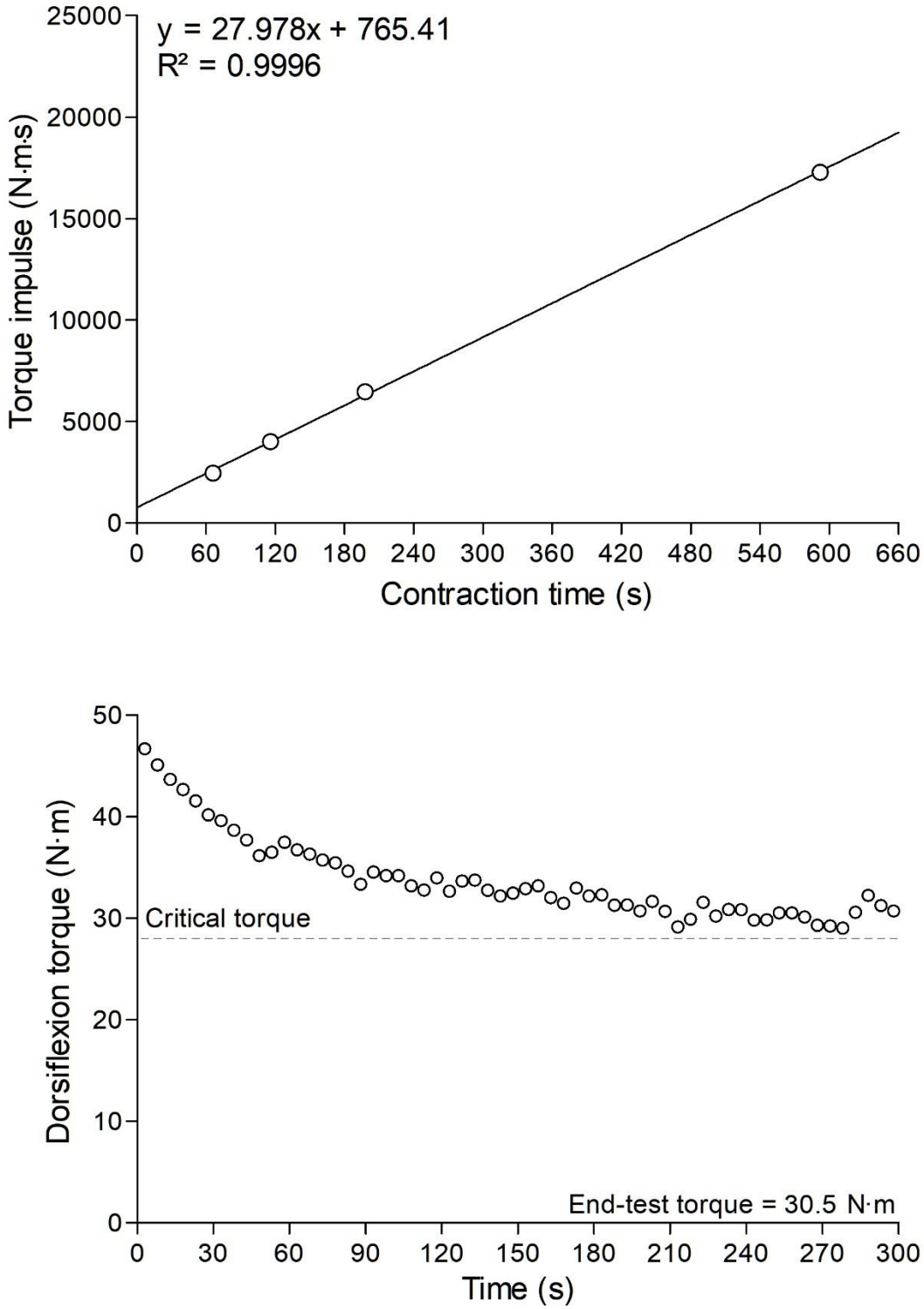

Figure 6.4. *Critical torque determined using the conventional method and end-test torque from the 5 min all-out test for a representative participant.* ***A****) The critical torque estimated using the impulse-time model across four separate submaximal tests performed to task failure.* ***B****) The mean torque profile of the 5 min all-out test. Note the lack of agreement with the critical torque from* ***A*** *during the final six contractions of the 5 min all-out test in* ***B****.*

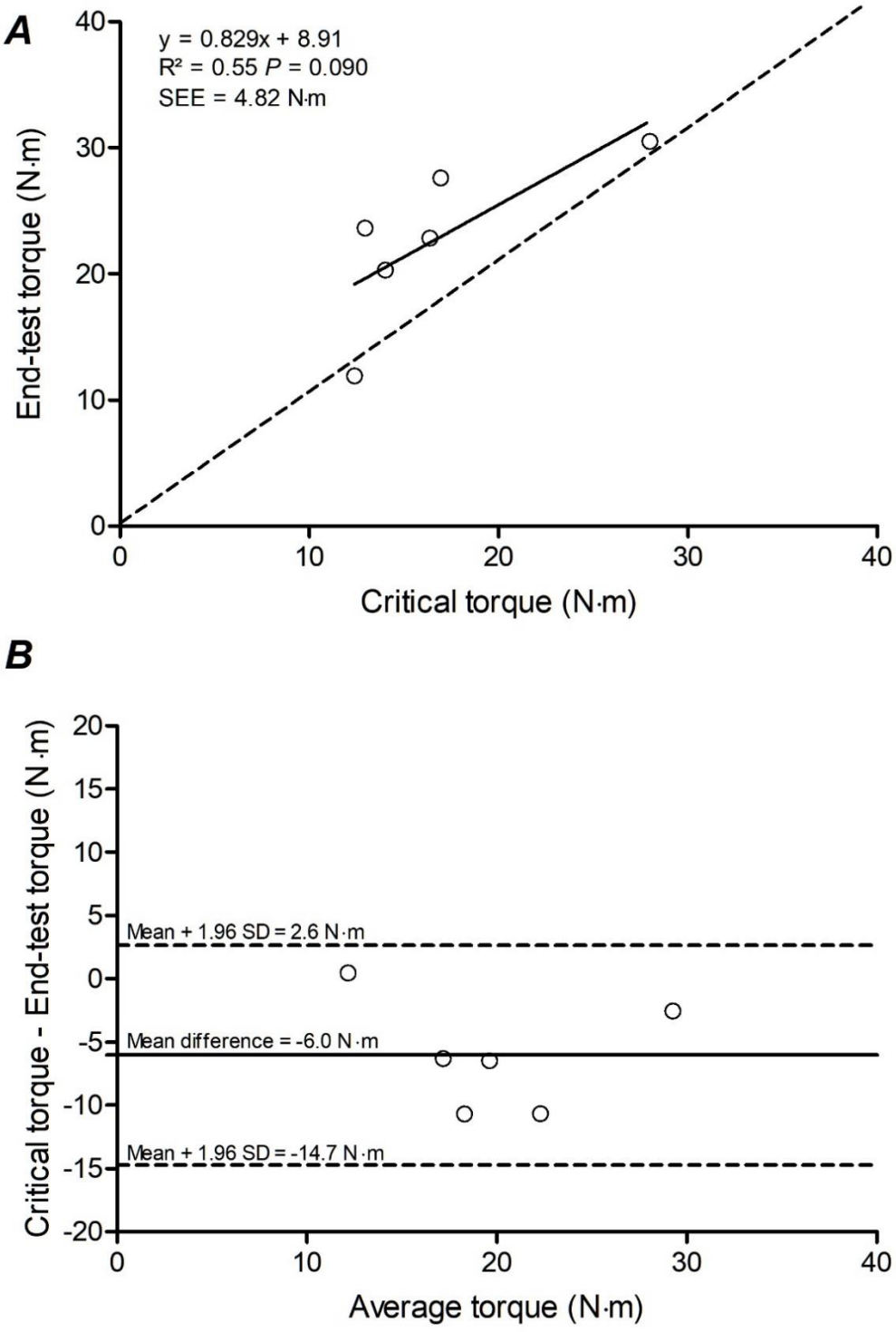

Figure 6.5. A*) The relationship between the critical torque estimated using the conventional method and the end-test torque from the 5 min all-out test for all participants. Linear regression was used to estimate the line of best fit (displayed at the solid line). The line of identity is represented by the dashed line.* ***B****) The bias and limits of agreement between the critical torque and the end-test torque. The mean difference between each estimate is indicated by the solid line, and the dashed lines represent the 95% limits of agreement. Open circles represent the values for each individual participant. SEE, standard error of the estimate.*

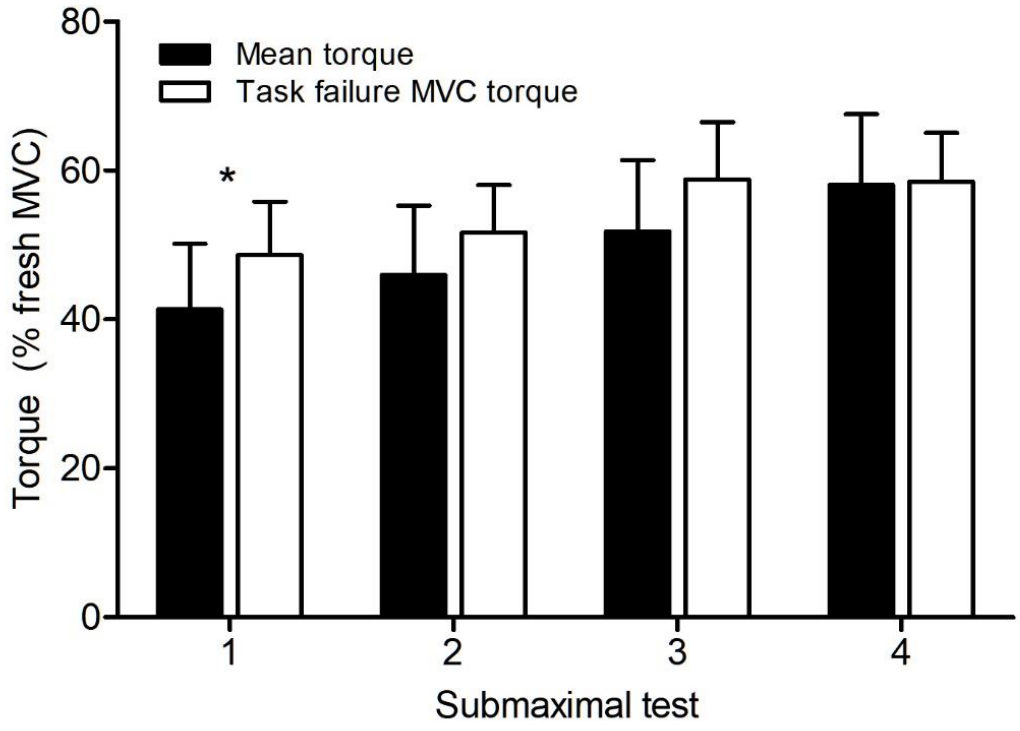

Figure 6.6. *Group torque responses during the submaximal exercise tests used in the conventional estimation of the critical torque. The submaximal tests are ordered from the lowest (test 1) to highest (test 4) target torque attempted by each participant. The mean torque for each test and the MVC torque at task failure are each shown as a percentage of fresh MVC torque. Error bars represent SD. *Significantly different from mean torque (P < 0.05).*

Discussion

The current study aimed to compare the end-test dorsiflexor torque during the last 30 s of the 5 min all-out test and the critical torque estimated using the conventional method involving multiple submaximal tests performed to task failure. In contrast to the stated hypothesis, the data showed that the end-test torque from the 5 min all-out test does not closely approximate the critical torque estimated using the conventional method. The present study is the first to extend the critical torque concept to the dorsiflexor muscles, which are central to many HDsEMG studies, and

provides the first evidence that the dorsiflexor critical torque occurs at a higher fraction of MVC than that of the knee extensors.

The results of the current study suggest that the 5 min all-out test does not provide a valid measure of the critical torque in the dorsiflexors when compared to the “gold standard” method involving multiple submaximal tests. Although the 5 min all-out test is sufficient for the attainment of a steady state in the knee extensors (Burnley, 2009), its use here overestimated the critical torque by ~15% MVC, indicating that it is necessary to extend the duration of the all-out test in the dorsiflexors beyond 5 min. Using intermittent handgrip exercise with an adapted 1 s contraction to 2 s relaxation duty cycle, Kellawan and Tchakovsky (2014) recently developed an all-out test lasting 10 min. The authors postulated that an extended test was required to attain a plateau in force, given the smaller mass of the forearm musculature and the lower duty cycle, relative to the knee extensors and the 5 min all-out test, respectively. Indeed, in a model-based estimation of the critical torque in the similarly less fatigable elbow flexor muscle group, it was suggested that durations of up to 60 min may be necessary to attain a true steady state during the end-test torque (Herold & Sommer, 2020). It would appear that when using all-out tests across muscle groups, applying a uniform approach to the duration of the test is likely to result in an overestimation of the critical torque. It should be noted that Abdalla et al. (2018) did use the 5 min all-out test in the plantar flexors, and reported an end-test torque of ~40% MVC, which is higher than the estimate of dorsiflexor critical torque reported here. However, the critical torque was not estimated using the conventional method, meaning no comparison could be made between that and the end-test torque.

It is pertinent to mention that attempts by some research groups to estimate the critical power using the 3 min all-out test in cycling (from which the 5 min all-out test was derived) have also resulted in overestimations when compared to the conventional approach (Bartram et al., 2017; Bergstrom et al., 2014; Muniz-Pumares et al., 2019; Nicolò et al., 2017). Bartram et al. (2017) and Nicolò et al.

(2017) challenged the validity of the 3 min all-out test in predicting critical power in well-trained cyclists after “end-test” power was reported to overestimate the critical power and subsequent time trial performance, respectively. However, in one study participants were not familiarised with the 3 min all-out test (Bergstrom et al., 2014), and both Bartram et al. (2017) and Nicolò et al. (2017) were unable to rule out the possibility that pacing strategy, whether conscious or subconscious, influenced the end-test power. We attempted as far as possible to limit such methodological factors in the present study. Participants were familiarised with the 5 min all-out test during their first visit, instructed to produce maximal effort during each and every contraction of the test, and were given strong verbal encouragement throughout.

Like the critical power, which demarcates the boundary between heavy and severe intensity exercise and therefore the threshold of the metabolic steady-state during exercise (Craig et al., 2019; Jones et al., 2019), the critical torque represents an important threshold for neuromuscular fatigue development (Burnley et al., 2012). The limitations of using estimates of surface EMG amplitude to infer changes in the neural drive to the muscle due to the phenomenon of amplitude cancellation are well known, with amplitude cancellation increasing in magnitude alongside the intensity of muscle activation (Farina, Merletti et al., 2014). Nevertheless, bipolar surface EMG was recorded from the tibialis anterior to allow for comparisons to the work of Burnley (2009). Though not measured in the current study, a ~26% fall in voluntary action, indicative of central fatigue, was reported by Burnley (2009) during the 5 min all-out test for the knee extensors. This decline in voluntary activation was accompanied by significant reductions in the vastus lateralis average rectified EMG, with each time point of the first 90 s greater than the value at 300 s. In contrast, while a significant reduction in EMG_{RMS} was also observed in the current study during the all-out test, the only value that was significantly different to the end-test EMG_{RMS} was that of the 0-30 s time bin. Indeed, post-hoc comparisons revealed that the EMG_{RMS} during the 0-30 s time bin was significantly different to all other time bin values; no other differences were observed in the comparisons involving time bins from 30-60 s onwards (the inclusion of participant 3, who demonstrated a steep decline in EMG_{RMS} across the test, resulted in much greater variance in the

EMG_{RMS} responses; Figure 6.3*D-F*). This finding suggests that after an initial decline, neural drive may have been sustained throughout the remainder of the all-out test (Bigland-Ritchie et al., 1983). Future research could employ HDsEMG decomposition techniques, removing the aforementioned limitations of bipolar surface EMG, and from which the behaviour of individual motor units can be extracted (Martinez-Valdes, Laine et al., 2016). However, the motor unit decomposition technique presented in the General Methods (Chapter 3) is currently limited to isometric contractions lasting at least 10 s (Negro et al., 2016), requiring a greatly altered duty cycle to those used in the all-out tests developed thus far.

For one participant (participant 3; Table 6.1), it would appear that the 5 min all-out test was long enough in duration to provide an accurate estimate of the critical torque when compared to the conventional method (11.9 N·m vs. 12.4 N·m). The same participant also had the lowest critical torque relative to MVC (22%), suggesting that the lower the relative critical torque, the shorter the duration of all-out test needed. Additionally, in contrast to all other participants and in line with the findings of Burnley (2009), the impulse above end-test torque was greater than the curvature constant (*W'*; 2340.6 N·m·s vs. 1573.4 N·m·s).

In the current study, the impulse accumulated above the end-test torque during the 5 min all-out test was not significantly different to the curvature constant (*W'*) calculated from the submaximal trials (Table 6.1). However, this lack of difference is likely due to the large variance (quantified by the SD), rather than the two estimates being of similar value. In all but one participant, *W'* was greater than the impulse accumulated above the end-test torque. This is in contrast to Burnley (2009), who unexpectedly found impulse accumulated above the end-test torque to be significantly greater than *W'* for the knee extensors. Given that *W'* can be considered a "fatigability constant", thought to be related to intramuscular substrate depletion and, consequently, to represent a muscular accumulation of metabolites (e.g., P_i, ADP, or H+; Poole et al., 2016), this led to the suggestion that the two values do not represent the same physiological parameter (Burnley, 2009).

Interestingly, for only one participant in Burnley (2009) was the *W'* greater than the impulse accumulated above the end-test torque (participant 3), and this participant also had the biggest overestimation of critical torque (~6% MVC). Combined with the findings of the current study, this suggests that, even if the two values do indeed represent different physiological quantities, an impulse accumulated above end-test torque greater than *W'* might be correlated with a closer agreement between the critical torque and end-test torque and vice versa. However, if an estimate of dorsiflexor *W'* is required, a conventional series of submaximal tests performed to task failure must be used, as is also the case for the knee extensor muscle group.

In the current study, the conventional method involving a series of submaximal exercise tests performed to task failure yielded a critical torque of ~36% MVC for the dorsiflexors. This is higher than the critical torque of ~28% MVC reported for the knee extensors by Burnley (2009), indicating that the dorsiflexor muscles are less fatigable. Other studies to have estimated the critical torque for the knee extensors have yielded values of between ~27 and 35% MVC (Abdalla et al., 2018; Ansdell et al., 2019b; Burnley et al., 2012; de Menezes Bassan et al., 2019; Pethick et al., 2016; Pethick et al., 2020). The finding that the dorsiflexors are more fatigue-resistant than the knee extensors is consistent with the analysis of endurance times reported by Frey-Law and Avin (2010). While the current study employed an intermittent, isometric model of exercise, Frey-Law and Avin (2010) carried out a systematic review of sustained contractions and found the ankle joint to be the most fatigue-resistant when compared to the trunk, elbow, handgrip, knee, and shoulder, with similar endurance time “power fatigue” curves predicted for both plantarflexion and dorsiflexion contractions. To the author’s knowledge, the only other muscle group for which the critical torque/force has been calculated empirically is the forearm muscles, but this was not reported as a value relative to MVC (Kellawan & Tchakovsky, 2014).

Limitations

In the current study, only one 5 min all-out test was used for analyses, whereas Burnley (2009) used two. This allowed Burnley (2009) to compare the end-test torque between tests, confirming the reliability of the measure, and use the grouped average values for each participant for any subsequent comparisons with the critical torque from the conventional method. In addition, the all-out test used in the present study was limited to 5 min. A study design incorporating a longer all-out test or more visits could have been employed, but without knowing when torque would be predicted to plateau, this would have been difficult. As previously mentioned, durations of up to 60 min have been suggested for other muscle groups using a model-based approach (Herold & Sommer, 2020). Further work could utilise similar models to predict a "time to end-test torque" before confirming this experimentally.

Finally, the small sample size in the current study makes it difficult to generalise to a wider population, and only male participants were recruited. It has previously been shown that females have a higher critical force for the knee extensors relative to MVC when compared to males (Ansdell et al., 2019a). Future work is necessary to establish if similar sex differences are also apparent in the dorsiflexor muscle group.

Conclusions

In summary, the performance of a 5 min all-out test in the ankle dorsiflexors resulted in an end-test torque of ~50% MVC, which was significantly higher than the critical torque estimated from the conventional method involving a series of submaximal contractions performed to task failure (~36% MVC). This finding suggests that, unlike in the knee extensors (Burnley, 2009), a duration of 5 min is not long enough to attain a plateau in torque which closely approximates the critical torque during the final 30 s of maximal ankle dorsiflexor contractions. Additionally, the current study is the first to extend the critical torque concept to ankle dorsiflexion and provides the first evidence that the critical torque for the dorsiflexors occurs at a higher fraction of MVC than that of the knee extensors in a similar participant sample to the work of Burnley (2009). Given that the ankle dorsiflexor muscles (most notably the tibialis anterior) are commonly used in studies utilising HDsEMG techniques, this finding is

of importance as it demonstrates that the target torque for fatiguing intermittent contractions should be set above this relative value. Future studies should look to confirm this finding. Given the importance of the critical torque as a neuromuscular fatigue threshold, and the fact that fatigue-induced losses of complexity are only evident above this threshold, further work is required to establish the optimal duration for an all-out test in the dorsiflexors using both the duty cycle of the current study (3 s contraction: 2 s rest), but also other duty cycles more typical of those used in HDsEMG studies (e.g., intermittent contractions incorporating a 10 s hold phase).

CHAPTER 7 – THE EFFECTS OF PRIMING EXERCISE ON MOTOR UNIT BEHAVIOUR IN THE TIBIALIS ANTERIOR

Introduction

In healthy young adults, the transition from rest to constant-load, moderate-intensity exercise is characterised by the attainment of steady-state pulmonary oxygen uptake ($\dot{V}O_2$) within 2-3 min (Whipp et al., 1982). The $\dot{V}O_2$ response can be partitioned into three phases (Burnley & Jones, 2007). The cardiodynamic phase (Phase I), characterised by a 10-20 s delay in the $\dot{V}O_2$ response to exercise, is caused by pulmonary $\dot{V}O_2$ not immediately reflecting muscle $\dot{V}O_2$ (Burnley & Jones, 2007). This leads to Phase II, the primary component, consisting of an exponential increase in $\dot{V}O_2$, which ultimately results in the attainment of steady-state after 2-3 min of exercise (Phase III). However, during heavy or severe exercise (performed above the lactate threshold and the critical power, respectively), $\dot{V}O_2$ rises above the predicted 'steady-state', with the amplitude of this response signifying an increased metabolic inefficiency as exercise continues, termed the $\dot{V}O_2$ "slow component" (Barstow et al., 1990; Jones, Koppo et al., 2003). The importance of $\dot{V}O_2$ kinetics and how they relate to exercise tolerance was introduced in the Review of Literature (Chapter 2). Consequently, interventions designed to speed overall $\dot{V}O_2$ kinetics and attenuate the amplitude of the $\dot{V}O_2$ slow component during high-intensity exercise have been extensively explored with a view to improving exercise performance.

Warm-up exercise is a universally accepted practice performed by athletes prior to subsequent exercise, training, or competition (Bishop, 2003; Jones, Koppo et al., 2003). The use of heavy warm-up exercise, or "priming", is known to lead to a speeding of $\dot{V}O_2$ kinetics during a subsequent bout of heavy exercise (Gerbino et al., 1996; MacDonald et al., 1997). Subsequent work determined that priming exercise did not speed the phase II $\dot{V}O_2$ kinetics (Burnley et al., 2000), but instead the overall speeding of $\dot{V}O_2$ kinetics was attributed to an increased phase II amplitude and a reduced $\dot{V}O_2$ slow component amplitude (Burnley et al., 2001; Koppo & Bouckaert, 2001). The effects on the $\dot{V}O_2$ response are preserved for at least 30-45 min following prior heavy exercise (Burnley, Doust, & Jones, 2006). Provided sufficient recovery time is allowed (>9-10 min), priming exercise performed

in the heavy or severe intensity domain has also been shown to lead to increases in time to exhaustion of between 10-60% in a subsequent bout of exercise (Bailey et al., 2009; Burnley et al., 2011; Carter et al., 2005; Jones, Wilkerson, et al., 2003). Despite this, the mechanisms responsible for the above-mentioned changes in $\dot{V}O_2$ kinetics remain a contended issue.

One long-held hypothesis for the effect of priming on the $\dot{V}O_2$ kinetics response is a change in motor unit recruitment patterns (Burnley et al., 2001; Whipp, 1994). It is important to note that some studies have been unable to detect significant changes in the integrated electromyogram (iEMG) of the leg muscles when priming exercise was followed by a subsequent bout of heavy exercise (Scheuermann et al., 2001; Tordi et al., 2003). Nevertheless, the data from both Scheuermann et al. (2001) and Tordi et al. (2003) were suggestive of a trend for increased iEMG values during the subsequent heavy exercise bout. In line with this, Burnley, Doust, Ball et al. (2002) reported an elevated primary $\dot{V}O_2$ amplitude during the second of two bouts of heavy cycle exercise (separated by 12 min recovery), accompanied by a significant 19% increase in the iEMG of three leg muscles (gluteus maximus, vastus lateralis, and vastus medialis) at the onset of the second bout. It was suggested that the observed elevated primary $\dot{V}O_2$ amplitude may be due to increased motor unit recruitment at the onset of exercise (Burnley, Doust, Ball et al., 2002). Additionally, the observed increase in iEMG was less steep during the final 3 min of the second exercise bout, providing further (albeit qualitative) support to the notion that the continual recruitment of additional motor units could also explain the reduction in the amplitude of the $\dot{V}O_2$ slow component.

The aforementioned differences in iEMG findings between cycling studies highlight the limited sensitivity of bipolar surface EMG in detecting subtle changes in motor unit behaviour during dynamic, multi-joint exercise (Burnley, et al., 2005). Unlike cycle ergometry, the use of isokinetic dynamometry provides an opportunity to investigate the effect of priming exercise on motor unit behaviour using an isolated muscle model. Layec et al. (2009) investigated the effects of a prior 6 min bout of

high-intensity knee-extension exercise (35% of MVC) on energy production and muscle fibre recruitment during a subsequent 6 min heavy-intensity knee-extension exercise. The two exercise bouts were separated by 6 min of rest and surface EMG was recorded from the vastus lateralis muscle of the left leg. The authors calculated the ratio between iEMG and power output (W) and observed an increase during the early part of the subsequent exercise bout without an increase in energy cost (Layec et al., 2009). This increase in the iEMG/W ratio was interpreted to represent the recruitment of additional motor units following priming exercise. However, the use of single-channel bipolar surface EMG techniques, even in an isolated muscle model, is limited since the amplitude and frequency content of the signal can only provide coarse approximations of motor unit behaviour (Farina, 2008; Holobar, et al., 2016).

In studies of individual motor unit behaviour, it has been demonstrated that the recruitment (and de-recruitment) thresholds of motor units are altered following a bout of fatiguing exercise (Adam & De Luca, 2003; Carpentier et al., 2001; Enoka et al., 1989). Carpentier et al. (2001) observed decreases and increases in recruitment threshold for high threshold and low threshold motor units, respectively, during submaximal fatiguing contractions (50% MVC) of the first dorsal interosseous. In contrast, Adam and De Luca (2003) reported decreases in the recruitment threshold of all observed motor units during submaximal fatiguing contractions (20% MVC) in the vastus lateralis muscle, regardless of whether motor units were classified as a high or low threshold. Moreover, and in line with the effects reported after prior heavy whole body exercise on the $\dot{V}O_2$ response, the time taken for restoration of the original recruitment thresholds in motor units appears to be similar, lasting between 15-30 min after cessation of exercise (Carpentier et al., 2001).

The above findings were obtained using traditional motor unit recording techniques, which typically involve the use of intramuscular electrodes (Adam & De Luca, 2003; Carpentier et al., 2001) or subcutaneous electrodes (Enoka et al., 1989). Though

these methods have been widely used in research and clinical settings, they present some fundamental limitations due to their inherent selectivity and invasive nature. Furthermore, these invasive approaches are typically suited to low-level muscle contractions and often result in relatively few motor units being sampled at a time (Farina et al., 2008). In contrast, the development of high-density surface EMG (HDsEMG) presents the opportunity to non-invasively identify a more representative sample of motor units in the active muscle (Merletti et al., 2008). Recent advances in HDsEMG decomposition algorithms have enabled the identification of larger pools of motor units from a range of muscles and contraction levels (Holobar, et al., 2014; Negro et al., 2016).

The aim of the present study was to investigate the effects of prior 'heavy' exercise on motor unit behaviour of the tibialis anterior muscle. This chapter extends the area of priming research to include HDsEMG recordings during isometric ankle dorsiflexion contractions. The experimental hypotheses were: 1) priming exercise would lead to a reduction in motor unit recruitment threshold during subsequent contractions; and 2) priming exercise would result in an increase in HDsEMG amplitude during a subsequent bout of 'heavy' exercise.

Methods

Participants

Following approval from the SSES REAG at the University of Kent, and in accordance with the Declaration of Helsinki, six physically active male adults (mean ± SD: age 29 ± 7 years; stature 181 ± 5 cm; body mass 74 ± 11 kg) volunteered to participate in the study and provided written informed consent. Participants were instructed to attend each session well rested and well hydrated, to not consume caffeine or eat in the 2 h prior to exercise, and to not consume alcohol or undergo heavy exercise in the preceding 24 h. Participants were requested to wear shorts to allow access to the HDsEMG electrode site.

Experimental Design

Participants were required to visit the laboratory on three separate occasions, with at least 48 hours between visits. Sessions were conducted at the same time of day (± 2 h) to minimise the influence of diurnal variation on muscle contractility (Racinais et al., 2005). The first visit was used to familiarise participants with all equipment and procedures, and record individual chair settings (during *Visit 1* from Chapter 6). *Visits 2* and *3* were used to investigate the effects of "priming" exercise on motor unit behaviour. The order of the second and third visits was randomised.

Experimental Set-up

Torque: The methods used for the setup of the dynamometer are described in the General Methods (Chapter 3). The seating position was recorded during the first visit and replicated thereafter. During the 6 min heavy exercise bouts, participants were instructed to match a target torque displayed as a horizontal line on a computer monitor ~2 m away from them. During the ramp-and-hold contractions, a custom-written Spike2 script was used to display a trapezoidal torque target on the computer monitor, and participants were instructed to track this target as smoothly as possible.

High-density surface electromyography: The methods used for the placement of the HDsEMG electrode grid are described in the General Methods (Chapter 3). The location of the HDsEMG electrode grid was marked on the skin using a surgical pen and participants were asked to keep the area marked to allow consistent positioning across experimental visits.

Motor Unit Decomposition: The HDsEMG signals acquired during each submaximal isometric ramp-and-hold contraction were decomposed offline using OT BioLab (OT Bioelettronica, Torino, Italy) as described in the General Methods (Chapter 3). The SIL was set at 0.90 for each contraction in the first instance, and only lowered to 0.85 if fewer than 5 motor units were identified. In the event that fewer than 5 motor units were then identified after the SIL was lowered to 0.85, those motor units were discarded from further analysis. The torque values corresponding to the first and last motor unit action potentials were used as the recruitment and de-recruitment

thresholds, respectively. The average discharge rate for each motor unit was calculated from the first four action potentials to give the discharge rate at recruitment, from all action potentials identified during the steadiest 8 s of torque from the hold phase of the contraction, and from the last four action potentials to give the discharge rate at de-recruitment (Del Vecchio, Casolo et al., 2019).

Global surface EMG measurements: The root mean square value of the central signal of the HDsEMG grid was used to estimate EMG amplitude (EMG_{RMS}) during each 3 s contraction of the 6 min exercise bouts to provide a global measure of motor unit recruitment. Technical difficulties meant that the EMG_{RMS} data during the second 6 min bout for one participant failed to record, therefore these data are reported for five participants.

Experimental Protocol

Visit 1 – Familiarisation: Participants performed a series of three isometric MVCs, each lasting 3 s and separated by at least 1 min of recovery. After 5 min rest, participants were familiarised with the ramp-and-hold contractions at 10% and 40% MVC (5 s ramp-up, 10 s hold, 5 s ramp-down; Figure 7.1C).

Visit 2 – Priming exercise: After the HDsEMG electrode array was re-applied, participants completed a short warm-up then completed a series of three isometric MVCs, each lasting 3 s and separated by at least 1 min of recovery. Following the MVCs, 5 min of rest was given before participants completed the pre-exercise ramp-and-hold contractions as described in *Visit 1*. A further 5 min of rest was given after the baseline contractions before participants completed the 'priming' exercise. Participants performed intermittent submaximal ankle dorsiflexion contractions for 6 min or until task failure, whichever occurred sooner. This protocol used a duty cycle of 3 seconds contraction and 2 seconds rest, at a target torque set at 90% of the estimated critical torque (determined in Chapter 6). This intensity was chosen to ensure, as far as possible, participants exercised in the 'heavy' intensity domain. Ramp-and-hold contractions were then performed immediately after the priming exercise. A schematic of the procedures for *Visit 3* can be seen in Figure 7.1.

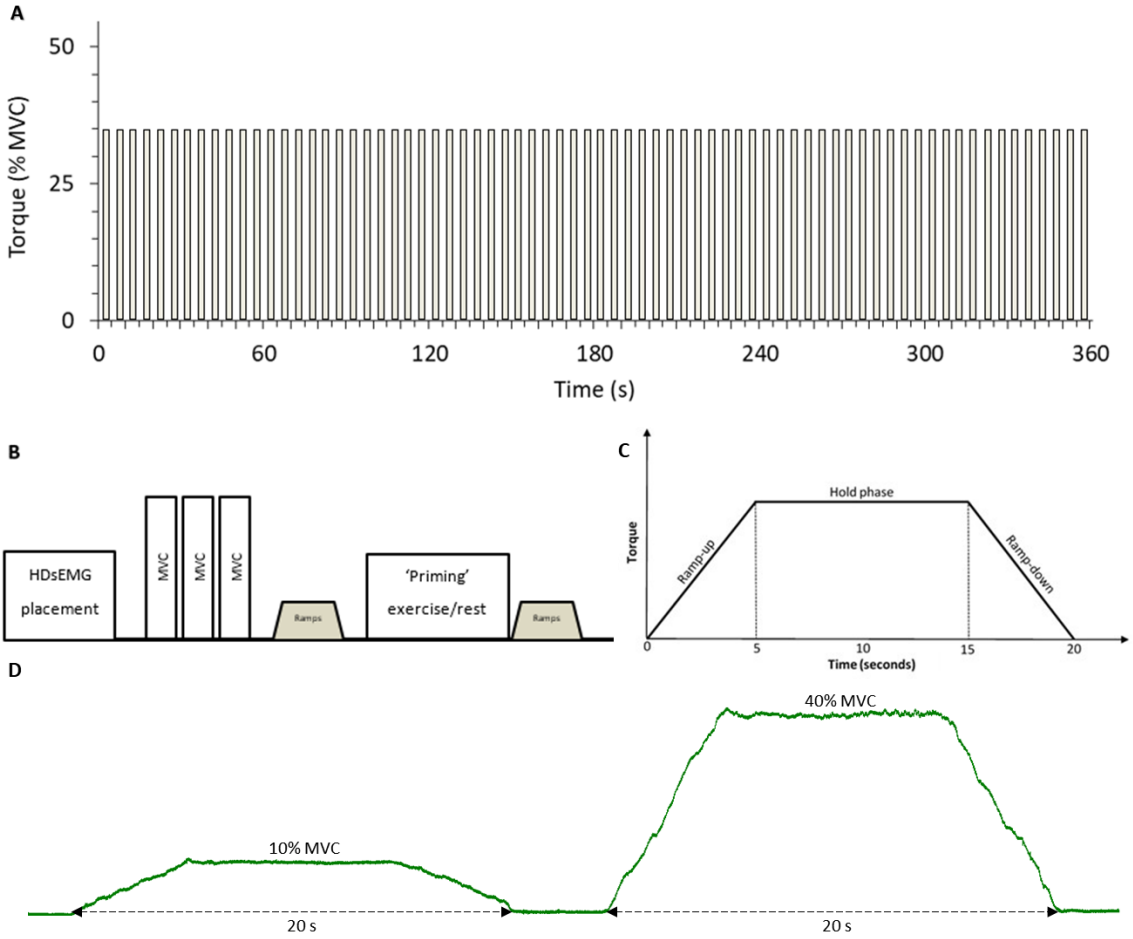

Figure 7.1. *A: Contraction protocol for the 6 min priming and subsequent exercise bouts. B: Schematic of the experimental trial procedures. C: Each repeat of the ramp-and-hold contractions consisted of a 5 s incline, a 10 s hold phase, and a 5 s decline. D: Torque output for a representative participant from the ramp-and-hold contractions performed immediately after the 6 min priming bout at 10% and 40% MVC.*

Visit 3 – Effects of priming on a subsequent exercise bout: The HDsEMG electrode grid was re-applied and participants completed a short warm-up before completing a series of three MVCs separated by 1 min rest, and resting for 5 min. Participants then performed the same priming bout as outlined in *Visit 2* before resting for 12 min (Burnley et al., 2001). After this rest period, participants completed a second 6 min bout of exercise, performed at the same intensity as the priming bout. HDsEMG was continuously sampled during both exercise bouts.

Data Acquisition

HDsEMG signals were sampled at 2048 Hz and converted to digital data by a 12-bit analogue-to-digital converter (EMG-USB2+, 64-channel EMG amplifier; OT Bioelettronica, Torino, Italy; 3 dB, bandwidth 10-500 Hz). To avoid signal saturation, which could affect decomposition results, HDsEMG signals were amplified using a gain of 2000, 1000, 500, and 500 for the contractions at 10% MVC, 40% MVC, MVC, and the 6 min heavy exercise bouts respectively. Torque data was sampled at 2048 Hz in Spike2 (Version 7; Cambridge Electronic Design, Cambridge, UK) via a CED Micro 1401-3 (Cambridge Electronic Design, Cambridge, UK) and stored on a computer hard disk before offline analysis. HDsEMG and torque signals were synchronised using a trigger delivered using Spike2.

Statistical Analysis

Student's paired-samples t-tests and 95% confidence intervals were used to investigate differences between pre-exercise and post-exercise values for discharge rates at recruitment, during the hold phase, and at de-recruitment, as well as recruitment thresholds and de-recruitment thresholds of the contractions performed at 10% and 40% MVC. Global EMG_{RMS} data from the third visit was compared using a two-way (exercise bout × time) repeated measures ANOVA. *Post-hoc* Bonferroni-adjusted pairwise comparisons were performed to identify specific differences when significant main or interaction effects were observed.

Results

MVC torque and target torque during heavy exercise

Fresh peak MVC torque was taken from Chapter 6. The target torque for the 6 min heavy exercise bouts was set at 90% of the critical torque calculated in Chapter 6, which was 15.1 ± 5.2 N·m (32.3 ± 8.4% MVC). All participants completed the entirety of the second 6 min heavy exercise bout during *Visit 3*. The individual target torque values are shown in Table 7.1.

Motor unit behaviour

For two participants, fewer than 5 motor units were identified during the contractions performed at 10% MVC and were discarded from further analysis, therefore data for these contractions is reported for 4 participants. The total number of motor units accepted for data processing after decomposition across both contraction intensities and timepoints was 296. This included 87 (mean per participant: 22 ± 6) from the pre-exercise contraction and 88 (22 ± 6) from the post-exercise contraction performed at 10% MVC. 66 motor units were accepted from the pre-exercise contraction (11 ± 3) and 55 (9 ± 4) from the post-exercise contraction performed at 40% MVC.

Table 7.1. *Target torque values for the 6 min heavy exercise bouts.*

		Critical Torque		Target Torque for Priming Exercise	
Participant	MVC, N·m	N·m	% MVC	N·m	% MVC
1	57.4	28.0	48.8	25.2	43.9
2	41.5	12.9	31.2	11.7	28.1
3	57.0	12.4	21.7	11.1	19.6
4	46.9	16.9	36.1	15.2	32.5
5	39.9	14.0	35.1	12.6	31.6
6	38.4	16.4	42.6	14.7	38.3
Mean	46.8	16.8	35.9	15.1	32.3
SD	8.5	5.8	9.3	5.2	8.4

MVC, maximal voluntary contraction; critical torque, calculated across submaximal exercise tests performed to task failure using the impulse-time model in Chapter 6.

Figure 7.2 shows the mean discharge rates at recruitment, during the hold phase, and at de-recruitment for each contraction before and immediately after 6 min of priming exercise. Discharge rate at recruitment was significantly lower in the post-exercise contraction when compared to the pre-exercise contraction performed at 10% MVC (mean difference; 95 CIs: -0.7 pps; -1.1, -0.2 pps; t = -4.83, P = 0.017; Figure 7.2A). There were no significant differences between discharge rate during the hold phase (mean difference; 95 CIs: -0.03 pps; -0.5, 0.4 pps; t = -0.20, P = 0.851; Figure 7.2B) or at de-recruitment (mean difference; 95 CIs: -0.6 pps; -2.0, 0.8 pps; t = -1.39, P = 0.258; Figure 7.2C) during the post-exercise contraction compared to the pre-exercise contraction performed at 10% MVC. There were no

significant differences between discharge rate at recruitment (mean difference; 95 CIs: -0.7 pps; -3.1, 1.7 pps; t = -0.77, P = 0.475; Figure 7.2A), during the hold phase (mean difference; 95 CIs: 0.1 pps; -0.9, 1.0 pps; t = 0.14, P = 0.895; Figure 7.2B), or at de-recruitment (mean difference; 95 CIs: 0.1 pps; -0.9, 1.2 pps; t = 0.31, P = 0.766; Figure 2C), in the post-exercise contraction when compared to the pre-exercise contraction performed at 40% MVC.

Mean recruitment and de-recruitment thresholds for the motor units identified during each contraction before and immediately after 6 min of priming exercise are shown in Figure 7.3. There were no significant differences between mean recruitment threshold (mean difference; 95 CIs: 0.58 N·m; -3.1, 4.2 N·m; t = 0.50, P = 0.650; Figure 7.3A) or de-recruitment threshold (mean difference; 95 CIs: -0.1 N·m; -2.1, 2.0 N·m; t = -0.12, P = 0.910; Figure 3C) during the post-exercise contraction compared to the pre-exercise contraction performed at 10% MVC. Likewise, no significant differences in recruitment threshold (mean difference; 95 CIs: -0.6 N·m; -2.1, 1.0 N·m; t = -0.97, P = 0.895; Figure 3A) or de-recruitment threshold (mean difference; 95 CIs: -0.4 N·m; -2.0, 1.3 N·m; t = -0.58, P = 0.586; Figure 7.3C) were observed when the post-exercise contraction was compared to the pre-exercise contraction performed at 40% MVC.

Global EMG response

The two-way repeated measures ANOVA revealed no main effect of condition ($F_{5, 20}$ = 7.07, P = 0.056, η_p^2 = 0.64) and a significant effect of time ($F_{5, 20}$ = 3.29, P = 0.025, η_p^2 = 0.45) for global EMG_{RMS}. There was a significant interaction effect (exercise bout × time) for global EMG_{RMS} ($F_{5, 20}$ = 2.78, P = 0.046, η_p^2 = 0.41; Figure 7.4A). Therefore, simple main effects were run. Global EMG_{RMS} (normalised to a pre-test MVC) was significantly lower in the second bout of heavy exercise compared to the first bout at min 1 (mean difference; 95% CIs: -1.16%; -2.10, -0.22; $F_{1, 4}$ = 11.67, P = 0.027), min 2 (mean difference; 95% CIs: -0.86%; -1.41, -0.30%; $F_{1, 4}$ = 18.52, P = 0.013), and min 3 (mean difference; 95% CIs: -1.30%; -2.03, -0.56%; $F_{1, 4}$ = 24.05, P < 0.008). There were no significant differences between global EMG_{RMS} in the final 3 min of the second bout compared to the first bout (all

$P > 0.05$). Due to the significant interaction effect, the effects of time were examined in each exercise bout separately. Global EMG_{RMS} did not significantly change over time during the first bout of heavy exercise ($F_{5, 20} = 2.20$, $P = 0.094$, $\eta_p^2 = 0.36$). However, EMG_{RMS} significantly increased over time during the second bout of heavy exercise ($F_{5, 20} = 3.91$, $P = 0.012$, $\eta_p^2 = 0.50$). Individual EMG_{RMS} responses are outlined in Figure 7.4B.

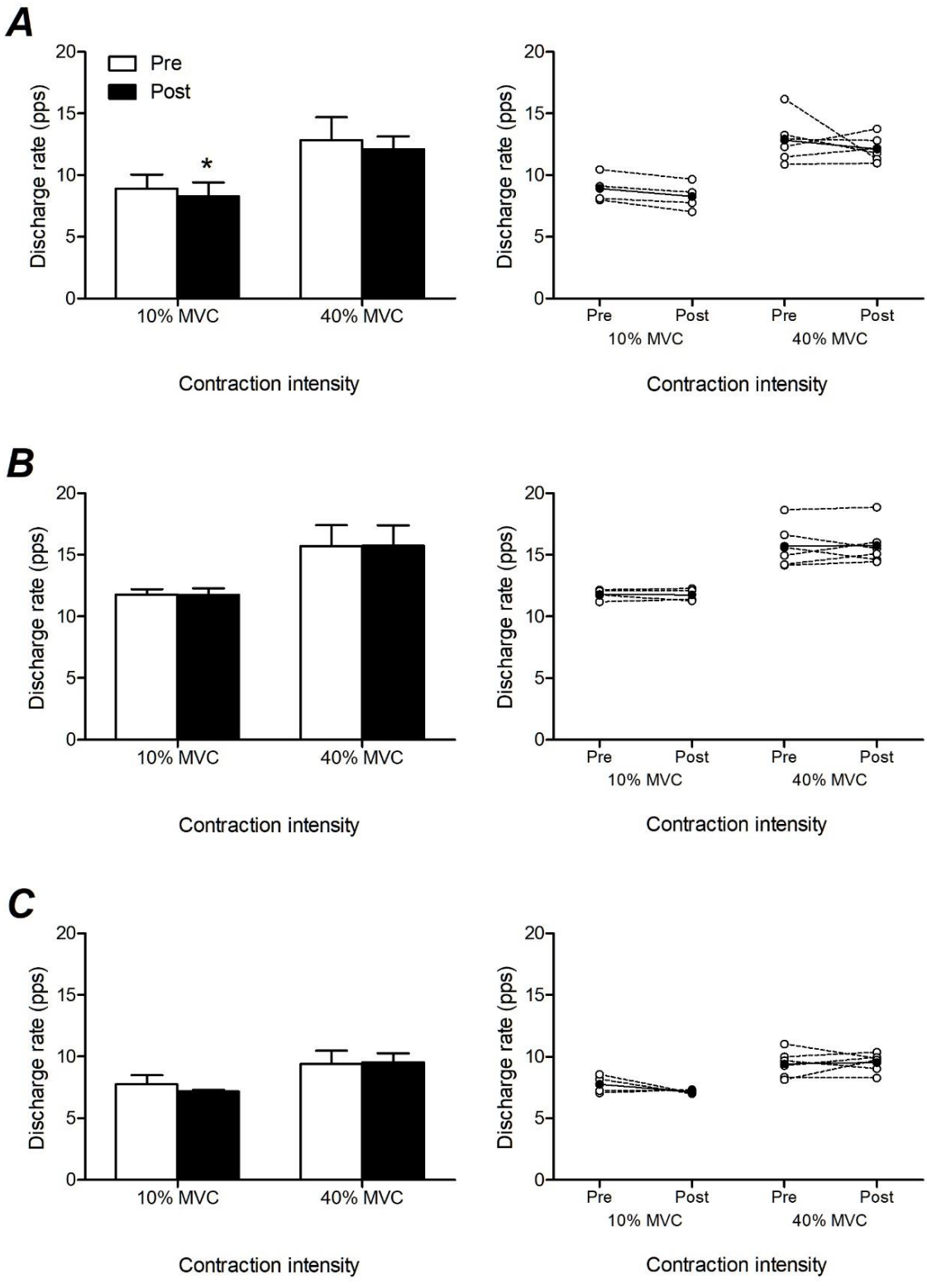

Figure 7.2. *Mean discharge rates during ramp-and-hold contractions performed at 10% MVC and 40% MVC before and immediately after 6 min of priming exercise. A, Discharge rate during motor unit recruitment. B, Discharge rate during the hold phase of the contraction. C, Discharge rate during motor unit de-recruitment. Group mean values are shown on the left panel (error bars represent SD) and individual values are shown on the right panel (filled circles and solid lines represent group mean values). pps, pulses per second. * Significantly different from pre-exercise contraction. Data for contractions at 10% MVC are reported for n = 4.*

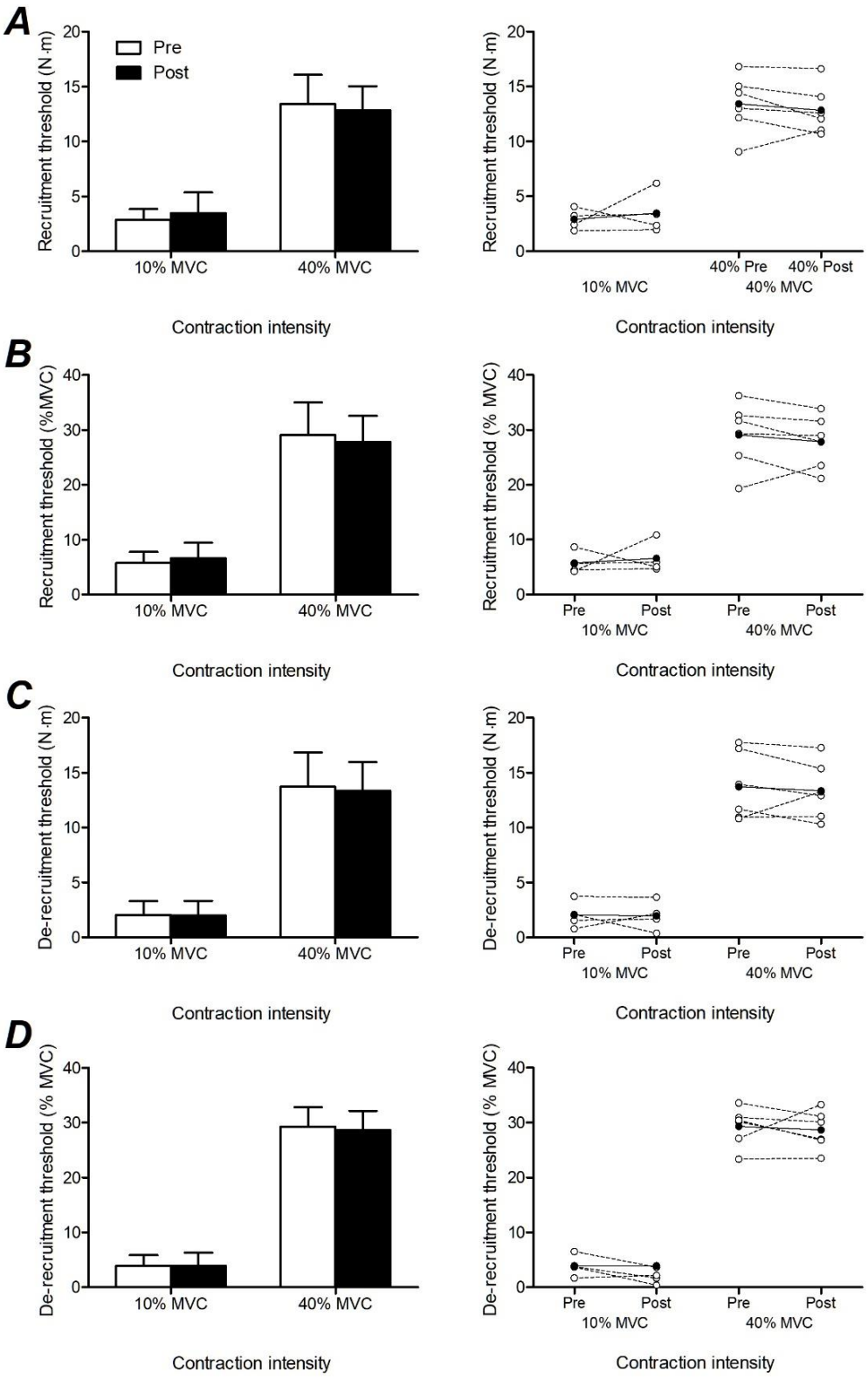

Figure 7.3. *Mean recruitment (A and B) and de-recruitment (C and D) thresholds during ramp-and-hold contractions performed at 10% MVC and 40% MVC before and immediately after 6 min of priming exercise. A and C are absolute torque values and B and D are expressed as % MVC. Group mean values are shown on the left panel (error bars represent SD) and individual values are shown on the right panel (filled circles and solid lines represent group mean values). Data for contractions at 10% MVC are reported for n = 4.*

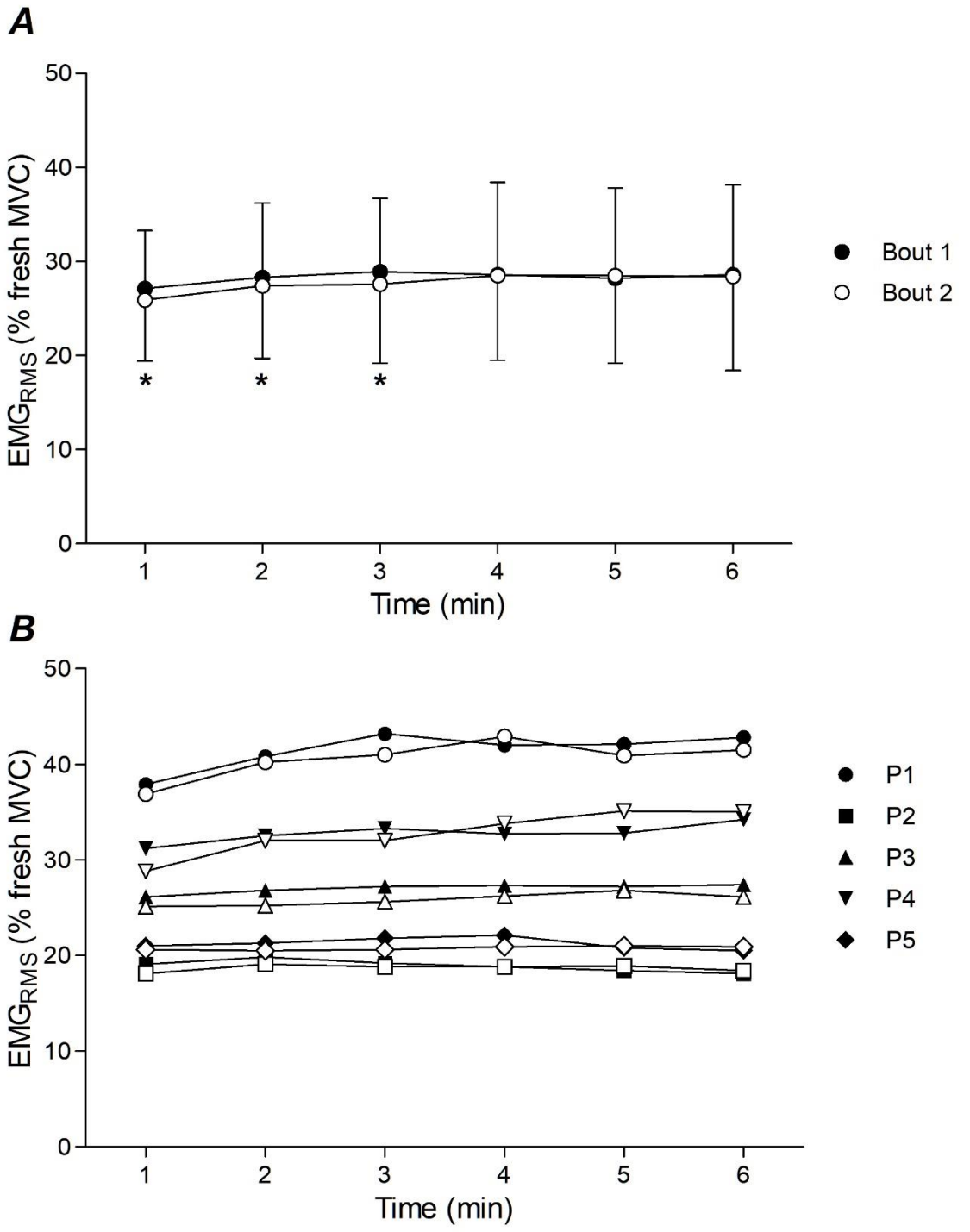

Figure 7.4. *Tibialis anterior global HDsEMG root mean square (EMG_{RMS}) responses during 6 min of 'heavy' priming exercise (open symbols) and a subsequent bout of 6 min 'heavy' exercise (filled symbols). Values were normalised to a fresh MVC and 1 min time bins (consisting of 12 contractions each) were used for analysis. Group mean ± SD responses are shown in A, and individual responses in B. * Significantly different from the corresponding value during bout 1. NB. Data are reported for n = 5.*

Discussion

The present study aimed to investigate the effects of a 6 min bout of intermittent 'heavy' ankle dorsiflexion contractions on motor unit behaviour of the tibialis anterior muscle. Contrary to the first hypothesis, the data showed that motor unit behaviour in the tibialis anterior was largely unchanged after priming exercise performed in the heavy domain. However, there was a small but significant reduction in discharge rate during the recruitment phase of the ramp-and-hold contraction performed at 10% MVC. A secondary aim of the current study was to assess the effect of a prior 6 min bout of heavy exercise on global EMG amplitude of the tibialis anterior during a subsequent 6 min heavy exercise bout. Again in contrast to the hypothesis, a small but significant reduction in EMG_{RMS} was observed during the subsequent exercise bout. Together, the results of the present study suggest that the changes in motor unit recruitment previously observed for the knee extensors following a bout of heavy priming exercise (Burnley, Doust, Ball et al., 2002; Layec et al., 2009) are absent in the tibialis anterior.

It was long suspected that the development of the $\dot{V}O_2$ slow component during heavy exercise resulted from increases in motor unit recruitment (Poole et al., 1991; Whipp, 1994), and observations that the slow component developed concomitantly with increases in the iEMG during heavy exercise provided experimental support for this hypothesis (Perrey et al., 2001; Saunders et al., 2000; Shinohara & Moritani, 1992). It is now well established that prior heavy exercise speeds the overall $\dot{V}O_2$ kinetics without any change in the primary $\dot{V}O_2$ time constant, instead resulting in an increased primary component amplitude and a reduced $\dot{V}O_2$ slow component amplitude (Burnley et al., 2000; Burnley et al., 2001; Koppo & Bouckaert, 2001; Poole & Jones, 2012). Given the association between the iEMG and the $\dot{V}O_2$ slow component development during heavy exercise, it was suggested that alterations in motor unit recruitment patterns might also be responsible for the reduction in the amplitude of the slow component $\dot{V}O_2$ amplitude after priming exercise (Burnley et al., 2001). Burnley et al. (2001) reasoned that increased motor unit recruitment may also cause the increase in primary component amplitude observed during a

subsequent heavy exercise bout. This was investigated in a subsequent study, and proportional increases in both the primary amplitude and the iEMG of three knee extensor muscles were reported for the second of two heavy cycling exercise bouts (Burnley, Doust, Ball et al., 2002). The finding that increased motor unit recruitment was evident during the early part of a subsequent heavy exercise bout was corroborated by Layec et al. (2009), who reported an increase in the ratio between iEMG and power output (W) during the second of two bouts of heavy knee-extension exercise. However, two other studies to have employed bipolar surface EMG were unable to detect significant changes in the leg muscle EMG signal (Scheuermann et al., 2001; Tordi et al., 2003), despite trends toward higher iEMG values in the subsequent heavy exercise bout.

It is now recognised that global EMG amplitude measures display a weak association with progressive motor unit recruitment (Del Vecchio et al., 2017), and the mixed findings discussed above further highlight the limited sensitivity of bipolar surface EMG to infer changes in motor unit recruitment strategies, particularly during cycling exercise. The present study was therefore designed to explore the immediate effects of priming on individual motor unit behaviour using HDsEMG decomposition before and immediately after exercise using an isolated muscle group, and measures of global EMG amplitude across two bouts of heavy exercise were used to directly compare to previous work. However, no differences were observed for motor unit discharge rates at 40% MVC or for recruitment thresholds during contractions performed immediately after priming exercise at either 10% MVC or 40% MVC, though a minor reduction in discharge rate was observed during recruitment for contractions performed at 10% MVC. Additionally, small but significant decreases in EMG_{RMS} were observed during the first 3 min of the second bout of heavy exercise, a finding unlike those reported for the knee extensors.

The finding from the current study that motor unit behaviour was largely unchanged after priming exercise offers two potential explanations. The first is that the lack of changes in either motor unit behaviour or EMG_{RMS} reported here, combined with the equivocal results reported for measures of bipolar EMG amplitude in earlier studies

(Burnley, Doust, Ball et al., 2002; Layec et al., 2009; Scheuermann et al., 2001; Tordi et al., 2003), presents the possibility that changes in motor unit recruitment patterns are not responsible for the beneficial effects on $\dot{V}O_2$ kinetics and/or subsequent performance associated with prior heavy exercise. Several alternative mechanisms have been proposed to contribute to changes in $\dot{V}O_2$ kinetics following priming exercise including elevated muscle temperature, improved muscle perfusion, and increased mitochondrial substrate availability, but the evidence for these mechanisms is scant or inconclusive (Poole & Jones, 2012). For example, passive leg warming (achieving muscle temperatures of both ~2°C greater than and muscle temperatures equivalent to that achieved during priming exercise) was found to have no effect on $\dot{V}O_2$ kinetics during a subsequent bout of heavy cycling exercise (Burnley, Doust & Jones, 2002; Koppo et al., 2002) and is therefore not thought to account for the effects of priming exercise on the $\dot{V}O_2$ response.

Despite consistent evidence that following priming exercise O_2 delivery is increased at the onset of a subsequent heavy exercise bout (e.g., Bangsbo et al., 2001; Burnley, Doust, Ball et al., 2002), which would be expected to speed the primary $\dot{V}O_2$ kinetics (i.e., reduce the primary time constant value), a number of studies have found no effect on the primary $\dot{V}O_2$ time constant (Whipp et al., 2002). It would appear that for a priming effect to materialise in the working muscle(s), improved blood flow to the muscle is not essential (Endo et al., 2005, Fukuba et al., 2004), but the primary component and $\dot{V}O_2$ slow component might be sensitive to O_2 delivery in certain situations, such as supine exercise (Koga et al., 1999) and hyperoxia (MacDonald et al., 1997).

Prior exercise has also been proposed to speed $\dot{V}O_2$ kinetics through increased activation of the pyruvate dehydrogenase complex (PDC) resultant to increased substrate availability (Campbell-O'Sullivan et al., 2002). However, administration of dichloroacetate, which increases PDC activation by inhibition of pyruvate dehydrogenase kinase, actually *reduced* the amplitude of the primary component (Rossiter et al., 2003), meaning it is unlikely that the priming effect of heavy exercise

is a result of increased mitochondrial substrate availability. Therefore, by process of elimination, changes in motor unit recruitment seems the most plausible mechanism for the increased primary and reduced $\dot{V}O_2$ slow component previously observed after prior heavy exercise. An alternative explanation for the lack of discernible changes in motor unit behaviour after prior heavy exercise in the present study is detailed below.

The alternative explanation is that the effects of prior heavy exercise on motor unit recruitment previously inferred from bipolar EMG measurements for the knee extensor muscles are absent in the tibialis anterior (and possibly the dorsiflexor muscle group), owing to histological differences between these muscles/muscle groups. This is plausible because the proportion of type II muscle fibres is typically lower in the tibialis anterior (~30%; Henriksson- Larsén et al., 1983; Helliwell et al., 1987) when compared to the vastus lateralis (~60%; Staron et al., 2000). Furthermore, the proportion of type II muscle fibres increases toward the deeper regions of the tibialis anterior (Henriksson- Larsén et al., 1983), meaning the sample pool of motor units detected by HDsEMG techniques (up to ~10% of the active motor units) might be more biased toward type I fibres since the decomposed motor units are likely drawn from those with fibres closest to the skin (Holobar et al., 2016; Gallina et al., 2022).

The fibre-type composition of the exercising muscle(s) and the pattern in which these muscle fibre-types are recruited may have a considerable impact on $\dot{V}O_2$ kinetics (Poole & Jones, 2012). For example, later-recruited type II muscle fibres are thought to display slower $\dot{V}O_2$ kinetics and a far greater energetic cost relative to earlier-recruited type I fibres, partly based on the observation that $\dot{V}O_2$ kinetics are significantly slower in mouse muscle comprised predominantly of type II fibres compared to muscle consisting of mainly type I fibres (Crow & Kushmerick, 1982; Jones et al., 2004). The manipulation of pedal rates during constant heavy cycling exercise to preferentially recruit type II fibres using extreme pedal rates (115 rpm) led to a lower $\dot{V}O_2$ primary component amplitude and an increased absolute and relative amplitude of the $\dot{V}O_2$ slow component compared to exercise using low pedal

rates (35 rpm; Pringle et al., 2003b). In line with this finding, Carter et al. (2004) preferentially reduced the contribution of type II fibres by means of glycogen depletion and reported an increased $\dot{V}O_2$ primary component amplitude and reduced $\dot{V}O_2$ slow component during heavy exercise. In addition, a lower fraction of type I muscle fibres in the vastus lateralis is associated with a greater relative contribution of the $\dot{V}O_2$ slow component to end exercise $\dot{V}O_2$ during 6 min of heavy cycling (Barstow et al., 1996; Poole & Jones, 2012; Pringle et al., 2003a). Therefore, type II fibre recruitment likely elevates the O_2 cost of exercise and plays a vital role in the development of the $\dot{V}O_2$ slow component.

If the motor units initially recruited during heavy exercise in the tibialis anterior consisted predominantly of type I muscle fibres, fatigue development would be delayed (relative to equivalent heavy exercise for the knee extensors) and the need to recruit additional motor units to maintain torque output during the onset of the second bout would be lessened. If fewer motor units consisting of type II fibres are neither needed nor available for recruitment, this would in theory limit the associated deleterious effects of type II fibre recruitment on $\dot{V}O_2$ kinetics (i.e., reduced efficiency, elevated O_2 cost of exercise, and $\dot{V}O_2$ slow component development). In line with this supposition, the dorsiflexors appear to be more fatigue-resistant than the knee extensors; the findings of Chapter 6 confirmed that the critical torque for the dorsiflexors occurs at a higher fraction of MVC than that previously reported for the knee extensors. It is reasonable to assume that the response to heavy exercise in the dorsiflexors is different to that of the knee extensors (and other more fatigable muscle groups) and further research should look to confirm this finding. Interestingly, the fatigue-resistant properties of the tibialis anterior might present a muscle model for investigation within which repeated bouts of heavy exercise can be performed without any observable ‘priming’ effects.

One consistent finding in the studies that have investigated bipolar EMG outcomes after priming exercise was that no changes in the mean or median power frequency of the surface EMG were reported (Burnley, Doust, Ball et al., 2002; Layec et al., 2009; Scheuermann et al., 2001; Tordi et al., 2003). These findings have been used

to infer that, even in the event of additional motor unit recruitment (Burnley, Doust, Ball et al., 2002; Layec et al., 2009), the muscle fibres of the newly recruited motor units were not of a higher order nor did they display an increased discharge rate, which is in line with the results of the current study. However, it should be noted that although the median power frequency is thought to be highly correlated to mean spike frequency (the average number of spikes per unit of time; Gabriel et al., 2001), spectral properties of the surface EMG signal have more recently been shown to be poorly correlated with motor unit recruitment strategies, at least for the tibialis anterior, leading to calls for such inferences to be abandoned (Del Vecchio et al., 2017).

Limitations

The participants involved in the current study were the same as those in Chapter 6 and this therefore presents similar limitations to those highlighted previously surrounding a small, male-only sample. It is worth noting that previous studies have included female participants, and priming effects were seemingly observed in these participants (e.g., Burnley et al., 2001). However, it is currently unknown whether sex differences exist regarding the effects of priming exercise on motor unit behaviour, and future work should aim to address this issue.

As was also discussed in Chapter 6, the motor unit decomposition algorithm used in the present study is currently limited to contractions lasting at least 10 s (Negro et al., 2016). This meant it was not possible assess individual motor unit behaviour during the 6 min priming bout, nor was this possible during the subsequent heavy exercise bout. Future work should look to incorporate motor unit decomposition techniques during contractions of the priming bout, which would likely require a different duty cycle to the one employed here. That said, similar decomposition approaches derived from the convolutive blind source separation method (Holobar & Zazula, 2007; Negro et al., 2016) have recently been applied to HDsEMG signals of the tibialis anterior during rapid dorsiflexion contractions (reaching a target force/torque as quickly as possible before holding for 3 s) to assess motor unit

behaviour before and after short-term isometric strength training (Del Vecchio, Negro et al., 2019; Del Vecchio et al., 2021), and could therefore be employed in study designs using the contraction duty cycle of the current study.

The motor units identified in the current study were not tracked across contractions, meaning it is not possible to state with certainty that the same population of motor units was sampled before and after the 6 min priming bout; comparisons were therefore based on motor unit pool differences, rather than at the level of individual motor units (Del Vecchio, Casolo et al., 2019). The decomposition feature of the software utilised here is free to use, but does not include motor unit tracking (Martinez-Valdes, Negro et al., 2017); at this time tracking features are not open source, limiting widespread application, and restricting their availability to a few select research groups (Felici & Del Vecchio, 2020). However, previous work has shown similar findings in motor unit behaviour (decreases in recruitment threshold and increases in discharge rate at the target force, but no changes in discharge rate at recruitment or de-recruitment) between matched and unmatched units after 4 weeks of isometric strength training (Del Vecchio, Casolo et al., 2019). Thus, even though motor units were not tracked here, provided the sample is large enough this should still be representative of the muscle as a whole.

Because the subsequent 6 min bout during *Visit 3* was performed at the same intensity as the 6 min priming bout (90% of the critical torque), exercise was limited to the heavy intensity domain. As a result, it is reasonable to assume that exercise would have continued beyond 30 min had the subsequent exercise bout been performed until task failure. The current study did not attempt to identify if the time to task failure during subsequent ‘severe’ intensity exercise (i.e., contractions performed above the critical torque) would have been prolonged by 6 min of heavy priming exercise, as has been demonstrated for cycle ergometer work (Bailey et al., 2009; Burnley et al., 2011), and future work should look to investigate this.

Conclusions

In summary, the performance of 6 min intermittent heavy exercise resulted in no changes, save for a decrease in discharge rate at recruitment at 10% MVC, in motor unit behaviour of the tibialis anterior muscle. The absence of any noticeable changes in motor unit behaviour after priming exercise involving isometric dorsiflexor contractions suggests that the effects previously observed during knee extensor exercise are not necessarily generalisable to other muscles and/or muscle groups. Further research incorporating HDsEMG techniques is required to assess effects of priming exercise on motor unit behaviour, both to confirm the findings of the present study pertaining to the dorsiflexors, but also for other muscle groups, particularly the knee extensors.

CHAPTER 8 – GENERAL DISCUSSION

Recapitulation of experimental studies and summary of main findings

The overall aim of the present thesis was to investigate the neural control of muscle torque during isometric exercise using HDsEMG decomposition in healthy young adults. The dorsiflexor muscles, specifically the tibialis anterior (primary ankle dorsiflexor), were chosen as the focus of the experimental chapters owing to their high motor unit yield relative to other leg muscles and their prominent role in locomotion and postural control.

The first experimental chapter (Chapter 4) aimed to investigate the methodological aspects of HDsEMG signal acquisition and decomposition within our laboratory setup; key amongst this was skin preparation, the reduction of HDsEMG signal noise, and the motor unit yield at different contraction intensities, as well as after different decomposition acceptance criteria were applied. Isometric trapezoidal (ramp-and-hold) and rectangular 20 s dorsiflexion contractions were performed at varying intensities (10%, 30%, 50%, and 70% MVC) after three different treatments (rubbing with alcohol, rubbing with abrasive paste, and cleaning with water) were applied to the skin. In addition, the ground electrode configuration was iteratively tested to inform the experimental setup pertaining to the reduction of HDsEMG signal noise.

In Chapter 4, no differences in motor unit yield were observed between skin treatments, which suggests that skin preparation, rather than treatment *per se*, is more important at the skin-electrode interface. The use of at least four ground electrodes resulted in significant reductions to the baseline noise of the HDsEMG signal, which informed the experimental setup of subsequent chapters, and the use of an adjusted acceptance criteria during the decomposition process provided a greater motor unit yield compared to the original conditions. Moreover, it was shown that as ankle dorsiflexion contraction intensity increased, motor unit yield decreased, and that contractions in subsequent experimental chapters should be performed below 50% MVC.

Chapter 4 also highlighted an obvious sex difference in motor unit yield after HDsEMG decomposition. Although the sample size of female participants used here was small (n = 3), across 72 contractions the greatest sample of motor units reliably identified in a single contraction was four and this yield was achieved only once (it should be noted here that five motor units were identified after a subsection of contractions were reprocessed using expanded decomposition acceptance criteria; Chapter 4, Figure 4.6). This led to the remainder of experimental chapters consisting of male participants only, which prevented any subsequent investigations into sex differences surrounding complexity, the critical torque, and the effects of priming exercise on motor unit behaviour. This issue is discussed in detail later in this chapter.

Chapter 5 investigated the effects of fatiguing exercise performed at 30% MVC on muscle torque and motor unit cumulative spike train complexity, in which it was necessary to apply arterial occlusion to the working muscle to accelerate fatigue development. It was demonstrated that after fatiguing intermittent isometric exercise performed at 30% MVC under arterial occlusion, reductions in the complexity of the tibialis anterior motor unit cumulative spike train were concomitant with a loss of dorsiflexor muscle torque complexity. An increase in tibialis anterior motor unit discharge rate accompanied these losses in complexity. This was the first application of complexity statistics to ankle dorsiflexion torque, and the first time that the complexity of the cumulative spike train has been reported after fatiguing exercise.

The findings of Chapter 5 indicate that losses in muscle torque complexity, including those previously reported for the knee extensors, are likely a reflection of increased transmission of the common synaptic input to the muscle as task failure approaches, in conjunction with an attenuated transmission of independent synaptic input. Losses of physiological complexity have previously been assumed to represent a

loss of system adaptability, but this work points to an attempt to *maintain* adaptability, at least in response to increasing levels of neuromuscular fatigue.

Chapter 6 extended the critical torque concept to intermittent ankle dorsiflexion exercise, and involved a comparison between a 5 min all-out test and the conventional method, consisting of multiple submaximal exercise bouts performed until task failure. It was demonstrated that the 5 min all-out test, previously validated for the knee extensors, overestimates the critical torque for the ankle dorsiflexors compared to the critical torque estimated using the conventional method. In addition, the ankle dorsiflexor critical torque occurs at a greater fraction of MVC than that of the knee extensors, providing further evidence that the dorsiflexor muscles are highly fatigue-resistant. It is likely that an all-out test of longer duration is required to attain an end-test torque which closely approximates the critical torque in this muscle group. The critical torque estimated from the conventional method was subsequently used to set the heavy-intensity exercise in Chapter 7.

Lastly, the final experimental study (Chapter 7) investigated the effects of 6 min prior heavy intermittent isometric exercise, or 'priming', on motor unit behaviour and global surface EMG amplitude for the tibialis anterior. Chapter 7 demonstrated that the performance of 6 min priming exercise resulted in no meaningful changes in motor unit behaviour or measures of global EMG amplitude. This was unlike previously reported findings for the knee extensors and suggests that the tibialis anterior (and possibly the dorsiflexor muscle group) is not subject to the same 'priming' effects. It was speculated that this difference is due to the greater proportion of type I muscle fibres typically found in the tibialis anterior relative to the vasti muscles, leading to an absence of discernible alterations to motor unit recruitment. The below sections provide explanations for the previously discussed findings, and suggestions for future research are presented therein.

Fatigue-induced losses of motor unit cumulative spike train complexity in the tibialis anterior

It has been shown that fatigue-induced losses in knee-extensor muscle torque complexity occur after maximal and submaximal isometric contractions (Pethick et al., 2015), with such losses occurring exclusively during contractions performed above the critical torque (Pethick et al., 2016; 2020), and the work of this thesis extends these findings to the dorsiflexor muscle group. Chapter 5 demonstrated a loss of dorsiflexor torque complexity in tandem with a loss of cumulative spike train complexity in the tibialis anterior after fatiguing contractions performed to task failure, whereas no losses in the complexity of either output were observed after less-fatiguing contractions performed for 30 min. Though the dorsiflexor contractions in Chapter 5 were performed at 30% MVC, the use of arterial occlusion effectively reduced the critical torque to 0 N·m (Broxterman et al., 2015), thereby 'simulating' exercise above the critical torque.

The accelerated rate of fatigue development during exercise performed with arterial occlusion compared to during exercise without is in line with the expected responses to exercise performed above and below the critical torque (Burnley et al., 2012; Poole et al., 2016). Resultantly, this led to qualitatively similar losses in complexity to those observed for the knee extensors (Pethick et al., 2015), albeit with uniformly lower ApEn values (likely owing to the necessary filtering of the torque signal to remove high-frequency system noise). However, the increase in DFA α exponent was not statistically significant, despite being significantly greater during the final minute of exercise than during the corresponding timepoint in the open circulation condition.

Arterial occlusion was a necessary compromise in Chapter 5, balancing motor unit yield (demonstrated to decrease at contraction intensities above 30% MVC in Chapter 4 and elsewhere; Del Vecchio, Holobar et al., 2020) with the fatigue-resistant properties of the dorsiflexors (confirmed in Chapter 6 and discussed below;

the critical torque was shown to be greater than that typically observed for the knee extensors). The use of arterial occlusion likely accentuated the development of peripheral fatigue, possibly resulting from metabolite accumulation (e.g., P_i, ADP, H^+ and/or K^+) and depletion (e.g., PCr and/or ATP). Such changes within the muscle can lead to reductions in muscle force responses for a given level of stimulation (Allen et al., 2008), requiring increases in excitatory drive to the motor neuron pool to maintain a target force as task failure approaches (Castronovo et al., 2015; Taylor et al., 2016). The likelihood of the above mechanism explaining (at least partially) the findings of Chapter 5 is supported by the work of Pethick et al. (2018b), wherein peripheral fatigue recovery after contractions performed to task failure was prevented by arterial occlusion of the exercised leg, which also inhibited the restoration of torque complexity ahead of a subsequent bout of exercise.

Castronovo et al. (2015) previously demonstrated that an increase in net excitatory input to the motor neurons, in response to increasing contraction intensity and fatigue, results in relative increases in the proportion of common synaptic input (received by all motor neurons) compared to the independent input (received by individual motor neurons). Specifically, increases in the coherence values between motor unit spike trains in the low-frequency bands (1-10 Hz) for the lowest contraction intensity (20% MVC) were evident at task failure, and coherence in these frequency bands was also positively correlated with force variability (Castronovo et al., 2015). The fatiguing contractions used in the work of Castronovo et al. (2015) were likely performed above the critical torque, which typically occurs at ~14-18% MVC for sustained isometric contractions (Hendrix et al., 2009; Monod & Scherrer, 1965); however, the critical torque for sustained dorsiflexion contractions may be higher, as reported for intermittent contractions in Chapter 6. Given that the total common input delivered to motor neurons is the main determinant of force fluctuations during sustained contractions (Farina, Negro et al., 2014), it is reasonable to assume that an increase in common synaptic input relative to independent input would also affect muscle torque complexity.

We propose that the data of Chapter 5, namely concomitant losses in the complexity of the cumulative spike train and muscle torque outputs, signify an emergence and amplification of common synaptic input as fatigue develops and task failure approaches. This offers a significant conceptual advance on the “loss of complexity hypothesis” (whereby a loss of complexity is thought to represent a reduction in the adaptive capacity of a system; Lipsitz & Goldberger, 1992; Peng et al., 2009) in relation to neuromuscular fatigue. Thus, rather than a loss of system adaptability, the observed loss of cumulative spike train complexity, in tandem with losses of muscle torque complexity, represents an attempt to *maintain* adaptability in response to neuromuscular fatigue.

While a reduction in the complexity of the common synaptic input to the muscle itself in response to fatigue could explain the losses in motor unit cumulative spike train complexity, this remains to be seen. Therefore, a fatigue-induced, attenuated independent synaptic input and an emergent and strengthened common drive as the system attempts to maintain adaptability presents the most plausible explanation for the findings of Chapter 5. However, further work is needed to confirm the main findings of Chapter 5 in other muscles.

Fatigue-resistant properties of the dorsiflexor muscles

The ankle joint is known to be more fatigue-resistant during sustained contractions than most other joints of the human body (Frey-Law & Avin, 2010), and the dorsiflexors in turn appear to be more fatigue-resistant than the plantar flexors, at least in certain conditions (Fourchet et al., 2012). The data from Chapters 6 and 7 provide further support for the fatigue-resistant properties of this muscle group. In Chapter 6, the critical torque for intermittent isometric ankle dorsiflexion contractions was calculated as 36% MVC. This is considerably higher than most estimates of the critical torque previously reported in male participants for the knee extensors, which range from ~27 to 30% MVC (Abdalla et al., 2018; Burnley, 2009; de Menezes Bassan et al., 2019; Pethick et al., 2016; Pethick et al., 2020), though values of 34%

(Burnley et al., 2012) and 35% MVC (Ansdell et al., 2019b) have also been reported. Furthermore, the fatigue-resistant properties of the dorsiflexors meant that the end-test torque calculated from the final 30 s of the 5-min all-out test (previously validated for the knee extensors by Burnley [2009]) in Chapter 6 overestimated the critical torque by ~15% MVC. Future research is required to establish the optimal duration for an all-out test in the dorsiflexors, given the importance of the critical torque concept and the prominence of the tibialis anterior muscle in HDsEMG research.

Changes in motor unit recruitment provide the most plausible explanation for the effects of heavy prior exercise on $\dot{V}O_2$ kinetics during a subsequent heavy exercise bout, namely an increase in the primary component amplitude and a reduction in the amplitude of the slow component (Burnley et al., 2001). However, after the 'heavy' priming exercise performed in Chapter 7, motor unit behaviour of the tibialis anterior was unchanged, a finding at odds with previous research in the knee extensors (Burnley, Doust, Ball et al., 2002; Layec et al., 2009). While such divergent outcomes could simply be an example of the limited sensitivity of inferences made from the amplitude and frequency content of bipolar surface EMG to detect meaningful changes in motor unit behaviour (Farina, 2008; Holobar et al., 2016), a more likely explanation lies in the histological differences between the muscles of interest.

The proportion of type I muscle fibres in the tibialis anterior (~70%; Henriksson-Larsén et al., 1983; Helliwell et al., 1987) is greater when compared to the vastus lateralis (~40%; Staron et al., 2000). In addition, the motor units detected by HDsEMG techniques are thought to be biased toward those with fibres closest to the skin (Holobar et al., 2016; Gallina et al., 2022), which are more likely to predominantly consist of type I muscle fibres than those toward deeper regions of the tibialis anterior (Henriksson- Larsén et al., 1983). Given that type I muscle fibres are more fatigue-resistant than type II fibres (Schiaffino & Reggiani, 2011), the fibre-type composition and the order of recruitment of these fibres at the exercising muscles are thought to have a considerable impact on $\dot{V}O_2$ kinetics (Poole & Jones,

2012). Furthermore, the relative contribution of the $\dot{V}O_2$ slow component to end exercise $\dot{V}O_2$ during heavy cycling work is smaller when the working muscle comprises a greater proportion of type I muscle fibres (Barstow et al., 1996; Poole & Jones, 2012; Pringle et al., 2003a).

It is reasonable to assume that, if a greater proportion of motor units consisting of type I fibres were recruited during heavy exercise in the tibialis anterior, recruitment of fewer additional motor units would have been necessary as exercise progressed compared to equivalent exercise in the knee extensors. This, in turn, would limit the effects of type II fibre recruitment on $\dot{V}O_2$ kinetics, such as $\dot{V}O_2$ slow component development, and the classical 'priming' effects would therefore be absent. Further research is needed to confirm the results of Chapter 7, both in the tibialis anterior and the knee extensors. It is also unclear whether the priming exercise performed in Chapter 7 would have led to improvements in time to task failure during a subsequent bout of 'severe' exercise (i.e., contractions performed above the critical torque) in line with previous cycling exercise (Bailey et al., 2009; Burnley et al., 2011), and future work should look to confirm this.

The small sample size used in Chapters 6 and 7 was an unavoidable result of limits on recruitment during the Coronavirus Restrictions of late 2020, and the results of both studies should therefore be taken with caution. Nonetheless, their combined findings lead to the interesting possibility that the tibialis anterior presents a muscle model that is robust to the effects of fatigue, whereby repeated 'heavy' exercise bouts could be performed without any discernible 'priming' effects. In summary, while the tibialis anterior might be a reliable muscle for HDsEMG signal decomposition, yielding greater numbers of motor units that most other muscles (Del Vecchio, Holobar et al., 2020), findings from studies of tibialis anterior motor unit behaviour are not necessarily generalisable to other muscles (e.g., the vasti muscles).

High-density surface electromyography – a powerful, yet limited technique

Though a powerful technique offering a window into the neural control of muscle torque, the use of HDsEMG decomposition methods is not without some major limitations. Firstly, there is a scarcity of data for female participants in studies that have utilised HDsEMG signal decomposition. The algorithm used in the present thesis is based on the convolutive blind source separation technique developed by Negro et al. (2016). This approach and other similar blind source separation decomposition methods have only been validated using male participants (Holobar et al., 2014; Marateb et al., 2011). Therefore, it is perhaps unsurprising that consistently low motor unit yields for female participants such as those reported in Chapter 4 have also been reported elsewhere (Afsharipour et al., 2020; Del Vecchio, Holobar et al., 2020; Hug, Avrillon et al., 2021; Taylor et al., 2022).

The reason for such a marked sex difference in motor unit yield is presently unclear, and although recent work has started to investigate this issue (Taylor et al., 2022), there is still more to do. Over two-thirds of HDsEMG decomposition research published since 2002 has consisted solely of male participants (Taylor et al., 2022), meaning the vast majority of information garnered from the technique might not be wholly representative of true human motor behaviour. Furthermore, recent work using intramuscular EMG has reported female participants to have lower ankle dorsiflexion force steadiness and tibialis anterior CoV_{isi} (Inglis & Gabriel, 2021), and higher vastus lateralis motor unit discharge rates during maximal and submaximal contractions when compared to male participants (Inglis & Gabriel, 2020; Guo et al., 2022).

The absence of female participants in Chapters 5 to 7 precluded any investigation into the potential sex differences in both the critical torque and the ‘priming’ response (or lack of) for the dorsiflexors and/or the tibialis anterior muscle. During matched-intensity isometric contractions performed to task failure, female

participants are usually less fatigable than their male counterparts (Hunter, 2014). For example, it has been shown that females exhibit a higher critical force (as a fraction of MVC) for contractions of the knee extensors when compared to males (Ansdell, et al., 2019a), a finding partially attributed to the higher proportional area of fatigue-resistant type I muscle fibres in the female vastus lateralis relative to males (Hunter, 2014). However, sex differences in fatigability are smaller in the ankle dorsiflexors (Russ & Kent-Braun, 2003; Russ et al., 2005) compared to the knee extensors (Martin & Rattey, 2007; Wüst et al., 2008). While females generally have a greater proportion of type I muscle fibres than males (Hunter, 2014), this disparity appears to be less pronounced in the tibialis anterior compared to the muscles of the knee extensors (Porter et al., 2002; Simoneau & Bouchard, 1989). Nevertheless, future work is necessary to establish if a sex difference exists for the critical torque of the ankle dorsiflexors.

Another issue pertaining to the widespread applicability of HDsEMG decomposition techniques is the reduction in motor unit yields with increasing contraction intensity and across investigated muscles (Del Vecchio, Holobar et al. 2020). We initially envisaged the vastus lateralis as the muscle of focus for this thesis, due to its prominent role in locomotion and the body of previous work from our group using knee extensor exercise (e.g., Pethick et al., 2015). However, during pilot work we encountered difficulties in decomposing adequate motor unit numbers, even in male participants. Regarding work with the vastus lateralis muscle, in personal communication with more experienced users of the technique we were advised to recruit lean (and ideally well-trained) male participants, and to re-recruit those participants with greater motor unit yields during subsequent studies. This would suggest that previous research focuses on a small pool of participants meeting very specific criteria, and likely focusing on those possessing certain morphological features of the vasti muscles. Subsequently, the tibialis anterior was chosen instead, owing to its high relative motor unit yield across the full recruitment range compared to other muscles (Del Vecchio, Holobar et al. 2020; Del Vecchio & Farina, 2019). The reasons for such divergent motor unit yields between muscles are not clear, but it is thought that the greater discriminative features between motor unit action

potentials of muscles with varying anatomy (such as the tibialis anterior) are more easily identified by HDsEMG decomposition algorithms in comparison to those from muscles with more uniformly parallel fibres (Del Vecchio, Holobar et al., 2020).

Because the coherence between common input and the cumulative spike train approaches unity when a sample of ~10 motor units is used for a given contraction (Farina, Negro et al., 2014), it is assumed that such yields are sufficient to infer the neural control signal of muscle torque. Chapter 4 demonstrated that at lower contraction intensities (10% and 30% MVC), the motor unit yield for the majority of male participants reached or exceeded this number, whereas at higher contraction intensities (50% and 70% MVC) this was not the case. Consequently, the decision to set the contraction intensity of Chapter 5 at 30% MVC and apply arterial occlusion to accelerate fatigue development was based on these findings. It should be noted here that other groups have reported sufficient yields at higher intensities within the same muscle. For example, Martinez-Valdes, Negro, Farina et al. (2020) identified an average of 11 motor units at 70% MVC and Del Vecchio, Falla et al. (2019) identified 12 motor units at 75% MVC. Though these groups used a more extensive decomposition software program than that used in the current thesis (discussed below), large reductions (~30%) in the number of motor units that could be identified when the target force increased from 30% to 75% MVC have been reported (Del Vecchio & Farina, 2019), likely as a result of greater motor unit action potential superposition in the interference signal as contraction intensity increases (Del Vecchio, Casolo et al., 2019).

Finally, issues remain regarding the accessibility of HDsEMG techniques and the costs involved, with multichannel amplifiers costing upwards of £13,000 (Felici & Del Vecchio, 2020). Although the manufacturer of the HDsEMG amplifier does provide a free software program (OT BioLab), this has limited features in comparison to commercially available programs such as the DEMUSE tool (e.g., Avrillon et al., 2021). For example, when using the DEMUSE tool it is possible to track individual motor units across contractions based on the cross-correlation between motor unit

action potential profiles, presenting an opportunity to monitor motor unit behaviour between contractions or visits (Martinez-Valdes, Negro et al., 2017), and as many as 30% of decomposed motor units can be tracked between sessions in the tibialis anterior muscle (Del Vecchio, Casolo et al., 2019). However, the motor unit tracking technique is not open-source, limiting its usage to a few select research groups. Therefore, the motor units identified in the experimental chapters of this thesis were not tracked across contractions or visits, meaning any comparisons have been made on the basis of motor unit pool differences, rather than on an individual motor unit level (Del Vecchio, Casolo et al., 2019).

The most recent version of the free software used in this thesis (OT BioLab+; Version 1.5.7) introduced the ability to manually edit individual motor unit discharges, in line with the previously mentioned DEMUSE tool and as recommended by Gallina et al. (2022) in the Consensus for Experimental Design in Electromyography (CEDE). Additionally, the SIL (a normalised value used to assess the accuracy of the estimated discharge timings) of each identified motor unit is now calculated, providing a more individualised approach for assessing the authenticity of the decomposed motor unit spike trains (Figure 8.1). The decomposition function of the software, Decomponi, now also permits the removal of individual HDsEMG channels, such as those contaminated by noise or ‘dead’ channels, which may influence the decomposition results (Del Vecchio, Holobar et al., 2020). It remains to be seen whether motor unit tracking functionality will be included in future versions of OT BioLab+.

Regardless of the aforementioned updates, the decomposition feature of this software is currently limited to isometric contractions of at least 10 s in duration. Blind source separation algorithms similar to the one used in this thesis have recently been used to decompose the HDsEMG signal recorded during dynamic contractions in a range of muscles (Chen et al., 2020; Del Vecchio, Sylos-Labini et al., 2020; Oliveira & Negro, 2021). The recent development of wireless, wearable HDsEMG amplifiers (Martinez-Valdes et al., 2021; Yokoyama et al., 2022) suggests

that accurate motor unit decomposition during locomotory tasks might be viable in the near future, and potentially processed in real-time (Bräcklein et al., 2022). However, while attempts to validate existing HDsEMG decomposition methods during dynamic contractions of the tibialis anterior have suggested applicability for small range of motion (≤ 30°) tasks including slow walking (Yokoyama et al., 2021; Yokoyama et al., 2022), novel HDsEMG decomposition methods (e.g, Chen et al., 2020; Glaser & Holobar, 2019) are likely required before neural interfacing during more complex tasks such as fast locomotion is a possibility.

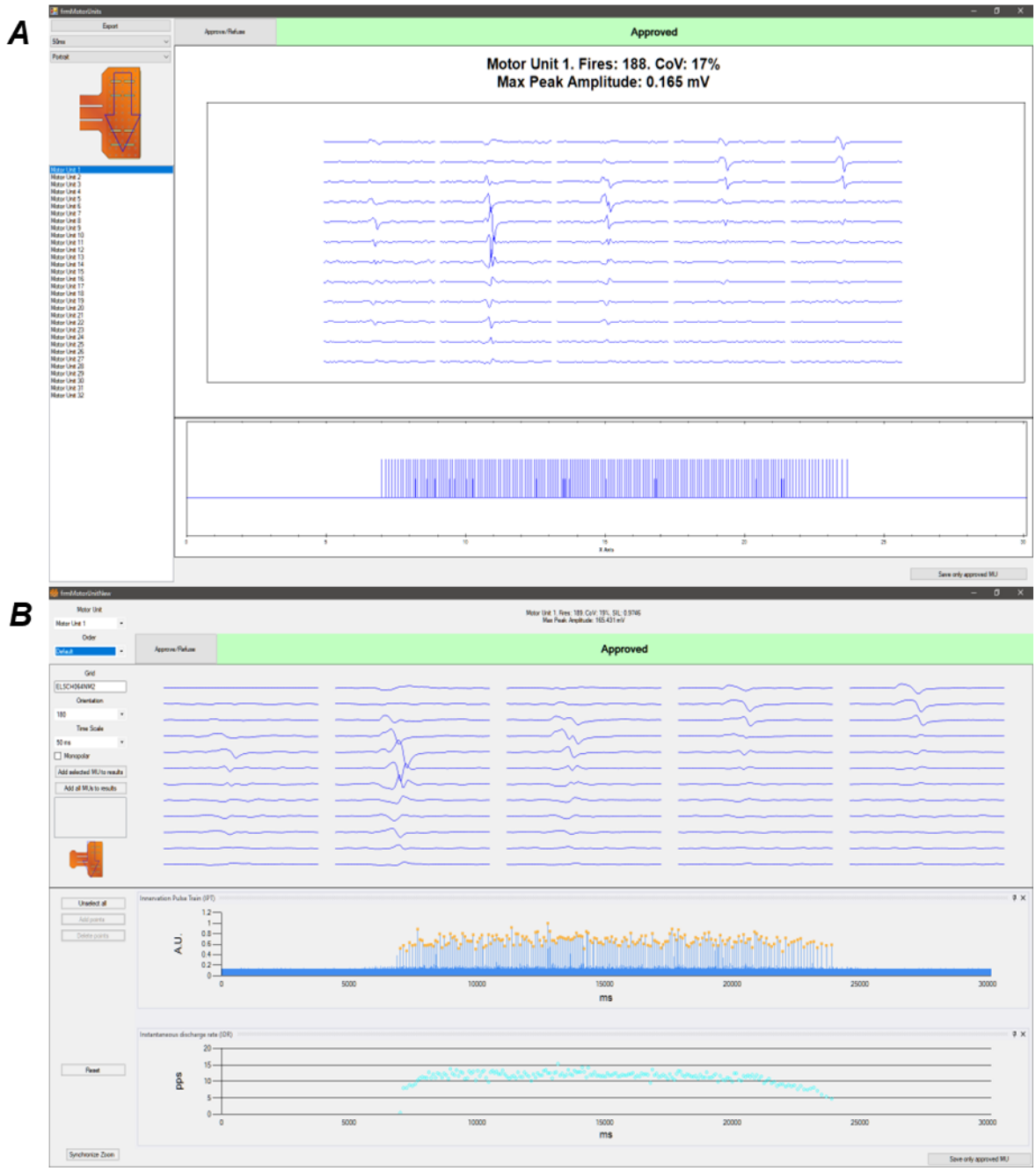

***Figure 8.1**. The decomposition review window presented after HDsEMG signal decomposition in A) OT BioLab and B) OT BioLab+. Note the additional features in OT BioLab+ including the pulse train outlining the original source of the discharges (blue spikes with yellow points) and the instantaneous discharge rate (cyan circles).*

Conclusions

The present thesis has studied the motor unit behaviour of the tibialis anterior in conjunction with the torque output of the dorsiflexor muscles to gain an insight into the mechanisms underlying the complexity of muscle torque, the critical torque, and the effects of prior heavy exercise, or priming, on subsequent exercise. The major novel finding of the thesis is that fatigue-induced losses in the complexity of muscle torque are accompanied by losses of motor unit cumulative spike train complexity in the tibialis anterior. The tibialis anterior is commonly investigated in research employing HDsEMG decomposition techniques, and this will likely continue due to its high motor unit yield relative to other locomotory muscles. The use of HDsEMG decomposition is potentially powerful in terms of the neuromuscular insights generated, but is subject to significant limitations in its practical application, particularly surrounding low motor unit yields for female participants and at higher contraction intensities. Nevertheless, the data presented in this thesis will inform future research into the three central themes of complexity, the critical torque, and priming exercise, but also serves as a reminder that the findings from motor unit behaviour of the tibialis anterior are not necessarily generalisable to other muscles, such as the knee extensors; for want of a better term, “a” muscle is not “the” muscle. Thus, general inferences about neuromuscular control using HDsEMG decomposition techniques should be made with caution.

REFERENCES

Abdalla, L. H. P., Denadai, B. S., Bassan, N. M., & Greco, C. C. (2018). Exercise tolerance during muscle contractions below and above the critical torque in different muscle groups. *Applied Physiology, Nutrition, and Metabolism*, *43*(2), 174-179.

Adam, A., & De Luca, C. J. (2003). Recruitment order of motor units in human vastus lateralis muscle is maintained during fatiguing contractions. *Journal of Neurophysiology*, *90*(5), 2919-2927.

Adrian, E. D., & Bronk, D. W. (1929). The discharge of impulses in motor nerve fibres: Part II. The frequency of discharge in reflex and voluntary contractions. *The Journal of Physiology*, *67*(2), i3.

Afsharipour, B., Manzur, N., Duchcherer, J., Fenrich, K. F., Thompson, C. K., Negro, F., ... & Gorassini, M. A. (2020). Estimation of self-sustained activity produced by persistent inward currents using firing rate profiles of multiple motor units in humans. *Journal of Neurophysiology*, *124*(1), 63-85.

Allen, D. G., Lamb, G. D., & Westerblad, H. (2008). Skeletal muscle fatigue: cellular mechanisms. *Physiological Reviews, 88*(1), 287-332.

Almuklass, A. M., Davis, L., Hamilton, L. D., Vieira, T. M., Botter, A., & Enoka, R. M. (2018). Motor unit discharge characteristics and walking performance of individuals with multiple sclerosis. *Journal of Neurophysiology, 119*(4), 1273-1282.

Ansdell, P., Brownstein, C. G., Škarabot, J., Hicks, K. M., Howatson, G., Thomas, K., ... & Goodall, S. (2019a). Sex differences in fatigability and recovery relative to the intensity–duration relationship. *The Journal of Physiology*, *597*(23), 5577-5595.

Ansdell, P., Brownstein, C. G., Škarabot, J., Hicks, K. M., Howatson, G., Thomas, K., ... & Goodall, S. (2019b). Methodological issues influence determination

of critical force during intermittent exercise: authors' reply. *The Journal of Physiology*, *597*(24), 5987-5989.

Arabi, H., Vandewalle, H., Kapitaniak, B., & Monod, H. (1999). Evaluation of wheelchair users in the field and in laboratory: Feasibility of progressive tests and critical velocity tests. *International Journal of Industrial Ergonomics*, *24*(5), 483-491.

Arsac, L. M., & Deschodt-Arsac, V. (2018). Detrended fluctuation analysis in a simple spreadsheet as a tool for teaching fractal physiology. *Advances in Physiology Education*, *42*(3), 493-499.

Avrillon, S., Del Vecchio, A., Farina, D., Pons, J. L., Vogel, C., Umehara, J., & Hug, F. (2021). Individual differences in the neural strategies to control the lateral and medial head of the quadriceps during a mechanically constrained task. *Journal of Applied Physiology*, *130*(1), 269-281.

Bailey, S. J., Vanhatalo, A., Wilkerson, D. P., DiMenna, F. J., & Jones, A. M. (2009). Optimizing the "priming" effect: influence of prior exercise intensity and recovery duration on O2 uptake kinetics and severe-intensity exercise tolerance. *Journal of Applied Physiology*, *107*(6), 1743-1756.

Bangsbo, J., Krustrup, P., González-Alonso, J., & Saltin, B. (2001). ATP production and efficiency of human skeletal muscle during intense exercise: effect of previous exercise. *American Journal of Physiology-Endocrinology and Metabolism, 280(6), E956-E964.*

Barbero, M., Merletti, R., & Rainoldi, A. (2012). *Atlas of muscle innervation zones: understanding surface electromyography and its applications*. Springer Science & Business Media.

Barker, T., Poole, D. C., Noble, M. L., & Barstow, T. J. (2006). Human critical power–oxygen uptake relationship at different pedalling frequencies. *Experimental Physiology*, *91*(3), 621-632.

Baron, B., Dekerle, J., Robin, S., Neviere, R., Dupont, L., Matran, R., ... & Pelayo, P. (2003). Maximal lactate steady state does not correspond to a complete

physiological steady state. *International Journal of Sports Medicine, 24*(8)*, 582-587.*

Barstow, T. J., Jones, A. M., Nguyen, P. H., & Casaburi, R. (1996). Influence of muscle fiber type and pedal frequency on oxygen uptake kinetics of heavy exercise. *Journal of Applied Physiology*, *81*(4), 1642-1650.

Barstow, T. J., Lamarra, N., & Whipp, B. J. (1990). Modulation of muscle and pulmonary O2 uptakes by circulatory dynamics during exercise. *Journal of Applied Physiology*, *68*(3), 979-989.

Bartram, J. C., Thewlis, D., Martin, D. T., & Norton, K. I. (2017). Predicting critical power in elite cyclists: questioning the validity of the 3-minute all-out test. *International Journal of Sports Physiology and Performance*, *12*(6), 783-787.

Bassingthwaighte, J. B., Liebovitch, L. S., & West, B. J. (2013). *Fractal physiology*. Springer.

Bellemare, F., & Grassino, A. (1982). Evaluation of human diaphragm fatigue. *Journal of Applied Physiology*, *53*(5), 1196-1206.

Beretta-Piccoli, M., D'Antona, G., Barbero, M., Fisher, B., Dieli-Conwright, C. M., Clijsen, R., & Cescon, C. (2015). Evaluation of central and peripheral fatigue in the quadriceps using fractal dimension and conduction velocity in young females. *PloS one*, *10*(4), e0123921.

Berger, N. J., & Jones, A. M. (2007). Pulmonary O2 uptake on-kinetics in sprint-and endurance-trained athletes. *Applied Physiology, Nutrition, and Metabolism, 32(3), 383-393.*

Bergstrom, H. C., Housh, T. J., Zuniga, J. M., Traylor, D. A., Lewis Jr, R. W., Camic, C. L., ... & Johnson, G. O. (2014). Differences among estimates of critical power and anaerobic work capacity derived from five mathematical models and the three-minute all-out test. *The Journal of Strength and Conditioning Research*, *28*(3), 592-600.

Bigland-Ritchie, B., Furbush, F., & Woods, J. J. (1986). Fatigue of intermittent submaximal voluntary contractions: central and peripheral factors. *Journal of Applied Physiology, 61(2), 421-429.*

Bigland-Ritchie, B., Johansson, R., Lippold, O. C., & Woods, J. J. (1983). Contractile speed and EMG changes during fatigue of sustained maximal voluntary contractions. *Journal of Neurophysiology*, *50*(1), 313-324.

Billat, V. L., Mouisel, E., Roblot, N., & Melki, J. (2005). Inter-and intrastrain variation in mouse critical running speed. *Journal of Applied Physiology*, *98*(4), 1258-1263.

Bishop, D. (2003). Warm up I. *Sports Medicine*, *33*(6), 439-454.

Black, M. I., Jones, A. M., Blackwell, J. R., Bailey, S. J., Wylie, L. J., McDonagh, S. T., ... & Vanhatalo, A. (2017). Muscle metabolic and neuromuscular determinants of fatigue during cycling in different exercise intensity domains. *Journal of Applied Physiology*, *122*(3), 446-459.

Boccia, G., Dardanello, D., Beretta Piccoli, M., Cescon, C., Coratella, G., Rinaldo, N., ... & Rainoldi, A. (2016). Muscle fiber conduction velocity and fractal dimension of EMG during fatiguing contraction of young and elderly active men. *Physiological Measurement*, *37*(1), 162-74.

Bräcklein, M., Barsakcioglu, D. Y., Ibáñez, J., Eden, J., Burdet, E., Mehring, C., & Farina, D. (2022). The control and training of single motor units in isometric tasks are constrained by a common input signal. *eLife*, *11*, e72871.

Bradbury, R. R., & Reichelt, R. R. (1983). Fractal dimension of a coral reef at ecological scales. *Marine Ecology Progress Series, 10,* 169-171.

Brickley, G., Doust, J., & Williams, C. (2002). Physiological responses during exercise to exhaustion at critical power. *European Journal of Applied Physiology*, *88*(1-2), 146-151.

Broxterman, R. M., Ade, C. J., Craig, J. C., Wilcox, S. L., Schlup, S. J., & Barstow, T. J. (2015). Influence of blood flow occlusion on muscle oxygenation characteristics and the parameters of the power-duration relationship. *Journal of Applied Physiology*, *118*(7), 880-889.

Broxterman, R. M., Ade, C. J., Poole, D. C., Harms, C. A., & Barstow, T. J. (2013). A single test for the determination of parameters of the speed–time

relationship for running. *Respiratory Physiology and Neurobiology*, *185*(2), 380-385.

Broxterman, R. M., Layec, G., Hureau, T. J., Amann, M., & Richardson, R. S. (2017). Skeletal muscle bioenergetics during all-out exercise: mechanistic insight into the oxygen uptake slow component and neuromuscular fatigue. *Journal of Applied Physiology*, *122*(5), 1208-1217.

Bruce, E. N. (1996). Temporal variations in the pattern of breathing. *Journal of Applied Physiology*, *80*(4), 1079-1087.

Burke, R. E. (2007). Sir Charles Sherrington's the integrative action of the nervous system: a centenary appreciation. *Brain*, *130*(4), 887-894.

Burnley, M. (2009). Estimation of critical torque using intermittent isometric maximal voluntary contractions of the quadriceps in humans. *Journal of Applied Physiology*, *106*(3), 975-983.

Burnley, M., & Jones, A. M. (2007). Oxygen uptake kinetics as a determinant of sports performance. *European Journal of Sport Science, 7*(2), 63-79.

Burnley, M., & Jones, A. M. (2018). Power–duration relationship: physiology, fatigue, and the limits of human performance. *European Journal of Sport Science*, *18*(1), 1-12.

Burnley, M., Davison, G., & Baker, J. R. (2011). Effects of priming exercise on V̇O2 kinetics and the power-duration relationship. *Medicine and Science in Sports and Exercise*, *43*(11), 2171-2179.

Burnley, M., Doust, J. H., & Jones, A. M. (2002). Effects of prior heavy exercise, prior sprint exercise and passive warming on oxygen uptake kinetics during heavy exercise in humans. *European Journal of Applied Physiology*, *87*(4), 424-432.

Burnley, M., Doust, J. H., & Jones, A. M. (2006). Time required for the restoration of normal heavy exercise V̇O2 kinetics following prior heavy exercise. *Journal of Applied Physiology*, *101*(5), 1320-1327.

Burnley, M., Doust, J. H., & Vanhatalo, A. (2006). A 3-min all-out test to determine peak oxygen uptake and the maximal steady state. *Medicine and Science in Sports and Exercise*, *38*(11), 1995-2003.

Burnley, M., Doust, J. H., Ball, D., & Jones, A. M. (2002). Effects of prior heavy exercise on V̇O2 kinetics during heavy exercise are related to changes in muscle activity. *Journal of Applied Physiology*, *93*(1), 167-174.

Burnley, M., Doust, J. H., Carter, H., & Jones, A. M. (2001). Effects of prior exercise and recovery duration on oxygen uptake kinetics during heavy exercise in humans. *Experimental Physiology*, *86*(3), 417-425.

Burnley, M., Jones, A. M., Carter, H., & Doust, J. H. (2000). Effects of prior heavy exercise on phase II pulmonary oxygen uptake kinetics during heavy exercise. *Journal of Applied Physiology, 89*(4), 1387-1396.

Burnley, M., Koppo, K., & Jones, A. M. (2005). "Priming exercise" and V̇O2 kinetics. In Andrew M Jones & D. C. Poole (Eds.), *Oxygen uptake kinetics in sport, exercise and medicine* (pp. 230–260). Abingdon, UK: Routledge.

Burnley, M., Vanhatalo, A., & Jones, A. M. (2012). Distinct profiles of neuromuscular fatigue during muscle contractions below and above the critical torque in humans. *Journal of Applied Physiology*, *113*(2), 215-223.

Byrne, C. A., O'keeffe, D. T., Donnelly, A. E., & Lyons, G. M. (2007). Effect of walking speed changes on tibialis anterior EMG during healthy gait for FES envelope design in drop foot correction. *Journal of Electromyography and Kinesiology*, *17*(5), 605-616.

Campbell-O'Sullivan, S. P., Constantin-Teodosiu, D., Peirce, N., & Greenhaff, P. L. (2002). Low intensity exercise in humans accelerates mitochondrial ATP production and pulmonary oxygen kinetics during subsequent more intense exercise. *The Journal of Physiology*, *538*(3), 931-939.

Cannon, W. B. (1929). Organization for physiological homeostasis. *Physiological Reviews*, *9*(3), 399-431.

Carpentier, A., Duchateau, J., & Hainaut, K. (2001). Motor unit behaviour and contractile changes during fatigue in the human first dorsal interosseus. *The Journal of Physiology*, *534*(3), 903-912.

Carter, H., Grice, Y. V., Dekerle, J., Brickley, G., Hammond, A. J., & Pringle, J. S. (2005). Effect of prior exercise above and below critical power on exercise to exhaustion. *Medicine and Science in Sports and Exercise*, *37*(5), 775-781.

Carter, H., Pringle, J. S., Boobis, L., Jones, A. M., & Doust, J. H. (2004). Muscle glycogen depletion alters oxygen uptake kinetics during heavy exercise. *Medicine and Science in Sports and Exercise*, *36*(6), 965-972.

Caserta, F., Eldred, W. D., Fernandez, E., Hausman, R. E., Stanford, L. R., Bulderev, S. V., ... & Stanley, H. E. (1995). Determination of fractal dimension of physiologically characterized neurons in two and three dimensions. *Journal of Neuroscience Methods*, *56*(2), 133-144.

Caserta, F., Stanley, H. E., Eldred, W. D., Daccord, G., Hausman, R. E., & Nittmann, J. (1990). Physical mechanisms underlying neurite outgrowth: a quantitative analysis of neuronal shape. *Physical Review Letters*, *64*(1), 95.

Cashaback, J. G., Cluff, T., & Potvin, J. R. (2013). Muscle fatigue and contraction intensity modulates the complexity of surface electromyography. *Journal of Electromyography and Kinesiology*, *23*(1), 78-83.

Castronovo, A. M., Mrachacz-Kersting, N., Stevenson, A. J. T., Holobar, A., Enoka, R. M., & Farina, D. (2018). Decrease in force steadiness with aging is associated with increased power of the common but not independent input to motor neurons. *Journal of Neurophysiology*, *120*(4), 1616-1624.

Castronovo, A. M., Negro, F., Conforto, S., & Farina, D. (2015). The proportion of common synaptic input to motor neurons increases with an increase in net excitatory input. *Journal of Applied Physiology*, *119*(11), 1337-1346.

Chen, C., Ma, S., Sheng, X., Farina, D., & Zhu, X. (2020). Adaptive real-time identification of motor unit discharges from non-stationary high-density surface electromyographic signals. *IEEE Transactions on Biomedical Engineering*, *67*(12), 3501-3509.

Chen, Y. C., Lin, L. L., Lin, Y. T., Hu, C. L., & Hwang, I. S. (2017). Variations in static force control and motor unit behavior with error amplification feedback in the elderly. *Frontiers in Human Neuroscience*, *11*, 538.

Cheng, C. F., Yang, Y. S., Lin, H. M., Lee, C. L., & Wang, C. Y. (2012). Determination of critical power in trained rowers using a three-minute all-out rowing test. *European Journal of Applied Physiology*, *112*(4), 1251-1260.

Clingeleffer, A., Mc Naughton, L., & Davoren, B. (1994). Critical power may be determined from two tests in elite kayakers. *European Journal of Applied Physiology and Occupational Physiology*, *68*(1), 36-40.

Cogliati, M., Cudicio, A., Martinez-Valdes, E., Tarperi, C., Schena, F., Orizio, C., & Negro, F. (2020). Half marathon induces changes in central control and peripheral properties of individual motor units in master athletes. *Journal of Electromyography and Kinesiology*, *55*, 102472.

Cohen, J. (1973). Eta-squared and partial eta-squared in fixed factor ANOVA designs. *Educational and Psychological Measurement*, *33*(1), 107-112.

Contessa P, Adam A. & De Luca C. J. (2009). Motor unit control and force fluctuation during fatigue. *Journal of Applied Physiology, 107*(1), 235-243.

Copp, S. W., Hirai, D. M., Musch, T. I., & Poole, D. C. (2010). Critical speed in the rat: implications for hindlimb muscle blood flow distribution and fibre recruitment. *The Journal of Physiology*, *588*(24), 5077-5087.

Craig, J. C., Vanhatalo, A., Burnley, M., Jones, A. M., & Poole, D. C. (2019). Critical power: possibly the most important fatigue threshold in exercise physiology. In *Muscle and Exercise Physiology* (pp. 159-181). Academic Press.

Crow, M. T., & Kushmerick, M. J. (1982). Chemical energetics of slow-and fast-twitch muscles of the mouse. *The Journal of General Physiology, 79(1), 147-166.*

Cruz-Montecinos, C., Calatayud, J., Iturriaga, C., Bustos, C., Mena, B., España-Romero, V., & Carpes, F. P. (2018). Influence of a self-regulated cognitive dual task on time to failure and complexity of submaximal isometric force control. *European Journal of Applied Physiology*, *118*(9), 2021-2027.

De Luca, C. J., & Adam, A. (1999). Decomposition and analysis of intramuscular electromyographic signals. *Modern Techniques in Neuroscience Research*, (27), 757–776.

De Luca, C. J., & Nawab, S. H. (2011). Reply to Farina and Enoka: the reconstruct-and-test approach is the most appropriate validation for surface EMG signal decomposition to date. *Journal of Neurophysiology*, *105*(2), 983-984.

De Luca, C. J., Nawab, S. H., & Kline, J. C. (2015). Clarification of methods used to validate surface EMG decomposition algorithms as described by Farina et al.(2014). *Journal of Applied Physiology*, *118*(8), 1084-1084.

de Menezes Bassan, N., Denadai, B. S., de Lima, L. C. R., Caritá, R. A. C., Abdalla, L. H. P., & Greco, C. C. (2019). Effects of resistance training on impulse above end-test torque and muscle fatigue. *Experimental Physiology*, *104*(7), 1115-1125.

de Oliveira, D. S., Casolo, A., Balshaw, T. G., Maeo, S., Lanza, M. B., Martin, N. R., ... & Del Vecchio, A. (2022). Neural decoding from surface high-density EMG signals: influence of anatomy and synchronization on the number of identified motor units. *Journal of Neural Engineering*, *19*(4), 046029.

De Ruiter, C. J., Mallee, M. I., Leloup, L. E., & De Haan, A. (2014). A submaximal test for the assessment of knee extensor endurance capacity. *Medicine and Science in Sports and Exercise*, *46*(2), 398-406.

Degen, T., & Loeliger, T. (2007, August). An improved method to continuously monitor the electrode-skin impedance during bioelectric measurements. In *Engineering in Medicine and Biology Society, 2007. EMBS 2007. 29th Annual International Conference of the IEEE*, 6294-6297.

Dekerle, J., Baron, B., Dupont, L., Vanvelcenaher, J., & Pelayo, P. (2003). Maximal lactate steady state, respiratory compensation threshold and critical power. *European Journal of Applied Physiology*, *89*(3), 281-288.

Dekerle, J., Pelayo, P., Clipet, B., Depretz, S., Lefevre, T., & Sidney, M. (2005). Critical swimming speed does not represent the speed at maximal lactate steady state. *International Journal of Sports Medicine*, *26*(07), 524-530.

Del Vecchio, A., & Farina, D. (2019). Interfacing the neural output of the spinal cord: robust and reliable longitudinal identification of motor neurons in humans. *Journal of Neural Engineering*, *17*(1), 016003.

Del Vecchio, A., Casolo, A., Dideriksen, J., Aagaard, P., Felici, F., Falla, D., & Farina, D. (2021). Why humans are stronger but not faster after isometric strength training: specific neural, not muscular, motor unit adaptations. *bioRxiv*. Preprint. Available from: https://doi.org/10.1101/2021.03.20.436242

Del Vecchio, A., Casolo, A., Negro, F., Scorcelletti, M., Bazzucchi, I., Enoka, R., ... & Farina, D. (2019). The increase in muscle force after 4 weeks of strength training is mediated by adaptations in motor unit recruitment and rate coding. *The Journal of Physiology*, *597*(7), 1873-1887.

Del Vecchio, A., Falla, D., Felici, F., & Farina, D. (2019). The relative strength of common synaptic input to motor neurons is not a determinant of the maximal rate of force development in humans. *Journal of Applied Physiology*, *127*(1), 205-214.

Del Vecchio, A., Holobar, A., Falla, D., Felici, F., Enoka, R. M., & Farina, D. (2020). Tutorial: Analysis of motor unit discharge characteristics from high-density surface EMG signals. *Journal of Electromyography and Kinesiology*, *53*, 102426.

Del Vecchio, A., Negro, F., Felici, F., & Farina, D. (2017). Associations between motor unit action potential parameters and surface EMG features. *Journal of Applied Physiology*, *123*(4), 835-843.

Del Vecchio, A., Negro, F., Holobar, A., Casolo, A., Folland, J. P., Felici, F., & Farina, D. (2019). You are as fast as your motor neurons: speed of recruitment and maximal discharge of motor neurons determine the maximal rate of force development in humans. *The Journal of Physiology*, *597*(9), 2445-2456.

Del Vecchio, A., Sylos-Labini, F., Mondì, V., Paolillo, P., Ivanenko, Y., Lacquaniti, F., & Farina, D. (2020). Spinal motoneurons of the human newborn are highly synchronized during leg movements. *Science Advances*, *6*(47), eabc3916.

Del Vecchio, A., Ubeda, A., Sartori, M., Azorin, J. M., Felici, F., & Farina, D. (2018). Central nervous system modulates the neuromechanical delay in a broad range for the control of muscle force. *Journal of Applied Physiology*, *125*(5), 1404-1410.

Dideriksen, J. L., Enoka, R. M., & Farina, D. (2011). Neuromuscular adjustments that constrain submaximal EMG amplitude at task failure of sustained isometric contractions. *Journal of Applied Physiology*, *111*(2), 485-494.

Dideriksen, J. L., Negro, F., Enoka, R. M., & Farina, D. (2012). Motor unit recruitment strategies and muscle properties determine the influence of synaptic noise on force steadiness. *Journal of Neurophysiology*, *107*(12), 3357-3369.

Dideriksen, J., Elias, L. A., Zambalde, E. P., Germer, C. M., Molinari, R. G., & Negro, F. (2022). Influence of central and peripheral motor unit properties on isometric muscle force entropy: A computer simulation study. *Journal of Biomechanics*, *139*, 110866.

Eke, A., Herman, P., Kocsis, L., & Kozak, L. R. (2002). Fractal characterization of complexity in temporal physiological signals. *Physiological Measurement*, *23*(1), R1.

Enders, H., Nigg, B. M., & Von Tscharner, V. (2015). Neuromuscular Strategies during Cycling at Different Muscular Demands. *Medicine and Science in Sports and Exercise*, *47*(7), 1450-1459.

Endo, M., Okada, Y., Rossiter, H. B., Ooue, A., Miura, A., Koga, S., & Fukuba, Y. (2005). Kinetics of pulmonary $\dot{V}O_2$ and femoral artery blood flow and their relationship during repeated bouts of heavy exercise. *European Journal of Applied Physiology, 95*(5), 418-430.

Enoka, R. M., & Duchateau, J. (2008). Muscle fatigue: what, why and how it influences muscle function. *The Journal of Physiology*, *586*(1), 11-23.

Enoka, R. M., & Duchateau, J. (2015). Inappropriate interpretation of surface EMG signals and muscle fiber characteristics impedes understanding of the control of neuromuscular function. *Journal of Applied Physiology*, *119*(12), 1516-1518.

Enoka, R. M., & Duchateau, J. (2016). Translating fatigue to human performance. *Medicine and Science in Sports and Exercise*, *48*(11), 2228.

Enoka, R. M., & Duchateau, J. (2017). Rate coding and the control of muscle force. *Cold Spring Harbor Perspectives in Medicine*, *7*(10), a029702.

Enoka, R. M., & Farina, D. (2021). Force steadiness: from motor units to voluntary actions. *Physiology*, *36*(2), 114-130.

Enoka, R. M., & Fuglevand, A. J. (2001). Motor unit physiology: some unresolved issues. *Muscle & Nerve: Official Journal of the American Association of Electrodiagnostic Medicine*, *24*(1), 4-17.

Enoka, R. M., Robinson, G. A., & Kossev, A. R. (1989). Task and fatigue effects on low-threshold motor units in human hand muscle. *Journal of Neurophysiology*, *62*(6), 1344-1359.

Erim, Z., & Lin, W. (2008). Decomposition of intramuscular EMG signals using a heuristic fuzzy expert system. *IEEE Transactions on Biomedical Engineering*, *55*(9), 2180-2189.

Farina, D. (2008). Last word on point: counterpoint: spectral properties of the surface EMG can characterize/do not provide information about motor unit recruitment and muscle fiber type. *Journal of Applied Physiology*, *105*(5), 1683-1683.

Farina, D., & Holobar, A. (2016). Characterization of human motor units from surface EMG decomposition. *Proceedings of the IEEE*, *104*(2), 353-373.

Farina, D., & Negro, F. (2012). Accessing the neural drive to muscle and translation to neurorehabilitation technologies. IEEE *Reviews in Biomedical Engineering, 5*, 3–14.

Farina, D., & Negro, F. (2015). Common synaptic input to motor neurons, motor unit synchronization, and force control. *Exercise and Sport Sciences Reviews*, *43*(1), 23-33.

Farina, D., Cescon, C., & Merletti, R. (2002). Influence of anatomical, physical, and detection-system parameters on surface EMG. *Biological Cybernetics*, *86*(6), 445-456.

Farina, D., Holobar, A., Merletti, R., & Enoka, R. M. (2010). Decoding the neural drive to muscles from the surface electromyogram. *Clinical Neurophysiology*, *121*(10), 1616-1623.

Farina, D., Merletti, R., & Enoka, R. M. (2014). The extraction of neural strategies from the surface EMG: an update. *Journal of Applied Physiology*, *117*(11), 1215-1230.

Farina, D., Merletti, R., & Enoka, R. M. (2015). Reply to De Luca, Nawab, and Kline: The proposed method to validate surface EMG signal decomposition remains problematic. *Journal of Applied Physiology*, *118*(8), 1085-1085.

Farina, D., Negro, F., & Dideriksen, J. L. (2014). The effective neural drive to muscles is the common synaptic input to motor neurons. *The Journal of Physiology*, *592*(16), 3427-3441.

Farina, D., Negro, F., Muceli, S., & Enoka, R. M. (2016). Principles of motor unit physiology evolve with advances in technology. *Physiology*, *31*(2), 83-94.

Farina, D., Yoshida, K., Stieglitz, T., & Koch, K. P. (2008). Multichannel thin-film electrode for intramuscular electromyographic recordings. *Journal of Applied Physiology*, *104*(3), 821-827.

Feinstein, B., Lindegård, B., Nyman, E., & Wohlfart, G. (1955). Morphologic studies of motor units in normal human muscles. *Cells Tissues Organs*, *23*(2), 127-142.

Felici, F., & Del Vecchio, A. (2020). Surface electromyography: what limits its use in exercise and sport physiology?. *Frontiers in Neurology*, *11*, 578504.

Fitts, R. H. (1994). Cellular mechanisms of muscle fatigue. *Physiological Reviews*, *74*(1), 49-94.

Fourchet, F., Millet, G. P., Tomazin, K., Guex, K., Nosaka, K., Edouard, P., ... & Millet, G. Y. (2012). Effects of a 5-h hilly running on ankle plantar and dorsal flexor force and fatigability. *European Journal of Applied Physiology*, *112*(7), 2645-2652.

Frey Law, L. A., & Avin, K. G. (2010). Endurance time is joint-specific: a modelling and meta-analysis investigation. *Ergonomics*, *53*(1), 109-129.

Fukuba, Y., Ohe, Y., Miura, A., Kitano, A., Endo, M., Sato, H., ... & Fukuda, O. (2004). Dissociation between the time courses of femoral artery blood flow and pulmonary V̇O2 during repeated bouts of heavy knee extension exercise in humans. *Experimental Physiology, 89*(3), 243-253.

Fukunaga, T., Roy, R. R., Shellock, F. G., Hodgson, J. A., & Edgerton, V. R. (1996). Specific tension of human plantar flexors and dorsiflexors. *Journal of Applied Physiology*, *80*(1), 158-165.

Full, R. J. (1986). Locomotion without lungs: energetics and performance of a lungless salamander. *American Journal of Physiology-Regulatory, Integrative and Comparative Physiology*, *251*(4), R775-R780.

Full, R. J., & Herreid, C. F. (1983). Aerobic response to exercise of the fastest land crab. *American Journal of Physiology-Regulatory, Integrative and Comparative Physiology*, *244*(4), R530-R536.

Furness P, Jessop J & Lippold, O. C. J., (1977). Long-lasting increases in the tremor of human hand muscles following brief, strong effort. *The Journal of Physiology*, *265*(3), 821-831.

Gabriel, D. A., Basford, J. R., & An, K. N. (2001). Training-related changes in the maximal rate of torque development and EMG activity. *Journal of Electromyography and Kinesiology*, *11*(2), 123-129.

Gaesser, G. A., & Poole, D. C. (1996). The slow component of oxygen uptake kinetics in humans. *Exercise and Sport Sciences Reviews*, *24*(1), 35-70.

Galganski, M. E., Fuglevand, A. J., & Enoka, R. M. (1993). Reduced control of motor output in a human hand muscle of elderly subjects during submaximal contractions. *Journal of Neurophysiology*, *69*(6), 2108-2115.

Gallina, A., Disselhorst-Klug, C., Farina, D., Merletti, R., Besomi, M., Holobar, A., ... & Hodges, P. W. (2022). Consensus for experimental design in electromyography (CEDE) project: High-density surface electromyography matrix. *Journal of Electromyography and Kinesiology*, *64*, 102656.

Gandevia, S. C. (2001). Spinal and Supraspinal Factors in Human Muscle Fatigue. *Physiological Reviews*, *81*(4), 1725-1725.

Gerbino, A., Ward, S. A., & Whipp, B. J. (1996). Effects of prior exercise on pulmonary gas-exchange kinetics during high-intensity exercise in humans. *Journal of Applied Physiology*, *80*(1), 99-107.

Gitter, J. A., & Czerniecki, M. J. (1995). Fractal analysis of the electromyographic interference pattern. *Journal of Neuroscience Methods*, *58*(1-2), 103-108.

Glaser, V., & Holobar, A. (2018). Motor unit identification from high-density surface electromyograms in repeated dynamic muscle contractions. *IEEE Transactions on Neural Systems and Rehabilitation Engineering*, *27*(1), 66-75.

Glenny, R. W. (2011). Emergence of matched airway and vascular trees from fractal rules. *Journal of Applied Physiology*, *110*(4), 1119-1129.

Glenny, R. W., Robertson, H. T., Yamashiro, S., & Bassingthwaighte, J. B. (1991). Applications of fractal analysis to physiology. *Journal of Applied Physiology*, *70*(6), 2351-2367.

Goldberger, A. L. (1996). Non-linear dynamics for clinicians: chaos theory, fractals, and complexity at the bedside. *The Lancet*, *347*(9011), 1312-1314.

Goldberger, A. L. (1991). Is the normal heartbeat chaotic or homeostatic? *Physiology*, *6*(2), 87-91.

Goldberger, A. L. (1992). Fractal mechanisms in the electrophysiology of the heart. *IEEE Engineering in Medicine and Biology Magazine*, *11*(2), 47-52.

Goldberger, A. L. (2006). Giles F. Filley lecture. Complex systems. *Proceedings of the American Thoracic Society*, *3*(6), 467-471.

Goldberger, A. L., Amaral, L. A., Hausdorff, J. M., Ivanov, P. C., Peng, C. K., & Stanley, H. E. (2002). Fractal dynamics in physiology: alterations with disease and aging. *Proceedings of the National Academy of Sciences*, *99*(suppl_1), 2466-2472.

Goldberger, A. L., Bhargava, V., West, B. J., & Mandell, A. J. (1985). On a mechanism of cardiac electrical stability. The fractal hypothesis. *Biophysical Journal*, *48*(3), 525-528.

Goldberger, A. L., Peng, C. K., & Lipsitz, L. A. (2002). What is physiologic complexity and how does it change with aging and disease?. *Neurobiology of Aging*, *23*(1), 23-26.

Grimnes, S. (1983). Impedance measurement of individual skin surface electrodes. *Medical and Biological Engineering and Computing*, *21*(6), 750-755.

Guo, Y., Jones, E. J., Inns, T. B., Ely, I. A., Stashuk, D. W., Wilkinson, D. J., ... & Piasecki, M. (2022). Neuromuscular recruitment strategies of the vastus lateralis according to sex. *Acta Physiologica*, *235*(2), e13803.

Gutin, B., Stewart, K., Lewis, S., & Kruper, J. (1976). Oxygen consumption in the first stages of strenous work as a function of prior exercise. *Journal of Sports Medicine and Physical Fitness*, *16*(1), 60-65.

Hagberg, M. (1981). Muscular endurance and surface electromyogram in isometric and dynamic exercise. *Journal of Applied Physiology*, *51*(1), 1-7.

Hardstone, R., Poil, S. S., Schiavone, G., Jansen, R., Nikulin, V. V., Mansvelder, H. D., & Linkenkaer-Hansen, K. (2012). Detrended fluctuation analysis: a scale-free view on neuronal oscillations. *Frontiers in Physiology*, *3*, 450.

Hase, K., & Stein, R. B. (1998). Analysis of rapid stopping during human walking. *Journal of Neurophysiology*, *80*(1), 255-261.

Hausdorff, J. M., Peng, C. K., Ladin, Z. V. I., Wei, J. Y., & Goldberger, A. L. (1995). Is walking a random walk? Evidence for long-range correlations in stride interval of human gait. *Journal of Applied Physiology*, *78*(1), 349-358.

Heckman, C. J., & Enoka, R. M. (2012). Motor unit. *Comprehensive Physiology*, *2*(4), 2629–2682.

Helliwell, T. R., Coakley, J., Smith, P. E. M., & Edwards, R. H. T. (1987). The morphology and morphometry of the normal human tibialis anterior muscle. *Neuropathology and Applied Neurobiology, 13*(4), 297-307.

Hendrix, C. R., Housh, T. J., Johnson, G. O., Mielke, M., Camic, C. L., Zuniga, J. M., & Schmidt, R. J. (2009). Comparison of critical force to EMG fatigue thresholds during isometric leg extension. *Medicine and Science in Sports and Exercise, 41*(4), 956-964.

Henneman, E. (1985). The size-principle: a deterministic output emerges from a set of probabilistic connections. *Journal of Experimental Biology*, *115*(1), 105-112.

Henriksson-Larsén, K. B., Lexell, J., & Sjöström, M. (1983). Distribution of different fibre types in human skeletal muscles. I. Method for the preparation and analysis of cross-sections of whole tibialis anterior. *The Histochemical Journal, 15*(2), 167-178.

Hernandez, L. R., & Camic, C. L. (2019). Fatigue-mediated loss of complexity is contraction-type dependent in vastus lateralis electromyographic signals. *Sports*, *7*(4), 78.

Herold, J. L., & Sommer, A. (2020). A model-based estimation of critical torques reduces the experimental effort compared to conventional testing. *European Journal of Applied Physiology*, *120*(6), 1263-1276.

Hill, A. V. (1925). The Physiological Basis of Athletic Records. *Nature*, *116*, 544-548.

Hill, A. V., & Lupton, H. (1923). Muscular exercise, lactic acid, and the supply and utilization of oxygen. *QJM: An International Journal of Medicine*, (62), 135-171.

Hill, D. W., Alain, C., & Kennedy, M. D. (2003). Modeling the relationship between velocity and time to fatigue in rowing. *Medicine and Science in Sports and Exercise*, *35*(12), 2098-2105.

Hill, D. W., Poole, D. C., & Smith, J. C. (2002). The relationship between power and the time to achieve VO2max. *Medicine and Science in Sports and Exercise*, *34*(4), 709-714.

Holobar, A., & Zazula, D. (2007). Multichannel blind source separation using convolution kernel compensation. *IEEE Transactions on Signal Processing*, *55*(9), 4487-4496.

Holobar, A., Farina, D., & Zazula, D. (2016). Surface EMG decomposition. *Surface Electromyography: Physiology, Engineering, and Applications*, 180-209.

Holobar, A., Farina, D., Gazzoni, M., Merletti, R., & Zazula, D. (2009). Estimating motor unit discharge patterns from high-density surface electromyogram. *Clinical Neurophysiology*, *120*(3), 551-562.

Holobar, A., Minetto, M. A., & Farina, D. (2014). Accurate identification of motor unit discharge patterns from high-density surface EMG and validation with a novel signal-based performance metric. *Journal of Neural Engineering*, *11*(1), 016008.

Holobar, A., Minetto, M. A., Botter, A., Negro, F., & Farina, D. (2010). Experimental analysis of accuracy in the identification of motor unit spike trains from high-density surface EMG. *IEEE Transactions on Neural Systems and Rehabilitation Engineering*, *18*(3), 221-229.

Hu, K., Ivanov, P. C., Chen, Z., Carpena, P., & Stanley, H. E. (2001). Effect of trends on detrended fluctuation analysis. *Physical Review E*, *64*(1), 011114.

Hug, F., Avrillon, S., Del Vecchio, A., Casolo, A., Ibanez, J., Nuccio, S., ... & Farina, D. (2021). Analysis of motor unit spike trains estimated from high-density surface electromyography is highly reliable across operators. *Journal of Electromyography and Kinesiology*, *58*, 102548.

Hug, F., Del Vecchio, A., Avrillon, S., Farina, D., & Tucker, K. (2021). Muscles from the same muscle group do not necessarily share common drive: evidence from the human triceps surae. *Journal of Applied Physiology*, *130*(2), 342-354.

Hughson, R. L., Orok, C. J., & Staudt, L. E. (1984). A high velocity treadmill running test to assess endurance running potential. *International Journal of Sports Medicine*, *5*(01), 23-25.

Hunter, S. K. (2014). Sex differences in human fatigability: mechanisms and insight to physiological responses. *Acta Physiologica*, *210*(4), 768-789.

Hunter, S. K. (2016). The relevance of sex differences in performance fatigability. *Medicine and Science in Sports and Exercise*, *48*(11), 2247.

Hunter, S. K., & Enoka, R. M. (2003). Changes in muscle activation can prolong the endurance time of a submaximal isometric contraction in humans. *Journal of Applied Physiology*, *94*(1), 108-118.

Huysmans, M. A., Hoozemans, M. J. M., Van der Beek, A. J., De Looze, M. P., & Van Dieën, J. H. (2008). Fatigue effects on tracking performance and muscle activity. *Journal of Electromyography and Kinesiology*, *18*(3), 410-419.

Ingjer, F., & Strømme, S. B. (1979). Effects of active, passive or no warm-up on the physiological response to heavy exercise. *European Journal of Applied Physiology and Occupational Physiology*, *40*(4), 273-282.

Inglis, J. G., & Gabriel, D. A. (2020). Sex differences in motor unit discharge rates at maximal and submaximal levels of force output. *Applied Physiology, Nutrition, and Metabolism, 45*(11), 1197-1207.

Inglis, J. G., & Gabriel, D. A. (2021). Sex differences in the modulation of the motor unit discharge rate leads to reduced force steadiness. *Applied Physiology, Nutrition, and Metabolism, 46*(9), 1065-1072.

Iyengar, N., Peng, C. K., Morin, R., Goldberger, A. L., & Lipsitz, L. A. (1996). Age-related alterations in the fractal scaling of cardiac interbeat interval dynamics.

American Journal of Physiology-Regulatory, Integrative and Comparative Physiology, *271*(4), R1078-R1084.

Jenkins, D. G., & Quigley, B. M. (1990). Blood lactate in trained cyclists during cycle ergometry at critical power. *European Journal of Applied Physiology and Occupational Physiology*, *61*(3-4), 278-283.

Jones, A. M., & Poole, D. C. (2009). Physiological demands of endurance exercise. *Olympic Textbook of Science in Sport. Chichester (UK): Blackwell Publishing*, 43-55.

Jones, A. M., Burnley, M., Black, M. I., Poole, D. C., & Vanhatalo, A. (2019). The maximal metabolic steady state: redefining the 'gold standard'. *Physiological Reports*, *7*(10), e14098.

Jones, A. M., Koppo, K., & Burnley, M. (2003). Effects of prior exercise on metabolic and gas exchange responses to exercise. *Sports Medicine*, *33*(13), 949-971.

Jones, A. M., Vanhatalo, A., Burnley, M., Morton, R. H., & Poole, D. C. (2010). Critical power: implications for determination of V O2max and exercise tolerance. *Medicine and Science in Sports and Exercise*, *42*(10), 1876-1890.

Jones, A. M., Wilkerson, D. P., Burnley, M., & Koppo, K. (2003). Prior heavy exercise enhances performance during subsequent perimaximal exercise. Medicine and Science in Sports and Exercise, 35(12), 2085-2092.

Jones, A. M., Wilkerson, D. P., DiMenna, F., Fulford, J., & Poole, D. C. (2008). Muscle metabolic responses to exercise above and below the "critical power" assessed using 31P-MRS. *American Journal of Physiology- Regulatory, Integrative and Comparative Physiology*, *294*(2), R585-R593.

Jones, A., Pringle, J., & Carter, H. (2004). Influence of muscle fibre type and motor unit recruitment on pulmonary O2 kinetics. In *Oxygen Uptake Kinetics in Health and Disease: Research and Practical Applications* (pp. 261-293). London: Routledge.

Jordan, K., Jesunathadas, M., Sarchet, D. M., & Enoka, R. M. (2013). Long-range correlations in motor unit discharge times at low forces are modulated by visual gain and age. *Experimental Physiology*, *98*(2), 546-555.

Kaplan, D. T., Furman, M. I., Pincus, S. M., Ryan, S. M., Lipsitz, L. A., & Goldberger, A. L. (1991). Aging and the complexity of cardiovascular dynamics. *Biophysical Journal*, *59*(4), 945-949.

Karastergiou, K., Smith, S. R., Greenberg, A. S., & Fried, S. K. (2012). Sex differences in human adipose tissues–the biology of pear shape. *Biology of Sex Differences*, *3*(1), 13.

Kellawan, J. M., & Tschakovsky, M. E. (2014). The single-bout forearm critical force test: a new method to establish forearm aerobic metabolic exercise intensity and capacity. *PLoS One*, *9*(4), e93481.

Koga, S., Shiojiri, T., Kondo, N., & Barstow, T. J. (1997). Effect of increased muscle temperature on oxygen uptake kinetics during exercise. *Journal of Applied Physiology*, *83*(4), 1333-1338.

Koga, S., Shiojiri, T., Shibasaki, M., Kondo, N., Fukuba, Y., & Barstow, T. J. (1999). Kinetics of oxygen uptake during supine and upright heavy exercise. *Journal of Applied Physiology*, *87*(1), 253-260.

Koppo, K., & Bouckaert, J. (2001). The effect of prior high-intensity cycling exercise on the V̇O2 kinetics during high-intensity cycling exercise is situated at the additional slow component. *International Journal of Sports Medicine*, *22*(1), 21-26.

Koppo, K., Jones, A. M., & Bouckaert, J. (2002). Effect of prior exercise on $\dot{V}O_2$ slow component is not related to muscle temperature. *Medicine and Science in Sports and Exercise*, *34*(10), 1600-1604.

Kuiken, T. A., Lowery, M. M., & Stoykov, N. S. (2003). The effect of subcutaneous fat on myoelectric signal amplitude and cross-talk. *Prosthetics and Orthotics International*, *27*(1), 48-54.

Lauderdale, M. A., & Hinchcliff, K. W. (1999). Hyperbolic relationship between time-to-fatigue and workload. *Equine Veterinary Journal*, *31*(S30), 586-590.

Layec, G., Bringard, A., Le Fur, Y., Vilmen, C., Micallef, J. P., Perrey, S., ... & Bendahan, D. (2009). Effects of a prior high-intensity knee-extension exercise on muscle recruitment and energy cost: a combined local and global investigation in humans. *Experimental Physiology*, *94*(6), 704-719.

Liddell, E. G. T., & Sherrington, C. S. (1925). Recruitment and some other features of reflex inhibition. *Proceedings of the Royal Society of London. Series B, Containing Papers of a Biological Character*, *97*(686), 488-518.

Liebovitch, L. S., Fischbarg, J., Koniarek, J. P., Todorova, I., & Wang, M. (1987). Fractal model of ion-channel kinetics. *Biochimica et Biophysica Acta (BBA)-Biomembranes*, *896*(2), 173-180.

Lipsitz, L. A. (2002). Dynamics of stability: the physiologic basis of functional health and frailty. *The Journals of Gerontology Series A: Biological Sciences and Medical Sciences*, *57*(3), B115-B125.

Lipsitz, L. A., & Goldberger, A. L. (1992). Loss of 'complexity' and aging: potential applications of fractals and chaos theory to senescence. *Journal of the American Medical Association*, *267*(13), 1806-1809.

Lucas, K. (1905). On the gradation of activity in a skeletal muscle-fibre. *The Journal of Physiology*, *33*(2), 125–137.

Lucas, K. (1909). The “all or none” contraction of the amphibian skeletal muscle fibre. *The Journal of Physiology*, *38*(2–3), 113–133.

Macdonald, M., Pedersen, P. K., & Hughson, R. L. (1997). Acceleration of $\dot{V}O_2$ kinetics in heavy submaximal exercise by hyperoxia and prior high-intensity exercise. *Journal of Applied Physiology*, *83*(4), 1318-1325.

Mandelbrot, B. (1967). How long is the coast of Britain? Statistical self-similarity and fractional dimension. *Science*, *156*(3775), 636-638.

Mandelbrot, B. (1977). *Fractals*. San Francisco: Freeman.

Mandelbrot, B. (1982). *The fractal geometry of nature* (Vol. 1). New York: WH Freeman.

Marateb, H. R., McGill, K. C., Holobar, A., Lateva, Z. C., Mansourian, M., & Merletti, R. (2011). Accuracy assessment of CKC high-density surface EMG decomposition in biceps femoris muscle. *Journal of Neural Engineering*, *8*(6), 066002.

Marsh, D. J., Osborn, J. L., & Cowley Jr, A. W. (1990). 1/f fluctuations in arterial pressure and regulation of renal blood flow in dogs. *American Journal of Physiology-Renal Physiology*, *258*(5), F1394-F1400.

Marsh, E., Sale, D., McComas, A. J., & Quinlan, J. (1981). Influence of joint position on ankle dorsiflexion in humans. *Journal of Applied Physiology*, *51*(1), 160-167.

Martin, P. G., & Rattey, J. (2007). Central fatigue explains sex differences in muscle fatigue and contralateral cross-over effects of maximal contractions. *Pflügers Archiv-European Journal of Physiology*, *454*(6), 957-969.

Martinez-Valdes, E., Guzman-Venegas, R. A., Silvestre, R. A., Macdonald, J. H., Falla, D., Araneda, O. F., & Haichelis, D. (2016). Electromyographic adjustments during continuous and intermittent incremental fatiguing cycling. *Scandinavian Journal of Medicine and Science in Sports*, *26*(11), 1273-1282.

Martinez-Valdes, E., Laine, C. M., Falla, D., Mayer, F., & Farina, D. (2016). High-density surface electromyography provides reliable estimates of motor unit behavior. *Clinical Neurophysiology*, *127*(6), 2534-2541.

Martinez-Valdes, E., Negro, F., Botter, A., Pincheira, P. A., Cerone, G. L., Falla, D., ... & Cresswell, A. G. (2021). Modulations in motor unit discharge are related to changes in fascicle length during isometric contractions. *bioRxiv*. Preprint. https://doi.org/10.1101/2021.04.27.441619

Martinez-Valdes, E., Negro, F., Falla, D., Dideriksen, J. L., Heckman, C. J., & Farina, D. (2020). Inability to increase the neural drive to muscle is associated with task failure during submaximal contractions. *Journal of Neurophysiology*, *124*(4), 1110-1121.

Martinez-Valdes, E., Negro, F., Farina, D., & Falla, D. (2020). Divergent response of low-versus high-threshold motor units to experimental muscle pain. *The Journal of Physiology*, *598*(11), 2093-2108.

Martinez-Valdes, E., Negro, F., Laine, C. M., Falla, D., Mayer, F., & Farina, D. (2017). Tracking motor units longitudinally across experimental sessions with high-density surface electromyography. *The Journal of Physiology*, *595*(5), 1479-1496.

Masuda, T., Miyano, H. and Sadoyama, T. (1985). The position of innervation zones in the biceps brachii investigated by surface electromyography. *IEEE Transactions on Biomedical Engineering, 32*(1), 36-42.

Mattioni Maturana, F., Fontana, F. Y., Pogliaghi, S., Passfield, L., & Murias, J. M. (2018). Critical power: How different protocols and models affect its determination. *Journal of Science and Medicine in Sport*, *21*(7), 742-747.

McNeil, C. J., Giesebrecht, S., Gandevia, S. C., & Taylor, J. L. (2011). Behaviour of the motoneurone pool in a fatiguing submaximal contraction. *The Journal of Physiology*, *589*(14), 3533-3544.

Merletti, R., & Farina, D. (Eds.). (2016). Surface electromyography: physiology, engineering and applications. John Wiley & Sons.

Merletti, R., Holobar, A., & Farina, D. (2008). Analysis of motor units with high-density surface electromyography. *Journal of Electromyography and Kinesiology*, *18*(6), 879-890.

Mesin, L., Dardanello, D., Rainoldi, A., & Boccia, G. (2016). Motor unit firing rates and synchronisation affect the fractal dimension of simulated surface electromyogram during isometric/isotonic contraction of vastus lateralis muscle. *Medical Engineering and Physics*, *38*(12), 1530-1533.

Milner, N. P. (1996). *Vegetius: Epitome of Military Science*. *2nd revised edition.* Liverpool, England: Liverpool University Press.

Mines, G. R. (1913). On the summation of contractions. *The Journal of Physiology*, *46*(1), 1-27.

Mitchell, E. A., Martin, N. R., Bailey, S. J., & Ferguson, R. A. (2018). Critical power is positively related to skeletal muscle capillarity and type I muscle fibers in endurance-trained individuals. *Journal of Applied Physiology*, *125*(3), 737-745.

Miura, A., Endo, M., Sato, H., Sato, H., Barstow, T. J., & Fukuba, Y. (2002). Relationship between the curvature constant parameter of the power-duration curve and muscle cross-sectional area of the thigh for cycle ergometry in humans. *European Journal of Applied Physiology*, *87*(3), 238-244.

Miura, A., Kino, F., Kajitani, S., Sato, H., Sato, H., & Fukuba, Y. (1999). The effect of oral creatine supplementation on the curvature constant parameter of the power-duration curve for cycle ergometry in humans. *The Japanese Journal of Physiology*, *49*(2), 169-174.

Miura, A., Sato, H., Sato, H., Hipp, B. J., & Fukuba, Y. (2000). The effect of glycogen depletion on the curvature constant parameter of the power-duration curve for cycle ergometry. *Ergonomics*, *43*(1), 133-141.

Monod, H., & Scherrer, J. (1965). The work capacity of a synergic muscular group. *Ergonomics*, *8*(3), 329-338.

Moritani, T., Nagata, A., deVries, H. A., & Muro, M. (1981). Critical power as a measure of physical work capacity and anaerobic threshold. *Ergonomics*, *24*(5), 339-350.

Morton, R. H., Redstone, M. D., & Laing, D. J. (2014). The critical power concept and bench press: Modeling 1RM and repetitions to failure. *International Journal of Exercise Science*, *7*(2), 6.

Muceli, S., Poppendieck, W., Negro, F., Yoshida, K., Hoffmann, K. P., Butler, J. E., … Farina, D. (2015). Accurate and representative decoding of the neural drive to muscles in humans with multi-channel intramuscular thin-film electrodes. *The Journal of Physiology*, *593*(17), 3789–3804.

Muniz-Pumares, D., Karsten, B., Triska, C., & Glaister, M. (2019). Methodological approaches and related challenges associated with the determination of critical power and curvature constant. *The Journal of Strength and Conditioning Research*, *33*(2), 584-596.

Murgatroyd, S. R., Ferguson, C., Ward, S. A., Whipp, B. J., & Rossiter, H. B. (2011). Pulmonary O2 uptake kinetics as a determinant of high-intensity exercise tolerance in humans. *Journal of Applied Physiology*, *110*(6), 1598-1606.

Murphy, S., Durand, M., Negro, F., Farina, D., Hunter, S., Schmit, B., ... & Hyngstrom, A. (2019). The relationship between blood flow and motor unit firing rates in response to fatiguing exercise post-stroke. *Frontiers in Physiology, 10, 545.*

Neder, J. A., Jones, P. W., Nery, L. E., & Whipp, B. J. (2000). Determinants of the exercise endurance capacity in patients with chronic obstructive pulmonary disease: the power–duration relationship. *American Journal of Respiratory and Critical Care Medicine*, *162*(2), 497-504.

Negro, F., Holobar, A., & Farina, D. (2009). Fluctuations in isometric muscle force can be described by one linear projection of low-frequency components of motor unit discharge rates. *The Journal of Physiology*, *587*(24), 5925-5938.

Negro, F., Muceli, S., Castronovo, A. M., Holobar, A., & Farina, D. (2016). Multi-channel intramuscular and surface EMG decomposition by convolutive blind source separation. *Journal of Neural Engineering*, *13*(2), 026027.

Nicolò, A., Bazzucchi, I., & Sacchetti, M. (2017). Parameters of the 3-Minute All-Out test: overestimation of competitive-cyclist time-trial performance in the severe-intensity domain. *International Journal of Sports Physiology and Performance*, *12*(5), 655-661.

Oliveira, A. S., & Negro, F. (2021). Neural control of matched motor units during muscle shortening and lengthening at increasing velocities. *Journal of Applied Physiology*, *130*(6), 1798-1813.

Peitgen, H. O., Jürgens, H., Saupe, D., & Feigenbaum, M. J. (1992). *Chaos and fractals: new frontiers of science* (Vol. 7). New York: Springer.

Pendergast, D., Leibowitz, R., Wilson, D., & Cerretelli, P. (1983). The effect of preceding anaerobic exercise on aerobic and anaerobic work. *European Journal of Applied Physiology and Occupational Physiology*, *52*(1), 29-35.

Peng, C. K., Buldyrev, S. V., Havlin, S., Simons, M., Stanley, H. E., & Goldberger, A. L. (1994). Mosaic organization of DNA nucleotides. *Physical Review E*, *49*(2), 1685.

Peng, C. K., Costa, M., & Goldberger, A. L. (2009). Adaptive data analysis of complex fluctuations in physiologic time series. *Advances in Adaptive Data Analysis*, *1*(01), 61-70.

Peng, C. K., Hausdorff, J. M., & Goldberger, A. L. (2000). Fractal mechanisms in neuronal control: human heartbeat and gait dynamics in health and disease. *Self-organized biological dynamics and nonlinear control*, 66-96.

Peng, C. K., Havlin, S., Stanley, H. E., & Goldberger, A. L. (1995). Quantification of scaling exponents and crossover phenomena in nonstationary heartbeat time series. *Chaos*, *5*(1), 82-87.

Peng, C. K., Mietus, J. E., Liu, Y., Lee, C., Hausdorff, J. M., Stanley, H. E., ... & Lipsitz, L. A. (2002). Quantifying fractal dynamics of human respiration: age and gender effects. *Annals of Biomedical Engineering*, *30*(5), 683-692.

Peng, C.K., Buldyrev, S.V, Havlin, S., Simon, M., Stanley, H.E. and Goldberger, A.L. (1994). Mosaic organization of DNA nucleotides. *Physical Review E, 49*(2), 1685-1689.

Perrey, S., Betik, A., Candau, R., Rouillon, J. D., & Hughson, R. L. (2001). Comparison of oxygen uptake kinetics during concentric and eccentric cycle exercise. *Journal of Applied Physiology*, *91*(5), 2135-2142.

Pethick, J., Casselton, C., Winter, S. L., & Burnley, M. (2021). Ischemic preconditioning blunts loss of knee extensor torque complexity with fatigue. *Medicine and Science in Sports and Exercise*, *53*(2), 306.

Pethick, J., Whiteaway, K., Winter, S. L., & Burnley, M. (2019). Prolonged depression of knee-extensor torque complexity following eccentric exercise. *Experimental Physiology*, *104*(1), 100-111.

Pethick, J., Winter, S. L., & Burnley, M. (2015). Fatigue reduces the complexity of knee extensor torque fluctuations during maximal and submaximal intermittent isometric contractions in man. *The Journal of Physiology*, *593*(8), 2085-2096.

Pethick, J., Winter, S. L., & Burnley, M. (2016). Loss of knee extensor torque complexity during fatiguing isometric muscle contractions occurs exclusively above the critical torque. *American Journal of Physiology-Regulatory, Integrative and Comparative Physiology*, *310*(11), R1144-R1153.

Pethick, J., Winter, S. L., & Burnley, M. (2018a). Caffeine Ingestion Attenuates Fatigue-induced Loss of Muscle Torque Complexity. *Medicine and Science in Sports and Exercise*, *50*(2), 236-245.

Pethick, J., Winter, S. L., & Burnley, M. (2018b). Effects of ipsilateral and contralateral fatigue and muscle blood flow occlusion on the complexity of knee-extensor torque output in humans. *Experimental Physiology*, *103*(7), 956-967.

Pethick, J., Winter, S. L., & Burnley, M. (2019a). Fatigue reduces the complexity of knee extensor torque during fatiguing sustained isometric contractions. *European Journal of Sport Science*, *19*(10), 1349-1358.

Pethick, J., Winter, S. L., & Burnley, M. (2019b). Relationship between muscle metabolic rate and muscle torque complexity during fatiguing intermittent isometric contractions in humans. *Physiological Reports*, *7*(18), e14240.

Pethick, J., Winter, S. L., & Burnley, M. (2020). Physiological evidence that the critical torque is a phase transition, not a threshold. *Medicine and Science in Sports and Exercise*, *52*(11), 2390.

Pethick, J., Winter, S. L., & Burnley, M. (2021). Physiological complexity: influence of ageing, disease and neuromuscular fatigue on muscle force and torque fluctuations. *Experimental Physiology*, *106*(10), 2046-2059.

Pettitt, R. W., Jamnick, N., & Clark, I. E. (2012). 3-min all-out exercise test for running. *International Journal of Sports Medicine*, *33*(06), 426-431.

Piatrikova, E., Sousa, A. C., Gonzalez, J. T., & Williams, S. (2018). Validity and reliability of the 3-minute all-out test in national and international competitive swimmers. *International Journal of Sports Physiology and Performance*, *13*(9), 1190-1198.

Piervirgili, G., Petracca, F., & Merletti, R. (2014). A new method to assess skin treatments for lowering the impedance and noise of individual gelled Ag–AgCl electrodes. *Physiological Measurement*, *35*(10), 2101.

Pincus, S. M. (1991). Approximate entropy as a measure of system complexity. *Proceedings of the National Academy of Sciences*, *88*(6), 2297-2301.

Pincus, S. M. (2001). Assessing serial irregularity and its implications for health. *Annals of the New York Academy of Sciences*, *954*(1), 245-267.

Pincus, S. M. (2006). Approximate entropy as a measure of irregularity for psychiatric serial metrics. *Bipolar Disorders*, *8*, 430-440.

Place, N., Bruton, J. D., & Westerblad, H. (2009). Mechanisms of fatigue induced by isometric contractions in exercising humans and in mouse isolated single muscle fibres. *Clinical and Experimental Pharmacology and Physiology*, *36*(3), 334-339.

Poole, D. C., & Jones, A. M. (2012). Oxygen uptake kinetics. *Comprehensive Physiology*, *2*(2), 933-96.

Poole, D. C., Burnley, M., Vanhatalo, A., Rossiter, H. B., & Jones, A. M. (2016). Critical power: an important fatigue threshold in exercise physiology. *Medicine and Science in Sports and Exercise*, *48*(11), 2320.

Poole, D. C., Schaffartzik, W., Knight, D. R., Derion, T., Kennedy, B., Guy, H. J., ... & Wagner, P. D. (1991). Contribution of excising legs to the slow component of oxygen uptake kinetics in humans. *Journal of Applied Physiology*, *71*(4), 1245-1260.

Poole, D. C., Ward, S. A., & Whipp, B. J. (1990). The effects of training on the metabolic and respiratory profile of high-intensity cycle ergometer exercise. *European Journal of Applied Physiology and Occupational Physiology*, *59*(6), 421-429.

Poole, D. C., Ward, S. A., Gardner, G. W., & Whipp, B. J. (1988). Metabolic and respiratory profile of the upper limit for prolonged exercise in man. *Ergonomics*, *31*(9), 1265-1279.

Porter, M. M., Stuart, S., Boij, M., & Lexell, J. (2002). Capillary supply of the tibialis anterior muscle in young, healthy, and moderately active men and women. *Journal of Applied Physiology*, *92*(4), 1451-1457.

Pringle, J. S., & Jones, A. M. (2002). Maximal lactate steady state, critical power and EMG during cycling. *European Journal of Applied Physiology*, *88*(3), 214-226.

Pringle, J. S., Doust, J. H., Carter, H., Tolfrey, K., Campbell, I. T., & Jones, A. M. (2003a). Oxygen uptake kinetics during moderate, heavy and severe intensity 'submaximal' exercise in humans: the influence of muscle fibre type and capillarisation. *European Journal of Applied Physiology*, *89*(3), 289-300.

Pringle, J. S., Doust, J. H., Carter, H., Tolfrey, K., & Jones, A. M. (2003b). Effect of pedal rate on primary and slow-component oxygen uptake responses during heavy-cycle exercise. *Journal of Applied Physiology*, *94*(4), 1501-1507.

Racinais, S., Blonc, S., Jonville, S., & Hue, O. (2005). Time of day influences the environmental effects on muscle force and contractility. Medicine and Science in Sports and Exercise, 37(2), 256-261.

Richman, J. S., & Moorman, J. R. (2000). Physiological time-series analysis using approximate entropy and sample entropy. *American Journal of Physiology-Heart and Circulatory Physiology*, *278*(6), H2039-H2049.

Rohmert, W. (1960). Ermittlung von Erholungspausen für statische Arbeit des Menschen. *Internationale Zeitschrift für Angewandte Physiologie einschließlich Arbeitsphysiologie*, *18*(2), 123-164.

Rose, M. H., Bandholm, T., & Jensen, B. R. (2009). Approximate entropy based on attempted steady isometric contractions with the ankle dorsal-and plantarflexors: reliability and optimal sampling frequency. *Journal of Neuroscience Methods*, *177*(1), 212-216.

Rossato, J., Tucker, K., Avrillon, S., Lacourpaille, L., Holobar, A., & Hug, F. (2022). Less common synaptic input between muscles from the same group allows for more flexible coordination strategies during a fatiguing task. *Journal of Neurophysiology*, *127*(2), 421-433.

Rossiter, H. B., Ward, S. A., Doyle, V. L., Howe, F. A., Griffiths, J. R., & Whipp, B. J. (1999). Inferences from pulmonary O2 uptake with respect to intramuscular [phosphocreatine] kinetics during moderate exercise in humans. *The Journal of Physiology*, *518*(3), 921-932.

Rossiter, H. B., Ward, S. A., Howe, F. A., Wood, D. M., Kowalchuk, J. M., Griffiths, J. R., & Whipp, B. J. (2003). Effects of dichloroacetate on VO2 and intramuscular 31P metabolite kinetics during high-intensity exercise in humans. *Journal of Applied Physiology*, *95*(3), 1105-1115.

Russ, D. W., & Kent-Braun, J. A. (2003). Sex differences in human skeletal muscle fatigue are eliminated under ischemic conditions. *Journal of Applied Physiology*, *94*(6), 2414-2422.

Russ, D. W., Lanza, I. R., Rothman, D., & Kent-Braun, J. A. (2005). Sex differences in glycolysis during brief, intense isometric contractions. *Muscle and Nerve*, *32*(5), 647-655.

Saugen, E., Vollestad, N. K., Gibson, H., Martin, P. A., & Edwards, R. H. (1997). Dissociation between metabolic and contractile responses during intermittent isometric exercise in man. *Experimental Physiology, 82*(1), 213-226.

Saunders, M. J., Evans, E. M., Arngrimsson, S. A., Allison, J. D., Warren, G. L., & Cureton, K. J. (2000). Muscle activation and the slow component rise in oxygen uptake during cycling. *Medicine and Science in Sports and Exercise*, *32*(12), 2040-2045.

Scheuermann, B. W., Hoelting, B. D., Noble, M. L., & Barstow, T. J. (2001). The slow component of O2 uptake is not accompanied by changes in muscle EMG during repeated bouts of heavy exercise in humans. *The Journal of Physiology*, *531*(1), 245-256.

Schiaffino, S., & Reggiani, C. (2011). Fiber types in mammalian skeletal muscles. *Physiological Reviews*, *91*(4), 1447-1531.

Schneider, E. D., & Kay, J. J. (1994). Life as a manifestation of the second law of thermodynamics. *Mathematical and Computer Modelling*, *19*(6-8), 25-48.

Seely, A. J. E., & Macklem, P. (2012). Fractal variability: an emergent property of complex dissipative systems. *Chaos: An Interdisciplinary Journal of Nonlinear Science*, *22*(1), 013108.

Seely, A. J., & Macklem, P. T. (2004). Complex systems and the technology of variability analysis. *Critical Care*, *8*(6), R367.

Sherrington, C. S. (1906). *The integrative action of the nervous system*. C Scribner and Sons, New York.

Sherrington, C. S. (1925). Remarks on some aspects of reflex inhibition. *Proceedings of the Royal Society of London. Series B, Containing Papers of a Biological Character*, *97*(686), 519-545.

Shinohara, M. & Moritani, T. (1992). Increase in neuromuscular activity and oxygen uptake during heavy exercise. *The Annals of Physiological Anthropology*, *11*(3), 257-262.

Simoneau, J. A., & Bouchard, C. (1989). Human variation in skeletal muscle fiber-type proportion and enzyme activities. *American Journal of Physiology-Endocrinology And Metabolism*, *257*(4), E567-E572.

Simpson, L. P., Jones, A. M., Skiba, P. F., Vanhatalo, A., & Wilkerson, D. (2015). Influence of hypoxia on the power-duration relationship during high-intensity exercise. *International Journal of Sports Medicine*, *36*(02), 113-119.

Škarabot, J., Ansdell, P., Temesi, J., Howatson, G., Goodall, S., & Durbaba, R. (2019). Neurophysiological responses and adaptation following repeated

bouts of maximal lengthening contractions in young and older adults. *Journal of Applied Physiology*, *127*(5), 1224-1237.

Slifkin, A. B., & Newell, K. M. (1999). Noise, information transmission, and force variability. *Journal of Experimental Psychology: Human Perception and Performance*, *25*(3), 837.

Smith Jr, T. G., Marks, W. B., Lange, G. D., Sheriff Jr, W. H., & Neale, E. A. (1989). A fractal analysis of cell images. *Journal of Neuroscience Methods*, *27*(2), 173-180.

Smith, J. C., & Hill, D. W. (1993). Stability of parameter estimates derived from the power/time relationship. *Canadian Journal of Applied Physiology*, *18*(1), 43-47.

Smith, J. L., Martin, P. G., Gandevia, S. C., & Taylor, J. L. (2007). Sustained contraction at very low forces produces prominent supraspinal fatigue in human elbow flexor muscles. *Journal of Applied Physiology, 103(2), 560-568.*

Søgaard, K., Gandevia, S. C., Todd, G., Petersen, N. T., & Taylor, J. L. (2006). The effect of sustained low-intensity contractions on supraspinal fatigue in human elbow flexor muscles. *The Journal of Physiology*, *573*(2), 511-523.

Spinelli, E. M., Mayosky, M. A., & Pallás-Areny, R. (2006). A practical approach to electrode-skin impedance unbalance measurement. *IEEE Transactions on Biomedical Engineering, 53*(7), 1451-1453.

Staron, R. S., Hagerman, F. C., Hikida, R. S., Murray, T. F., Hostler, D. P., Crill, M. T., ... & Toma, K. (2000). Fiber type composition of the vastus lateralis muscle of young men and women. *Journal of Histochemistry and Cytochemistry, 48*(5), 623-629.

Stergiou, N., & Decker, L. M. (2011). Human movement variability, nonlinear dynamics, and pathology: is there a connection? *Human Movement Science*, *30*(5), 869-888.

Tamm, A. S., Lagerquist, O., Ley, A. L., & Collins, D. F. (2009). Chronotype influences diurnal variations in the excitability of the human motor cortex and the ability to generate torque during a maximum voluntary contraction. *Journal of Biological Rhythms*, *24*(3), 211-224.

Taylor, C. A., Kopicko, B. H., Negro, F., & Thompson, C. K. (2022). Sex differences in the detection of motor unit action potentials identified using high-density surface electromyography. *Journal of Electromyography and Kinesiology*, *65*, 102675.

Taylor, J. L., Amann, M., Duchateau, J., Meeusen, R., & Rice, C. L. (2016). Neural contributions to muscle fatigue: from the brain to the muscle and back again. *Medicine and Science in Sports and Exercise*, *48*(11), 2294.

Tordi, N., Perrey, S., Harvey, A., & Hughson, R. L. (2003). Oxygen uptake kinetics during two bouts of heavy cycling separated by fatiguing sprint exercise in humans. *Journal of Applied Physiology*, *94*(2), 533-541.

Trevino, M. A., Sterczala, A. J., Miller, J. D., Wray, M. E., Dimmick, H. L., Ciccone, A. B., ... & Herda, T. J. (2019). Sex-related differences in muscle size explained by amplitudes of higher-threshold motor unit action potentials and muscle fibre typing. *Acta Physiologica*, *225*(4), e13151.

Vaillancourt, D. E., & Newell, K. M. (2003). Aging and the time and frequency structure of force output variability. *Journal of Applied Physiology*, *94*(3), 903-912.

Van Cutsem, M., Feiereisen, P., Duchateau, J., & Hainaut, K. (1997). Mechanical properties and behaviour of motor units in the tibialis anterior during voluntary contractions. *Canadian Journal of Applied Physiology*, *22*(6), 585-597.

Vanhatalo, A., Black, M. I., DiMenna, F. J., Blackwell, J. R., Schmidt, J. F., Thompson, C., ... & Jones, A. M. (2016). The mechanistic bases of the power–time relationship: muscle metabolic responses and relationships to muscle fibre type. *The Journal of Physiology*, *594*(15), 4407-4423.

Vanhatalo, A., Doust, J. H., & Burnley, M. (2007). Determination of critical power using a 3-min all-out cycling test. *Medicine and Science in Sports and Exercise*, *39*(3), 548-555.

Vanhatalo, A., Doust, J. H., & Burnley, M. (2008). Robustness of a 3 min all-out cycling test to manipulations of power profile and cadence in humans. *Experimental Physiology*, *93*(3), 383-390.

Vanhatalo, A., Fulford, J., DiMenna, F. J., & Jones, A. M. (2010). Influence of hyperoxia on muscle metabolic responses and the power–duration relationship during severe-intensity exercise in humans: a 31P magnetic resonance spectroscopy study. *Experimental Physiology*, *95*(4), 528-540.

Vanhatalo, A., Jones, A. M., & Burnley, M. (2011). Application of critical power in sport. *International Journal of Sports Physiology and Performance*, *6*(1), 128-136.

Vanhatalo, A., Poole, D. C., DiMenna, F. J., Bailey, S. J., & Jones, A. M. (2011). Muscle fiber recruitment and the slow component of O2 uptake: constant work rate vs. all-out sprint exercise. *American Journal of Physiology-Regulatory, Integrative and Comparative Physiology*, *300*(3), R700-R707.

Vieira, T. M., Loram, I. D., Muceli, S., Merletti, R., & Farina, D. (2011). Postural activation of the human medial gastrocnemius muscle: are the muscle units spatially localised?. *The Journal of Physiology*, *589*(2), 431-443.

Wagner, C. D., & Persson, P. B. (1995). Nonlinear chaotic dynamics of arterial blood pressure and renal blood flow. *American Journal of Physiology-Heart and Circulatory Physiology*, *268*(2), H621-H627.

Wakayoshi, K., Ikuta, K., Yoshida, T., Udo, M., Moritani, T., Mutoh, Y., & Miyashita, M. (1992). Determination and validity of critical velocity as an index of swimming performance in the competitive swimmer. *European Journal of Applied Physiology and Occupational Physiology*, *64*(2), 153-157.

Walton, C., Kalmar, J. M., & Cafarelli, E. (2002). Effect of caffeine on self-sustained firing in human motor units. *The Journal of Physiology*, *545*(2), 671-679.

Walton, C., Kalmar, J., & Cafarelli, E. (2003). Caffeine increases spinal excitability in humans. *Muscle and Nerve*, *28*(3), 359-364.

West, B. J. (2010). Fractal physiology and the fractional calculus: a perspective. *Frontiers in Physiology*, *1*, 12.

Whipp, B. J. (1994). The slow component of O2 uptake kinetics during heavy exercise. *Medicine and Science in Sports and Exercise*, *26*(11), 1319-1326.

Whipp, B. J., Huntsman, B. J., Storer, T., Lamarra, N., & Wasserman, K. (1982). A constant which determines the duration of tolerance to high-intensity work. *Fed Proc, 41,* 1591.

Whipp, B. J., Rossiter, H. B., & Ward, S. A. (2002). Exertional oxygen uptake kinetics: a stamen of stamina?. *Biochemical Society Transactions*, *30*(2), 237-247.

Whipp, B. J., Ward, S. A., & Hassall, M. (1996). Estimating the metabolic rate of marching Roman Legionaries. *Journal of Physiology (London), 491P*, 60.

Whipp, B. J., Ward, S. A., & Hassall, M. W. (1998). Paleo-bioenergetics: the metabolic rate of marching Roman legionaries. *British Journal of Sports Medicine*, *32*(3), 261.

Whipp, B. J., Ward, S. A., Lamarra, N., Davis, J. A., & Wasserman, K. (1982). Parameters of ventilatory and gas exchange dynamics during exercise. *Journal of Applied Physiology*, *52*(6), 506-1513.

Wilkie, D. R., (1980). Equations describing power input by humans as a function of duration of exercise. In: Exercise Bioenergetics and Gas Exchange (pp. 75-80). Elsevier

Wüst, R. C., Morse, C. I., De Haan, A., Jones, D. A., & Degens, H. (2008). Sex differences in contractile properties and fatigue resistance of human skeletal muscle. *Experimental Physiology*, *93*(7), 843-850.

Yentes, J. M., Hunt, N., Schmid, K. K., Kaipust, J. P., McGrath, D., & Stergiou, N. (2013). The appropriate use of approximate entropy and sample entropy with short data sets. *Annals of Biomedical Engineering*, *41*(2), 349-365.

Yokoyama, H., Kaneko, N., Sasaki, A., Saito, A., & Nakazawa, K. (2022). Firing behavior of single motor neurons of the tibialis anterior in human walking as non-invasively revealed by HDsEMG decomposition. *bioRxiv*. Preprint. https://doi.org/10.1101/2022.04.03.486869

Yokoyama, H., Sasaki, A., Kaneko, N., Saito, A., & Nakazawa, K. (2021). Robust Identification of Motor Unit Discharges From High-Density Surface EMG in Dynamic Muscle Contractions of the Tibialis Anterior. *IEEE Access, 9, 123901-123911.*

Yoon, T., Schlinder Delap, B., Griffith, E. E., & Hunter, S. K. (2007). Mechanisms of fatigue differ after low-and high-force fatiguing contractions in men and women. *Muscle and Nerve, 36(4), 515-524.*

APPENDIX

Ethical Approval Codes

Study 1 (Chapter 4): Prop 99_2017_18

Study 2 (Chapter 5): Prop 72_2018_19

Study 3 & 4 (Chapters 6 & 7): Prop 32_2019_20

HEALTH QUESTIONNAIRE

Code Number……

Age……

Please answer these questions truthfully and completely. The sole purpose of this questionnaire is to ensure that you are in a fit and healthy state to complete an exercise test. ANY INFORMATION CONTAINED HEREIN WILL BE TREATED AS CONFIDENTIAL.

SECTION 1: GENERAL HEALTH QUESTIONS

Please read the 10 questions below carefully and answer each one honestly: check YES or NO.

	YES	NO
1. Has your doctor ever said that you have a heart condition or high blood pressure?	□	□
2. Do you feel pain in your chest at rest, during your daily activities of living, or when you do physical activity?	□	□
3. Do you lose balance because of dizziness or have you lost consciousness in the last 12 months? (Please answer NO if your dizziness was associated with over-breathing including vigorous exercise).	□	□
4. Have you ever been diagnosed with another chronic medical condition (other than heart disease or high blood pressure)?	□	□
If yes, please list condition(s) here:		
5. Are you currently taking prescribed medications for a chronic medical condition?	□	□
If yes, please list condition(s) and medications here:		
6. Do you currently have (or have you had within the past 12 months) a bone, joint or soft tissue (muscle, ligament, or tendon) problem that could be made worse by becoming more physically active? Please answer NO if you had a problem in the past but it *does not limit your ability* to be physically active.	□	□
If yes, please list condition(s) here:		
7. Has your doctor ever said that you should only do medically supervised physical activity?	□	□
8. Are you, or is there any chance you could be, pregnant?	□	□
9. Are you currently taking any nutritional supplement? **If 'YES' please inform the researcher what supplements are being taken**	□	□
10. Are you involved in any other research project? **If 'YES' please inform the researcher about details of the project**	□	□

If you answered NO to all of the questions above, you are cleared to take part in the exercise test

Go to SECTION 3 to sign the form. You do not need to complete section 2.

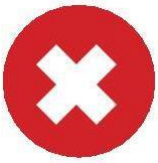

If you answered YES to one or more of the questions in Section 1 - PLEASE GO TO SECTION 2.

SECTION 2: CHRONIC MEDICAL CONDITIONS

Please read the questions below carefully and answer each one honestly: check YES or NO.

		YES	NO
1.	**Do you have arthritis, osteoporosis, or back problems?** If YES answer questions 1a-1c. If NO go to Question 2.	□	□
1a.	Do you have difficulty controlling your condition with medications or other physician-prescribed therapies? (Answer NO if you are not currently taking any medications or other treatments).	□	□
1b.	Do you have joint problems causing pain, a recent fracture or fracture caused by osteoporosis or cancer, displaced vertebrae (e.g. spondylolisthesis), and/or spondyloysis/pars defect (a crack in the bony ring on the back of the spinal column)?	□	□
1c.	Have you had steroid injections or taken steroid tablets regularly for more than 3 months?	□	□
2.	**Do you have cancer of any kind?** If YES answer questions 2a-2b. If NO, go to Question 3.	□	□
2a.	Does your cancer diagnosis include any of the following types: lung/bronchogenic, multiple myeloma (cancer of plasma cells), head and neck?	□	□
2b.	Are you currently receiving cancer therapy (such as chemotherapy or radiotherapy)?	□	□
3.	**Do you have heart disease or cardiovascular disease? This includes coronary artery disease, high blood pressure, heart failure, diagnosed abnormality or heart rhythm.** If YES answer questions 3a-3e. If NO go to Question 4.	□	□
3a.	Do you have difficulty controlling your condition with medications or other physician-prescribed therapies? (Answer NO if you are not currently taking any medications or other treatments).	□	□
3b.	Do you have an irregular heartbeat that requires medical management? (e.g. atrial fibrillation, premature ventricular contraction)	□	□
3c.	Do you have chronic heart failure?	□	□
3d.	Do you have a resting blood pressure equal to or greater than 160/90mmHg with or without medication? Answer YES if you do not know your resting blood pressure.	□	□
3e.	Do you have diagnosed coronary artery (cardiovascular) disease and have not participated in regular physical activity in the last 2 months?	□	□

		YES	NO
4.	**Do you have any metabolic conditions? This includes Type 1 Diabetes, Type 2 Diabetes and Pre-Diabetes.** If YES answer questions 4a-4c. If NO, go to Question 5.	□	□
4a.	Is your blood sugar often above 13mmol/L? (Answer YES if you are not sure).	□	□
4b.	Do you have any signs or symptoms of diabetes complications such as heart or vascular disease and/or complications affecting your eyes, kidneys, OR the sensation in your toes and feet?	□	□
4c.	Do you have other metabolic conditions (such as thyroid disorders, current pregnancy related diabetes, chronic kidney disease, or liver problems)?	□	□
5.	**Do you have any mental health problems or learning difficulties?** This includes Alzheimer's, dementia, depression, anxiety disorder, eating disorder, psychotic disorder, intellectual disability and down syndrome. If YES answer questions 5a-5b. If NO go to Question 6.	□	□
5a.	Do you have difficulty controlling your condition with medications or other physician-prescribed therapies? (Answer NO if you are not currently taking any medications or other treatments).	□	□
5b.	Do you also have back problems affecting nerves or muscles?	□	□
6.	**Do you have a respiratory disease?** This includes chronic obstructive pulmonary disease, asthma, pulmonary high blood pressure. If YES answer questions 6a-6d. If NO, go to Question 7.	□	□
6a.	Do you have difficulty controlling your condition with medications or other physician-prescribed therapies? (Answer NO if you are not currently taking any medications or other treatments).	□	□
6b.	Has your doctor ever said you blood oxygen level is low at rest or during exercise and/or that you require supplemental oxygen therapy?	□	□
6c.	If asthmatic, do you currently have symptoms of chest tightness, wheezing, laboured breathing, consistent cough (more than 2 days/week), or have you used your rescue medication more than twice in the last week?	□	□
6d.	Has your doctor ever said you have high blood pressure in the blood vessels of your lungs?	□	□
7.	**Do you have a spinal cord injury?** This includes tetraplegia and paraplegia. If YES answer questions 7a-7c. If NO, go to Question 8.	□	□
7a.	Do you have difficulty controlling your condition with medications or other physician-prescribed therapies? (Answer NO if you are not currently taking any medications or other treatments).	□	□
7b.	Do you commonly exhibit low resting blood pressure significant enough to cause dizziness, light-headedness, and/or fainting?	□	□
7c.	Has your physician indicated that you exhibit sudden bouts of high blood pressure (known as autonomic dysreflexia)?	□	□

		YES	NO
8.	**Have you had a stroke?** This includes transient ischemic attack (TIA) or cerebrovascular event. If YES answer questions 8a-8c. If NO go to Question 9.	□	□
8a.	Do you have difficulty controlling your condition with medications or other physician-prescribed therapies? (Answer NO if you are not currently taking any medications or other treatments).	□	□
8b.	Do you have any impairment in walking or mobility?	□	□
8c.	Have you experienced a stroke or impairment in nerves or muscles in the past 6 months?	□	□
9.	**Do you have any other medical condition which is not listed above or do you have two or more medical conditions?** If you have other medical conditions, answer questions 9a-9c. If NO go to Question 10.	□	□
9a.	Have you experienced a blackout, fainted, or lost consciousness as a result of a head injury within the last 12 months OR have you had a diagnosed concussion within the last 12 months?	□	□
9b.	Do you have a medical condition that is not listed (such as epilepsy, neurological conditions, and kidney problems)?	□	□
9c.	Do you currently live with two or more medical conditions?	□	□
	Please list your medical condition(s) and any related medications here:		
10.	**Have you had a viral infection in the last 2 weeks (cough, cold, sore throat, etc.)?** If YES please provide details below:	□	□
11.	**Is there any other reason why you cannot take part in this exercise test?** If YES please provide details below:	□	□
12.	**Please provide brief details of your current weekly levels of physical activity (sport, physical fitness or conditioning activities), using the following classification for exertion level:** **L = light (slightly breathless)** **M = moderate (breathless)** **V = vigorous (very breathless)** **Activity** **Duration (mins.)** **Level (L/M/V)** **Monday** **Tuesday** **Wednesday** **Thursday** **Friday** **Saturday** **Sunday**		

Please see below for recommendations for your current medical condition and sign this document:

If you answered NO to all of the follow-up questions about your medical condition, you are cleared to take part in the exercise test.

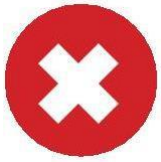

If you answered YES to one or more of the follow-up questions about your medical condition it is strongly advised that you should seek further advice from a medical professional before taking part in the exercise test.

This health questionnaire is based around the PAR-Q+, which was developed by the Canadian Society for Exercise Physiology www.csep.ca

CONSENT FORM

Title of project: The effects of priming exercise on motor unit behaviour

Name of investigator: Robert Hunter

Participant Identification Number for this project:

Please initial box

1. I confirm I have read and understand the information sheet dated xx/xx/xxxx (Version x.x) for the above study. I have had the opportunity to consider the information, ask questions and have had these answered satisfactorily. ☐

2. I understand that my participation is voluntary and that I am free to withdraw at any time without giving any reason. If I wish to withdraw I may contact Robert Hunter (RH567@kent.ac.uk). ☐

3. I understand that my results will be anonymised before analysis. I give permission for members of the research team to have access to my anonymised data. ☐

4. I understand that I must read the health questionnaire (PAR-Q+) carefully and answer the questions to the best of my ability, and that the researchers will use my answers to this questionnaire to assess my suitability for participation. ☐

5. I agree to take part in the above research project. ☐

Name of participant	Date	Signature
Name of person taking consent *(if different from lead researcher)*	Date	Signature
Lead researcher	Date	Signature

To be signed and dated in presence of the participant

Copies when completed: 1 for participant; 1 for researcher site file; 1 (original) to be kept in main file.